UNIVERSITY OF PADUA

DEPARTMENT OF INFORMATION ENGINEERING

MASTER'S DEGREE IN
CONTROL SYSTEMS ENGINEERING

HYBRID RIGIDITY THEORY

A Unifying Mathematical Framework for Heterogeneous Multi-Agent Systems with Mixed Measurements

Supervisor
Prof. Angelo Cenedese
University of Padova

Co-supervisor
Prof. Giulia Michieletto
University of Padova

Candidate
Nicolò Baseggio
ID: 2159165

ACADEMIC YEAR 2025/2026

To my family
and
my friends.

ABSTRACT

Rigidity theory has emerged as a cornerstone for addressing coordination problems in multi-agent systems (MASs), particularly when absolute positioning is unavailable or lacks the precision required for the task, necessitating a strict reliance on relative inter-agent measurements. Current methodologies rely on distinct rigidity paradigms tailored to specific sensor capabilities, such as distance, displacement, and bearing measurements.

Driven by the need to model complex real-world scenarios, recent research has shifted toward heterogeneous MASs, characterized by agents with distinct dynamics evolving on different manifolds. However, although the framework proposed by Michieletto et al. successfully addresses heterogeneous configurations based exclusively on bearing measurements, the literature still lacks a systematic methodology for handling MASs defined by mixed measurement topologies.

To bridge this gap, this thesis introduces Hybrid Rigidity Theory: a unifying mathematical framework designed to accommodate multi-agent systems featuring both heterogeneous dynamics and mixed sensing modalities.

By seamlessly integrating different measurement paradigms, the proposed theory provides a rigorous foundation for the distributed coordination and control of fully heterogeneous MASs. Furthermore, the theoretical framework is validated through a comprehensive set of case studies. Notably, these case studies demonstrate the broad effectiveness of the proposed approach across a variety of scenarios, including successful applications to complex settings where agents are subject to submanifold-constrained dynamics.

EXTENDED ABSTRACT

Rigidity theory has emerged as a cornerstone for addressing distributed coordination problems in MASs, particularly when absolute positioning is unavailable and operations must rely solely on relative inter-agent measurements. Existing methodologies, however, generally depend on distinct paradigms tailored to specific sensing modalities, such as distance, displacement, or bearing.

Driven by the need to model complex real-world scenarios, recent research has shifted toward heterogeneous MASs, whose agents' dynamics is modeled in different manifolds. Although existing frameworks successfully address heterogeneous configurations characterized exclusively by bearing measurements, the literature still lacks a systematic methodology for handling MASs endowed with different measurements.

To bridge this gap, this thesis formally introduces a *Hybrid Rigidity Theory*, a unifying mathematical framework that accommodates MASs with both heterogeneous agent dynamics and mixed sensing modalities. The flexibility of this new framework yields significant practical advantages for modern MAS design, by allowing "advanced" and "basic" sensors to cooperate within cost-effective architectures. The fusion of diverse measurements further facilitates synergistic performance optimization and enhanced robustness, since combining different sensing modalities helps the network avoid the vulnerabilities typical of unimodal measurements.

The **first chapter** provides a comprehensive introduction, reviewing the state of the art in MASs and rigidity theory. It outlines the primary challenges in modern heterogeneous networks and introduce the core contributions of this thesis.

The **second chapter** proposes a novel extension of classical rigidity theory, extending the gourp-theoretic generalized rigidity concepts into a graph-based formalism wherein it is necessary to explicitly define the type of measurement represented by any edge. With this premise, we completely reformulate the standard theory by defining rigidity with respect to a specific smooth group action acting on the agent domain. Conceptually, choosing a specific group action can be thought of as imposing a particular graph completion to achieve the desired notion of rigidity. Through this abstraction, not only we reformulate key well-stated rigidity properties, but also we derive new characterizations with a clear physical interpretation.

The **third chapter** is devoted to characterizing the measurement function, which conceals all the underlying complexity of handling heterogeneous agents and sensors. We describe it as a composition of smooth maps between manifolds, each representing a logical step in the measurement process; this decomposition clarifies how the mathematical model accounts for heterogeneity. Nonetheless, working directly with heterogeneous manifolds is an algebraically delicate and complex operation. An effective way to overcome this challenge is to embed all agents and measurements into a

common homogeneous abstract space. Properly characterizing the agents within this space requires an intermediate formulation that incorporates extrinsic parameters.

We introduce a category-theoretic approach to formalize how the measurement function is formulated across these different representation spaces and to elucidate the relationships between spaces expressed in different realizations. In this sense, category theory offers a natural and elegant language for expressing structural connections, serving as a methodological guide for formally modeling the measure process. This theory also accommodates all the structural connections seamlessly, making the underlying network relationships explicit. We define three distinct network realizations: a native kinematic formulation, an augmented formulation explicitly handling extrinsic variables, and a fully embedded one. The three resulting global network configurations, described in their respective spaces, represent the exact same physical reality and, consequently, are naturally linked. For each of these realizations, the rigidity properties of the framework can be analyzed with respect to a specific smooth group action on its respective state space, naturally inducing three distinct analytical paradigms:

- **Kinematic Φ_{kin}-rigidity** analyzes the rigidity of the native agent configurations, directly assessing the true physical formation of the network.
- **Augmented Φ_{aug}-rigidity** analyzes the rigidity of the state explicitly expanded with extrinsic parameters.
- **Embedded Φ_{emb}-rigidity** analyzes the rigidity of the fully homogenized space.

Although these three notions of rigidity are mathematically deeply connected, they differ profoundly in their physical interpretation, making therefore essential to distinguish between abstract mathematical degrees of freedom and physically realizable motions. Notably, this methodology is highly modular: it can be seamlessly extended by adding or removing intermediate realization, depending on the specific structural characteristics one need to highlight.

Building upon the embedded formulation, the **fourth chapter** investigates the algebraic structure of the embedded rigidity matrix. It systematically analyzes the matrix assembly process for networks relying on pure distance, pure bearing, and mixed modalities, providing explicit analytical Jacobians.

The **fifth chapter** validates the theoretical framework through a set of case studies. It demonstrates the effectiveness and operational utility of the proposed approach by applying the unified theory to complex practical scenarios, where agents are constrained to specific submanifold dynamics and interact through mixed measurements.

Finally, the **sixth chapter** concludes the thesis, summarizing the theoretical advancements and practical implications of the proposed hybrid framework, while outlining promising directions for future research.

DISCLAIMERS

- AI tools were used to support the writing and revision of this manuscript. All AI-assisted content was carefully reviewed, verified, and approved by the author.
- The main mathematical definitions used in this work are reported in the Appendix, with the exception of differential geometry, which is assumed as background knowledge.
- Classical rigidity theory is deliberately omitted from this work to avoid confusion, and readers are referred to the cited literature.

CONTENTS

1 INTRODUCTION

1.1 MULTI-AGENT SYSTEM (MAS)

Over the past few decades, the study of Multi-Agent Systems (MASs) has become an established paradigm across a range of research domains. Initially rooted in computer science as a subfield of Distributed Artificial Intelligence for software coordination, the MAS framework has been extended mathematically and adopted across different engineering domains such as autonomous robotics, aerospace engineering, telecommunications, and smart power grids.

> **Definition 1.1** (Multi-Agent System). A Multi-Agent System (MAS) is a distributed network of agents, ranging from mobile robots and sensors to generic dynamical systems, that interact, share information, and cooperate to achieve complex, system-level objectives.

The cooperation within a MAS generates a collective capability greater than the sum of its individual parts, enabling the execution of tasks that would otherwise be impossible or significantly less efficient.

Initially, MAS served primarily as an analytical tool, providing the mathematical foundation required to model and analyze network dynamics. As engineering challenges increased in complexity, the paradigm extended into synthesis and active problem-solving. Nowadays, the MAS framework is used not only to address natively distributed problems but also to re-engineer classically solved ones, achieving levels of efficiency and robustness that standard single-agent strategies cannot attain.

The adoption of MAS architectures is driven by the cooperation among agents, which offers several fundamental advantages. Some of the most important include:

- **Enhanced Perception and Distributed Actuation:** Spatially distributing agents improves both environmental perception and actuation. Sensing from distinct vantage points allows the system to gather multi-modal data, effectively mitigating issues related to environmental occlusions and measurement uncertainty. Simultaneously, through active collaboration, the network achieves collective capabilities that far exceed the simple sum of its individual parts. Agents working in cooperation can perform complex or physically demanding tasks that would otherwise be either impossible or significantly less efficient.

- **Modularity and Economic Efficiency:** By distributing capabilities across a network of simpler, cost-effective agents rather than concentrating resources into a single monolithic platform, MASs significantly reduce both initial development expenditures and long-term maintenance costs. This modular structure allows individual units to be upgraded, repaired, or replaced independently without overhauling the entire infrastructure.

- **Operational Robustness and Fault Tolerance:** A decentralized architecture removes the vulnerability of single-point failures. In the event of hardware malfunctions, localized damage, or the loss of an individual unit, cooperative control algorithms allow the network to dynamically reconfigure its operational topology. This is further supported by designing formations with redundant sensing edges: should a sensory link fail, the system can absorb the loss without compromising its overall structural cohesion, redistributing tasks among the surviving agents.

- **Scalability and Adaptability:** Agents can be introduced or removed dynamically to accommodate evolving task requirements or unforeseen obstacles without requiring a complete redesign of the underlying control laws, granting the system high adaptability in unstructured environments.

- **Heterogeneity and Synergy:** Combining agents with distinct kinematic constraints and sensing modalities allows the network to exploit asymmetric capabilities. The synergistic fusion of diverse data streams optimizes performance and enables the execution of complex tasks that would be inaccessible to any single or homogeneous platform. Furthermore, mixing different sensing modalities significantly increases the system's robustness, avoiding the vulnerabilities typical of single-measurement configurations. Ultimately, combining heterogeneous agents further enriches the collective actuation and sensing capabilities of the entire network.

The study of MAS involves a wide variety of aspects and problems. In this thesis, we focus on the geometric aspects. Within this framework, the work concentrates on two fundamental problems where the structural cohesion of the network is central:

- **Formation Control:** Design of control strategies that coordinate a group of agents to achieve and maintain a prescribed spatial configuration over time, enabling the network to navigate as a single coherent group.

- **Network Localization:** Estimate the spatial states (typically the positions and orientations) of all agents based solely on available sensing data and the underlying communication topology.

While this work draws on examples from mobile robotics to illustrate these spatial interactions, the underlying theoretical framework remains agnostic to the specific application, and the term "agent" may represent a broader class of dynamical entities.

1.2 THE ROLE OF RIGIDITY THEORY

Classically, the execution of spatially structured tasks has depended on the availability of absolute global positioning data, typically provided by external infrastructure such as the Global Positioning System (GPS) or indoor motion-capture systems. However, this dependence introduces a critical limitation: in a range of scenarios such as deep-space exploration, underwater and subterranean navigation, search and rescue in collapsed structures, or operation in cluttered urban environments, global positioning signals are either denied, degraded, or lack the accuracy required for the task.

Consequently, control and estimation architectures must shift away from dependence on absolute global coordinate frames toward decentralized approaches based on local relative measurements. Since the full relative state is generally unavailable in practice, these systems typically employ partial relative measurements, such as inter-agent distances or bearings. In this approach, agents utilize onboard exteroceptive sensors (such as vision systems, LiDAR, or ultra-wideband radios) to acquire inter-agent state information, reducing the reliance on absolute quantities to a minimum.

This paradigm is strongly inspired by collective biological phenomena, such as the flocking of birds, the schooling of fish, and the foraging behavior of insect colonies. In these natural groups, it is often only a single leader or a small fraction of the collective that possesses knowledge of the absolute destination or global heading. The majority of individuals maintain their positions to preserve the cohesive structure of the group, relying exclusively on local interactions and the direct perception of their immediate neighbors.

Drawing on this biologically inspired distributed intelligence, engineers design MASs that translate relative inter-agent measurements into coordinated emergent behaviors. Through this approach, networks depending on local relative quantities can execute complex operations and function robustly without relying on global positioning.

While bypassing the need for external infrastructure is practically advantageous, shifting from absolute to relative sensing introduces mathematical complexities. When a MAS operates solely on distributed local interactions, guaranteeing the global structural cohesion of the system becomes non-trivial. The primary challenge lies in the ambiguity of relative constraints: a given set of local measurements does not automatically guarantee that the overall network will hold a unique geometric shape. Without the correct underlying topology and an appropriate choice of measurement modalities, the formation might be susceptible to unwanted continuous deformations or folding motions, leading to failures in coordination and estimation.

It is within this context that Rigidity Theory provides the relevant mathematical framework. The formalization of this concept has historical roots dating back to early geometry and analytical mechanics. Among the first to investigate the rigidity properties of geometric shapes was Leonhard Euler, whose initial conjectures on polyhedra in 1766 (Euler's rigidity conjecture) [1] laid the groundwork. It was ultimately

Augustin-Louis Cauchy, with his Rigidity Theorem of 1813 [2], who demonstrated that a convex polyhedral shell is an intrinsically rigid structure, laying the formal foundations of Rigidity Theory.

The transition from analyzing continuous polyhedral surfaces to discrete structural frameworks was pioneered shortly thereafter by James Clerk Maxwell. In his 1864 work [3], motivated by the engineering necessity to analyze the statics of trusses and bridges, Maxwell formulated the algebraic conditions relating the number of joints to the number of connecting bars required to prevent internal mechanisms (Maxwell's counting rules). A few years later, in 1869 [4], he expanded this combinatorial intuition into the realm of internal forces, introducing the concept of reciprocal figures. This later work laid the mathematical foundation for the analysis of structural stresses, which constitutes a backbone of global rigidity analysis and stress matrix formulations in modern control architectures.

Maxwell's insights bridged the gap between structural mechanics and modern graph theory, culminating in the late twentieth century with the work of Gerard Laman. In 1970 [5], Laman formalized Maxwell's initial counting rules, establishing the combinatorial conditions for the generic rigidity of planar graphs. This led to the algebraic contributions of Asimow and Roth (1978, 1979) [6], [7]. A central outcome of their research was the mathematical description of rigid systems through the notion of a *bar-and-joint framework*. By coupling the abstract graph topology with a geometric realization in space, they formalized the concepts of infinitesimal and static rigidity using the rigidity matrix, providing the analytical tools to analyze the infinitesimal motions and continuous deformations of spatial frameworks.

Broadly speaking, a structure is defined as *rigid* if it cannot undergo continuous deformations, flexions, or bendings without violating the constraints imposed between its components. Translating this into Asimow and Roth's formalization, a bar-and-joint framework can be envisioned as an architecture of movable joints connected by inextensible solid bars. In this specific context, the system is rigid if the only way to alter its geometric shape is to break or modify the length of a connecting link. In the absence of such deformations, the framework lacks any internal degrees of freedom; consequently, the network is restricted to moving through space as a single, cohesive body, permitted to undergo only global rigid-body motions: global translations and rotations.

Over the centuries, rigidity theory has expanded from its geometric origins to a wide range of scientific disciplines and very different scales (for an overview, see [8] and the references therein). Applications range from the macroscopic level, such as in architecture and civil engineering, where it constitutes the foundational principle for the static analysis and design of trusses, bridges, and scaffolds, ensuring that built infrastructures exhibit no internal degrees of freedom that would lead to structural collapse. Scaling down to the microscopic level, the theory extends to structural chemistry and molecular biology, where rigidity is employed to study the spatial conformation of molecules and the processes of protein folding. In these domains, atoms are modeled as vertices and chemical bonds act as distance constraints, allowing researchers to predict the macroscopic properties of the compound.

Due to its mathematical versatility, rigidity theory has recently been further abstracted. Moving beyond the traditional physical interpretation of standard bar-and-joint frameworks, the theory has been extended to MASs [9], [10]. In this domain, the concept of rigidity is detached from its mechanical origins. The vertices of the structure no longer represent static elements such as steel joints or microscopic atoms, but rather dynamical systems such as mobile agents, sensors, or other robotic platforms. Moreover, the physical linkages connecting these vertices are transformed into *virtual* constraints. These virtual dependencies represent sensing relations and constraints, defined exclusively by relative inter-agent measurements acquired by onboard exteroceptive sensors. Consequently, the classical concept of a framework has been redefined, broadening its applicability to advanced settings where states and measurements require description on non-flat manifolds rather than the standard n-dimensional Euclidean space.

In these scenarios, rigidity theory emerges as a structural property of the MAS, serving as the core that bridges classical geometry and robotic coordination. Rooted at the intersection of algebraic geometry and graph theory, the theory formalizes how localized measurement constraints dictate the global structural integrity of the system. It provides a systematic framework to determine whether a specific sensing network locks a formation into a unique spatial configuration. By mathematically guaranteeing this structural uniqueness, the theory enables decentralized formation control and network localization from relative sensing alone. In such a scenario, when a formation is considered rigid, a group of physically disconnected yet virtually constrained agents can behave with the same cohesion as a single rigid body.

1.3 STATE OF THE ART

Historically rooted in structural mechanics, the initial application of Rigidity Theory to MASs relied on inter-agent distance measurements. An early synthesis of this transition is provided by Anderson et al. [11], whose work on distance-rigidity graph control architectures details the advantages, limitations, applications, and open problems of distance-based autonomous formations.

Following this, technological advances introduced new sensors capable of measuring different relative quantities. Each sensing modality possesses operational advantages and physical limitations, rendering it particularly suited for specific operational scenarios and environments. To accommodate these distinct capabilities, the classical rigidity theory branched into sensor-specific paradigms.

Each of these formulations represents an independent theoretical branch tailored to the operational traits of its corresponding hardware. Within these dedicated frameworks, researchers investigate the specific topological conditions required for rigidity and the design of specialized algorithms.

Currently, the literature is dominated by the following formulations:

- **Displacement Rigidity:** This framework relies on measuring the full relative position vectors between neighboring agents [12]. Its associated formation control architectures leverage the displacement rigidity matrix to construct gradient-based control laws [13].

- **Distance Rigidity:** This is the classical and most widely adopted formulation, relying exclusively on inter-agent distance measurements [11]. From an application perspective, this paradigm has driven the fields of sensor network localization [14] and decentralized formation control, typically utilizing gradient descent strategies [15].

- **Bearing Rigidity:** This paradigm relies on inter-agent bearing (or line-of-sight) measurements, typically acquired in body-fixed frames [16], to quantify the relative direction between interacting agents. Driven by the pervasive use of onboard vision sensors, bearing-based approaches have recently seen a surge in popularity due to their enhanced robustness and reliability. This paradigm shift has opened new avenues in bearing-only network localization and enabled scale-invariant formation control strategies. Emphasizing the profound impact of these techniques on modern control architectures, Zhao and Zelazo framed this evolution as an exploration of "life beyond distance rigidity" [17].

- **Angle Rigidity:** More recently, alternative paradigms such as angle-based rigidity [18] have been explored. These rely on the internal subtended angles between neighbors, offering a crucial advantage: the measurements are invariant to local reference frames, providing robust solutions even when agents lack a common global orientation

The transition toward these more complex measurement paradigms exposes the limits of classical modeling assumptions, requiring an extension of the theory.

A primary requirement is the relaxation of the bidirectional sensing constraint, a need that arises because modern interaction models exhibit different symmetry properties. While scalar constraints like distance are inherently symmetric (meaning the measurement from agent i to agent j is identical to that from j to i), allowing the framework to rely on underlying undirected graphs, vectorial quantities are generally asymmetric. For instance, measurements that depend on the observer's local reference frame, such as bearings, are intrinsically directional. Since these measurements are strictly defined from the measuring agent i to the target agent j, the theoretical framework must be extended to encompass directed underlying topologies. To capture this reality, classical theory was generalized into the framework of *Directed Rigidity* [19], which dictates a shift from undirected to directed interaction topologies.

This paradigm shift accommodates practical hardware limitations, restricted sensor fields of view, and communication bottlenecks. Furthermore, from a control perspective, the adoption of directed graphs enables an asymmetric distribution of the responsibility to maintain specific formation constraints among the agents.

To formalize this asymmetric assignment of tasks, the shift to directed frameworks led to the introduction of *persistent graphs*. While standard rigidity ensures that a network possesses a unique geometric shape, persistence guarantees that this shape can be actively and consistently maintained. Specifically, it ensures that no individual agent is assigned more directed constraints than it can physically satisfy, rendering the formation feasible for autonomous, decentralized control.

Driven by this new paradigm, new analysis and control challenges have emerged in the literature. Moving from pure structural analysis to active coordination, control laws have subsequently been developed to guarantee formation stabilization directly under these directed interaction topologies [20].

Although persistence is a fundamental property, its explicit analysis falls outside the scope of this work. Instead, we proceed under the assumption that the MAS is always capable of maintaining the assigned formation constraints.

However, the emergence of these new sensing paradigms exposed another limitation of standard rigidity theory: its reliance on agents evolving exclusively within simple Euclidean spaces. Historically, classical rigidity analysis has been strictly confined to $\mathbb{R}^d$, leveraging well-established combinatorial tools (such as Maxwell's counting rules) to assess the structural integrity of positional point-mass networks. In general, this framework is no longer restricted to Euclidean spaces. For instance, when dealing with sensing paradigms that incorporate orientation information, accounting for the agents' attitude and full pose evolution requires a shift from flat Euclidean spaces to non-flat manifolds.

A representative example of this mathematical shift is found in the study of bearing rigidity. Because bearing measurements are explicitly tied to the measuring agents' local reference frames, the state representation must inherently incorporate full pose (position and orientation). This necessitates modeling the system state on the Special Euclidean groups $SE(d)$ (for $d \in \{2, 3\}$, $d = 2$), which are non-flat manifolds. Significant contributions toward accommodating these full pose kinematics were made by Zelazo et al. [21], who extended classical frameworks to $SE(2)$ to enable bearing-only control for nonholonomic vehicles, and subsequently by Michieletto et al. [22], who formalized bearing rigidity theory directly in $SE(3)$ to address full 3D pose dynamics.

Transitioning into these non-Euclidean domains implies that the classical rigidity theorems and geometric guarantees are no longer valid, requiring a rigorous theoretical extension. While some preliminary counting conditions have been formulated for specific non-Euclidean spaces, the literature remains sparse. Specifically for bearing-based frameworks, Michieletto et al. [23] formalized the primary combinatorial and rank conditions required to ensure structural uniqueness across these generalized abstract manifolds.

Despite these theoretical advancements in non-Euclidean geometry, the frameworks discussed thus far share a fundamental limitation: the assumption of network homogeneity. Traditional models strictly require all agents to share the same kinematic structure, forcing them to evolve on the same manifold.

In modern real-world deployments, this restriction becomes severely limiting. To overcome this barrier, recent research has shifted toward heterogeneous MASs, where agents possess distinct dynamics evolving across different manifolds. The work by Michieletto et al. [23] addressed this problem for bearing rigidity by embedding the agents' dynamics into a common abstract homogeneous manifold. Specifically, $SE(3)$ was chosen as this unified space, as it is sufficiently general to encompass a wide class of heterogeneous MASs.

While the idea proposed by Michieletto et al. could be extended to other sensing modalities, a strict limitation still holds: the sensing network itself must remain homogeneous. This means that the inter-agent relative measurements across the network must consist of the same type (e.g., exclusively distances or exclusively bearings)

1.4 MOTIVATIONS AND CONTRIBUTIONS

Despite their individual theoretical successes, the literature remains fundamentally constrained by this assumption of *homogeneous sensing networks*. In modern real-world scenarios, this requirement is highly restrictive. It is rarely possible or optimal to guarantee a uniform measurement type across all agents, particularly within heterogeneous MAS. To overcome this structural barrier, this thesis embraces the paradigm of *mixed-measurement sensing networks*, seamlessly integrating diverse sensing modalities within a single interacting architecture.

The transition toward this mixed-measurement paradigm is motivated by several additional advantages:

- **Asymmetric Hardware Efficiency:** Uniform sensor distribution is rarely optimal. A mixed-measurement framework enables an asymmetric sensing network, where a small subgroup of agents is equipped with *advanced* sensors (high-fidelity, power-intensive devices like heavy 3D LiDARs), while others rely on *basic* sensors (standard, cost-effective, and faster alternatives such as lightweight cameras). This reduces total mission cost, payload, and energy consumption without sacrificing structural rigidity, enabling optimal resource allocation for the MAS.

- **Improved Accuracy and Performance:** Each sensing modality possesses intrinsic limitations. By combining heterogeneous measurements, the system leverages their complementary strengths, overcoming these individual limitations and effectively filtering out uncorrelated noise. This ensures that the most effective measurement strategy is used for a given spatial configuration, improving the overall performance of the formation and leading to more precise state estimations.

- **Expanded Environmental Perception:** Beyond tracking the internal state of the formation, a heterogeneous sensor suite allows the network to observe a richer set of external/environmental information. Different sensors can capture diverse physical features, enabling essential tasks like obstacle detection, target identification, and terrain mapping, which greatly enhances the overall situational awareness of the system.
- **Increased Robustness and Fault Tolerance:** In a homogeneous network, a single external disturbance can compromise the entire sensing topology and lead to a loss of cohesion. A mixed architecture relies on different physical principles that rarely fail simultaneously under the same perturbations. This reduces vulnerability to individual sensor failures, signal loss, or localized disturbances, achieving fault tolerance through technological diversification rather than mere component duplication, which remains susceptible to the exact same environmental disturbances.
- **Symmetry-Breaking:** Homogeneous sensing networks often suffer from structural ambiguities, such as scale ambiguity in bearing-based formations or reflection ambiguities in distance-based ones. Combining heterogeneous measurements may effectively break these spatial symmetries.
- **Enhanced System Observability:** Integrating diverse data sources allows for the estimation of complex states or variables that would otherwise remain unobservable using a single measurement type. Overcoming these limitations guarantees the global observability of the entire network state.

As previously discussed, the study of heterogeneous MASs has experienced rapid expansion, driven by the escalating complexity of modern real-world applications. While the theoretical frameworks governing heterogeneous agents are studied, their integration with mixed-measurement paradigms poses a non-trivial mathematical challenge.

To establish the mathematical foundation required for such a framework, this thesis draws on and extends the work of Stacey and Mahony [24]. By departing from traditional graph-theoretic models of MAS, their research generalizes the concept of rigidity through the lens of differential geometry and group theory. This geometric perspective is broad enough to accommodate the complexities of both heterogeneous dynamics and mixed-measurement topologies. However, while providing a rigorous theoretical background for analyzing systems with diverse kinematics and measurements, these concepts remain largely abstract, lacking a systematic and constructive methodology to handle such heterogeneity.

This thesis extends the work of Stacey and Mahony through graph-theoretic structures by introducing *Hybrid Rigidity Theory*. This unifying mathematical framework is specifically designed to systematically govern MASs characterized by heterogeneity in both agent kinematics and mixed-measurement topologies.

It is worth noting that *Hybrid Rigidity Theory* is general enough to encompass all other specialized rigidity theories (classical, heterogeneous, and mixed-measurement) as special cases. Consequently, it inherently accommodates any combination of homogeneity and heterogeneity across both agent kinematics and sensing topologies.

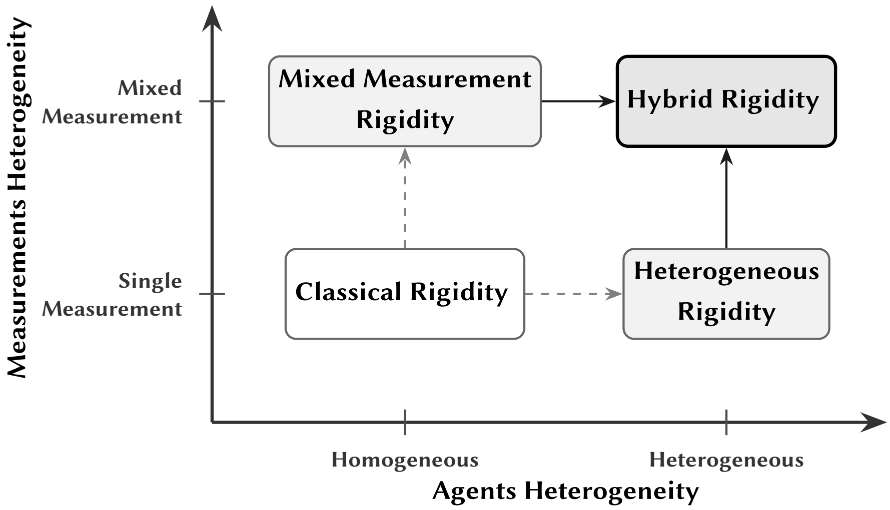

Working directly with heterogeneous manifolds is an delicate and complex task. An effective strategy to overcome this challenge is to embed all agents and measurements into common abstract homogeneous spaces, subsequently defining an embedded measurement map between them.

In classical frameworks, however, measurement mappings are constrained to depend exclusively on the interacting agents' internal states. This imposes a severe structural limitation when dealing with heterogeneous dynamics, where measurements often occur between states residing in disparate manifolds and thus require additional parameters to be fully characterized.

The proposed *Hybrid Rigidity Theory* overcomes classical limitations. The embedding process uses external information to properly characterize the state within the common homogeneous space. This allows the framework to seamlessly handle diverse measurements whether they utilize the agents' full kinematic state, rely on a specific subset of it, or extend it by incorporating extra information. Furthermore, the framework can manage measurements across different spaces and introduces a novel concept of robustness analysis under extrinsic variable perturbations, opening up a promising avenue for future research.

Looking forward, this approach suggests that these extrinsic parameters can eventually participate in the rigidity analysis in the exact same manner as intrinsic agent variables. This implies that the framework could integrate not only static parameters but also accommodate the active dynamics of external variables. Additionally, as another promising direction for future research, one could investigate the potential benefits of integrating these parameters directly into the measurement space as well. While this advanced paradigm is conceptually introduced in this work, its comprehensive mathematical analysis is left to future research.

A central contribution of this work is the mathematical characterization of the measurement function, which abstracts all the underlying complexity of handling heterogeneous agents and measurements. By structuring the measurement modeling process as a sequence of composed mappings, this approach yields a systematic methodology for rigidity analysis. These mappings represent the exact steps required to formalize inter-agent measurements. They clearly highlight how the mathematical model handles heterogeneity, and how state information is either filtered or augmented with external parameters to compute the final measurement.

As will become evident, the measurement function can be characterized in various ways through the strategic selection of intermediate manifolds and mappings, effectively transforming this choice into a design degree of freedom. Specifically, in this work, particular attention is devoted to the rigidity matrix structure that arises when all intermediate manifolds are homogeneous, propagating the embedded state of the agents via appropriate filtering and padding operations.

To formalize how the measurement function is formulated across these different representation spaces (native, augmented with parameters and embedded), and to elucidate the relationships between spaces expressed in different realizations, we introduce a category-theoretic approach. Although the framework could, in principle, be constructed without it, category theory offers a natural and elegant language for expressing structural connections, serving as a methodological guide for formally modeling the measurement process. It accommodates these realizations seamlessly, making the underlying relationships explicit.

We define three distinct network realizations: a native kinematic formulation, an augmented formulation explicitly handling extrinsic variables, and a fully embedded formulation. While these three describe the exact same physical reality, they utilize different agent state representations and are therefore intrinsically linked. For each realization, the structural rigidity of the framework can be analyzed with respect to a specific smooth group action on its respective state space, naturally inducing three distinct analytical paradigms:

- **Kinematic Φ_{kin}-rigidity:** Analyzes the rigidity of the native agent configurations, directly assessing the true physical geometry of the network.
- **Augmented Φ_{aug}-rigidity:** Analyzes the rigidity of the augmented state, which explicitly incorporates extrinsic parameters.
- **Embedded Φ_{emb}-rigidity:** Analyzes the rigidity of the network within the fully homogenized abstract space.

Although these three notions of rigidity are mathematically deeply connected, they differ profoundly in their physical interpretation. When analyzing infinitesimal or continuous rigidity, it is therefore essential to distinguish between abstract mathematical degrees of freedom and physically realizable motions.

Notably, this methodology is highly modular: it can be seamlessly extended by adding or removing intermediate realizations, depending on the specific structural characteristics that need to be highlighted. While the specific chain of mappings proposed herein is tailored to the most prevalent sensing modalities in the literature, this inherent modularity allows the framework to be modified by introducing or omitting steps. This effortlessly adapts it to new measurement paradigms. Regardless of the specific sensor types, this work provides a conceptual baseline for the procedural steps required to construct a valid measurement function.

The incorporation of extrinsic variables paves the way for the study of submanifold-constrained systems. In such scenarios, a minimal kinematic state does not always contain all the information required to evaluate the measurement map. For instance, agents constrained to distinct rails possess 1-dimensional kinematic states, yet they may rely on measurements that require 3D spatial awareness, such as 3-dimensional relative distances or bearings. To evaluate these interactions, the kinematic state must be augmented with external geometric parameters; this fully characterizes the agents' state within the environment and enables the computation of the measurement map. As a preliminary example of its applicability, this work explores the rigidity analysis of a multi-agent system wherein individual agents are kinematically restricted to predefined distict parallel 1D geometric structures, such as rectilinear rails, embedded in a 3D environment. The comprehensive mathematical formalization of generalized constrained systems is left to future research.

This illustrates the adaptability of the approach, yielding a solution for the coordination of constrained robotic systems while reserving a more rigorous mathematical treatment for future research.

2 HYBRID RIGIDITY THEORY

This chapter establishes the theoretical foundations of the proposed *Hybrid Rigidity* framework. Specifically, it formalizes the representation of a MAS featuring heterogeneous agents and mixed measurements as a framework, providing the mathematical foundation for the rigidity analysis. This analysis extends the definitions originally proposed by Stacey and Mahony [24] with a rigorous graph-theoretic formalism. Based on this synthesis, several fundamental results and characterizations are presented.

2.1 FRAMEWORKS

To model a MAS and its underlying sensing network, it is necessary to translate the physical reality of the agents and their sensory interactions into the language of graph theory.

Consider a MAS comprising n interacting agents. The state of each agent, denoted by $\mathbf{x}_i$, evolves within a specific smooth manifold $\mathscr{D}_i$, i.e., $\mathbf{x}_i \in \mathscr{D}_i$.

While the agents rely on onboard sensors for inter-agent measurements, the framework does not require every agent to possess sensing capabilities. A subset of actively sensing agents is sufficient, and individual sensors may concurrently acquire data from multiple neighbors.

By assuming a local communication network for information sharing, we can abstract this physical sensing process and model the distributed network purely as a set of m distinct pairwise measurement constraints. Thus, each k-th measurement (with $k \in \{1, \dots, m\}$) is fully characterized by a value $y_k \in \mathscr{M}_k$, where $\mathscr{M}_k$ denotes its corresponding measurement smooth manifold.

The distribution and topology of these n agents and m sensory links are encoded using a finite graph $\mathscr{G} = (\mathscr{V}, \mathscr{E})$. Here, the vertex set $\mathscr{V}$ models the agents, and the edge set $\mathscr{E}$ models the active inter-agent measurements.

From a general topological perspective, the nodes in $\mathscr{V}$ could represent indistinguishable agents. In such a case, the graph cannot be ordered; this anonymity is also propagated to the edge set $\mathscr{E}$. Consequently, in these *non-ordered* frameworks, both the global state space and the global measurement space must account for combinatorial permutations, since swapping any two identical agents yields an equivalent macroscopic configuration.

However, in typical real-world applications, agents are rarely anonymous. Therefore, it is standard practice to model a MAS with distinctly labeled and enumerated agents and measurements. Under this realistic assumption, we formally treat the underlying topology $\mathscr{G}$ as an *ordered graph*. This implies the existence of a strict bijection between the vertex set $\mathscr{V}$ and the index set $\{1, \ldots, n\}$, as well as between the edge set $\mathscr{E}$ and the index set $\{1, \ldots, m\}$.

Depending on the specific sensory modalities and the system architecture, the underlying interaction graph can be modeled as either directed or undirected. The necessity for directed edges typically arises from three distinct domains:

- **Nature of the measurement:** The intrinsic symmetry of a sensory constraint dictates the underlying topology of the graph. A measurement is considered *symmetric* if the information acquired by agent i relative to agent j is equivalent to that acquired by j relative to i. Scalar quantities, such as Euclidean distance, are inherently symmetric and are thus naturally modeled using *undirected edges*. Conversely, vectorial measurements that depend strictly on the observer's local reference frame, such as relative bearing or line-of-sight, are intrinsically asymmetric. This necessitates the use of *directed edges* to explicitly distinguish the measuring agent (the source node i) from the observed agent (the target node j).

- **Physical hardware limitations:** Restricted sensor fields of view, occlusions, communication bottlenecks, and heterogeneous equipment frequently result in asymmetric sensing topologies. In such cases, only one agent in a given pair might be physically capable of acquiring the measurement, naturally inducing a directed sensing link.

- **Control strategies and task assignment:** From an architectural standpoint, the directionality of an edge is intrinsically linked to the assignment of task responsibilities within the formation. Even in the presence of mathematically symmetric constraints and ideal hardware, the underlying control architecture dictates which agent must actively enforce the constraint. If the task of maintaining this constraint is assigned jointly to a pair of agents, the relationship is mutual and thus appropriately modeled by an *undirected edge*. Conversely, the control architecture may delegate this responsibility to a single agent (e.g., agent i is tasked with maintaining a prescribed distance from agent j, while j acts independently and remains completely unaware of i). Under such conditions, the interaction is fundamentally asymmetric, and the constraint must be represented by a *directed edge* originating from the agent responsible for its enforcement.

It is worth noting that a directed graph formalism serves as a natural generalization of undirected topologies. Specifically, any undirected edge can be equivalently represented as a pair of directed edges sharing the same endpoints but having opposite orientations. Consequently, adopting a directed framework provides the mathematical flexibility to seamlessly encompass both symmetric and asymmetric interactions within a unified structure.

In formation control problems, a measurement might only be available to a single agents, as previously discussed. This inherent asymmetry naturally enables the explicit assignment of control responsibilities across the network, a scenario where the question of graph persistence typically arises. However, in this work, we assume the existence of a sufficient communication infrastructure that allows agents to cooperate effectively in satisfying any given constraint. Consequently, the specific challenges associated with persistence are not considered. Crucially, this capability to communicate does not imply that the underlying physical measurements become symmetric; the sensing topology remains fundamentally directed.

In control problems, a measurement might be available to a single agent only, or the responsibility to maintain a specific constraint may be assigned to just one node of the edge, explicit assignment of control responsibilities across the network. To formalize this asymmetric task allocation, the shift toward directed frameworks in the literature led to the introduction of *persistent graphs*. While standard rigidity ensures that a network possesses a unique geometric shape, persistence guarantees that this shape can be actively and consistently maintained. Specifically, it ensures that no individual agent is assigned more directed constraints than its degrees of freedom can physically satisfy, rendering the formation feasible for autonomous, decentralized control.

However, in this work, we assume the existence of a robust communication infrastructure that allows agents to cooperate effectively and that all agents are physically capable of satisfying any prescribed constraint. Consequently, the specific theoretical challenges associated with directed persistence fall beyond the scope of this analysis. Crucially, this communication capability does not imply that the underlying physical measurements become symmetric; the physical sensing topology remains fundamentally directed.

The topological graph alone is insufficient to completely model a MAS and its associated sensing network. To fully characterize the system through a graph, each vertex must be characterized by a specific physical state, and each edge must be mapped to a specific inter-agent measurement to model the sensing constraints. This mapping process is formally captured by the concept of a framework.

> **Definition 2.1** (Ordered Smooth Framework). Consider a MAS composed of n agents, where the physical state of the i-th agent evolves within a specific smooth manifold $\mathscr{D}_i$, meaning it can be fully characterized by $x_i \in \mathscr{D}_i$. Concurrently, the system features m active inter-agent measurements, where each k-th measurement takes values in a specific smooth measurement manifold $\mathscr{M}_k$, characterized by $y_k \in \mathscr{M}_k$.
>
> Let the underlying interaction topology be represented by a finite graph $\mathscr{G} = (\mathscr{V}, \mathscr{E})$, with $|\mathscr{V}| = n$ and $|\mathscr{E}| = m$, which may be directed or undirected depending on the specific modeling requirements. We assume $\mathscr{G}$ is an ordered graph.

We define the global vertex state space as an open subset of the Cartesian product of the individual agent manifolds, $\mathscr{D}_g \subseteq \prod_{i=1}^{n} \mathscr{D}_i$, and the global edge measurement space as a subset of the Cartesian product of the individual measurement manifolds, $\mathscr{M}_g \subseteq \prod_{k=1}^{m} \mathscr{M}_k$.

While $\mathscr{D}_g$ and $\mathscr{M}_g$ directly reflect the physical topology of the distributed network, it is often mathematically more convenient to map these product manifolds into isomorphic spaces via diffeomorphisms, i.e., $\overline{\mathscr{D}} \cong \mathscr{D}_g$ and $\overline{\mathscr{M}} \cong \mathscr{M}_g$.

To fully characterize the MAS, we must associate the vertices with the agent states and the edges with the relative inter-agent measurements. Consequently, we define two fundamental local mappings:

- A local *vertex-state map* $\mathscr{X}_i$, which assigns each vertex v_i to a physical node state $x_i \in \mathscr{D}_i$.
- A local *edge-measurement map*$\mathscr{Y}_k$, which assigns each explicit edge e_k to a specific measurement instance $y_k \in \mathscr{M}_k$.

To build the global configurations, we extend these concepts by defining:

- A global *vertex-state map* $\mathscr{X}$, which assigns to an ordered vertex n-tuple $\mathbf{v} = (v_1, \dots, v_n)$ the global agent configuration $x \in \overline{\mathscr{D}}$.

  Since the vertices are ordered, the map $\mathscr{X}$ is bijectively identified by its resulting vector. Therefore, the abstract map can be effectively replaced by the global agent configuration $x \in \overline{\mathscr{D}}$.

- A global *edge-measurement map* $\mathscr{Y}$, which assigns to an ordered m-tuple of the graph's edges $\mathbf{e} = (e_1, \dots, e_m)$ the global measurement configuration $y \in \overline{\mathscr{M}}$.

  Since the edges are ordered, the map $\mathscr{Y}$ is bijectively identified by its resulting vector. Therefore, the abstract map can be safely replaced by the global measurement configuration $y \in \overline{\mathscr{M}}$.

The underlying graph topology $\mathscr{G}$ and the inter-agent relative nature of the measurements motivate the introduction of a smooth *(global) measurement/sensing map*

$$h : \overline{\mathscr{D}} \to \overline{\mathscr{M}}. \tag{1}$$

This function analytically bridges the node configuration with the edge configuration, mapping the states of the agents into the resulting sensory outputs such that $y = h(x)$. Consistent with the graph topology, the k-th component of the sensing map, $h_k(x) \in \mathscr{M}_k$, depends exclusively on the states of the specific agents incident to the edge e_k.

The combination of the topological graph, the node configuration, and the global sensing map yields the complete mathematical characterization of the system. We formally define this structure as the *Ordered Smooth Framework*, denoted by the triplet $\Gamma = (\mathscr{G}, x, h)$.

In the classical rigidity literature, a framework is traditionally defined as the ordered pair $(\mathscr{G}, x)$, treating the measurement function as a separate external entity. While this decoupled approach is sufficient for standard formulations where the sensing network is strictly homogeneous, it falls short when dealing with the heterogeneous sensing topologies considered in this work. To properly accommodate these mixed modalities, the underlying graph topology must be explicitly coupled with the specific nature of the sensory edges. By elevating the measurement map h to a core component of the framework to form the triplet $\Gamma = (\mathscr{G}, x, h)$, we fully encapsulate the MAS within a single unified entity. This formulation yields a flexible mathematical model that accurately reflects the physical reality, enabling new sensory characteristics and rigidity properties to be intrinsically tied to the framework itself.

Furthermore, despite this comprehensive formulation, adopting the concise triplet $(\mathscr{G}, x, h)$ entails no loss of information. Specifically, the abstract vertex-state map $\mathscr{X}$ can be safely replaced by the global node configuration x, because the explicitly ordered nature of $\mathscr{G}$ ensures a unique bijection between the two. Additionally, the edge-measurement map $\mathscr{Y}$ (along with its induced configuration y) is intentionally omitted to avoid functional redundancy, since the sensory output can be fully reconstructed at any time via the evaluation $y = h(x)$. Consequently, the triplet $(\mathscr{G}, x, h)$ avoids unnecessary complexities while providing all the essential ingredients. The graph $\mathscr{G}$ dictates the topology and contains the vertex and edge sets, while the definition of the map $h : \overline{\mathscr{D}} \to \overline{\mathscr{M}}$ inherently carries both the state and measurement manifolds, defining how they are linked. Thanks to this integrated information, the node configuration x alone is sufficient to completely characterize the current agents and measuremets state of the framework.

The global state space $\mathscr{D}_g$ is defined as an *open subset* of the product manifold $\prod_{i=1}^{n} \mathscr{D}_i$. This restriction serves to remove singular configurations from the domain. A practical example arises in spatial multi-robot systems, where this formulation systematically prevents unfeasible geometric states by explicitly excluding inter-agent collisions.

Conversely, the measurement space $\mathscr{M}_g$ is not required to be an open subset. Its individual components $\mathscr{M}_k$ are typically natural smooth manifolds (e.g., the positive real line $\mathbb{R}_{>0}$ for distances, or $\mathbb{S}^1$ and $\mathbb{S}^2$ for bearings). These spaces are boundaryless smooth manifolds by construction, which is sufficient to support the differential structure of the map h. Physical sensing constraints restrict the image $h(\overline{\mathscr{D}})$ without altering the smooth manifold properties of the codomain.

> **Definition 2.2** (Homogeneous and Heterogeneous Frameworks)**.** Let $(\mathscr{G}, x, h)$ be an ordered smooth framework. We classify its structure based on the uniformity of its underlying manifolds:
>
> - **Node/Agent Homogeneity:** The framework is *node/agent-homogeneous* if all agents evolve on the same differential state manifold, i.e., $\mathscr{D}_i = \mathscr{D}$ for all $i \in \{1, \ldots, n\}$, yielding the global state space $\mathscr{D}_g = \mathscr{D}^n$.

Conversely, if at least two agents operate on distinct state manifolds, the framework is *node/agent-heterogeneous*.

- **Edge/Measurement Homogeneity:** The framework is *edge/measurement-homogeneous* if all sensory links evaluate to the same differential measurement manifold, i.e., $\mathscr{M}_k = \mathscr{M}$ for all $k \in \{1, \ldots, m\}$, yielding the global measurement space $\mathscr{M}_g = \mathscr{M}^m$.

  Conversely, if at least two measurements belong to distinct manifolds, the framework is *edge/measurement-heterogeneous*.

The proposed framework is general enough to accommodate all possible combinations of such homogeneity and heterogeneity for both agents and measurments.

2.2 RIGIDITY PROPERTIES OF ORDERED SMOOTH FRAMEWORKS

Definition 2.3 (Node-Equivalent Frameworks). Let $\Gamma = (\mathscr{G}, x, h)$ and $\Gamma' = (\mathscr{G}, x', h)$ be two frameworks sharing the same underlying ordered topological graph $\mathscr{G}$ and global sensing map h. The two frameworks are said to be *node-equivalent* if their respective global node configurations $x, x' \in \overline{\mathscr{D}}$ yield identical global sensory outputs under h. Formally, this measurement equivalence is expressed as:

$$y = h(x) = h(x') = y' \tag{2}$$

Definition 2.4 (Preimage). Let $f : X \to Y$ be a map between two sets X and Y, and let $S \subseteq Y$ be a subset of the codomain. The *preimage* (or inverse image) of S under f, denoted by $f^{-1}(S)$, is the set of all elements in the domain X that map into S:

$$f^{-1}(S) := \{x \in X \mid f(x) \in S\} \tag{3}$$

Definition 2.5 (Fiber). Let $f : X \to Y$ be a map between two sets X and Y, and let $y \in Y$ be a specific, single element of the codomain. The *fiber* of the map f over the point y is defined as the preimage of the singleton set $\{y\}$. It is typically denoted as $f^{-1}(y)$:

$$f^{-1}(y) := f^{-1}\big(\{y\}\big) = \{x \in X \mid f(x) = y\} \tag{4}$$

Definition 2.6 (Node-Equivalent Set). Let $\Gamma = (\mathscr{G}, x, h)$ be a framework with global node configuration $x \in \overline{\mathscr{D}}$. The *node-equivalent set* associated with the framework Γ is the collection of all valid configurations within the smooth product manifold $\overline{\mathscr{D}}$

that yield the same global sensory output as x. Formally, this set coincides with the fiber of the sensing map h over the specific sensory output $y = h(x)$:

$$\mathcal{Q}(\Gamma) := h^{-1}\big(h(x)\big) = \big\{x' \in \overline{\mathcal{D}} \mid h(x') = h(x)\big\} \tag{5}$$

In *mixed-signal* networks, the classical definition of congruence known in the literature [23] cannot be applied, as there is no single measurement type that defines the completion of the graph. To overcome this limitation, we adopt a more general geometric formulation based on Lie group theory, inspired by the approach proposed in [24].

Definition 2.7 (Measurement Φ-Invariant Framework)**.** Let G be a Lie group acting smoothly on the node configuration space $\overline{\mathcal{D}}$ via the left group action $\Phi : G \times \overline{\mathcal{D}} \to \overline{\mathcal{D}}$. A framework $\Gamma = (\mathcal{G}, x, h)$ is said to be *measurement Φ-invariant* if its global sensing map h is invariant under the action of G. Formally:

$$h(\Phi(g, x)) = h(x) \quad \forall g \in G,\ \forall x \in \overline{\mathcal{D}}. \tag{6}$$

Proposition 2.1 (Φ-Invariance of the Equivalent Set)**.** *Let $\Gamma = (\mathcal{G}, x, h)$ be a measurement Φ-invariant framework. Then, its associated node-equivalent set (or fiber) $\mathcal{Q}(\Gamma)$ is a Φ-invariant set.*

Proof. By definition, a subset $S \subseteq \overline{\mathcal{D}}$ is strictly Φ-invariant if $\Phi(g, S) = S$ for all $g \in G$. To prove this for $\mathcal{Q}(\Gamma)$, let $x' \in \mathcal{Q}(\Gamma)$ be an arbitrary configuration within the equivalent set. By the definition of the fiber, it holds that $h(x') = h(x)$.

Let $g \in G$ be an arbitrary element of the Lie group. We must determine whether the transformed configuration $\Phi(g, x')$ remains within the equivalent set. Because the framework is measurement Φ-invariant, the global sensing map h is unaffected by the group action, yielding:

$$h\big(\Phi(g, x')\big) = h(x'). \tag{7}$$

Substituting the identity $h(x') = h(x)$ into this equation gives:

$$h\big(\Phi(g, x')\big) = h(x). \tag{8}$$

This outcome satisfies the inclusion criteria for the fiber, therefore $\Phi(g, x') \in \mathcal{Q}(\Gamma)$. Since this holds for any chosen $x' \in \mathcal{Q}(\Gamma)$, we establish the structural inclusion:

$$\Phi\big(g, \mathcal{Q}(\Gamma)\big) \subseteq \mathcal{Q}(\Gamma) \tag{9}$$

To prove strict equality, we must demonstrate the reverse inclusion:

$$\mathcal{Q}(\Gamma) \subseteq \Phi\big(g, \mathcal{Q}(\Gamma)\big) \tag{10}$$

Because g was chosen arbitrarily, the forward inclusion established in (9) must analogously hold for its inverse element $g^{-1} \in G$:

$$\Phi\big(g^{-1}, \mathcal{Q}(\Gamma)\big) \subseteq \mathcal{Q}(\Gamma) \tag{11}$$

Let $y \in \mathcal{Q}(\Gamma)$ be an arbitrary element. By the relation above, applying the inverse action yields a point $z = \Phi(g^{-1}, y)$ that strictly belongs to $\mathcal{Q}(\Gamma)$. By exploiting the fundamental property of group actions, we can reconstruct the original point y as:

$$y = \Phi\big(g, \Phi(g^{-1}, y)\big) = \Phi(g, z) \tag{12}$$

Since $z \in \mathcal{Q}(\Gamma)$, it immediately follows that $y \in \Phi\big(g, \mathcal{Q}(\Gamma)\big)$. This establishes the reverse inclusion:

$$\mathcal{Q}(\Gamma) \subseteq \Phi\big(g, \mathcal{Q}(\Gamma)\big) \tag{13}$$

Since both inclusions hold, we conclude that the node-equivalent set is strictly invariant under the group action:

$$\mathcal{Q}(\Gamma) = \Phi\big(g, \mathcal{Q}(\Gamma)\big) \tag{14}$$

Thus, the node-equivalent set $\mathcal{Q}(\Gamma)$ is proven to be a Φ-invariant set. □

Definition 2.8 (Node Φ-Congruent Frameworks)**.** Let G be a Lie group acting smoothly on $\overline{\mathcal{D}}$ via the left action Φ. Two measurement Φ-invariant frameworks $\Gamma = (\mathcal{G}, x, h)$ and $\Gamma' = (\mathcal{G}, x', h)$ are said to be *node Φ-congruent* (or simply Φ-congruent) if their respective global node configurations $x, x' \in \overline{\mathcal{D}}$ are related by a global symmetry transformation. Formally, there must exist a group element $g \in G$ such that:

$$\Phi(g, x) = x'. \tag{15}$$

Definition 2.9 (Node Φ-Congruent Set)**.** Let G be a Lie group acting smoothly on $\overline{\mathcal{D}}$ via the left action Φ. Let $\Gamma = (\mathcal{G}, x, h)$ be a measurement Φ-invariant framework with global node configuration $x \in \overline{\mathcal{D}}$. The *$\Phi$-congruent node configuration set* (or orbit) associated with the framework represents the collection of all spatial node assignments that can be reached via a global symmetry transformation. Formally, it is defined as the group orbit of x under Φ:

$$\mathscr{C}(\Gamma) := \mathrm{Orb}(x) = \mathrm{Im}(\Phi_x) = \{\Phi(g, x) \in \overline{\mathcal{D}} \mid g \in G\} \tag{16}$$

Proposition 2.2 (Φ-Invariance of the Congruent Set)**.** *Let $\Gamma = (\mathcal{G}, x, h)$ be a framework. Its associated node-congruent set (or orbit) $\mathscr{C}(\Gamma)$ is a Φ-invariant set.*

Proof. By definition, the node-congruent set is the group orbit generated by the configuration x, formally expressed as $\mathscr{C}(\Gamma) = \{\Phi(k, x) \mid k \in G\}$.

Let $g \in G$ be an arbitrary element of the Lie group. Applying the group action $\Phi(g, \cdot)$ to the entire orbit yields:

$$\Phi\big(g, \mathscr{C}(\Gamma)\big) = \big\{\Phi\big(g, \Phi(k, x)\big) \mid k \in G\big\}. \tag{17}$$

By the fundamental composition axiom of group actions, applying two successive transformations is equivalent to applying the transformation of their group product, hence $\Phi\big(g, \Phi(k, x)\big) = \Phi(g \circ k, x)$.

Substituting this property gives:

$$\Phi\big(g, \mathscr{C}(\Gamma)\big) = \{\Phi(g \circ k, x) \mid k \in G\}. \tag{18}$$

In group theory, left-translation by any element $g \in G$ is a bijection from the group onto itself. Therefore, as k ranges over all elements of G, the product $(g \circ k)$ perfectly spans the entire group G once again (i.e., $g \circ G = G$).

This allows us to rewrite the set exactly as the original orbit:

$$\Phi\big(g, \mathscr{C}(\Gamma)\big) = \{\Phi(k', x) \mid k' \in G\} = \mathscr{C}(\Gamma). \tag{19}$$

This proves that the congruent set is perfectly mapped onto itself, satisfying the definition of a Φ-invariant set. □

Lemma 2.3 (Orbit-Fiber Inclusion). *Let $\Gamma = (\mathscr{G}, x, h)$ be a measurement Φ-invariant framework. Then, its associated node-congruent set is always a subset of its node-equivalent set:*

$$\mathscr{C}(\Gamma) \subseteq \mathscr{Q}(\Gamma). \tag{20}$$

Proof. Let $x' = \Phi(g, x) \in \mathscr{C}(\Gamma)$ be an arbitrary configuration in the orbit of x. By the definition of measurement Φ-invariance for the global sensing map h, it follows that $h(x') = h(\Phi(g, x)) = h(x)$. Consequently, $x' \in h^{-1}\big(h(x)\big) = \mathscr{Q}(\Gamma)$, which concludes the proof. □

Definition 2.10 (Φ-Rigidity). Let G be a Lie group acting smoothly on the state space $\overline{\mathscr{D}}$ via the left group action $\Phi : G \times \overline{\mathscr{D}} \to \overline{\mathscr{D}}$, and let $\Gamma = (\mathscr{G}, x, h)$ be a measurement Φ-invariant framework.

The framework Γ is said to be locally rigid with respect to Φ (or simply *locally Φ-rigid*) if there exists an open neighborhood $\mathscr{U}_x \subseteq \overline{\mathscr{D}}$ of x such that:

$$\mathscr{Q}(\Gamma) \cap \mathscr{U}_x = \mathscr{C}(\Gamma) \cap \mathscr{U}_x. \tag{21}$$

If this condition holds for $\mathscr{U}_x = \overline{\mathscr{D}}$, the framework is said to be globally rigid with respect to Φ (or simply *globally Φ-rigid*).

Corollary 2.4 (Simplification of Rigidity Conditions)**.** *Let $\Gamma = (\mathcal{G}, x, h)$ be a measurement Φ-invariant framework. By virtue of the Orbit-Fiber Inclusion Lemma, the rigidity conditions simplify as follows:*

- *Γ is locally Φ-rigid if and only if there exists an open neighborhood $\mathcal{U}_x \subseteq \overline{\mathcal{D}}$ such that:*
$$\mathcal{Q}(\Gamma) \cap \mathcal{U}_x \subseteq \mathcal{C}(\Gamma) \cap \mathcal{U}_x. \tag{22}$$
- *Γ is globally Φ-rigid if and only if:*
$$\mathcal{Q}(\Gamma) \subseteq \mathcal{C}(\Gamma). \tag{23}$$

Proof. By the Orbit-Fiber Inclusion Lemma, the structural inclusion $\mathcal{C}(\Gamma) \subseteq \mathcal{Q}(\Gamma)$ holds over the entire state space $\overline{\mathcal{D}}$. Consequently, for any open neighborhood $\mathcal{U}_x$, the local inclusion $\mathcal{C}(\Gamma) \cap \mathcal{U}_x \subseteq \mathcal{Q}(\Gamma) \cap \mathcal{U}_x$ is also satisfied.

Since the standard definition of Φ-rigidity requires exact set equality between the equivalent set and the congruent set (locally or globally), and one direction of the inclusion is already guaranteed, the equality holds if and only if the reverse inclusion is verified. □

Proposition 2.5. *A globally Φ-rigid framework $\Gamma = (\mathcal{G}, x, h)$ is also locally Φ-rigid.*

Proof. By definition, for a globally Φ-rigid framework, it holds that $\mathcal{Q}(\Gamma) = \mathcal{C}(\Gamma)$. Consequently, the condition for local rigidity, $\mathcal{Q}(\Gamma) \cap \mathcal{U}_x = \mathcal{C}(\Gamma) \cap \mathcal{U}_x$, is trivially satisfied for any open neighborhood $\mathcal{U}_x \subseteq \overline{\mathcal{D}}$ of x. This demonstrates that global rigidity is a sufficient condition for local rigidity. □

Definition 2.11 (Φ-Rigidity of a Φ-invariant Set)**.** Let $S \subseteq \overline{\mathcal{D}}$ be a Φ-invariant subset, meaning that $\Phi(g, S) = S$ for all $g \in G$.

The set S is said to be *locally* (respectively, *globally*) Φ-rigid if every configuration $x' \in S$ induces a framework $\Gamma' = (\mathcal{G}, x', h)$ that is locally (respectively, globally) Φ-rigid.

Corollary 2.6. *A globally Φ-rigid Φ-invariant Set is also locally Φ-rigid.*

Proof. The proof follows trivially from the previous proposition applied to every configuration $x' \in \mathcal{Q}(\Gamma)$. □

Theorem 2.7 (Invariance of Local Φ-Rigidity)**.** *Let G be a Lie group acting smoothly on $\overline{\mathcal{D}}$ via the left action Φ. Let $\Gamma = (\mathcal{G}, x, h)$ be a measurement Φ-invariant framework with global node configuration $x \in \overline{\mathcal{D}}$, and let $\mathcal{C}(\Gamma) \subseteq \overline{\mathcal{D}}$ be its associated node-congruent set.*

The framework Γ is locally Φ-rigid if and only if its associated node-congruent set $\mathscr{C}(\Gamma)$ is locally Φ-rigid.

Proof. ($\Longleftarrow$)

Let $e \in G$ be the identity element of the Lie group. By the fundamental axioms of group actions, applying the identity element to the action map yields the identity map on the state space, i.e., $\Phi(e,\cdot) = \mathrm{id}$. Consequently, the original node configuration x trivially belongs to its own orbit, since $x = \Phi(e,x) \in \mathscr{C}(\Gamma)$.

By hypothesis, the node-congruent set $\mathscr{C}(\Gamma)$ is locally Φ-rigid, which means that every configuration within it induces a locally Φ-rigid framework. Since we established that $x \in \mathscr{C}(\Gamma)$, it follows that the specific framework $\Gamma = (\mathscr{G}, x, h)$ must also be locally Φ-rigid.

($\Longrightarrow$) Suppose Γ is locally Φ-rigid. By the Simplification Corollary derived from the Orbit-Fiber Inclusion Lemma, there exists an open neighborhood $\mathscr{U}_x \subseteq \overline{\mathscr{D}}$ of x such that:

$$\mathscr{Q}(\Gamma) \cap \mathscr{U}_x \subseteq \mathscr{C}(\Gamma) \cap \mathscr{U}_x. \tag{24}$$

Let $x' = \Phi(g,x) \in \mathscr{C}(\Gamma)$ be an arbitrary configuration in the orbit. Since G acts smoothly, the map $\Phi(g,\cdot) : \overline{\mathscr{D}} \to \overline{\mathscr{D}}$ is a diffeomorphism; we can thus define $\mathscr{U}_{x'} := \Phi(g, \mathscr{U}_x)$, which is an open neighborhood containing x'.

Since $\Phi(g,\cdot)$ is a bijection, applying it to both sides preserves the subset inclusion and commutes with set intersections. Using the fact that $\mathscr{Q}(\Gamma)$ is a Φ-invariant set ($\Phi(g, \mathscr{Q}(\Gamma)) = \mathscr{Q}(\Gamma)$) and that $\mathscr{C}(\Gamma)$ is an orbit ($\Phi(g, \mathscr{C}(\Gamma)) = \mathscr{C}(\Gamma)$), we obtain:

$$\Phi\big(g, \mathscr{Q}(\Gamma) \cap \mathscr{U}_x\big) \subseteq \Phi\big(g, \mathscr{C}(\Gamma) \cap \mathscr{U}_x\big) \tag{25}$$

$$\Phi\big(g, \mathscr{Q}(\Gamma)\big) \cap \Phi\big(g, \mathscr{U}_x\big) \subseteq \Phi\big(g, \mathscr{C}(\Gamma)\big) \cap \Phi\big(g, \mathscr{U}_x\big) \tag{26}$$

$$\mathscr{Q}(\Gamma) \cap \mathscr{U}_{x'} \subseteq \mathscr{C}(\Gamma) \cap \mathscr{U}_{x'}. \tag{27}$$

Finally, since $x' \in \mathscr{C}(\Gamma)$, their respective equivalent sets and orbits coincide entirely ($\mathscr{Q}(\Gamma) = \mathscr{Q}(\Gamma')$ and $\mathscr{C}(\Gamma) = \mathscr{C}(\Gamma')$). Substituting these yields:

$$\mathscr{Q}(\Gamma') \cap \mathscr{U}_{x'} \subseteq \mathscr{C}(\Gamma') \cap \mathscr{U}_{x'}. \tag{28}$$

By the Simplification Corollary, this inclusion guarantees that the framework induced by x' is locally Φ-rigid. Given the arbitrariness of x', the entire node-congruent set $\mathscr{C}(\Gamma)$ is locally Φ-rigid. □

Theorem 2.8 (Invariance of Global Φ-Rigidity)**.** *Let G be a Lie group acting smoothly on $\overline{\mathscr{D}}$ via the left action Φ. Let $\Gamma = (\mathscr{G}, x, h)$ be a measurement Φ-invariant framework with global node configuration $x \in \overline{\mathscr{D}}$, and let $\mathscr{C}(\Gamma) \subseteq \overline{\mathscr{D}}$ be its associated node-congruent set.*

The framework Γ is globally Φ-rigid if and only if its associated node-congruent set $\mathscr{C}(\Gamma)$ is globally Φ-rigid.

Proof. ($\Longrightarrow$) Suppose the framework Γ is globally Φ-rigid, which by definition means $\mathcal{Q}(\Gamma) = \mathcal{C}(\Gamma)$. Let x' be any configuration in the orbit $\mathcal{C}(\Gamma)$. Because x' belongs to the orbit of x, it generates the exact same orbit: $\mathcal{C}(\Gamma') = \mathcal{C}(\Gamma)$. Furthermore, since $\mathcal{C}(\Gamma)$ and Γ is globally rigid, x' is also in $\mathcal{Q}(\Gamma)$, meaning it yields the same global measurements as x. Thus, its equivalent set is identical: $\mathcal{Q}(\Gamma') = \mathcal{Q}(\Gamma)$. Substituting these equalities yields $\mathcal{Q}(\Gamma') = \mathcal{C}(\Gamma')$, proving that the induced framework $\Gamma' = (\mathcal{G}, x', h)$ is globally Φ-rigid. Since this holds for every $x' \in \mathcal{C}(\Gamma)$, the entire congruent set is globally Φ-rigid.

($\Longleftarrow$) Let $e \in G$ be the identity element of the Lie group. By the fundamental axioms of group actions, the transformation associated with the identity element is the identity map on the state space, meaning $\Phi_e = \text{id}$. As a direct consequence, the initial configuration x trivially resides within its own orbit, since $x = \Phi(e, x) \in \mathcal{C}(\Gamma)$.

By hypothesis, the node-congruent set $\mathcal{C}(\Gamma)$ is globally Φ-rigid, which implies by definition that every configuration contained within it induces a globally Φ-rigid framework. Since we have established that $x \in \mathcal{C}(\Gamma)$, it follows that the original framework $\Gamma = (\mathcal{G}, x, h)$ must also be globally Φ-rigid. □

Definition 2.12 (Rigid Component of the Node-Equivalent Set)**.** Let $\Gamma = (\mathcal{G}, x, h)$ be a measurement Φ-invariant framework, and let $\mathcal{Q}(\Gamma) \subseteq \overline{\mathcal{D}}$ be its associated node-equivalent set.

If a configuration $x' \in \mathcal{Q}(\Gamma)$ induces a locally Φ-rigid framework $\Gamma' = (\mathcal{G}, x', h)$, then its corresponding Φ-congruent set (orbit) $\mathcal{C}(\Gamma') \subseteq \mathcal{Q}(\Gamma)$ is termed a *rigid component* of the node-equivalent set $\mathcal{Q}(\Gamma)$.

The proposed framework is sufficiently general to seamlessly accommodate any combination of homogeneity and heterogeneity across both agents and measurements. Furthermore, it can effectively handle sensory modalities that utilize the agents' full kinematic state, rely on a specific subset of it, or extend this state by properly integrating additional information.

The formulation presented thus far inherently addresses an *analysis* problem: given a predefined framework, we verify whether it is rigid with respect to a given Lie group action Φ operating on the agents' configuration space.

However, this mathematical foundation naturally paves the way for the inverse problem. Suppose we are given a system of n agents that must be made rigid with respect to a specific group action Φ. The dual challenge lies in systematically designing the graph topology and assigning the appropriate measurement functions to the edges in order to achieve Φ-rigidity for a desired family of smooth ordered frameworks.

This problem will be formalized and addressed in future work.

2.3 UNIFICATION OF CLASSICAL RIGIDITY PARADIGMS WITH Φ-RIGIDITY

To provide a concrete geometric perspective, it is instructive to observe how the proposed Lie group formulation encapsulates and unifies classical rigidity paradigms. The standard frameworks well-known in the literature can be recovered by specifying the appropriate symmetry group G and its corresponding action Φ.

Below, we detail how this applies to Distance, Relative Position, Relative Pose, Body-Fixed Bearing, and Inertial Direction rigidity paradigms.

The Euclidean Groups Framework

- **Distance Rigidity:** In the classical 3-dimensional distance-based framework, agent states are spatial positions $x_i, x_j \in \mathbb{R}^3$. A distance measurement is defined by the Euclidean norm:

  $$y_k = h_k(x_i, x_j) = \|x_i - x_j\| \in \mathbb{R}_{>0}. \tag{29}$$

  We consider a global Euclidean transformation applied to all states using an element $g = (Q, \xi)$ belonging to the Euclidean group $\mathbb{E}(3)$, where $Q \in \mathbb{O}(3)$ represents an orthogonal transformation (encompassing both rotations and reflections) and $\xi \in \mathbb{R}^3$ is a translation vector. For a configuration $x = (x_1, \dots, x_n)$, the global group action is defined component-wise as:

  $$\Phi(g, x_i) = Qx_i + \xi. \tag{30}$$

  Evaluating the measurement map on the transformed states yields:

  $$h_k\big(\Phi(g, x_i), \Phi(g, x_j)\big) = \|(Qx_i + \xi) - (Qx_j + \xi)\| = \|Q(x_i - x_j)\|.$$

  Because orthogonal matrices strictly preserve the Euclidean norm, $\|Q(x_i-x_j)\| = \|x_i-x_j\| = h_k(x_i, x_j)$. This formally demonstrates the well-known result that relative distances are invariant to rigid-body translations, rotations, and reflections, proving that classical distance rigidity is equivalent to Φ-rigidity under $\mathbb{E}(3)$.

  It is worth noting that in practical multi-robot systems, physical reflections are kinematically unrealizable. By removing reflections from $\mathbb{E}(3)$, we obtain the Special Euclidean group $\mathbb{SE}(3)$:

  $$\mathbb{SE}(3) = \big\{(R, \xi) \in \mathbb{E}(3) \mid R \in \mathbb{SO}(3)\big\}. \tag{31}$$

  Since $\mathbb{SE}(3)$ is a proper subgroup ($\mathbb{SE}(3) \subset \mathbb{E}(3)$), we can restrict the group action to $\mathbb{SE}(3)$, defining $\Phi|_{\mathbb{SE}(3)} : \mathbb{SE}(3) \times \mathbb{R}^3 \to \mathbb{R}^3$. The distance measurements are trivially invariant to this restricted action, because a function that is invariant with respect to a group is guaranteed to be invariant under any of its subgroups.

- **Relative Pose Rigidity:** When dealing with agents and measurements that require full 3-dimensional poses, agents are modeled as rigid bodies whose states are represented by homogeneous transformation matrices $X_i, X_j \in \mathbb{SE}(3) \subset \mathbb{R}^{4\times4}$, explicitly defined as:

$$X_i = \begin{bmatrix} R_i & t_i \\ {}_{1\times3} & 1 \end{bmatrix} \tag{32}$$

where $R_i \in \mathbb{SO}(3)$ is a rotation matrix and $t_i \in \mathbb{R}^3$ is the translation vector.

The relative pose of agent j as measured by agent i is given by:

$$y_k = h_k(X_i, X_j) = X_i^{-1} X_j \tag{33}$$

which intrinsically maps the global pose of agent j into the local body frame of agent i.

The natural symmetry group associated with global rigid-body transformations is $\mathbb{SE}(3) \subset \mathbb{R}^{4\times4}$, acting via left multiplication. For a transformation $S \in \mathbb{SE}(3)$, the global action on the configuration vector $X = (X_1, \dots, X_n)$ is defined as:

$$\Phi(S, X) = (SX_1, \dots, SX_n). \tag{34}$$

Applying this transformation to the relative pose measurement yields:

$$\begin{aligned} h_k\big(\Phi(S, X_i), \Phi(S, X_j)\big) &= (SX_i)^{-1}(SX_j) \\ &= X_i^{-1} S^{-1} S X_j \\ &= X_i^{-1} X_j = y_k. \end{aligned}$$

Thus, relative pose measurements are intrinsically Φ-invariant under the left action of $\mathbb{SE}(3)$.

- **Relative Position Rigidity:** In scenarios where sensors measure only the 3-dimensional relative positions (displacements) between agents rather than full 6-DOF poses, the agent states still naturally reside in $X_i, X_j \in \mathbb{SE}(3) \subset \mathbb{R}^{4\times4}$ (since agents are physical bodies with orientations), but the measurement space is reduced to $\mathbb{R}^3$.

The relative position of agent j as measured by agent i, expressed in the local body frame of agent i, is explicitly defined as:

$$y_k = h_k(X_i, X_j) = R_i^T (t_j - t_i) \in \mathbb{R}^3. \tag{35}$$

Geometrically, this takes the global displacement vector $(t_j - t_i)$ and projects it into the local coordinate system of agent i via the inverse rotation R_i^T.

Algebraically, this measurement corresponds exactly to the translational block (the upper-right 3×1 subvector) of the relative pose matrix $X_i^{-1} X_j$, as shown by block matrix multiplication:

$$X_i^{-1} X_j = \begin{bmatrix} R_i^T & -R_i^T t_i \\ \mathbf{0}_{1\times3} & 1 \end{bmatrix} \begin{bmatrix} R_j & t_j \\ \mathbf{0}_{1\times3} & 1 \end{bmatrix} = \begin{bmatrix} R_i^T R_j & \mathbf{R_i^T(t_j - t_i)} \\ \mathbf{0}_{1\times3} & 1 \end{bmatrix}.$$

As established in the relative pose case, the complete transformation matrix is strictly Φ-invariant under the left action of any global transformation $S \in \mathbb{SE}(3)$:

$$(SX_i)^{-1}(SX_j) = X_i^{-1}S^{-1}SX_j = X_i^{-1}X_j.$$

Because the entire 4×4 matrix remains completely unchanged under the group action, every individual sub-block within it is necessarily invariant as well. Consequently, the local relative position measurement $y_k = R_i^T(t_j - t_i)$ inherently shares the exact same strict Φ-invariance under $\mathbb{SE}(3)$.

The Similarity Groups Framework

To model bearing and direction measurements, we must extend our transformation families to include scale. We define the **Similarity Group** $\mathbb{S}(3)$, consisting of elements $S = (Q, \xi, \rho)$, where $Q \in \mathbb{O}(3)$, $\xi \in \mathbb{R}^3$, and $\rho \in \mathbb{R}_{>0}$ is a positive scaling factor.

The action of the Special Similarity group $S = (Q, \xi, \rho) \in \mathbb{SS}(3)$ on an individual agent's pose $X_i = (R_i, t_i) \in \mathbb{SE}(3)$ is defined as:

$$\tilde{\Phi}(S, X_i) = \big(QR_i,\ \rho(Qt_i + \xi)\big). \tag{36}$$

For a full network configuration of poses $X = (X_1, \dots, X_n) \in \mathbb{SE}(3)^n$, this action extends globally by applying the transformation component-wise:

$$\tilde{\Phi}(S, X) = \big(\tilde{\Phi}(S, X_1), \dots, \tilde{\Phi}(S, X_n)\big). \tag{37}$$

From this general group, we derive two crucial subgroups:

- **Special Similarity Group** $\mathbb{SS}(3)$: The subgroup obtained by restricting $Q \in \mathbb{SO}(3)$ (pure rotations, no reflections). Because $\mathbb{SS}(3)$ preserves the $\det(Q) = 1$ property, it is the appropriate symmetry group to act on rigid-body poses.
- **Scaled Translations** $\mathbb{ST}(3)$: A subgroup of $\mathbb{SS}(3)$ where $Q = I_3$ (no rotation, only scaling and translation).

For these subgroups, the group action on an individual agent's state $X_i = (R_i, t_i) \in \mathbb{SE}(3)$ is defined locally as:

$$\tilde{\Phi}(S, X_i) = \big(QR_i,\ \rho(Qt_i + \xi)\big). \tag{38}$$

For a full network configuration of poses $X = (X_1, \dots, X_n) \in \mathbb{SE}(3)^n$, this action extends globally by applying the transformation component-wise:

$$\tilde{\Phi}(S, X) = \big(\tilde{\Phi}(S, X_1), \dots, \tilde{\Phi}(S, X_n)\big). \tag{39}$$

Note that the broader similarity group $\mathbb{S}(3)$ cannot act on $\mathbb{SE}(3)$ in this manner, as physical reflections would mathematically map rotation matrices out of $\mathbb{SO}(3)$.

The corresponding rigidity paradigms are:

- **Body-Fixed Bearing Rigidity:** Consider two oriented agents $X_i, X_j \in \mathbb{SE}(3)$. The body-fixed-frame bearing from agent i to agent j is the direction of t_j observed from t_i, strictly expressed in the local body-fixed orientation R_i:

$$y_k = h_k(X_i, X_j) = R_i^T \frac{t_j - t_i}{\|t_j - t_i\|} \in \mathbb{S}^2. \tag{40}$$

(Note: This measurement is ill-defined if $t_i = t_j$, necessitating the removal of collision configurations to ensure smoothness).

To demonstrate the invariance of this measurement, we evaluate the measurement map under the global action of the Special Similarity group $S = (Q, \xi, \rho) \in \mathbb{SS}(3)$, utilizing the previously defined action $\tilde{\Phi}$:

$$h_k\big(\tilde{\Phi}(S, X_i), \tilde{\Phi}(S, X_j)\big) = (QR_i)^T \frac{\rho(Qt_j + \xi) - \rho(Qt_i + \xi)}{\|\rho(Qt_j + \xi) - \rho(Qt_i + \xi)\|}.$$

By factoring out the scaling factor ρ and the orthogonal matrix Q:

$$= R_i^T Q^T \frac{\rho Q(t_j - t_i)}{\rho\|Q(t_j - t_i)\|}.$$

Since $\rho > 0$ cancels out, and orthogonal matrices preserve norms ($\|Qv\| = \|v\|$), the expression simplifies to:

$$= R_i^T Q^T Q \frac{t_j - t_i}{\|t_j - t_i\|} = R_i^T \frac{t_j - t_i}{\|t_j - t_i\|} = h_k(X_i, X_j).$$

This proves that body-fixed bearings are $\tilde{\Phi}$-invariant under $\mathbb{SS}(3)$, meaning they are unaffected by global translations, rotations, and uniform scaling.

- **Inertial Direction Rigidity:** When an agent's orientation is known or unnecessary, the bearing can be expressed directly in the global inertial reference frame. For agents with positions $x_i, x_j \in \mathbb{R}^3$, an inertial direction measurement is described by:

$$y_k = h_k(x_i, x_j) = \frac{x_j - x_i}{\|x_j - x_i\|} \in \mathbb{S}^2. \tag{41}$$

If we attempt to act on this measurement with the full Similarity group $\mathbb{S}(3)$, we obtain:

$$\begin{aligned} h_k\big(\Phi(S, x_i), \Phi(S, x_j)\big) &= \frac{\rho(Qx_j + \xi) - \rho(Qx_i + \xi)}{\|\rho(Qx_j + \xi) - \rho(Qx_i + \xi)\|} \\ &= \frac{Q(x_j - x_i)}{\|x_j - x_i\|} = Qh_k(x_i, x_j). \end{aligned}$$

Because the result is Qy_k rather than y_k, the measurement is **equivariant** (rather than invariant) with respect to global rotations. In rigidity theory, this implies that a global rotation or reflection directly alters the observed inertial direction, meaning the framework cannot treat arbitrary rotations as valid rigid symmetries.

However, by restricting the symmetry group to the Scaled Translations subgroup $\mathbb{ST}(3)$ where $Q = I_3$, the rotation matrix evaluates to the identity, yielding:

$$I_3 h_k(x_i, x_j) = h_k(x_i, x_j).$$

Consequently, inertial direction frameworks are Φ-invariant exclusively under $\mathbb{ST}(3)$, relying solely on the invariance to translation and global scaling.

By abstracting these spatial symmetries into a general Lie group action Φ, our formulation is no longer restricted to a single, homogeneous measurement type; instead, it provides a mathematical foundation for the structural analysis of heterogeneous (*mixed-signal*) multi-agent networks, where the overall system invariance emerges from the intersection of different transformation subgroups.

2.4 INFINITESIMAL RIGIDITY PROPERTIES OF ORDERED SMOOTH FRAMEWORKS

2.4.1 Coordinate-Free

Definition 2.13 (Φ-Rigidity Differential)**.** Let $\Gamma = (\mathcal{G}, x, h)$ be a smooth framework, where $h : \overline{\mathcal{D}} \to \overline{\mathcal{M}}$ is the measurement map. The rigidity differential of Γ at the configuration x is defined as the exact pushforward:

$$dh|_x : T_x\overline{\mathcal{D}} \to T_{h(x)}\overline{\mathcal{M}} \tag{42}$$

This linear map completely governs the first-order kinematics of the framework, translating abstract infinitesimal variations of the node configuration $\delta x \in T_x\overline{\mathcal{D}}$ into their corresponding infinitesimal measurement changes in $T_{h(x)}\overline{\mathcal{M}}$.

Definition 2.14 (Infinitesimal Motion)**.** Let $\Gamma = (\mathcal{G}, x, h)$ be a smooth framework, where the measurement map $h : \overline{\mathcal{D}} \to \overline{\mathcal{M}}$ is a smooth map between smooth manifolds. A first-order infinitesimal variation of the framework at x is defined as a tangent vector $\delta x \in T_x\overline{\mathcal{D}}$.

An infinitesimal variation δx is called a *measurement-preserving infinitesimal motion* (or simply *infinitesimal motion*) if it induces zero first-order variation in the sensory output. Formally, this occurs when:

$$dh|_x(\delta x) = 0 \tag{43}$$

where 0 denotes the zero vector in $T_{h(x)}\overline{\mathscr{M}}$, and $dh|_x : T_x\overline{\mathscr{D}} \to T_{h(x)}\overline{\mathscr{M}}$ is the differential (or pushforward map) of h evaluated at x. Consequently, the vector space of all infinitesimal motions coincides with the kernel of the differential, explicitly defined as:

$$\ker(dh|_x) = \{\delta x \in T_x\overline{\mathscr{D}} \mid dh|_x(\delta x) = 0\}. \tag{44}$$

Geometrically, an infinitesimal motion of the configuration x represents a first-order displacement that instantaneously preserves the sensory measurements $y = h(x)$. Given a smooth curve of configurations $x(t)$ such that $x(0) = x$ and its initial velocity is an infinitesimal motion $\dot{x}(0) = \delta x \in \ker(dh|_x)$, the rate of change of the sensory output is strictly zero at the first order:

$$\frac{d}{dt}y(t)\bigg|_{t=0} = \frac{d}{dt}h(x(t))\bigg|_{t=0} = dh|_x(\dot{x}(0)) = dh|_x(\delta x) = 0. \tag{45}$$

Physically, the vectors spanning $\ker(dh|_x)$ can be interpreted as allowable infinitesimal maneuvers of the framework. They define the exact geometric directions in which the node configuration can be actively steered while preserving the constraints imposed by the measurement map. Consequently, this space of infinitesimal motions lays the theoretical foundation for constraint-preserving formation control, allowing a MAS to maneuver collectively. However, the explicit design of such dynamic control laws remains beyond the scope of this work.

Definition 2.15 (Trivial Infinitesimal Motion). Let $\Gamma = (\mathscr{G}, x, h)$ be a Φ-invariant smooth framework under the action of a Lie group G. An infinitesimal variation $\delta x \in T_x\overline{\mathscr{D}}$ is called a *trivial infinitesimal motion* if it is induced purely by the smooth action of G on the global state space $\overline{\mathscr{D}}$.

Let $\mathfrak{g}$ be the Lie algebra associated with G, and let $\Phi_x : G \to \overline{\mathscr{D}}$ be the orbit map defined by $\Phi_x(g) = \Phi(g, x)$. A motion δx is trivial if there exists an element $\xi \in \mathfrak{g}$ such that:

$$\delta x = d\Phi_x|_e(\xi) = \frac{d}{dt}\bigg|_{t=0} \Phi\big(\exp(t\xi), x\big) \tag{46}$$

where e is the identity element of G, exp is the Lie group exponential map, and $d\Phi_x|_e : \mathfrak{g} \to T_x\overline{\mathscr{D}}$ is the differential of the orbit map evaluated at the identity.

Formally, the vector space of all trivial infinitesimal motions corresponds strictly to the image of the differential of the orbit map evaluated at the identity element $e \in G$. We denote this subspace as $\mathscr{T}(x)$, which inherently satisfies:

$$\mathscr{T}(x) = \mathrm{Im}\big(d\Phi_x|_e\big) \tag{47}$$

Lemma 2.9 (Infinitesimal Orbit-Kernel Inclusion). *Let $\Gamma = (\mathscr{G}, x, h)$ be a measurement Φ-invariant framework where the sensing map $h : \overline{\mathscr{D}} \to \overline{\mathscr{M}}$ is a smooth map between smooth manifolds.*

Let $dh|_x : T_x\overline{\mathscr{D}} \to T_{h(x)}\overline{\mathscr{M}}$ be the differential of the measurement map evaluated at x, and let $d\Phi_x|_e : \mathfrak{g} \to T_x\overline{\mathscr{D}}$ be the differential of the orbit map at the identity.

The measurement Φ-invariance globally implies that every trivial infinitesimal motion preserves the sensory output. Consequently, the space of trivial motions is a subspace of the kernel of the measurement map's differential:

$$\mathrm{Im}\big(d\Phi_x|_e\big) \subseteq \ker(dh|_x). \tag{48}$$

Proof. By the definition of measurement Φ-invariance, the sensory output is identical for any configuration along the orbit. Formally, we can express this using the orbit map Φ_x as a composition:

$$h(\Phi_x(g)) = h(x) \quad \text{for all } g \in G.$$

This implies that the composed map $h \circ \Phi_x : G \to \overline{\mathscr{M}}$ is strictly constant.

Taking the differential of this composition at the identity element $e \in G$, and applying the chain rule, we obtain:

$$d(h \circ \Phi_x)|_e = dh|_{\Phi_x(e)} \circ d\Phi_x|_e = dh|_x \circ d\Phi_x|_e.$$

Because the differential of a constant map is universally the zero operator, it follows that: $dh|_x \circ d\Phi_x|_e = 0$.

This operator identity directly implies that the entire image of the orbit map's differential is mapped to the zero vector by $dh|_x$, yielding the structural inclusion:

$$\mathrm{Im}\big(d\Phi_x|_e\big) \subseteq \ker(dh|_x).$$

□

Definition 2.16 (Infinitesimal Φ-Rigidity)**.** Let $\Gamma = (\mathscr{G}, x, h)$ be a measurement Φ-invariant framework, where G is a Lie group with Lie algebra $\mathfrak{g}$ acting smoothly on the state space $\overline{\mathscr{D}}$.

The framework is said to be infinitesimally rigid with respect to Φ (or simply *infinitesimally Φ-rigid*) if every infinitesimal motion is identically a trivial infinitesimal motion.

Formally, for every vector $\delta x \in \ker(dh|_x)$, there must exist an element $u \in \mathfrak{g}$ such that:

$$\delta x = d\Phi_x|_e(u) \tag{49}$$

where $d\Phi_x|_e : \mathfrak{g} \to T_x\overline{\mathscr{D}}$ is the differential of the orbit map $\Phi_x(g) = \Phi(g, x)$ evaluated at the identity element $e \in G$.

This means that the space of infinitesimal motions perfectly coincides with the space of trivial motions:

$$\ker(dh|_x) = \mathrm{Im}\big(d\Phi_x|_e\big). \tag{50}$$

Corollary 2.10 (Dimensional Condition for Infinitesimal Φ-Rigidity). *Let $\Gamma = (\mathscr{G}, x, h)$ be a measurement Φ-invariant framework. The framework is infinitesimally Φ-rigid at x if and only if the dimension of the differential's kernel equals the dimension of the space of trivial motions:*

$$\dim\big(\ker(dh|_x)\big) = \dim\Big(\mathrm{Im}\big(d\Phi_x|_e\big)\Big). \tag{51}$$

Proof. By definition, infinitesimal Φ-rigidity holds if and only if $\ker(dh|_x) = \mathrm{Im}\big(d\Phi_x|_e\big)$.

The necessary condition ($\Longrightarrow$) is trivial: if the two vector spaces are identical, their dimensions must be equal.

For the sufficient condition ($\Longleftarrow$), we exploit the Φ-invariance of the measurement function h. By the Infinitesimal Orbit-Kernel Inclusion Lemma, we have the guaranteed subspace inclusion:

$$\mathrm{Im}\big(d\Phi_x|_e\big) \subseteq \ker(dh|_x).$$

From fundamental linear algebra, if a finite-dimensional subspace is contained within another and they share the exact same dimension, the two spaces must coincide entirely. Therefore, the assumption $\dim(\ker(dh|_x)) = \dim(\mathrm{Im}(d\Phi_x|_e))$ directly forces the exact set equality $\ker(dh|_x) = \mathrm{Im}\big(d\Phi_x|_e\big)$, satisfying the definition of infinitesimal rigidity. $\square$

Definition 2.17 (Ordered Smooth Framework Family over A). Consider a subset A of the agent space manifold $\bar{\mathscr{D}}$. We define the ordered smooth A-framework as:

$$(\mathscr{G}, A, h) = \{(\mathscr{G}, x, h) \mid x \in A\} \tag{52}$$

Definition 2.18 (Infinitesimal Φ-rigidity of Ordered Smooth Framework Family over A). Let $(\mathscr{G}, A, h)$ be a smooth framework family over a subset $A \subseteq \bar{\mathscr{D}}$. We say that the family is **infinitesimally Φ-rigid** if, for every configuration $x \in A$, the individual framework $(\mathscr{G}, x, h)$ is infinitesimally Φ-rigid.

2.4.2 Local Coordinate

To translate the infinitesimal properties of the measurement map $h : \overline{\mathscr{D}} \to \overline{\mathscr{M}}$ into a computable algebraic framework, we transition from coordinate-free geometry to local representations.

Given a configuration $x \in \overline{\mathscr{D}}$, let $\mathscr{U}_x \subset \overline{\mathscr{D}}$ be an open neighborhood containing x. We introduce a smooth local coordinate chart $\phi : \mathscr{U}_x \to \mathbb{R}^{n_d}$, where $n_d = \dim(\overline{\mathscr{D}})$. This chart provides the local state coordinates $q = \phi(x)$.

Similarly, for the corresponding sensory output $y = h(x) \in \overline{\mathscr{M}}$, we consider an open neighborhood $\mathscr{V}_y \subset \overline{\mathscr{M}}$ containing y and introduce a smooth coordinate chart $\psi : \mathscr{V}_y \to \mathbb{R}^m$, where $m = \dim(\overline{\mathscr{M}})$. This yields the local output coordinates $p = \psi(y)$.

By employing these local maps, the abstract measurement map h can be expressed in local coordinates as a function $\hat{h} : \mathbb{R}^{n_d} \to \mathbb{R}^m$, defined by the composition:

$$p = \hat{h}(q) = \left(\psi \circ h \circ \phi^{-1}\right)(q). \tag{53}$$

Unlike the original map h acting between smooth manifolds, its local representation $\hat{h}$ operates entirely within Euclidean spaces. This allows us to compute its local Jacobian matrix, leading to the computational local counterpart of the rigidity differential.

Definition 2.19 (Φ-Rigidity Matrix)**.** Let $\Gamma = (\mathcal{G}, x, h)$ be a smooth framework defined on an n_d-dimensional state manifold $\overline{\mathcal{D}}$ and an m-dimensional measurement manifold $\overline{\mathcal{M}}$.

Let $\phi : \mathcal{U} \to \tilde{\mathcal{U}} \subseteq \mathbb{R}^{n_d}$ be a local coordinate chart defined on an open neighborhood $\mathcal{U} \subseteq \overline{\mathcal{D}}$ containing x, and let $\psi : \mathcal{V} \to \tilde{\mathcal{V}} \subseteq \mathbb{R}^m$ be a local coordinate chart defined on an open neighborhood $\mathcal{V} \subseteq \overline{\mathcal{M}}$ containing $h(x)$.

Given the local coordinate representation of the measurement map $\hat{h} = \psi \circ h \circ \phi^{-1} : \tilde{\mathcal{U}} \to \tilde{\mathcal{V}}$, the *rigidity matrix* of the framework at the configuration x, denoted by $R(x) \in \mathbb{R}^{m \times n_d}$, is defined as the differential of $\hat{h}$ evaluated at the numerical coordinate state $q = \phi(x)$:

$$R(x) := d\hat{h}|_{\phi(x)} = \left.\frac{\partial \hat{h}(q)}{\partial q}\right|_{q=\phi(x)}. \tag{54}$$

Algebraically, the rigidity matrix $R(x)$ is the unique matrix representation of the coordinate-free rigidity differential $dh|_x : T_x\overline{\mathcal{D}} \to T_{h(x)}\overline{\mathcal{M}}$, constructed with respect to the chosen bases of the local Euclidean spaces.

Because the local coordinate charts ϕ and ψ are smooth diffeomorphisms, their respective differentials $d\phi|_x$ and $d\psi|_{h(x)}$ act as linear isomorphisms. From a purely differential geometry perspective, these isomorphisms inherently preserve all algebraic properties of the abstract differential $dh|_x$, such as subspace inclusions and kernel dimensions. Consequently, the infinitesimal properties derived in the coordinate-free framework map directly to the rigidity matrix $R(x)$.

Nevertheless, although mathematically redundant, the explicit algebraic translation of these conditions is deliberately reported in this section. This is done for the sake of clarity and completeness, as the entirety of the computational framework relies strictly on these local matrix representations.

Proposition 2.11 (Local Coordinate Set Condition for Infinitesimal Φ-Rigidity)**.** *Let $\Gamma = (\mathcal{G}, x, h)$ be a measurement Φ-invariant framework defined on a state manifold $\overline{\mathcal{D}}$.*

Let $\phi : \mathcal{U} \to \tilde{\mathcal{U}} \subseteq \mathbb{R}^{n_d}$ be a local coordinate chart defined on an open neighborhood $\mathcal{U} \subseteq \overline{\mathcal{D}}$ containing x, and let $\psi : \mathcal{V} \to \tilde{\mathcal{V}} \subseteq \mathbb{R}^m$ be a local coordinate chart defined on an open neighborhood $\mathcal{V} \subseteq \overline{\mathcal{M}}$ containing $h(x)$.

The framework Γ is infinitesimally Φ-rigid at x if and only if the numerical null space $\ker(R(x))$ *and the abstract space of trivial motions* $\mathrm{Im}(d\Phi_x|_e)$ *are strictly equal via the chart differential* $d\phi|_x$*:*

$$\ker(R(x)) = d\phi|_x\Big(\mathrm{Im}\big(d\Phi_x|_e\big)\Big). \tag{55}$$

Proof. From the chain rule applied to the local representation $\hat{h} = \psi \circ h \circ \phi^{-1}$, the rigidity matrix represents the composed differential:

$$R(x) = d\psi|_{h(x)} \circ dh|_x \circ (d\phi|_x)^{-1}.$$

The differentials of the local charts, $d\phi|_x : T_x\overline{\mathscr{D}} \to \mathbb{R}^{n_d}$ and $d\psi|_{h(x)} : T_{h(x)}\overline{\mathscr{M}} \to \mathbb{R}^m$, are linear isomorphisms by the definition of a smooth chart. Since $d\phi|_x$ and $d\psi|_{h(x)}$ are isomorphisms, they are invertible and their kernels are trivial.

We can explicitly derive the relationship between the null space of the rigidity matrix and the kernel of the abstract differential. Let $v \in \mathbb{R}^{n_d}$ be a coordinate vector. By definition, $v \in \ker(R(x))$ if and only if $R(x)v = 0$. Expanding the matrix yields:

$$d\psi|_{h(x)}\Big(dh|_x\big((d\phi|_x)^{-1}(v)\big)\Big) = 0.$$

Because $d\psi|_{h(x)}$ has a trivial kernel, the inner term must be strictly zero:

$$dh|_x\big((d\phi|_x)^{-1}(v)\big) = 0 \quad \iff \quad (d\phi|_x)^{-1}(v) \in \ker(dh|_x).$$

Applying the isomorphism $d\phi|_x$ to both sides yields the strict equality of the mapped spaces:

$$\ker(R(x)) = d\phi|_x\big(\ker(dh|_x)\big). \tag{56}$$

To evaluate infinitesimal rigidity, we must mathematically compare this local space $\ker(R(x))$ of infinitesimal motions with the space of trivial motions generated by the group action, i.e., $\mathrm{Im}\big(d\Phi_x|_e\big)$. However, a structural discrepancy arises: the trivial motions reside in the tangent space $\mathrm{Im}\big(d\Phi_x|_e\big) \subseteq T_x\overline{\mathscr{D}}$, whereas the null space of the rigidity matrix resides in the coordinate space $\ker(R(x)) \subseteq \mathbb{R}^{n_d}$.

Since ϕ is a smooth local diffeomorphism, $d\phi|_x$ represents the unique linear isomorphism that maps every abstract velocity vector directly to its corresponding numerical coordinate vector in $\mathbb{R}^{n_d}$. To resolve the discrepancy, we use this isomorphism to translate the abstract space of trivial motions into the numerical coordinate space, defining the mapped set $d\phi|_x\big(\mathrm{Im}(d\Phi_x|_e)\big)$.

By definition, the abstract condition for infinitesimal Φ-rigidity requires $\ker(dh|_x) = \mathrm{Im}\big(d\Phi_x|_e\big)$. Applying the linear isomorphism $d\phi|_x$ to both sides of this abstract equality directly yields the local coordinate condition $\ker(R(x)) = d\phi|_x\big(\mathrm{Im}(d\Phi_x|_e)\big)$, completing the proof. □

Lemma 2.12 (Local Infinitesimal Orbit-Kernel Inclusion). *Let $\Gamma = (\mathscr{G}, x, h)$ be a measurement Φ-invariant framework, and let $R(x)$ be its associated rigidity matrix* *evaluated in a local coordinate chart ϕ. The space of abstract trivial motions, when mapped into the local coordinate space via the chart differential, is always a subspace of the numerical null space of the rigidity matrix:*

$$d\phi|_x\Big(\mathrm{Im}\big(d\Phi_x|_e\big)\Big) \subseteq \ker(R(x)). \tag{57}$$

Proof. By the abstract Infinitesimal Orbit-Kernel Inclusion Lemma, the physical Φ-invariance of the measurement function guarantees the strict subspace inclusion $\mathrm{Im}\big(d\Phi_x|_e\big) \subseteq \ker(dh|_x)$. Applying the linear isomorphism $d\phi|_x$ to both sides of this inclusion translates the relationship into the Euclidean coordinate space:

$$d\phi|_x\Big(\mathrm{Im}\big(d\Phi_x|_e\big)\Big) \subseteq d\phi|_x\big(\ker(dh|_x)\big).$$

From Equation (56) in Proposition 2.11, we established that $d\phi|_x\big(\ker(dh|_x)\big) = \ker(R(x))$. Substituting this exact set equality into the right-hand side directly yields the localized inclusion (57), completing the proof. □

Proposition 2.13 (Dimensional Condition for Local Coordinate Φ-Infinitesimal Rigidity). *Let $\Gamma = (\mathcal{G}, x, h)$ be a measurement Φ-invariant framework. The framework is infinitesimally Φ-rigid at x if and only if the numerical null space of the rigidity matrix and the abstract space of trivial motions share the exact same dimension:*

$$\dim\big(\ker(R(x))\big) = \dim\Big(\mathrm{Im}\big(d\Phi_x|_e\big)\Big). \tag{58}$$

Proof. The necessary condition ($\Longrightarrow$) follows directly from Proposition 2.11. If the framework is infinitesimally rigid, the mapped trivial motions and the numerical null space are strictly identical sets in $\mathbb{R}^{n_d}$, implying their dimensions must be equal.

To prove the sufficient condition ($\Longleftarrow$), we rely on the Local Infinitesimal Orbit-Kernel Inclusion Lemma (Lemma 2.12), which guarantees the structural inclusion:

$$d\phi|_x\Big(\mathrm{Im}\big(d\Phi_x|_e\big)\Big) \subseteq \ker(R(x)).$$

From fundamental linear algebra, if a finite-dimensional subspace is contained within another and they share the exact same dimension, the two spaces must coincide entirely. Therefore, assuming the dimensional equality (58) directly forces the exact set equality:

$$\ker(R(x)) = d\phi|_x\Big(\mathrm{Im}\big(d\Phi_x|_e\big)\Big).$$

By Proposition 2.11, this strict set equality constitutes the necessary and sufficient condition for infinitesimal Φ-rigidity, thereby completing the proof. □

Other results can be found in the literature, and their translation into this new generalized framework will be addressed in future work.

3 CHARACTERIZATION OF THE MEASUREMENT MAP

Every notion developed in the previous chapter is stated purely in terms of the global measurement map h and its differential $dh|_x$. The measurement function is thus the central mathematical object of the entire theory.

So far, h has been treated as an unstructured smooth map between two smooth manifolds. This abstraction is precisely what allowed the preceding analysis to remain agnostic to specific agent kinematics and sensing modalities, enabling it to handle any combination of heterogeneity and homogeneity for both agents and measurements. While treating h as a generic map is sufficient for the theoretical results established, providing it with an explicit internal structure enables the examination of properties stemming directly from how a measurement is physically constructed.

3.1 MEASUREMENT MAP AS A COMPOSITION OF MAPPINGS

The measurement map h models the sensing network, linking global node configurations to global edge configurations. The measurements considered in the rigidity framework are inter-agent measurements across the network. By analyzing how this process works, we can distinguish several independent operations.

Specifically, we characterize the measurement map h by decomposing it into an ordered composition of intermediate mappings, each fulfilling a specific role within the measurement process. This modular approach makes it possible to isolate, analyze, and subsequently modify each stage independently, with the overall system properties emerging from their composition. Furthermore, this decomposition provides deeper insights into the mathematical characterization of each stage, which is especially critical when dealing with heterogeneous agents and mixed-measurement topologies.

In general, the choice of these composition stages, along with their associated spaces and mappings, introduces valuable design degrees of freedom in modeling the measurement function, allowing the framework to be tailored to specific application requirements.

3.2 EMBEDDING PROCESS

The framework built up to this point is, by design, general enough to accommodate node- and edge-heterogeneous formations. Yet, nothing in it explicitly dictates *how* such heterogeneity is actually handled: the mathematical machinery developed so far leaves this complexity implicitly buried inside the abstract function h.

This abstraction conceals a genuine analytical obstruction. The rigidity relies on a single Lie group acting on the whole configuration space $\overline{\mathscr{D}}$; however, there is generally no canonical group acting jointly on the product space $\prod_i \mathscr{D}_i$ when the agent manifolds $\mathscr{D}_i$ are not all identical. Working with heterogeneous agents poses significant algebraic and geometric challenges, visible even in the simplest geometric operations. For instance, computing a relative position via the algebraic difference between the states of two agents living in Euclidean spaces of different dimensions is undefined. Therefore, the measurement function must implicitly resolve this discrepancy before any relative quantity can be evaluated.

One effective method to resolve this complexity consists of embedding all heterogeneous quantities into a unified abstract space. This is precisely the approach taken by Michieletto et al. [23] for heterogeneous bearing rigidity. In their framework, every agent is lifted into a common ambient manifold (specifically, the Special Euclidean group $SE(3)$) through a padding process.

However, this uniformity comes at a cost. By embedding agents with fewer controllable degrees of freedom into a higher-dimensional space, they acquire abstract ”virtual” degrees of freedom that are not kinematically feasible. To account for these virtual motions, Michieletto et al. [23] construct the rigidity matrix in the common $6n$-dimensional tangent space and insert two selection matrices, $\mathbf{U}$ and $\mathbf{V}$, into its translational and rotational blocks, respectively, to zero out exactly the directions a restricted agent cannot actuate. Both matrices are tailored to each agent’s domain on a case-by-case basis.

The construction pursued in this work can be interpreted as a rigorous generalization of this mechanism. Rather than inserting selection matrices directly into the differential of the measurement function and verifying them case by case, we make the correspondence between an agent’s actual physical state and its common-space representation explicitly structural. We achieve this through a formal geometric embedding, paired with its left-inverse retraction. In this formulation, the selection matrices $\mathbf{U}$ and $\mathbf{V}$ coincide exactly with the Jacobian of the embedding, restricted respectively to the translational and rotational components.

To adapt this concept to general hybrid networks, where both agent states and measurements can be heterogeneous, we introduce tailored embedding-retraction pairs for the respective agent and measurement spaces.

Definition 3.1 (Smooth Embedding). Let $\mathscr{M}$ and $\mathscr{N}$ be smooth manifolds, with $\dim(\mathscr{M}) \leq \dim(\mathscr{N})$. A smooth map $\iota : \mathscr{M} \to \mathscr{N}$ is called a *smooth embedding* if it satisfies the following two properties:

1. It is an immersion, meaning that its differential $d\iota|_x : T_x\mathscr{M} \to T_{\iota(x)}\mathscr{N}$ is injective for all $x \in \mathscr{M}$.
2. It is a topological embedding, meaning it is a homeomorphism between $\mathscr{M}$ and its image $\iota(\mathscr{M}) \subseteq \mathscr{N}$, where $\iota(\mathscr{M})$ is equipped with the subspace topology induced from $\mathscr{N}$.

Definition 3.2 (Right Inverse). Let X and Y be sets, and let $f : X \to Y$ be a map. A map $h : Y \to X$ is called a *right inverse* of f if their composition satisfies:

$$f(h(y)) = y, \quad \forall y \in Y. \tag{1}$$

Equivalently, this can be denoted as $f \circ h = \mathrm{Id}_Y$, where Id_Y is the identity map on the set Y.

The existence of a right inverse guarantees that the original map f is surjective.

Definition 3.3 (Left Inverse). Let X and Y be sets, and let $f : X \to Y$ be a map. A map $g : Y \to X$ is called a *left inverse* of f if their composition satisfies:

$$g(f(x)) = x, \quad \forall x \in X. \tag{2}$$

Equivalently, this can be denoted as $g \circ f = \mathrm{Id}_X$, where Id_X is the identity map on the set X.

The existence of a left inverse guarantees that the original map f is injective.

In the context of category theory and abstract algebra, a right inverse of a morphism is formally called a *section*, and a left inverse of a morphism is called a *retraction*.

Remark 3.1. It is worth noting a terminological distinction regarding the word *retraction*. In topology, however, a retraction has a strictly different meaning: it denotes a continuous map from a space onto a subspace that leaves all points of the subspace fixed.

In the following, to align with the algebraic structures, mappings, and commutative diagrams employed in this framework, we adopt the categorical nomenclature. We use the term **retraction** to indicate a smooth left inverse, and more specifically, the smooth left inverse of a given embedding.

Consequently, by an **embedding-retraction pair** (ι, ρ), we strictly denote a tuple consisting of a smooth embedding $\iota : \mathscr{M} \to \mathscr{N}$ and its corresponding smooth left-inverse $\rho : \mathscr{N} \to \mathscr{M}$. These mappings are structurally coupled by the relation:

$$\rho \circ \iota = \mathrm{Id}_{\mathscr{M}}. \tag{3}$$

This algebraic coupling explicitly highlights a fundamental symmetry: just as ρ acts as the left-inverse of ι (making it the categorical *retraction*), ι simultaneously acts as the right-inverse of ρ (serving as its corresponding *section*).

Geometrically, this dual perspective is extremely powerful: while the left-inverse property guarantees that ι is injective (ensuring no kinematic information is lost during the embedding), the right-inverse property guarantees that the retraction ρ is surjective onto $\mathscr{M}$. This ensures that every valid physical state of the agent can be perfectly recovered when projecting back from the abstract ambient space.

This formulation provides a rigorous formal link between the framework expressed in the original space and its counterpart in the embedded space, enabling seamless transitions between the two representations. Consequently, the rigidity matrix of the system can be constructed in the embedded space, where computations are mathematically tractable due to spatial homogeneity, and then mapped back into the original spaces.

The framework provides the degree of freedom to choose the appropriate space and mapping at every stage of the pipeline. In particular, this flexibility allows for the selection of the most suitable embedded state space for the agents. While $SE(3)$ is a natural universal choice for the ambient space, lifting every agent into six dimensions is not always physically necessary and can introduce redundant variables and unnecessary computational overhead. By treating the embedding target as a design parameter, the ambient space can be scaled exactly to what a given formation requires, ranging from a minimal manifold sufficient for a specific task to a maximal, redundant representation.

Since h decomposes into a sequence of elementary stages, these pairings are carried out at every intermediate stage of the decomposition rather than solely at its endpoints, utilizing distinct pairs specifically adapted to the manifolds involved at each level. This stage-by-stage structural coupling naturally gives rise to an interconnected commutative diagram, providing a rigorous formal link between the original and embedded representations.

Crucially, because the choice of spaces acts as a design degree of freedom at every stage of the modeling chain, neither dimensional uniformity nor a fixed structural characterization is globally enforced across the pipeline. Consequently, when comparing alternative pipeline realizations, the functions that link them can be any pair consisting of a function and its left inverse properly chosen. This means that, in general, there is no requirement for them to be consistently coupled by embedding-retraction pairs in the same orientation, as they may feature an identical or inverted pair order. This fundamental flexibility in defining intermediate spaces implies that distinct pipelines may operate across entirely disparate ambient manifolds at corresponding stages.

Beyond dimensional adjustments, relying on standard informationless padding as an embedding strategy is often insufficient to handle the full complexity of system heterogeneity. To properly characterize the state of the agents within a common homogeneous space, the embedding process must introduce external information, utilizing both the native state and these extrinsic parameters to formulate the embedded state.

In classical frameworks, measurement mappings are constrained to depend exclusively on the complete interacting agents' internal states, imposing a structural limitation when dealing with interactions across disparate manifolds. The proposed framework overcomes this by integrating external information to properly characterize the agents' embedded states. By strategically defining this embedded space, the framework enables generalized measurements that can utilize an agent's full kinematic state, isolate a specific subset of it, or incorporate external parameters beyond the agent's native state.

Ultimately, the inclusion of external variables provides a comprehensive characterization of the embedding processes required for heterogeneous MAS and introduces a novel paradigm for robustness analysis. This formulation suggests that extrinsic parameters can be incorporated into the rigidity analysis in the exact same manner as the agents' intrinsic variables, allowing the framework to accommodate both static perturbations and the active dynamics of external elements.

As briefly mentioned so far, and as will be further investigated in the following, the pipeline realizations and the mappings between their spaces exhibit a strong commutative structure. This powerful feature enables us to explain how the measurement function works, how it implicitly handles the embedding operation, and how extrinsic parameters are introduced into the formulation. Furthermore, the stage-by-stage decomposition allows us to precisely isolate the specific components, highlighting how each step operates and how their structure drives the adaptation process. Ultimately, this characterization provides a deeper understanding of the measurement functions.

3.3 CHARACTERIZATION VIA CATEGORY THEORY

The structural abstraction and inherent commutativity of the system's mapping pipelines naturally motivate the use of category theory. It provides a rigorous mathematical language for expressing and guaranteeing relations across different model representations. Concretely, we define a base category encoding the high-level structure of the measurement process and translate it into smooth manifolds via functors to properly describe the MAS.

The categorical pipeline developed below is built around the measurement types most commonly treated in the literature. This approach yields three primary functorial realizations:

- A **Kinematic Functor**, modeling native agent states and idealized measurements without dimensional embedding.

- An **Augmented Functor**, serving as an intermediate, generally heterogeneous layer that incorporates native kinematics and extrinsic parameters. This realization allow to highlighting how the parameters enter into embedding process.
- An **Embedded Functor**, modeling the uniform ambient spaces into which parameterized agents and measurements are mapped.

Accommodating different measurements that remain compatible with the measurement model provided by the base category requires only specifying a new functorial realization, bypassing the need to re-derive the downstream rigidity machinery. This simply entails defining the objects and morphisms over the existing base category. Conversely, if a new measurement type does not fit the established model, or if we want to consider a richer or simpler measurement process to highlight different aspects, the base category itself must be adapted. It can be expanded with new objects and morphisms, simplified by removing unnecessary stages, or constructed entirely from scratch.

While this work focuses on these three specific functors to establish the general paradigm, the framework remains highly modular. Depending on task requirements, one can generate as many realizations as desired to describe different system properties and connect them through natural transformations.

To formalize this structure, classical measurement models are decomposed into four core stages:

(i) incorporating the graph topology dictating agent interactions;

(ii) filtering the state subset relevant to the task;

(iii) applying geometric operators to evaluate relative spatial configurations; and

(iv) computing the final measurements.

We first define the base category $\mathscr{C}$. Subsequently, we present the three geometric realizations of increasing structural complexity (namely the kinematic, augmented, and embedded realization introduced previously), alongside the natural transformations that interrelate them.

3.4 THE BASE CATEGORY $\mathscr{C}$

The measurement operation can be modeled by a single structural category that captures the abstract architecture of the network's measurement chain. The purpose of this category is to encode the structural dependencies between the different stages of the measurement process while remaining completely agnostic to the specific mathematical realization of the spaces involved.

To this end, we first introduce a directed quiver containing the formal objects and generating morphisms of the measurement pipeline. The corresponding base category is then defined as the free category generated by this quiver.

Definition 3.4 (Generating Quiver)**.** Let Q be the directed quiver associated with the abstract measurement pipeline. Its objects are

$$\mathrm{Ob}(Q) = \{\mathbb{V}, \mathbb{E}, \mathbb{T}, \mathbb{O}, \mathbb{M}\},$$

where each object represents a formal stage of the measurement architecture:

- $\mathbb{V}$ **(Node Space):** the abstract domain representing the localized information associated with an individual agent. It serves as a generic placeholder for node-level information.
- $\mathbb{E}$ **(Edge Space):** the abstract domain representing the relational information associated with interacting pairs of agents, as determined by the underlying network topology.
- $\mathbb{T}$ **(Task Edge Space):** the abstract domain containing the subset of relational information that is relevant for the cooperative task or for the subsequent measurement operation.
- $\mathbb{O}$ **(Observation Space):** the abstract domain representing the relative observation generated from the task-relevant edge information.
- $\mathbb{M}$ **(Measurement Space):** the terminal abstract domain representing the output of the measurement pipeline.

The generating arrows of Q are

$$\mathrm{Gen}(Q) = \{\sigma, \mu, \gamma, \Delta, \eta\},$$

with source and target assignments

$$\sigma : \mathbb{V} \longrightarrow \mathbb{E}, \qquad \mu : \mathbb{E} \longrightarrow \mathbb{V},$$

$$\gamma : \mathbb{E} \longrightarrow \mathbb{T}, \qquad \Delta : \mathbb{T} \longrightarrow \mathbb{O}, \qquad \eta : \mathbb{O} \longrightarrow \mathbb{M}.$$

The resulting quiver is

$$\begin{tikzcd} \mathbb{V} \arrow[r, shift left, "\sigma"] & \mathbb{E} \arrow[l, shift left, "\mu"] \arrow[r, "\gamma"] & \mathbb{T} \arrow[r, "\Delta"] & \mathbb{O} \arrow[r, "\eta"] & \mathbb{M}. \end{tikzcd}$$

The generating arrows have the following structural interpretation:

$\sigma : \mathbb{V} \to \mathbb{E}$ (**DISTRIBUTION MAP**)**:** a structural operation that propagates localized node-level information into the relational edge domain according to the underlying network incidence structure.

$\mu : \mathbb{E} \to \mathbb{V}$ **(AGGREGATION MAP):** a structural feedback operation that aggregates relational information back into the localized node domain.

$\gamma : \mathbb{E} \to \mathbb{T}$ **(TASK FILTRATION MAP):** a structural operation that retains the portion of the edge-level information required by the cooperative task or measurement model.

$\Delta : \mathbb{T} \to \mathbb{O}$ **(EDGE OBSERVATION MAP):** a structural operation that transforms the task-relevant relational information into an abstract relative observation.

$\eta : \mathbb{O} \to \mathbb{M}$ **(MEASUREMENT MAP):** a structural operation that transforms the abstract relative observation into the final abstract measurement output.

Definition 3.5 (Base Category $\mathscr{C}$)**.** The **Base Category** $\mathscr{C}$ is defined as the free category generated by the quiver Q:

$$\mathscr{C} := \mathbf{Free}(Q).$$

The objects of $\mathscr{C}$ are the objects of Q,

$$\mathrm{Ob}(\mathscr{C}) = \{\mathbb{V}, \mathbb{E}, \mathbb{T}, \mathbb{O}, \mathbb{M}\},$$

while its morphisms are all finite composable paths in Q, together with the identity morphisms.

More explicitly, for any two objects $X, Y \in \mathrm{Ob}(\mathscr{C})$, the hom-set

$$\mathrm{Hom}_{\mathscr{C}}(X, Y)$$

consists of all finite paths from X to Y constructed from the generating arrows of Q, together with the identity morphism id_X when $X = Y$.

Composition in $\mathscr{C}$ is given by concatenation of composable paths and is therefore associative by construction. The identity morphisms are the paths of length zero.

Consequently, $\mathscr{C}$ is a well-defined category whose structure is determined entirely by the abstract architecture of the measurement pipeline.

At this level, no object within the quiver Q or its induced base category $\mathscr{C}$ is assigned a particular mathematical realization. They should be interpreted as formal categorical objects, rather than as explicitly realized sets or manifolds. In particular, the label ”Space” is used solely to emphasize their semantic role within the measurement pipeline and does not impose any intrinsic geometric structure. Thus, no dimension, coordinate system, algebraic operation, topology, differentiable structure, or metric is specified at the level of $\mathscr{C}$. Likewise, the generating arrows within the quiver Q and the resulting morphisms in its induced base category $\mathscr{C}$ are regarded strictly as formal categorical morphisms; they are not yet interpreted as functions between specific sets or as smooth maps between manifolds. The concrete mathematical meaning of every element within the category is established only once a realization functor is chosen.

3.4.1 The Abstract Global Measurement Morphism

Because $\mathscr{C}$ is a category, the generating morphisms can be composed whenever the target of the first matches the source of the second. In particular, the forward measurement pipeline determines the composite morphism

$$\mathscr{M} = \eta \circ \Delta \circ \gamma \circ \sigma \ : \ \mathbb{V} \longrightarrow \mathbb{M}$$

This morphism is an element of the hom-set

$$\mathscr{M} \in \mathrm{Hom}_{\mathscr{C}}(\mathbb{V}, \mathbb{M})$$

and represents the abstract measurement pipeline.

Importantly, $\mathscr{M}$ is defined entirely within the base category and therefore does not depend on any particular choice of coordinates, dimension, manifold, or physical realization.

3.4.2 Geometric Realization of the Base Category

Once the abstract measurement architecture has been established, a specific geometric model can be introduced through a covariant functor

$$\mathscr{F} \ : \ \mathscr{C} \longrightarrow \mathbf{Man}$$

where **Man** is the category of smooth manifolds.

The functor assigns to each formal object $X \in \mathrm{Ob}(\mathscr{C})$ a smooth manifold

$$X \longmapsto \mathscr{F}(X),$$

and to each abstract morphism $f \ : \ X \to Y$ a smooth map

$$f \longmapsto \mathscr{F}(f) \ : \ \mathscr{F}(X) \longrightarrow \mathscr{F}(Y).$$

In particular, the generating morphisms are realized as

$$\mathscr{F}(\sigma) = \sigma_{\mathscr{F}}, \qquad \mathscr{F}(\mu) = \mu_{\mathscr{F}}, \qquad \mathscr{F}(\gamma) = \gamma_{\mathscr{F}},$$

$$\mathscr{F}(\Delta) = \Delta_{\mathscr{F}}, \qquad \mathscr{F}(\eta) = \eta_{\mathscr{F}}.$$

Since $\mathscr{F}$ is a functor, it preserves identities and composition. Therefore,

$$\mathscr{F}(\mathscr{M}) = \mathscr{F}(\eta \circ \Delta \circ \gamma \circ \sigma)$$

satisfies

$$\mathscr{F}(\mathscr{M}) = \mathscr{F}(\eta) \circ \mathscr{F}(\Delta) \circ \mathscr{F}(\gamma) \circ \mathscr{F}(\sigma)$$

Thus, for every realization functor compatible with the considered MAS, the abstract categorical measurement pipeline is preserved under the realization.

This relization mechanism bridges allow to instatiate the abstract category into a concrete realization that describe the physical reality in analysis.

The construction provides the fundamental separation

$$\text{Abstract measurement architecture} \quad \xrightarrow{\mathscr{F}} \quad \text{Concrete geometric realization.}$$

Different choices of $\mathscr{F}$ therefore yield different geometric realizations of the same underlying measurement structure, while the abstract category $\mathscr{C}$ remains unchanged.

Consequently, by tailoring the specific representation of these objects and their associated morphisms, one can construct multiple distinct functors, each providing a unique mathematical perspective on the same physical reality. Therefore, the choice of realization space and morphism becomes a strategic decision and a design degree of freedom, deliberately leveraged to highlight specific characteristics of the system.

It is important to note that the abstract category $\mathscr{C}$ admits multiple possible geometric realizations. However, not every realization is compatible with the physical and sensing structure of a given MAS. Only those realization functors whose assigned manifolds and smooth maps are consistent with the specific system architecture, agent states, communication topology, and available measurements provide a valid representation of the corresponding MAS. Therefore, for the remainder of this analysis, we fix the specific MAS and sensing network under consideration and restrict attention to realization functors that are compatible with this fixed system.

This restriction is adopted because our primary objective is to characterize the measurement function associated with a fixed MAS and sensing framework. If a different system is considered, the corresponding system-specific realization must be specified accordingly to differentiate them. This ensures that distinct architectures can be compared and interrelated without ambiguity. In other words, the proposed formulation must be properly adapted to accommodate different MAS realization.

In this study, we consider the following functors, which were selected as the primary tools to establish a logical baseline.

- **The Kinematic Functor ($\mathscr{F}_{kin}$)**
  The agent space realization and the measurement space realization coincide with the original heterogeneous agent and measurement spaces. The spaces in

the intermediate stages are built in order to properly bridge both, following the instructions of the base category.

$$\mathscr{F}_{kin}(\mathbb{V}) \underset{\mathscr{F}_{kin}(\mu)=\mu_{kin}}{\overset{\mathscr{F}_{kin}(\sigma)=\sigma_{kin}}{\rightleftarrows}} \mathscr{F}_{kin}(\mathbb{E}) \xrightarrow{\mathscr{F}_{kin}(\gamma)=\gamma_{kin}} \mathscr{F}_{kin}(\mathbb{T}) \xrightarrow{\mathscr{F}_{kin}(\Delta)=\Delta_{kin}} \mathscr{F}_{kin}(\mathbb{O}) \xrightarrow{\mathscr{F}_{kin}(\eta)=\eta_{kin}} \mathscr{F}_{kin}(\mathbb{M}) \tag{4}$$

The realization of the measurement function via this functor is:

$$\begin{aligned}
\mathbf{h}_{kin} &= \mathscr{F}_{kin}(\mathscr{M}) && (5)\\
&= \mathscr{F}_{kin}(\eta \circ \Delta \circ \gamma \circ \sigma) && (6)\\
&= \mathscr{F}_{kin}(\eta) \circ \mathscr{F}_{kin}(\Delta) \circ \mathscr{F}_{kin}(\gamma) \circ \mathscr{F}_{kin}(\sigma) && (7)\\
&= \eta_{kin} \circ \Delta_{kin} \circ \gamma_{kin} \circ \sigma_{kin} \;:\; \mathscr{F}_{kin}(\mathbb{V}) \to \mathscr{F}_{kin}(\mathbb{M}) && (8)
\end{aligned}$$

For example, one possible kinematic realization is:

$$\prod_{i=1}^{n} \mathscr{D}_i \underset{\mu_{kin}}{\overset{\sigma_{kin}}{\rightleftarrows}} \prod_{k=1}^{m} \mathscr{D}_{s(e_k)} \times \mathscr{D}_{t(e_k)} \xrightarrow{\gamma_{kin}} \prod_{k=1}^{m} \mathscr{T}_{s(e_k)} \times \mathscr{T}_{t(e_k)} \xrightarrow{\Delta_{kin}} \prod_{k=1}^{m} \mathscr{O}_k \xrightarrow{\eta_{kin}} \prod_{k=1}^{m} \mathscr{M}_k \tag{9}$$

where $s, t : \mathscr{E} \to \mathscr{V}$ denote the source and target maps, assigning each edge to its respective source and target nodes.

- **The Augmented Functor ($\mathscr{F}_{aug}$)**
The agent space realization consists of an augmented state that combines the kinematic state with the information useful to fully characterize the measurement. In this case, since all the parameters are incorporated into the agent state, one can choose to retain the original measurement space. The spaces in the intermediate stages are built in order to properly bridge both, following the instructions of the base category. Note that in this case, we still have structural heterogeneity across the spaces.

$$\mathscr{F}_{aug}(\mathbb{V}) \underset{\mathscr{F}_{aug}(\mu)=\mu_{aug}}{\overset{\mathscr{F}_{aug}(\sigma)=\sigma_{aug}}{\rightleftarrows}} \mathscr{F}_{aug}(\mathbb{E}) \xrightarrow{\mathscr{F}_{aug}(\gamma)=\gamma_{aug}} \mathscr{F}_{aug}(\mathbb{T}) \xrightarrow{\mathscr{F}_{aug}(\Delta)=\Delta_{aug}} \mathscr{F}_{aug}(\mathbb{O}) \xrightarrow{\mathscr{F}_{aug}(\eta)=\eta_{aug}} \mathscr{F}_{aug}(\mathbb{M}) \tag{10}$$

The realization of the measurement function via this functor is:

$$\begin{aligned}
\mathbf{h}_{aug} &= \mathscr{F}_{aug}(\mathscr{M}) && (11)\\
&= \mathscr{F}_{aug}(\eta) \circ \mathscr{F}_{aug}(\Delta) \circ \mathscr{F}_{aug}(\gamma) \circ \mathscr{F}_{aug}(\sigma) && (12)\\
&= \eta_{aug} \circ \Delta_{aug} \circ \gamma_{aug} \circ \sigma_{aug} \;:\; \mathscr{F}_{aug}(\mathbb{V}) \to \mathscr{F}_{aug}(\mathbb{M}) && (13)
\end{aligned}$$

Following this definition, one possible augmented realization is:

$$\prod_{i=1}^{n} \mathcal{P}_i \underset{\mu_{aug}}{\overset{\sigma_{aug}}{\rightleftarrows}} \prod_{k=1}^{m} \mathcal{P}_{s(e_k)} \times \mathcal{P}_{t(e_k)} \xrightarrow{\gamma_{aug}} \prod_{k=1}^{m} \mathcal{T}_{s(e_k)}^{aug} \times \mathcal{T}_{t(e_k)}^{aug} \xrightarrow{\Delta_{aug}} \prod_{k=1}^{m} \mathcal{O}_k \xrightarrow{\eta_{aug}} \prod_{k=1}^{m} \mathcal{M}_k \tag{14}$$

where $\mathcal{P}_i = (\mathcal{D}_i \times \Theta_i)$ denotes the augmented state space of the i-th agent, seamlessly combining its base kinematic space with any external parameters associated with it.

- **The Embedded Functor ($\mathcal{F}_{emb}$)**
  All the stages of the measurement function consist of homogeneous spaces, always strictly following the instructions of the base category.

$$\mathcal{F}_{emb}(\mathbb{V}) \underset{\mathcal{F}_{emb}(\mu)=\mu_{emb}}{\overset{\mathcal{F}_{emb}(\sigma)=\sigma_{emb}}{\rightleftarrows}} \mathcal{F}_{emb}(\mathbb{E}) \xrightarrow{\mathcal{F}_{emb}(\gamma)=\gamma_{emb}} \mathcal{F}_{emb}(\mathbb{T}) \xrightarrow{\mathcal{F}_{emb}(\Delta)=\Delta_{emb}} \mathcal{F}_{emb}(\mathbb{O}) \xrightarrow{\mathcal{F}_{emb}(\eta)=\eta_{emb}} \mathcal{F}_{emb}(\mathbb{M}) \tag{15}$$

The realization of the measurement function via this functor is:

$$\begin{aligned} \mathbf{h}_{emb} &= \mathcal{F}_{emb}(\mathcal{M}) && (16)\\ &= \mathcal{F}_{emb}(\eta) \circ \mathcal{F}_{emb}(\Delta) \circ \mathcal{F}_{emb}(\gamma) \circ \mathcal{F}_{emb}(\sigma) && (17)\\ &= \eta_{emb} \circ \Delta_{emb} \circ \gamma_{emb} \circ \sigma_{emb} \ : \ \mathcal{F}_{emb}(\mathbb{V}) \to \mathcal{F}_{emb}(\mathbb{M}) && (18) \end{aligned}$$

For example, by embedding the agents into the Special Euclidean group $SE(3)$, one possible entirely homogeneous realization is:

$$SE(3)^n \underset{\mu_{emb}}{\overset{\sigma_{emb}}{\rightleftarrows}} (SE(3) \times SE(3))^m \xrightarrow{\gamma_{emb}} (SE(3) \times SE(3))^m \xrightarrow{\Delta_{emb}} (SE(3))^m \xrightarrow{\eta_{emb}} (\mathcal{M}_{emb})^m \tag{19}$$

In this scenario, the augmented functor is designed to encapsulate the native state and the external information necessary to fully characterize the subsequent embedding into a common space. The embedding operation leverages this augemented state and introduces informationless padding to rigorously homogenize the state spaces.

Remark 3.2. Neither $\mathcal{F}_{aug}$ nor $\mathcal{F}_{emb}$ is a strict prescription; rather, they are flexible modeling choices. For example one can range beetween:

- **Universal/Maximal Embedded Realization:** Provides a realization with spaces large enough to integrate all possible states of a particular class of agents. For example, in the case of agents operating in a 3D environment, the state would encompass the full spatial pose described by $\mathbb{SE}(3)$. It serves as the foundational framework for generalized hybrid rigidity paradigms, enabling a unified mathematical treatment of all possible agent configurations within a specific class of MAS.
- **Minimal Embedded Realization:** Employs only the minimal set of parameters required to fully define the measurements. Correspondingly, it utilizes

the lowest-dimensional embedding necessary to encompass all heterogeneous agents in the MAS and rigorously compute the measurement function.

- **Task-Driven Realization:** Highly optimized for a specific objective. Here, the parameter set is restricted strictly to what the task demands, and the embedding space is designed to unify agents and measurements while actively projecting out state components that are irrelevant to the measurement process (i.e., unobservable variables).

3.5 NATURAL TRANSFORMATIONS BETWEEN FUNCTORS

In category theory, the rigorous bridge between two parallel functors acting between the same categories is defined as a *natural transformation.* Crucially, a natural transformation is not merely a localized mapping between two isolated spaces, but a global operation that acts systematically across the entire categorical structure. It provides a structurally consistent connecting morphism for every corresponding object instantiated by the two functors, strictly preserving the commutativity of the internal morphisms involved.

In our framework, we consider three distinct functors: the kinematic functor ($\mathscr{F}_{kin}$), the augmented functor ($\mathscr{F}_{aug}$), and the embedded functor ($\mathscr{F}_{emb}$). To highlight how the embedding process functions and how extrinsic parameters enter the analytical pipeline, we establish a strict dimensional hierarchy across the associated spaces. The hierarchy begins with the kinematic functor, which strictly captures the pure kinematic state of the system. This naturally progresses to the augmented functor, which incorporates the external parameters required to rigorously characterize the embedding in the common abstract space of agents and measurements. Finally, the embedded functor leverages this augmented state, introducing informationless padding to fully homogenize the ambient space.

Consistent with this description, we assume that all objects of the kinematic functor have dimensions less than or equal to those of the augmented functor, and that all objects of the augmented functor have dimensions less than or equal to those of the embedded functor. Consequently, the embedding-retraction pairs between the objects of any two realization functions in analysis maintain a consistent directionality

Since the measurement function is defined as a composition of morphisms mirroring the structure of the base category, the objects of different geometric functorial realizations of the same category can be related through specific transformations. Whenever these transformations guarantee commutativity, they establish a consistent correspondence between the objects and morphisms of two realization functors, thus inducing a natural transformation between them. For the purposes of our analysis, we assume that the three functorial realizations under consideration are properly constructed, ensuring that the embedding-retraction pairs between their objects form a valid natural transformation.

More precisely, let $\mathscr{F}, \mathscr{G} : \mathscr{C} \longrightarrow \mathbf{Man}$ be two functors representing two geometric realizations of the same base category. A natural transformation $\alpha : \mathscr{F} \Rightarrow \mathscr{G}$ consists of a family of smooth maps, called the *components* of α,

$$\alpha_X : \mathscr{F}(X) \longrightarrow \mathscr{G}(X), \qquad \forall X \in \mathrm{Ob}(\mathscr{C}),$$

such that these maps are compatible with every morphism of the base category. In particular, for every morphism

$$f : X \longrightarrow Y$$

in $\mathscr{C}$, the following naturality condition must hold:

$$\mathscr{G}(f) \circ \alpha_X = \alpha_Y \circ \mathscr{F}(f)$$

Equivalently, the following diagram must commute for every morphism $f : X \to Y$:

$$\begin{tikzcd}
\mathscr{F}(X) \arrow[r, "\mathscr{F}(f)"] \arrow[d, "\alpha_X"'] & \mathscr{F}(Y) \arrow[d, "\alpha_Y"] \\
\mathscr{G}(X) \arrow[r, "\mathscr{G}(f)"'] & \mathscr{G}(Y).
\end{tikzcd}$$

Thus, a natural transformation does not merely establish independent correspondences between the realized spaces. Rather, it requires these correspondences to be structurally compatible with all morphisms of $\mathscr{C}$.

In the present construction, the transition maps between the selected realizations are assumed to satisfy this naturality condition together with the prescribed embedding-retraction structure. In particular, when the component maps are embeddings,

$$\alpha_X : \mathscr{F}(X) \hookrightarrow \mathscr{G}(X),$$

their corresponding retractions

$$\beta_X : \mathscr{G}(X) \longrightarrow \mathscr{F}(X)$$

are required to satisfy

$$\beta_X \circ \alpha_X = \mathrm{id}_{\mathscr{F}(X)}$$

for every $X \in \mathrm{Ob}(\mathscr{C})$.

Under these assumptions, the transition between the two realizations is simultaneously a natural transformation and an embedding-retraction structure. The latter expresses the prescribed relation between the dimensions and information content of the corresponding realized spaces, while the naturality condition guarantees compatibility of this relation with the measurement architecture encoded by $\mathscr{C}$.

Within this structure, the morphisms linking the functor objects dictated by the natural transformations play a critical role in our work. Indeed, they explain how the elements of the objects are processed, how parameters enter the measurements, and how the embedding process is defined.

We formalize the natural transformations between the functors in analysis:

- **Kinematic-to-Augmented Natural Realization:**

  $$\iota_\alpha : \mathscr{F}_{kin} \to \mathscr{F}_{aug}$$

  A natural transformation bridging the kinematic baseline with the augemented realization.

  For any abstract object $X \in \mathrm{ob}(\mathscr{C})$, the component map

  $$\iota_{\alpha,X} : \mathscr{F}_{kin}(X) \hookrightarrow \mathscr{F}_{aug}(X)$$

  is an injective embedding that structurally expands the intrinsic state to incorporate necessary external parameters.

- **Augmented-to-Kinematic Natural Realization:**

  $$\rho_\alpha : \mathscr{F}_{aug} \to \mathscr{F}_{kin}$$

  A natural transformation acting as the left-inverse to the kinematic-to-augmented embedding.

  For any abstract object $X \in \mathrm{ob}(\mathscr{C})$, the component map

  $$\rho_{\alpha,X} : \mathscr{F}_{aug}(X) \twoheadrightarrow \mathscr{F}_{kin}(X)$$

  is a surjective retraction that filters out all extra-kinematic parameters, precisely isolating and recovering the original intrinsic state, acting as the left-inverse of $\iota_{\alpha,X}$.

- **Augmented-to-Embedded Natural Realization:**

  $$\iota_\varepsilon : \mathscr{F}_{aug} \to \mathscr{F}_{emb}$$

  A natural transformation managing the resolution of topological heterogeneity across the network.

For any abstract object $X \in \mathrm{ob}(\mathscr{C})$, the component map

$$\iota_{\varepsilon,X} : \mathscr{F}_{aug}(X) \hookrightarrow \mathscr{F}_{emb}(X)$$

is an injective embedding that maps the heterogeneous augmented state into the globally uniform manifold.

- **Embedded-to-Augmented Natural Realization:**

$$\rho_{\varepsilon} : \mathscr{F}_{emb} \to \mathscr{F}_{aug}$$

A natural transformation acting as the left-inverse to the augmented-to-embedded embedding.

For any abstract object $X \in \mathrm{ob}(\mathscr{C})$, the component map

$$\rho_{\varepsilon,X} : \mathscr{F}_{emb}(X) \twoheadrightarrow \mathscr{F}_{aug}(X)$$

is a surjective retraction that mathematically discards the structurally redundant topological padding, recovering the true heterogeneous augmented configuration, acting as the left-inverse of $\iota_{\varepsilon,X}$.

Furthermore, a fundamental property of natural transformations is their strict composability. By vertically composing the sequential mappings, we establish direct, structurally guaranteed bidirectional bridges between the pure kinematic baseline and the fully homogeneous embedded space:

- **Composite Kinematic-to-Embedded Natural Realization (Direct Embedding):**

$$\iota_{\varepsilon\alpha} : \mathscr{F}_{kin} \to \mathscr{F}_{emb}$$

A natural transformation formed by the vertical composition of sequential mappings, bridging the pure kinematic baseline with the fully homogeneous embedded space.

For any abstract object $X \in \mathrm{ob}(\mathscr{C})$, the component map

$$\iota_{\varepsilon\alpha,X} = \iota_{\varepsilon,X} \circ \iota_{\alpha,X} : \mathscr{F}_{kin}(X) \hookrightarrow \mathscr{F}_{emb}(X)$$

is a composite injective embedding that directly maps the native kinematic state into the globally uniform manifold.

- **Composite Embedded-to-Kinematic Natural Realization (Direct Retraction):**

$$\rho_{\alpha\varepsilon} : \mathscr{F}_{emb} \to \mathscr{F}_{kin}$$

A natural transformation acting as the left-inverse to the composite direct embedding, bypassing intermediate representations.

For any abstract object $X \in \mathrm{ob}(\mathscr{C})$, the component map

$$\rho_{\alpha\varepsilon,X} = \rho_{\alpha,X} \circ \rho_{\varepsilon,X} : \mathscr{F}_{emb}(X) \twoheadrightarrow \mathscr{F}_{kin}(X)$$

is a composite surjective retraction that projects the redundant global space all the way down to the bare intrinsic state, simultaneously discarding both the artificial topological padding and the external parameters, acting as the left-inverse of $\iota_{\varepsilon\alpha,X}$.

By integrating the three functors with their associated natural transformations and exploiting their intrinsic commutativity, we derive the commutative diagram presented in Figure 3.1. This construction holds under the assumption that the embedding-retraction maps serve as natural transformation components strictly compatible with the measurement morphisms.

$$\begin{tikzcd}
\mathscr{F}_{kin}(\mathbb{V}) \arrow[r, shift left, "\sigma_{kin}"] \arrow[d, hook, shift left, "\iota_{\alpha,\mathbb{V}}"] & \mathscr{F}_{kin}(\mathbb{E}) \arrow[l, shift left, "\mu_{kin}"] \arrow[r, "\gamma_{kin}"] \arrow[d, hook, shift left, "\iota_{\alpha,\mathbb{E}}"] & \mathscr{F}_{kin}(\mathbb{T}) \arrow[r, "\Delta_{kin}"] \arrow[d, hook, shift left, "\iota_{\alpha,\mathbb{T}}"] & \mathscr{F}_{kin}(\mathbb{O}) \arrow[r, "\eta_{kin}"] \arrow[d, hook, shift left, "\iota_{\alpha,\mathbb{O}}"] & \mathscr{F}_{kin}(\mathbb{M}) \arrow[d, hook, shift left, "\iota_{\alpha,\mathbb{M}}"] \\
\mathscr{F}_{aug}(\mathbb{V}) \arrow[u, two heads, shift left, "\rho_{\alpha,\mathbb{V}}"] \arrow[r, shift left, "\sigma_{aug}"] \arrow[d, hook, shift left, "\iota_{\varepsilon,\mathbb{V}}"] & \mathscr{F}_{aug}(\mathbb{E}) \arrow[u, two heads, shift left, "\rho_{\alpha,\mathbb{E}}"] \arrow[l, shift left, "\mu_{aug}"] \arrow[r, "\gamma_{aug}"] \arrow[d, hook, shift left, "\iota_{\varepsilon,\mathbb{E}}"] & \mathscr{F}_{aug}(\mathbb{T}) \arrow[u, two heads, shift left, "\rho_{\alpha,\mathbb{T}}"] \arrow[r, "\Delta_{aug}"] \arrow[d, hook, shift left, "\iota_{\varepsilon,\mathbb{T}}"] & \mathscr{F}_{aug}(\mathbb{O}) \arrow[u, two heads, shift left, "\rho_{\alpha,\mathbb{O}}"] \arrow[r, "\eta_{aug}"] \arrow[d, hook, shift left, "\iota_{\varepsilon,\mathbb{O}}"] & \mathscr{F}_{aug}(\mathbb{M}) \arrow[u, two heads, shift left, "\rho_{\alpha,\mathbb{M}}"] \arrow[d, hook, shift left, "\iota_{\varepsilon,\mathbb{M}}"] \\
\mathscr{F}_{emb}(\mathbb{V}) \arrow[u, two heads, shift left, "\rho_{\varepsilon,\mathbb{V}}"] \arrow[r, shift left, "\sigma_{emb}"] & \mathscr{F}_{emb}(\mathbb{E}) \arrow[u, two heads, shift left, "\rho_{\varepsilon,\mathbb{E}}"] \arrow[l, shift left, "\mu_{emb}"] \arrow[r, "\gamma_{emb}"] & \mathscr{F}_{emb}(\mathbb{T}) \arrow[u, two heads, shift left, "\rho_{\varepsilon,\mathbb{T}}"] \arrow[r, "\Delta_{emb}"] & \mathscr{F}_{emb}(\mathbb{O}) \arrow[u, two heads, shift left, "\rho_{\varepsilon,\mathbb{O}}"] \arrow[r, "\eta_{emb}"] & \mathscr{F}_{emb}(\mathbb{M}) \arrow[u, two heads, shift left, "\rho_{\varepsilon,\mathbb{M}}"]
\end{tikzcd}$$

Figure 3.1: The Commutative Grid

It is important to emphasize that the three realization functors proposed in this work ($\mathscr{F}_{kin}, \mathscr{F}_{aug}, \mathscr{F}_{emb}$) constitute a foundational theoretical baseline. The underlying categorical framework is inherently flexible: one can instantiate an arbitrary number of functors, each with its own characteristics such as the choice of manifolds in the functor realizations, and relate them through any appropriate mapping that are not restricted to embedding-retraction pairs, which can eventually form natural transformations.

Consequently, determining which functors to define, how to link them, and exactly how each object and morphism is mathematically realized becomes a strategic design choice and a powerful degree of freedom that can be deliberately leveraged to expose structural behaviors. An interesting example of another possible functor is one that intentionally filters unobservable or task-irrelevant variables out of the kinematic state, thereby simplifying the analysis by removing mathematical complications introduced by components irrelevant to the measurement.

However, it is important to recall that we are considering the modeling of a fixed MAS, and any functor realization must be consistent with this system and the measurement process imposed by the base category. Furthermore, if one wishes to analyze a different measurement process that cannot be described by the current base category, one can simply define a new base category, create its corresponding realizations, and eventually compare the different measurement processes.

3.6 INDUCED FRAMEWORKS FROM FUNCTORS

The realization functors studied so far, by assumption, describe the same MAS and sensing network from different points of view. By applying these realization functors, the abstract base category is concretely instantiated to model the physical system. This means that the underlying graph can be assumed constant across the different realizations.

Accordingly, for each specific realization, we can define the corresponding node configuration within its respective agent space. Given a native configuration $\mathbf{x}_{kin} \in \mathscr{F}_{kin}(\mathbb{V})$, the augmented and embedded configurations are recovered by applying the appropriate component mappings of the natural transformations, yielding:

$$\mathbf{x}_{aug} := \iota_{\alpha,\mathbb{V}}(\mathbf{x}_{kin}), \qquad \mathbf{x}_{emb} := \iota_{\varepsilon,\mathbb{V}}(\mathbf{x}_{aug}) = \iota_{\varepsilon,\mathbb{V}}\big(\iota_{\alpha,\mathbb{V}}(\mathbf{x}_{kin})\big).$$

This means that $\mathbf{x}_{kin}, \mathbf{x}_{aug}$, and $\mathbf{x}_{emb}$ are not independent states, but rather a single physical configuration expressed at three different levels of representation.

The measurements functions induced by the respective functors are formally linked according to the commutative diagram presented in Figure 3.1, which naturally arises from these natural transformations. Consequently, the following relations hold:

$$\mathbf{h}_{aug} \circ \iota_{\alpha,\mathbb{V}} = \iota_{\alpha,\mathbb{M}} \circ \mathbf{h}_{kin}, \tag{20}$$
$$\mathbf{h}_{emb} \circ \iota_{\varepsilon,\mathbb{V}} = \iota_{\varepsilon,\mathbb{M}} \circ \mathbf{h}_{aug}, \tag{21}$$
$$\mathbf{h}_{kin} \circ \rho_{\alpha,\mathbb{V}} = \rho_{\alpha,\mathbb{M}} \circ \mathbf{h}_{aug}, \tag{22}$$
$$\mathbf{h}_{aug} \circ \rho_{\varepsilon,\mathbb{V}} = \rho_{\varepsilon,\mathbb{M}} \circ \mathbf{h}_{emb}, \tag{23}$$
$$\mathbf{h}_{kin} = \rho_{\alpha,\mathbb{M}} \circ \mathbf{h}_{aug} \circ \iota_{\alpha,\mathbb{V}}, \tag{24}$$
$$\mathbf{h}_{aug} = \rho_{\varepsilon,\mathbb{M}} \circ \mathbf{h}_{emb} \circ \iota_{\varepsilon,\mathbb{V}}. \tag{25}$$

Once the node configuration and the measurement function are established in each realization, the associated edge configuration can also be straightforwardly determined. These elements fully characterize a smooth ordered framework associated with the realization. Consequently, any two smooth ordered frameworks induced by functorial realizations modeling the same physical reality are formally linked through the relations established by the natural transformations connecting their underlying functors.

Once these functorial realizations are defined, one can analyze the rigidity of the induced framework with respect to a specific smooth group action applied to its respective state space. In our specific case, this yields the following representations:

- **Kinematic functor** $\mathscr{F}_{kin}$:
  - The global node configuration induced by $\mathscr{F}_{kin}$ is denoted as $\mathbf{x}_{kin} \in \mathscr{F}_{kin}(\mathbb{V})$, representing the true physical states of the agents.

- The measurement function induced by $\mathscr{F}_{kin}$ is defined as

$$\mathbf{h}_{kin} : \mathscr{F}_{kin}(\mathbb{V}) \to \mathscr{F}_{kin}(\mathbb{M}) \tag{26}$$

  and is characterized in Equation 8, mapping the configuration to the kinematic observation space.

- The resulting kinematic framework realization is the ordered smooth framework $\Gamma_{kin} = (\mathscr{G}, \mathbf{x}_{kin}, \mathbf{h}_{kin})$.

- **Augmented functor** $\mathscr{F}_{aug}$:
  - The global node configuration induced by $\mathscr{F}_{aug}$ is denoted as $\mathbf{x}_{aug} \in \mathscr{F}_{aug}(\mathbb{V})$, expanding the state space to include auxiliary variables or decoupled degrees of freedom.
  - The measurement function induced by $\mathscr{F}_{aug}$ is defined as

$$\mathbf{h}_{aug} : \mathscr{F}_{aug}(\mathbb{V}) \to \mathscr{F}_{aug}(\mathbb{M}) \tag{27}$$

    and is characterized in Equation 13, evaluating the measurements within the augmented domain.
  - The resulting augmented framework realization is the ordered smooth framework $\Gamma_{aug} = (\mathscr{G}, \mathbf{x}_{aug}, \mathbf{h}_{aug})$.

- **Embedded functor** $\mathscr{F}_{emb}$:
  - The global node configuration induced by $\mathscr{F}_{emb}$ is denoted as $\mathbf{x}_{emb} \in \mathscr{F}_{emb}(\mathbb{V})$, embedding the non-Euclidean manifold coordinates into a higher-dimensional ambient Euclidean space.
  - The measurement function induced by $\mathscr{F}_{emb}$ is defined as

$$\mathbf{h}_{emb} : \mathscr{F}_{emb}(\mathbb{V}) \to \mathscr{F}_{emb}(\mathbb{M}) \tag{28}$$

    and is characterized in Equation 18, formulating the algebraic measurement constraints within the ambient space.
  - The resulting embedded framework realization is the ordered smooth framework $\Gamma_{emb} = (\mathscr{G}, \mathbf{x}_{emb}, \mathbf{h}_{emb})$.

For each of these realizations, defining the group action for each formulation (Φ_{kin}, Φ_{aug}, and Φ_{emb}), the rigidity properties of the framework can be analyzed with respect to a specific smooth group action on its respective state space, naturally inducing three distinct analytical paradigms:

- **Kinematic Φ_{kin}-rigidity** analyzes the rigidity of the native agent configurations, directly assessing the true physical formation of the network.
- **Augmented Φ_{aug}-rigidity** analyzes the rigidity of the state explicitly expanded with extrinsic parameters.

- **Embedded Φ_{emb}-rigidity** analyzes the rigidity of the fully homogenized space.

These framework realizations are formally linked through the natural transformations between their respective functors. By virtue of these established relations, the rigidity matrix of one induced framework can be rigorously mapped to that of another.

Although these three notions of rigidity are mathematically deeply connected thanks to the natural transformations, they differ profoundly in their physical interpretation, making it therefore essential to distinguish between abstract mathematical degrees of freedom and physically realizable motions.

Notably, this methodology is highly modular: it can be seamlessly extended by adding or removing intermediate realizations, depending on the specific structural characteristics one needs to highlight.

3.7 NATURALLY ISOMORPHIC FUNCTORS

In category theory, an isomorphism is defined as a structure-preserving morphism that is fully reversible via an inverse mapping. The fundamental interest in isomorphisms lies in the fact that two isomorphic objects exhibit the exact same structural characteristics. Consequently, isomorphic structures cannot be distinguished through their intrinsic properties alone. They are mathematically treated as identical up to an isomorphism.

Depending on the specific mathematical category under consideration, these preserved characteristics take distinct forms, for example:

- **Algebraic structures:** In vector spaces or groups, an isomorphism is a bijective homomorphism (or linear map) whose inverse is also a homomorphism. This mapping rigorously preserves the algebraic structure: mathematical operations, linear independence, and basis dimensions.

- **Topological structures:** In topological spaces, an isomorphism (a homeomorphism) is a bijective continuous map possessing a continuous inverse. This specific mapping preserves the topological structure: open sets, spatial continuity, and global connectedness.

- **Differential structures:** In differential manifolds, an isomorphism (a diffeomorphism) is a bijective smooth map equipped with a smooth inverse. This specific mapping preserves the differential structure: it ensures that the differential itself is an isomorphism, which guarantees a rigorous bijective mapping between tangent spaces.

- **Relational structures:** In graph theory and network models, an isomorphism is a bijection between vertex sets that strictly preserves edge adjacency. This mapping preserves the relational structure: node connectivity, incidence matrices, and the overall network topology.

- **Metric structures:** In metric spaces, an isomorphism (an isometry) is a bijective map that rigorously preserves the metric structure: the exact quantitative distances between any given pair of points.

When two functors F and G are linked by a natural isomorphism, namely a natural transformation in which all maps between corresponding objects are exclusively isomorphisms, they are classified as *naturally isomorphic functors* (denoted as $F \cong G$). This implies that both functors encapsulate and translate the exact same structural reality into their respective target categories, providing mathematically equivalent representations up to natural isomorphism.

When utilizing naturally isomorphic functors, every single object in the source category is linked to its counterpart via an isomorphism. This establishes commutative diagrams between the two functors, where the natural isomorphism ensures that every associated morphism is perfectly translated.

This dictates that the entire global structures generated by the two functors are identical up to isomorphism. Consequently, all structural properties are strictly preserved across the functors. Therefore, if a specific structural property is mathematically intractable under a functor realization F, one can simply identify a naturally isomorphic functor G where the property becomes tractable. Once the proof is established in the domain of G, the natural isomorphism guarantees that the property remains strictly valid for the original realization F.

Exploiting the induced commutativity between the objects of the isomorphic realization functors, we are not constrained to evaluate the entire map composition within a single monolithic realization. Instead, we can strategically transition between naturally isomorphic functors at different stages of the formulation by gluing them with the appropriate isomorphisms. By bridging these functorial paths through the maps induced by the natural isomorphism, one can assemble the measurement function $\mathbf{h}$ by selecting the most analytically or computationally convenient representation for each specific step of the chain.

We will specifically focus on dfferential structures.

3.8 NATURALLY DIFFEOMORPHIC FUNCTORS

In our specific framework, we formally model the physical state spaces of the agents as *smooth manifolds* and the associated measurement functions as smooth maps. For this reason, we employ realization functors that map from the base category to the category of smooth manifolds. Indeed, when operating within this category, the objects naturally correspond to smooth manifolds and the morphisms to smooth mappings.

Within this category, an isomorphism explicitly manifests as a *diffeomorphism*: a smooth bijection possessing a smooth inverse. By extension, when two functors mapping to smooth manifolds are connected by a natural isomorphism, every component of this transformation is a strict diffeomorphism. We refer to such a natural isomorphism as a *natural diffeomorphism*, and to the associated functors as *naturally diffeomorphic functors*.

The critical advantage of a diffeomorphism is that, in addition to preserving topological properties, it rigorously preserves all differential structures, rendering the manifolds diffeomorphically equivalent.

Because the mapping and its inverse are smooth, the associated differential map is an isomorphism between tangent spaces. Consequently, its local coordinate representation, the Jacobian matrix, is everywhere invertible (i.e., full rank). This guarantees that applying a diffeomorphism does not alter the differential properties and characteristics of the system; for instance, the rank of the Jacobian of a map remains invariant under diffeomorphic transformations.

As a result, when analyzing differential properties (e.g., the *infinitesimal rigidity* of the framework), the analysis can be safely and rigorously transferred across diffeomorphic spaces.

Note that this is a special case of the isomorphic formulation. Therefore, the previously explained approach of exploiting commutativity to relate properties and construct an advantageous measurement function also holds for this special case, with the further advantage that differential properties are preserved across diffeomorphisms.

The utility of this definition becomes particularly evident when considering, for example, a network of n homogeneous agents evolving in $SE(3)$. The global state space can be realized via a *coupled* functor mapping to $(\mathbb{R}^3 \times SO(3))^n$, or via a naturally diffeomorphic *decoupled* functor mapping to $\mathbb{R}^{3n} \times SO(3)^n$. While the coupled form is intuitive for defining distributed control laws, identifying structural decoupling is remarkably easier in the decoupled representation, which explicitly segregates all translational degrees of freedom from the rotational ones. In this decoupled space, the associated Jacobian matrices naturally assume a block-diagonal or highly structured form, significantly simplifying the algebraic computation of their rank. By virtue of the natural diffeomorphism, any topological or differential property proven in the decoupled functor space is intrinsically valid for the coupled formulation. This specific case will be thoroughly investigated in the subsequent section detailing the structure of the embedded rigidity matrix.

4 EMBEDDED RIGIDITY MATRICES

Building upon the abstract categorical architecture established in the previous chapter, this chapter investigates the algebraic structure of the Rigidity Matrix within the Maximal Embedded Functor Realization.

We consider a MAS comprising n agents and m edges, which may intrinsically feature either homogeneous or heterogeneous agents and measurements. Because this chapter specifically investigates the embedded realization of the system, the agent and measurement spaces are rendered homogeneous, even if the original ones are not. Consequently, we assume that the embedding process has already been performed, yielding completely homogeneous agent and measurement spaces across the entire network.

Our analysis focuses on sensory modalities that capture purely distance, purely bearing, or a combination of both quantities simultaneously. More specifically, we restrict our scope to agents operating in 3D space; thus, positions reside in a 3-dimensional Euclidean space ($\mathbb{R}^3$) and rotations belong to the Special Orthogonal group ($\mathbb{SO}(3)$). Consequently, to fully handle this setting, the embedding process must map all agent states into the Special Euclidean group ($\mathbb{SE}(3)$).

Throughout our formulation, we strictly assume a globally collision-free nominal configuration where no two agents in the system are co-located. Formally, the nominal relative distance must satisfy $\|\mathbf{p}_{ij}^*\| = \|\mathbf{p}_j^* - \mathbf{p}_i^*\| > 0$ for all agents $i \neq j$, and consequently for all valid edges in the network. This fundamental assumption guarantees that the measurement functions, the relative geometric mappings, and their corresponding analytical Jacobians remain globally well-defined and free of algebraic singularities.

We model the agents' embedded configuration space as the Special Euclidean group $\mathbb{SE}(3)^n$. Relying on $\mathbb{SE}(3)$ as the maximal ambient manifold for the individual agents represents a natural and non-restrictive choice because it constitutes the group of all rigid-body poses in three-dimensional space.

In general, the choice of intermediate manifolds in the measurement pipeline acts as a flexible design degree of freedom. However, by choosing to propagate this maximal representation across every intermediate stage, we obtain a universally valid realization functor across the entire class of MASs for distance, bearing, and their combinations (i.e., mixed measurements).

The use of this maximal functor realization is inherently general, as it can be applied to any MAS whose agents are embeddable in $\mathbb{SE}(3)^n$ for the measurements addressed in this chapter. Consequently, the resulting embedded rigidity matrices can be directly applied to any compatible system without further structural modification. Furthermore, this approach allows the framework to be easily extended to novel measurement types in the future, preserving the underlying methodology.

The analysis performed within the homogeneous spaces of this maximal embedded functor realization can be extended to heterogeneous MASs through the definition of appropriate embedding functions and their corresponding left inverses. As the subsequent chapter will demonstrate, this allows us to analyze agent rigidity directly within their diverse native spaces. This yields a powerful methodological approach: one can always perform the analysis within the abstract common homogeneous space designed to handle heterogeneity, and subsequently move back to the original spaces. This yields a powerful methodological approach: one can always perform the analysis within the abstract common homogeneous space designed to handle heterogeneity, and subsequently map the results back to the original spaces. This provides a highly flexible analytical framework, as the derived results can be systematically reused across different systems sharing the same embedded spaces.

This chapter formally defines two distinct naturally diffeomorphic geometric functor realizations for the maximal embedded architecture and derives their corresponding rigidity matrices structure. The first is the natively *coupled* embedded realization characterized by the global domain $\mathbb{SE}(3)^n$. The second is the *decoupled* embedded realization featuring the factorized global domain $(\mathbb{R}^3)^n \times \mathbb{SO}(3)^n$.

We conclude by highlighting that the ensuing derivation establishes a general methodology, which can be readily adapted if a different functor realization is selected.

4.1 EMBEDDED FUNCTOR REALIZATIONS

The chosen coupled embedded functor realization for a given measurement task, denoted as $\mathscr{F}^c$, evaluates the state purely on the Special Euclidean group $\mathbb{SE}(3)$. The categorical sequence for this coupled representation is defined as follows:

$$\mathbb{SE}(3)^n \underset{\mu^c_{\text{emb}}}{\overset{\sigma^c_{\text{emb}}}{\rightleftarrows}} (\mathbb{SE}(3) \times \mathbb{SE}(3))^m \xrightarrow{\gamma^c_{\text{emb}}} (\mathbb{SE}(3) \times \mathbb{SE}(3))^m \xrightarrow{\Delta^c_{\text{emb}}} \mathbb{SE}(3)^m \xrightarrow{\eta^c_{\text{emb}}} \mathscr{Y}^m \tag{1}$$

where $\mathscr{Y}^m$ represents the global homogeneous measurement codomain ($\mathscr{Y} = \mathbb{L} = \mathbb{S}^2 \subset \mathbb{R}^3$ for purely bearing edges, $\mathscr{Y} = \mathbb{R}_{>0}$ for purely distance edges, and $\mathscr{Y} = \mathbb{L} \times \mathbb{R}_{>0}$ for mixed measurements).

It is important to note that

$$\mathbb{S}^2 = \left\{ \mathbf{b} \in \mathbb{R}^3 \mid \|\mathbf{b}\|_2 = 1 \right\}$$

is compact and therefore cannot be diffeomorphic to any nonempty open subset of $\mathbb{R}^2$. Consequently, no single coordinate chart can cover $\mathbb{S}^2$ globally. In fact, it is a well-know fact that every smooth atlas of $\mathbb{S}^2$ must contain at least two charts.

Furthermore, it is impossible to define a globally nonsingular two-dimensional tangent coordinate frame on $\mathbb{S}^2$ due to the *Hairy Ball Theorem*, which ensures that every continuous tangent vector field on $\mathbb{S}^2$ must vanish at at least one point.

To avoid these coordinate singularities, we represent the bearing as a Cartesian unit vector using a three-dimensional parametrization, rather than a minimal two-dimensional coordinate representation. Although this representation introduces one redundant ambient coordinate, the vector is tightly constrained by $\|\mathbf{b}\|_2 = 1$, thereby preserving the two strictly intrinsic degrees of freedom of $\mathbb{S}^2$. Crucially, this geometric embedding completely bypasses the topological requirement of utilizing a multi-chart atlas. By operating directly within the ambient space rather than relying on minimal intrinsic coordinates, we eliminate the need to manage local maps or implement chart-switching mechanisms, thereby achieving a single globally valid and completely singularity-free algebraic formulation.

For any $\mathbf{b} \in \mathbb{S}^2$, the tangent space is given by $T_{\mathbf{b}}\mathbb{S}^2 = \left\{ \mathbf{v} \in \mathbb{R}^3 \mid \mathbf{b}^T\mathbf{v} = 0 \right\}$. The orthogonal projector onto this tangent space is defined as

$$\mathbf{\Pi}_{\mathbf{b}} = \mathbf{I}_3 - \mathbf{b}\mathbf{b}^T.$$

Thus, for any ambient vector $\mathbf{u} \in \mathbb{R}^3$, its tangent component at $\mathbf{b}$ is obtained as $\mathbf{u}_{\tan} = \mathbf{\Pi}_{\mathbf{b}}\mathbf{u} \in T_{\mathbf{b}}\mathbb{S}^2$.

It is worth noting that, for every $\mathbf{b} \in \mathbb{S}^2$, this orthogonal projector has constant rank equal to 2. Indeed, since $\|\mathbf{b}\|_2 = 1$, its null space is

$$\ker(\mathbf{\Pi}_{\mathbf{b}}) = \operatorname{span}\{\mathbf{b}\},$$

which corresponds to the radial direction of the sphere and clearly has dimension 1.

Consequently, for any ambient vector $\mathbf{u} \in \mathbb{R}^3$, $\mathbf{\Pi}_{\mathbf{b}}\mathbf{u} \in T_{\mathbf{b}}\mathbb{S}^2$, is precisely the component of $\mathbf{u}$ tangent to the sphere, while its radial component is discarded.

Thus, the projector provides a globally defined, smooth, and constant-rank mechanism for extracting the two-dimensional tangent component without introducing a specific angular coordinate chart. The rank deficiency of $\mathbf{\Pi}_{\mathbf{b}}$ is therefore intentional and structural: it removes the single nonphysical radial degree of freedom and preserves exactly the two intrinsic degrees of freedom of the bearing manifold.

Ultimately, the embedded representation avoids the coordinate singularities associated with angular parametrizations at the cost of using a redundant ambient representation. To make this choice explicit, we denote the bearing measurement space as $\mathbb{L} = \mathbb{S}^2 \subset \mathbb{R}^3$.

To explicitly expose the translational and rotational degrees of freedom, we exploit the natural Cartesian diffeomorphism $\mathbb{SE}(3) \cong \mathbb{R}^3 \times \mathbb{SO}(3)$ at the local agent level. By systematically lifting this factorization to the global network configuration, we establish the equivalence $\mathbb{SE}(3)^n \cong (\mathbb{R}^3)^n \times \mathbb{SO}(3)^n$ and seamlessly propagate this decoupled state space throughout the entire sequence. This yields the alternative, fully pose-decoupled functor realization $\mathscr{F}^d$:

$$(\mathbb{R}^3)^n \times \mathbb{SO}(3)^n \underset{\mu^d_{\text{emb}}}{\overset{\sigma^d_{\text{emb}}}{\rightleftarrows}} \left(\mathbb{R}^3 \times \mathbb{R}^3\right)^m \times (\mathbb{SO}(3) \times \mathbb{SO}(3))^m \xrightarrow{\gamma^d_{\text{emb}}} \left(\mathbb{R}^3 \times \mathbb{R}^3\right)^m \times (\mathbb{SO}(3) \times \mathbb{SO}(3))^m \xrightarrow{\Delta^d_{\text{emb}}} (\mathbb{R}^3)^m \times \mathbb{SO}(3)^m \xrightarrow{\eta^d_{\text{emb}}} \mathscr{Y}^m \tag{2}$$

Because all corresponding manifolds within the two realizations are diffeomorphic, and the structural mappings flawlessly preserve these differentiable structures, the two sequences represent naturally diffeomorphic functors ($\mathscr{F}^c \cong \mathscr{F}^d$). By explicitly tracing these transformations, we obtain the overarching commutative diagram:

$$\begin{tikzcd}
\mathbb{SE}(3)^n \arrow[r, shift left, "\sigma^c_{\text{emb}}"] \arrow[d, shift left, "\phi_{\mathscr{V}}"] \arrow[d, phantom, "\cong"] & (\mathbb{SE}(3) \times \mathbb{SE}(3))^m \arrow[l, shift left, "\mu^c_{\text{emb}}"] \arrow[r, "\gamma^c_{\text{emb}}"] \arrow[d, shift left, "\phi_{\mathscr{E}}"] \arrow[d, phantom, "\cong"] & (\mathbb{SE}(3) \times \mathbb{SE}(3))^m \arrow[r, "\Delta^c_{\text{emb}}"] \arrow[d, shift left, "\phi_{\mathscr{T}}"] \arrow[d, phantom, "\cong"] & \mathbb{SE}(3)^m \arrow[r, "\eta^c_{\text{emb}}"] \arrow[d, shift left, "\phi_{\mathscr{O}}"] \arrow[d, phantom, "\cong"] & \mathscr{Y}^m \arrow[d, shift left, "\text{id}"] \arrow[d, phantom, "="] \\
(\mathbb{R}^3)^n \times \mathbb{SO}(3)^n \arrow[r, shift left, "\sigma^d_{\text{emb}}"] \arrow[u, shift left, "\phi^{-1}_{\mathscr{V}}"] & \left(\mathbb{R}^3 \times \mathbb{R}^3\right)^m \times (\mathbb{SO}(3) \times \mathbb{SO}(3))^m \arrow[l, shift left, "\mu^d_{\text{emb}}"] \arrow[r, "\gamma^d_{\text{emb}}"] \arrow[u, shift left, "\phi^{-1}_{\mathscr{E}}"] & \left(\mathbb{R}^3 \times \mathbb{R}^3\right)^m \times (\mathbb{SO}(3) \times \mathbb{SO}(3))^m \arrow[r, "\Delta^d_{\text{emb}}"] \arrow[u, shift left, "\phi^{-1}_{\mathscr{T}}"] & (\mathbb{R}^3)^m \times \mathbb{SO}(3)^m \arrow[r, "\eta^d_{\text{emb}}"] \arrow[u, shift left, "\phi^{-1}_{\mathscr{O}}"] & \mathscr{Y}^m \arrow[u, shift left, "\text{id}"]
\end{tikzcd} \tag{3}$$

The vertical isomorphisms representing the natural diffeomorphism are specifically defined as follows:

- $\phi_{\mathscr{V}}$ applies the pose decoupling element-wise to the n global node states.
- $\phi_{\mathscr{E}}$ and $\phi_{\mathscr{T}}$ apply the analogous decoupling to the $2m$ source and target states associated with the network edges, before and after filtration.
- $\phi_{\mathscr{O}}$ factorizes the m relative poses derived from the kinematic observation mappings.
- id represents the identity mapping on the final measurement codomain, which is physically invariant and inherently requires no decoupling.

4.2 NOTATION AND CONVENTIONS

Throughout our derivations, we assume the system operates around a nominal configuration. Let the superscript $\tau \in \{c, d\}$ denote the specific functor realization under analysis, where:

- $\tau = c$ represents the *coupled* realization operating natively on $\mathbb{SE}(3)$ at the local agent level;

- $\tau = d$ represents the *decoupled* formulation operating on $\mathbb{R}^3 \times \mathbb{SO}(3)$ at the local agent level.

As the nominal state propagates through the functorial sequence, it defines specific evaluation points mapped onto each intermediate manifold, structured systematically across local edge descriptions and global network domains:

- **1. Initial Agents State:**
  - *Local (Agent level):*
    - Coupled: $\mathbf{x}_i^{c*} = (\mathbf{p}_i^*, \mathbf{R}_i^*) \in \mathbb{SE}(3)$
    - Decoupled: $\mathbf{x}_i^{d*} = (\mathbf{p}_i^*, \mathbf{R}_i^*) \in \mathbb{R}^3 \times \mathbb{SO}(3)$
  - *Global (Network level):*
    - Coupled: $\mathbf{x}^{c*} = (\mathbf{x}_1^*, \dots, \mathbf{x}_n^*) \in \mathbb{SE}(3)^n$
    - Decoupled: $\mathbf{x}^{d*} = \big((\mathbf{p}_1^*, \dots, \mathbf{p}_n^*), (\mathbf{R}_1^*, \dots, \mathbf{R}_n^*)\big) \in (\mathbb{R}^3)^n \times \mathbb{SO}(3)^n$
- **2. Edge State ($\mathbf{e}^{\tau*} = \sigma_{\text{emb}}^{\tau}(\mathbf{x}^{\tau*})$):**
  - *Local (k-th edge $e_k = (i, j)$):*
    - Coupled: $\mathbf{e}_k^{c*} = (\mathbf{x}_i^*, \mathbf{x}_j^*) = ((\mathbf{p}_i^*, \mathbf{R}_i^*), (\mathbf{p}_j^*, \mathbf{R}_j^*)) \in \mathbb{SE}(3) \times \mathbb{SE}(3)$
    - Decoupled: $\mathbf{e}_k^{d*} = \big((\mathbf{p}_i^*, \mathbf{p}_j^*), (\mathbf{R}_i^*, \mathbf{R}_j^*)\big) \in (\mathbb{R}^3 \times \mathbb{R}^3) \times (\mathbb{SO}(3) \times \mathbb{SO}(3))$
  - *Global (All edges):*
    - Coupled: $\mathbf{e}^{c*} = (\mathbf{e}_1^{c*}, \dots, \mathbf{e}_m^{c*}) \in (\mathbb{SE}(3) \times \mathbb{SE}(3))^m$
    - Decoupled: $\mathbf{e}^{d*} = \big(((\mathbf{p}_{s_1}^*, \mathbf{p}_{t_1}^*), \dots, (\mathbf{p}_{s_m}^*, \mathbf{p}_{t_m}^*)), ((\mathbf{R}_{s_1}^*, \mathbf{R}_{t_1}^*), \dots, (\mathbf{R}_{s_m}^*, \mathbf{R}_{t_m}^*))\big) \in \big(\mathbb{R}^3 \times \mathbb{R}^3\big)^m \times (\mathbb{SO}(3) \times \mathbb{SO}(3))^m$
- **3. Filtered Padded State ($\tilde{\mathbf{e}}^{\tau*} = \gamma_{\text{emb}}^{\tau}(\mathbf{e}^{\tau*})$):**
  - *Local (k-th edge $e_k = (i, j)$):*
    - Coupled: $\tilde{\mathbf{e}}_k^{c*} = ((\mathbf{p}_i^*, \tilde{\mathbf{R}}_i^*), (\mathbf{p}_j^*, \tilde{\mathbf{R}}_j^*)) \in \mathbb{SE}(3) \times \mathbb{SE}(3)$
    - Decoupled: $\tilde{\mathbf{e}}_k^{d*} = \big((\mathbf{p}_i^*, \mathbf{p}_j^*), (\tilde{\mathbf{R}}_i^*, \tilde{\mathbf{R}}_j^*)\big) \in (\mathbb{R}^3 \times \mathbb{R}^3) \times (\mathbb{SO}(3) \times \mathbb{SO}(3))$
  - *Global (All edges):*
    - Coupled: $\tilde{\mathbf{e}}^{c*} = (\tilde{\mathbf{e}}_1^{c*}, \dots, \tilde{\mathbf{e}}_m^{c*}) \in (\mathbb{SE}(3) \times \mathbb{SE}(3))^m$
    - Decoupled: $\tilde{\mathbf{e}}^{d*} = \big(((\mathbf{p}_{s_1}^*, \mathbf{p}_{t_1}^*), \dots, (\mathbf{p}_{s_m}^*, \mathbf{p}_{t_m}^*)), ((\tilde{\mathbf{R}}_{s_1}^*, \tilde{\mathbf{R}}_{t_1}^*), \dots, (\tilde{\mathbf{R}}_{s_m}^*, \tilde{\mathbf{R}}_{t_m}^*))\big) \in \big(\mathbb{R}^3 \times \mathbb{R}^3\big)^m \times (\mathbb{SO}(3) \times \mathbb{SO}(3))^m$
- **4. Relative Observation State ($\mathbf{o}^{\tau*} = \Delta_{\text{emb}}^{\tau}(\tilde{\mathbf{e}}^{\tau*})$):**
  - *Local (k-th edge $e_k = (i, j)$):*
    - Coupled: $\mathbf{o}_k^{c*} = (\tilde{\mathbf{p}}_{ij}^*, \tilde{\mathbf{R}}_{ij}^*) \in \mathbb{SE}(3)$

    * Decoupled: $\mathbf{o}_k^{d*} = (\tilde{\mathbf{p}}_{ij}^*, \tilde{\mathbf{R}}_{ij}^*) \in \mathbb{R}^3 \times \mathbb{SO}(3)$
  - *Global (All edges):*
    * Coupled: $\mathbf{o}^{c*} = (\mathbf{o}_1^{c*}, \dots, \mathbf{o}_m^{c*}) \in \mathbb{SE}(3)^m$
    * Decoupled: $\mathbf{o}^{d*} = \big((\tilde{\mathbf{p}}_{s_1t_1}^*, \dots, \tilde{\mathbf{p}}_{s_mt_m}^*), (\tilde{\mathbf{R}}_{s_1t_1}^*, \dots, \tilde{\mathbf{R}}_{s_mt_m}^*)\big) \in (\mathbb{R}^3)^m \times \mathbb{SO}(3)^m$

Note that while the tilde notation $\tilde{(\cdot)}$ generically denotes a filtered or padded quantity, its specific action depends entirely on the measurement model. For the distance and bearing measurements in 3D space considered in this chapter, positional information is strictly required to compute relative spatial vectors. Consequently, the filtration map leaves positional coordinates unaltered, yielding $\tilde{\mathbf{p}}_i^* = \mathbf{p}_i^*$ and $\tilde{\mathbf{p}}_{ij}^* = \tilde{\mathbf{p}}_j^* - \tilde{\mathbf{p}}_i^* = \mathbf{p}_{ij}^*$. Unobservable rotational information, instead, is selectively masked (e.g., padded with $\mathbf{I}_3$) based on the measurement modality and the agent's topological role.

We emphasize that this positional invariance is specific to the chosen setup. For different sensing paradigms, the framework remains fully adaptable, allowing the filtration map to be custom-tailored to actively mask or modify positions as well (i.e., $\tilde{\mathbf{p}}_i^* \neq \mathbf{p}_i^*$).

4.3 GEOMETRIC TANGENT SPACE FACTORIZATION

Before deriving the specific intermediate mappings for the coupled and decoupled realizations, it is crucial to establish how the differential geometry of the underlying state manifolds dictates the algebraic structure of all ensuing Jacobian matrices.

4.3.1 Representation and Tangent-Space Parameterization Conventions

To concretize the transition from abstract differentials to the explicit Jacobian matrices used throughout this chapter, we first establish the coordinate conventions for the agent states and their tangent-space variations. Recognizing the heterogeneous nature of the framework, we consider agents operating in d-dimensional Euclidean spaces (with $d \in \{2, 3\}$), distinguishing between the configuration representation and the coordinate representation of infinitesimal variations on the corresponding tangent spaces.

The position of agent i is denoted by $\mathbf{p}_i^W \in \mathbb{R}^d$, where the superscript W emphasizes the global world frame. Accordingly, translational variations are standard Euclidean increments:

$$\delta \mathbf{p}_i^W \in T_{\mathbf{p}_i^W} \mathbb{R}^d \cong \mathbb{R}^d. \tag{4}$$

The orientation representation depends on the spatial dimension of the agent's operational space. For 3D agents, orientation is represented by a rotation matrix $\mathbf{R}_i \in \mathbb{SO}(3)$

mapping coordinates from the agent's local (body) frame to the world frame, i.e., $\mathbf{v}^W = \mathbf{R}_i \mathbf{v}^i$. For infinitesimal rotational variations, we adopt the right-trivialized representation:

$$\delta \mathbf{R}_i = \mathbf{R}_i [\delta \boldsymbol{\theta}_i^B]_\times, \tag{5}$$

where $\delta \boldsymbol{\theta}_i^B \in \mathbb{R}^3$ denotes the minimal rotational variation expressed in the local body frame (indicated by the superscript B), and $[\cdot]_\times$ is the skew-symmetric matrix operator (satisfying $[\delta \boldsymbol{\theta}_i^B]_\times = \mathbf{R}_i^T \delta \mathbf{R}_i$). Conversely, for planar agents, the orientation is represented by $\mathbf{R}_i \in \mathbb{SO}(2)$. Since $\mathbb{SO}(2)$ is an Abelian Lie group, left and right trivializations coincide. Consequently, the choice of trivialization does not affect the resulting scalar rotational tangent coordinate. The Lie algebra $\mathfrak{so}(2)$ is one-dimensional, so the infinitesimal rotational variation is represented by a scalar $\delta\theta_i \in \mathbb{R}$, corresponding to the variation of the agent's planar heading angle.

The complete pose of each agent is defined on the Special Euclidean group $\mathbb{SE}(d)$, which we identify via its standard Cartesian factorization:

$$\mathbf{x}_i \in \mathbb{SE}(d) \cong \mathbb{R}^d \times \mathbb{SO}(d). \tag{6}$$

Consequently, the tangent space admits the product decomposition

$$T_{\mathbf{x}_i} \mathbb{SE}(d) \cong T_{\mathbf{p}_i^W} \mathbb{R}^d \oplus T_{\mathbf{R}_i} \mathbb{SO}(d), \tag{7}$$

which, under the chosen tangent-space coordinates, evaluates to

$$T_{\mathbf{x}_i} \mathbb{SE}(3) \cong T_{\mathbf{p}_i^W} \mathbb{R}^3 \oplus T_{\mathbf{R}_i} \mathbb{SO}(3) \cong \mathbb{R}^3 \times \mathbb{R}^3 \cong \mathbb{R}^6 \tag{8}$$

$$T_{\mathbf{x}_i} \mathbb{SE}(2) \cong T_{\mathbf{p}_i^W} \mathbb{R}^2 \oplus T_{\mathbf{R}_i} \mathbb{SO}(2) \cong \mathbb{R}^2 \times \mathbb{R}^1 \cong \mathbb{R}^3 \tag{9}$$

We define the corresponding tangent coordinates explicitly depending on the agent's operational space:

$$\delta \mathbf{x}_i = \begin{cases} \left[(\delta \mathbf{p}_i^W)^T \quad (\delta \boldsymbol{\theta}_i^B)^T \right]^T \in \mathbb{R}^6, & \text{for 3D agents} \\ \left[(\delta \mathbf{p}_i^W)^T \quad \delta\theta_i \right]^T \in \mathbb{R}^3, & \text{for 2D agents} \end{cases} \tag{10}$$

This mixed-frame convention combining world-frame translational increments with local-frame (or scalar) rotational increments is entirely intentional, as it significantly simplifies the analytical derivation of the Jacobian matrices in subsequent sections by decoupling translational kinematics from orientation.

It is crucial to distinguish these coordinates from the standard right-trivialized coordinates of the full Lie algebra. In a pure Lie-algebraic setting for 3D systems, the translational variation would also be expressed in the local frame (e.g., $\delta \boldsymbol{\rho}_i^B$) satisfying $\delta \mathbf{p}_i^W = \mathbf{R}_i \delta \boldsymbol{\rho}_i^B$. By directly employing $\delta \mathbf{p}_i^W$ alongside $\delta \boldsymbol{\theta}_i^B$ (or $\delta\theta_i$), we treat $\delta \mathbf{x}_i$ strictly as the coordinate representation induced by the product decomposition $\mathbb{SE}(d) \cong \mathbb{R}^d \times \mathbb{SO}(d)$.

Finally, for 3-dimensional directional quantities (such as line-of-sight measurements), the representation space is the unit sphere $\mathbb{L} = \mathbb{S}^2 \subset \mathbb{R}^3$. For a direction vector $\mathbf{b} \in \mathbb{S}^2$, any infinitesimal variation $\delta\mathbf{b} \in \mathbb{R}^3$ must lie strictly within the tangent plane at $\mathbf{b}$, imposing the geometric constraint $\mathbf{b}^T\delta\mathbf{b} = 0$. Throughout this work, this condition is algebraically enforced via the orthogonal projector $\mathbf{\Pi_b} = \mathbf{I}_3 - \mathbf{b}\mathbf{b}^T$.

These coordinate conventions fundamentally shape the algebraic interpretation of relative quantities. Because all agent positions are universally tracked in the common world frame, the relative position associated with a directed edge $e_k = (i, j)$ is simply evaluated via linear algebraic difference:

$$\mathbf{p}_{ij}^W = \mathbf{p}_j^W - \mathbf{p}_i^W, \tag{11}$$

with the corresponding tangent variation being naturally linear, $\delta\mathbf{p}_{ij}^W = \delta\mathbf{p}_j^W - \delta\mathbf{p}_i^W$. Note that rotational transformations are applied exclusively when a relative vector must be re-expressed in a local coordinate frame. For instance, the line-of-sight direction measured in the local frame of agent i is straightforwardly computed as:

$$\mathbf{b}_{ij} = \frac{\mathbf{R}_i^T\mathbf{p}_{ij}^W}{\|\mathbf{p}_{ij}^W\|}. \tag{12}$$

Having rigorously established these coordinate definitions, the frame superscripts (e.g., W and B) will be systematically omitted hereafter to lighten the notation, as the reference frames for both configurations and their tangent variations are now unambiguously fixed.

Once the tangent-space coordinates have been fixed, the Jacobians derived throughout this chapter follow specific evaluation conventions dictated by the geometric nature of their underlying mappings. Linear or purely selective mappings yield constant Jacobians that are completely independent of the state. In these cases, we explicitly drop the nominal evaluation points from the notation, as these invariant matrices apply universally to any evaluation point. A degenerate case consists of constant mappings and padding elements, where the exact differentials evaluate trivially to zero. Conversely, non-linear mappings require explicit evaluation at their respective propagated operational points. Consequently, any state variable appearing within an evaluated Jacobian matrix represents its value frozen at the nominal configuration.

4.3.2 General Principles of Product Manifolds

The geometric structure of a product manifold algebraically factorizes because its tangent space is naturally isomorphic to the direct sum of the individual tangent spaces. Formally, given a Cartesian product of manifolds $\mathscr{A} = \prod_{i=1}^n \mathscr{A}_i$ and a nominal point $\mathbf{x}^* = (\mathbf{x}_1^*, \dots, \mathbf{x}_n^*)$, this foundational isomorphism is expressed as:

$$T_{\mathbf{x}^*}(\mathscr{A}_1 \times \cdots \times \mathscr{A}_n) \equiv T_{\mathbf{x}^*}\left(\prod_{i=1}^n \mathscr{A}_i\right) \cong \bigoplus_{i=1}^n T_{\mathbf{x}_i^*}\mathscr{A}_i \equiv T_{\mathbf{x}_1^*}\mathscr{A}_1 \oplus \cdots \oplus T_{\mathbf{x}_n^*}\mathscr{A}_n. \tag{13}$$

Consequently, any infinitesimal variation $\delta\mathbf{x}$ within this joint tangent space is natively represented by the ordered vertical concatenation (stacking) of the local variations $\delta\mathbf{x}_i \in T_{\mathbf{x}_i^*}\mathscr{A}_i$:

$$\delta\mathbf{x} = \begin{bmatrix} \delta\mathbf{x}_1 \\ \vdots \\ \delta\mathbf{x}_n \end{bmatrix}. \tag{14}$$

Now, consider a smooth map $f : \mathscr{M} \to \mathscr{N}$ between two generic manifolds. The push-forward (or exact differential) $df_{\mathbf{x}^*} : T_{\mathbf{x}^*}\mathscr{M} \to T_{f(\mathbf{x}^*)}\mathscr{N}$ is fundamentally a coordinate-free linear operator acting between their respective tangent spaces.

To evaluate this differential computationally, we must transition to its local formulation. By establishing local charts around the nominal point $\mathbf{x}^*$ and its mapped image $f(\mathbf{x}^*)$, we map these abstract tangent spaces onto Euclidean vector spaces. The Jacobian matrix is precisely the local coordinate representation of the differential with respect to the bases induced by these chosen charts.

The Jacobian matrix rigorously inherits the abstract topological architecture of the tangent spaces, manifesting as a highly structured matrix. Specifically, a direct sum decomposition in the domain's tangent space ($\mathscr{M}$) induces a strict block-column partition in the Jacobian matrix, where each column-block captures the partial derivative with respect to an independent input subspace. Conversely, a direct sum decomposition in the codomain's tangent space ($\mathscr{N}$) induces a strict block-row partition, systematically segregating the independent output components.

Therefore, the block occupying row i and column j of the Jacobian represents the local coordinate mapping of the partial derivative of the i-th output local component with respect to the j-th input local component ($\partial\mathbf{y}_i/\partial\mathbf{x}_j$).

We will actively exploit this principle across two distinct geometric architectures. To facilitate the exposition, we distinguish between *local maps*, which operate on individual nodes or edges to compute local quantities, and *global maps*, which operate collectively across all nodes or edges to evaluate network-wide quantities.

For the MASs considered here, the local state of an individual agent resides in the Special Euclidean group $\mathbb{SE}(3)$. By exploiting the local Cartesian diffeomorphism $\mathbb{SE}(3) \cong \mathbb{R}^3 \times \mathbb{SO}(3)$, this local tangent space inherently decomposes into independent translational and rotational sub-domains:

$$T_{\mathbf{x}_i^*}\mathbb{SE}(3) \cong T_{\mathbf{p}_i^*}\mathbb{R}^3 \oplus T_{\mathbf{R}_i^*}\mathbb{SO}(3). \tag{15}$$

This internal structure forces any local derivative acting on a single agent to naturally partition into distinct positional and rotational sub-blocks.

4.3.3 Tangent Space Structure in the Coupled Architecture

When expanding to the local edge level, the domain encompasses the coupled state pairs of the interacting agents, $\mathbb{SE}(3)\times\mathbb{SE}(3)$. Its tangent space strictly factorizes into the direct sum of the source and target tangent spaces:

$$T_{\mathbf{e}_k^{c*}}\big(\mathbb{SE}(3)\times\mathbb{SE}(3)\big) \cong T_{\mathbf{x}_i^*}\mathbb{SE}(3)\oplus T_{\mathbf{x}_j^*}\mathbb{SE}(3) \cong \Big(T_{\mathbf{p}_i^*}\mathbb{R}^3 \oplus T_{\mathbf{R}_i^*}\mathbb{SO}(3)\Big)\oplus\Big(T_{\mathbf{p}_j^*}\mathbb{R}^3 \oplus T_{\mathbf{R}_j^*}\mathbb{SO}(3)\Big). \tag{16}$$

As a mathematical consequence, any local Jacobian mapping from this coupled edge space universally exhibits a foundational 12-column structure that strictly mirrors this hierarchical geometric decomposition. Primarily, the columns are partitioned into two independent 6-DOF nodal macro-blocks explicitly associated with the source agent i and the target agent j. Subsequently, as established above, each of these nodal macro-blocks further subdivides internally into a 3-DOF purely positional sub-block and a 3-DOF purely rotational sub-block.

At the global network level, the coupled state manifold is defined as $\overline{\mathscr{D}}^c = \mathbb{SE}(3)^n$. Its global tangent space expands into a sequentially ordered direct sum across all n agents:

$$T_{\mathbf{x}^{c*}}\overline{\mathscr{D}}^c \cong \bigoplus_{i=1}^{n} T_{\mathbf{x}_i^*}\mathbb{SE}(3) \cong \bigoplus_{i=1}^{n}\Big(T_{\mathbf{p}_i^*}\mathbb{R}^3 \oplus T_{\mathbf{R}_i^*}\mathbb{SO}(3)\Big). \tag{17}$$

Just as in the local formulation, this dictates a strict hierarchical column structure for any global mapping originating from this domain. Primarily, the global domain decomposes into n independent 6-DOF macro-blocks, isolating the full pose variations agent by agent. Subsequently, every single one of these n macro-blocks internally maintains the explicit separation between translational and rotational sub-blocks.

Similarly, the globally coupled edge manifold $\overline{\mathscr{M}}_e^c = (\mathbb{SE}(3)\times\mathbb{SE}(3))^m$ factorizes as the direct sum over all m independent edges. To fully expose this nested structure, we expand the direct sum down to its foundational sub-domains:

$$T_{\mathbf{e}^{c*}}\overline{\mathscr{M}}_e^c \cong \bigoplus_{k=1}^{m}\Big(T_{\mathbf{x}_{s_k}^*}\mathbb{SE}(3)\oplus T_{\mathbf{x}_{t_k}^*}\mathbb{SE}(3)\Big) \cong \bigoplus_{k=1}^{m}\bigg(\Big(T_{\mathbf{p}_{s_k}^*}\mathbb{R}^3 \oplus T_{\mathbf{R}_{s_k}^*}\mathbb{SO}(3)\Big)\oplus\Big(T_{\mathbf{p}_{t_k}^*}\mathbb{R}^3 \oplus T_{\mathbf{R}_{t_k}^*}\mathbb{SO}(3)\Big)\bigg). \tag{18}$$

This establishes a rigorous three-tiered hierarchical grid for any Jacobian mapping into or out of this edge space. Primarily, the matrix partitions into m distinct 12-DOF macro-blocks, segregating the network edge by edge. Subsequently, each edge block bifurcates into source node and target node 6-DOF components. Finally, these nodal components subdivide into their pure positional and rotational 3-DOF blocks.

Consequently, any overarching local and global Jacobians acting on the coupled architecture studied in this chapter systematically preserve this deeply structured form.

4.3.4 Tangent Space Structure in the Decoupled Architecture

While the coupled formulation groups kinematics by agent, the decoupled realization exploits the global Cartesian diffeomorphism to completely separate translational and rotational physics.

When expanding to the local edge level, the domain encompasses the decoupled state pairs of the interacting agents, $(\mathbb{R}^3 \times \mathbb{R}^3) \times (\mathbb{SO}(3) \times \mathbb{SO}(3))$. Its tangent space strictly factorizes into the direct sum of the positional and rotational tangent spaces:

$$T_{\mathbf{e}_k^{d*}} \mathcal{M}_e^d \cong \left(T_{\mathbf{p}_i^*}\mathbb{R}^3 \oplus T_{\mathbf{p}_j^*}\mathbb{R}^3\right) \oplus \left(T_{\mathbf{R}_i^*}\mathbb{SO}(3) \oplus T_{\mathbf{R}_j^*}\mathbb{SO}(3)\right). \tag{19}$$

As a mathematical consequence, any local Jacobian mapping from this decoupled edge space universally exhibits a foundational 12-column structure that strictly mirrors this hierarchical decomposition. Primarily, the columns are partitioned into two independent 6-DOF macroscopic macro-blocks explicitly associated with the purely positional and purely rotational streams. Subsequently, each of these macro-blocks further subdivides internally into a 3-DOF source agent sub-block and a 3-DOF target agent sub-block.

At the global network level, the decoupled state manifold is defined as $\overline{\mathcal{D}}^d = (\mathbb{R}^3)^n \times (\mathbb{SO}(3))^n$. Its global tangent space expands into a sequentially ordered direct sum perfectly segregated into macroscopic positional and rotational domains:

$$T_{\mathbf{x}^{d*}} \overline{\mathcal{D}}^d \cong \left(\bigoplus_{i=1}^{n} T_{\mathbf{p}_i^*}\mathbb{R}^3\right) \oplus \left(\bigoplus_{i=1}^{n} T_{\mathbf{R}_i^*}\mathbb{SO}(3)\right). \tag{20}$$

Just as in the local formulation, this dictates a strict hierarchical column structure for any global mapping originating from this domain. Primarily, the global domain decomposes into two $3n$-DOF macro-blocks, isolating all network positions from all network rotations. Subsequently, every single one of these two macro-blocks internally maintains the explicit separation agent by agent across the n individual nodal components.

Similarly, the globally decoupled edge manifold $\overline{\mathcal{M}}_e^d = \left(\mathbb{R}^3 \times \mathbb{R}^3\right)^m \times (\mathbb{SO}(3) \times \mathbb{SO}(3))^m$ factorizes as the direct sum segregating all m translational edge domains from all m rotational edge domains. To fully expose this nested structure, we expand the direct sum down to its foundational sub-domains:

$$T_{\mathbf{e}^{d*}} \overline{\mathcal{M}}_e^d \cong \left(\bigoplus_{k=1}^{m} \left(T_{\mathbf{p}_{s_k}^*}\mathbb{R}^3 \oplus T_{\mathbf{p}_{t_k}^*}\mathbb{R}^3\right)\right) \oplus \left(\bigoplus_{k=1}^{m} \left(T_{\mathbf{R}_{s_k}^*}\mathbb{SO}(3) \oplus T_{\mathbf{R}_{t_k}^*}\mathbb{SO}(3)\right)\right). \tag{21}$$

This establishes a rigorous three-tiered hierarchical grid for any Jacobian mapping into or out of this edge space. Primarily, the matrix partitions into two distinct $6m$-DOF macro-blocks, segregating the physical domains globally. Subsequently, each domain block bifurcates into m distinct 6-DOF components, segregating the network edge by edge. Finally, these edge components subdivide into their pure source node and target node 3-DOF blocks.

Consequently, any overarching local and global Jacobians acting on the decoupled architecture that we will study in the chapter systematically preserve this deeply structured form.

4.3.5 Algebraic Sparsity and Kronecker Construction

As established, the domain and codomain factorizations naturally cast the global Jacobian into a precise grid of blocks. The block occupying row i and column j explicitly represents the partial derivative of the i-th local output component with respect to the j-th local input component ($\partial \mathbf{y}_i / \partial \mathbf{x}_j$). Whenever an output component is functionally independent of a given input component, the corresponding cross-derivative vanishes identically, yielding a zero block.

When this independence occurs systematically across the network, such as when intermediate framework mappings process edge pairs completely independently, cross-edge derivatives inherently vanish, and the resulting global Jacobian becomes highly sparse. In the extreme, yet recurring, case where every output component depends on one isolated input component, all off-diagonal blocks vanish entirely, naturally collapsing the overarching Jacobian into a purely block-diagonal matrix.

To systematically construct these large sparse matrices and streamline the mathematical notation in the following sections, we extensively leverage the Kronecker product ($\otimes$) primarily in two distinct algebraic contexts:

- **Homogeneous Block-Diagonal Replication:** For a generic local matrix $\mathbf{M}$, the operation $\mathbf{I}_k \otimes \mathbf{M}$ naturally constructs a large block-diagonal matrix containing k identical copies of $\mathbf{M}$ along its main diagonal:

$$\mathbf{I}_k \otimes \mathbf{M} = \operatorname{blockdiag}_{i=1}^{k}(\mathbf{M}). \tag{22}$$

  We utilize this property to seamlessly elevate identical constant local mappings to the global network level.

- **Sparse Block-Selector Operators:** Let $\mathbf{u}_i \in \mathbb{R}^n$ denote the i-th canonical basis vector (having a 1 at the i-th position and 0 elsewhere). Let d denote the dimension of the local state block being extracted. The generic block-selector operator $\mathbf{u}_i^T \otimes \mathbf{I}_d \in \mathbb{R}^{d \times dn}$ algebraically extracts the i-th node's d-DOF contribution directly from the global state vector. Explicitly, it takes the form of a sparse block-row matrix:

$$\mathbf{u}_i^T \otimes \mathbf{I}_d = \begin{bmatrix} \mathbf{0}_{d\times d} & \cdots & \underbrace{\mathbf{I}_d}_{i\text{-th block}} & \cdots & \mathbf{0}_{d\times d} \end{bmatrix}. \tag{23}$$

  In the context of this chapter, $d = 3$ for isolated positional or rotational components in the decoupled framework, and $d = 6$ for the full coupled pose.

4.4 COUPLED EMBEDDED RIGIDITY MATRIX

In this section, we systematically analyze the natively coupled embedded functor realization, denoted as $\mathscr{F}^c$, and explicitly derive the algebraic structure of the corresponding coupled rigidity matrix. By analytically evaluating the local mappings and topologically assembling their Jacobians across the network, we construct the global embedded rigidity matrix.

4.4.1 Coupled Topological Distribution Map

The coupled topological distribution map $\boldsymbol{\sigma}^c_{\text{emb}}$ linearly aggregates the global states by duplicating and routing them to their corresponding edge slots. For a network of n agents and m edges, the mapping is formally defined as:

$$\begin{aligned} \boldsymbol{\sigma}^c_{\text{emb}} :\ \mathbb{SE}(3)^n &\to (\mathbb{SE}(3) \times \mathbb{SE}(3))^m \\ (\mathbf{x}_1, \dots, \mathbf{x}_n) &\mapsto \big((\mathbf{x}_{s_1}, \mathbf{x}_{t_1}), \dots, (\mathbf{x}_{s_m}, \mathbf{x}_{t_m})\big) \end{aligned} \tag{24}$$

where $e_k = (s_k, t_k)$ denotes the k-th directed edge originating from the source node s_k and pointing to the target node t_k.

Evaluated at the nominal global configuration $\mathbf{x}^{c*} = (\mathbf{x}^*_1, \dots, \mathbf{x}^*_n)$, the mapping produces the nominal edge state $\mathbf{e}^{c*} = \boldsymbol{\sigma}^c_{\text{emb}}(\mathbf{x}^{c*})$.

Because $\boldsymbol{\sigma}^c_{\text{emb}}$ is a pure linear selection mapping, its Jacobian is entirely state-invariant. Consequently, we explicitly drop the evaluation argument and express its global Jacobian $\mathbf{J}^c_\sigma \in \mathbb{R}^{12m\times 6n}$ as a universally constant sparse block matrix. Utilizing the coupled block-selector operators, the k-th block row for a generic edge $e_k = (i, j)$ is rigorously formulated as an incidence-selection matrix:

$$[\mathbf{J}^c_\sigma]_k = \begin{bmatrix} \mathbf{u}_i^T \otimes \mathbf{I}_6 \\ \mathbf{u}_j^T \otimes \mathbf{I}_6 \end{bmatrix} \in \mathbb{R}^{12\times 6n} \tag{25}$$

This explicitly extracts the coupled 6-DOF states of the source node i and target node j. The full constant global matrix $\mathbf{J}^c_\sigma$ is constructed by vertically stacking these m constant block rows:

$$\mathbf{J}^c_\sigma = \begin{bmatrix} [\mathbf{J}^c_\sigma]_1 \\ [\mathbf{J}^c_\sigma]_2 \\ \vdots \\ [\mathbf{J}^c_\sigma]_m \end{bmatrix} \in \mathbb{R}^{12m\times 6n}. \tag{26}$$

4.4.2 Coupled Task Filtration Maps

To isolate the measurable components from the fully embedded edge states, the Coupled Task Filtration Map filters out the unobservable degrees of freedom for a specific task and replaces them with neutral informationless padding.

Local Filtration Maps and Jacobians

Let the nominal unpadded edge state for the k-th edge be $\mathbf{e}_k^{c*} = \big((\mathbf{p}_i^*, \mathbf{R}_i^*), (\mathbf{p}_j^*, \mathbf{R}_j^*)\big)$. Depending on the sensory capability, the local task filtration map

$$\gamma_{\mathrm{mod}_k}^c : \mathbb{SE}(3) \times \mathbb{SE}(3) \to \mathbb{SE}(3) \times \mathbb{SE}(3) \tag{27}$$

isolates the required physical components to produce the filtered state

$$\tilde{\mathbf{e}}_k^{c*} = \big((\tilde{\mathbf{p}}_i^*, \tilde{\mathbf{R}}_i^*), (\tilde{\mathbf{p}}_j^*, \tilde{\mathbf{R}}_j^*)\big) = \big((\mathbf{p}_i^*, \tilde{\mathbf{R}}_i^*), (\mathbf{p}_j^*, \tilde{\mathbf{R}}_j^*)\big).$$

Because this mapping is composed strictly of constant identity selections (for observed states) and zero mappings (for masked states), its Jacobian is universally invariant to the operational point. Consequently, we drop the evaluation argument, yielding a state-independent local masking Jacobian $J_{\gamma,\mathrm{mod}_k}^c \in \mathbb{R}^{12\times 12}$.

Dictated by the direct sum structure of the coupled edge's tangent space, this local matrix naturally partitions into independent block-diagonal components for the source node i and the target node j:

$$J_{\gamma,\mathrm{mod}_k}^c = \mathrm{blockdiag}(J_{\gamma,i}^c, J_{\gamma,j}^c). \tag{28}$$

and each nodal block structurally decouples into distinct translational and rotational sub-blocks:

$$J_{\gamma,i}^c = \mathrm{blockdiag}(J_{\gamma,p,i}^c, J_{\gamma,R,i}^c). \tag{29}$$

Consequently, the complete local filtration Jacobian explicitly expands into a four-block diagonal architecture:

$$J_{\gamma,\mathrm{mod}_k}^c = \mathrm{blockdiag}(J_{\gamma,p,i}^c, J_{\gamma,R,i}^c, J_{\gamma,p,j}^c, J_{\gamma,R,j}^c). \tag{30}$$

Depending on the active modality, we explicitly define these sub-blocks:

- **Distance Edge (**dist**):** Both source and target attitudes are unobservable. The map extracts only the positions, padding the rotations with the identity matrix ($\tilde{\mathbf{R}}_i^* = \tilde{\mathbf{R}}_j^* = \mathbf{I}_3$):

$$\gamma_{\mathrm{dist}}^c(\mathbf{e}_k^{c*}) = \big((\mathbf{p}_i^*, \mathbf{I}_3),\ (\mathbf{p}_j^*, \mathbf{I}_3)\big) \tag{31}$$

$$J_{\gamma,\mathrm{dist}}^c = \mathrm{blockdiag}\left(\mathbf{I}_3, \mathbf{0}_{3\times 3}, \mathbf{I}_3, \mathbf{0}_{3\times 3}\right) \tag{32}$$

  where $J_{\gamma,i}^c = J_{\gamma,j}^c = \mathrm{blockdiag}(\mathbf{I}_3, \mathbf{0}_{3\times 3})$. Therefore, $J_{\gamma,p,i}^c = J_{\gamma,p,j}^c = \mathbf{I}_3$ and $J_{\gamma,R,i}^c = J_{\gamma,R,j}^c = \mathbf{0}_{3\times 3}$.

- **Bearing Edge** (bear)**:** Only the target's attitude is unobservable. The map preserves the full source pose while padding the target's rotation ($\tilde{\mathbf{R}}_i^* = \mathbf{R}_i^*$, $\tilde{\mathbf{R}}_j^* = \mathbf{I}_3$):

$$\gamma_{\text{bear}}^c(\mathbf{e}_k^{c*}) = \big((\mathbf{p}_i^*, \mathbf{R}_i^*), (\mathbf{p}_j^*, \mathbf{I}_3)\big) \tag{33}$$

$$J_{\gamma,\text{bear}}^c = \text{blockdiag}\left(\mathbf{I}_6, \mathbf{I}_3, \mathbf{0}_{3\times3}\right) \tag{34}$$

where $J_{\gamma,i}^c = \mathbf{I}_6$ and $J_{\gamma,j}^c = \text{blockdiag}(\mathbf{I}_3, \mathbf{0}_{3\times3})$. Consequently, the sub-blocks are $J_{\gamma,p,i}^c = \mathbf{I}_3$, $J_{\gamma,R,i}^c = \mathbf{I}_3$, while $J_{\gamma,p,j}^c = \mathbf{I}_3$, $J_{\gamma,R,j}^c = \mathbf{0}_{3\times3}$.

- **Mixed Edge** (mix)**:** The target's attitude remains unobservable ($\tilde{\mathbf{R}}_i^* = \mathbf{R}_i^*$, $\tilde{\mathbf{R}}_j^* = \mathbf{I}_3$). Thus, the filtration mapping and its Jacobian sub-blocks are structurally identical to the bearing case:

$$\gamma_{\text{mix}}^c(\mathbf{e}_k^{c*}) = \big((\mathbf{p}_i^*, \mathbf{R}_i^*), (\mathbf{p}_j^*, \mathbf{I}_3)\big) \tag{35}$$

$$J_{\gamma,\text{mix}}^c = \text{blockdiag}\left(\mathbf{I}_6, \mathbf{I}_3, \mathbf{0}_{3\times3}\right) \tag{36}$$

Global Filtration Map and Jacobian Assembly

The global task filtration map $\boldsymbol{\gamma}_{\text{emb}}^c$ applies the appropriate local filtration to every edge simultaneously. For a network of m edges, it is formally defined as:

$$\begin{aligned} \boldsymbol{\gamma}_{\text{emb}}^c :\ & (\mathbb{SE}(3) \times \mathbb{SE}(3))^m \to (\mathbb{SE}(3) \times \mathbb{SE}(3))^m \\ & (e_1, \dots, e_m) \mapsto \left(\gamma_{\text{mod}_1}^c(e_1), \dots, \gamma_{\text{mod}_m}^c(e_m)\right) \end{aligned} \tag{37}$$

Because the filtration of each edge is completely independent of the others and structurally state-invariant, the global constant Jacobian $\mathbf{J}_{\boldsymbol{\gamma}}^c \in \mathbb{R}^{12m\times12m}$ is strictly block-diagonal and independent of the evaluation point. In its most general form, it is assembled by explicitly concatenating the local filtration Jacobians ordered by the edge index $k = 1, \dots, m$:

$$\mathbf{J}_{\boldsymbol{\gamma}}^c = \text{blockdiag}\left(J_{\gamma,\text{mod}_1}^c, \dots, J_{\gamma,\text{mod}_m}^c\right). \tag{38}$$

However, depending on the network's homogeneity, this general block-diagonal formulation can be elegantly compacted using the Kronecker product ($\otimes$) for homogeneous block-diagonal replication:

- **Distance Network:** For a homogeneous network composed exclusively of distance measurements, the global Jacobian uniformly replicates the local distance mask across all m edges. The general formula elegantly collapses into a Kronecker product:

$$\mathbf{J}_{\boldsymbol{\gamma},\text{dist}}^c = \mathbf{I}_m \otimes J_{\gamma,\text{dist}}^c \tag{39}$$

- **Bearing Network:** Similarly, for a fully homogeneous bearing network, the global Jacobian applies the bearing-specific mask evenly across the entire graph:

$$\mathbf{J}_{\boldsymbol{\gamma},\text{bear}}^c = \mathbf{I}_m \otimes J_{\gamma,\text{bear}}^c \tag{40}$$

- **Mixed Network:** In heterogeneous networks, where uniform replication is impossible, the Kronecker product cannot be used. The overarching general block-diagonal formula applies directly, dynamically assembling the specific local masks:
$$\mathbf{J}^c_{\boldsymbol{\gamma}} = \text{blockdiag}\left(J^c_{\gamma,\text{mod}_1}, \dots, J^c_{\gamma,\text{mod}_m}\right) \tag{41}$$

4.4.3 Coupled Edge Observation Maps

The observation map computes the relative pose for each edge directly in $\mathbb{SE}(3)$, relying on the filtered inputs provided by the preceding task filtration stage.

Local Observation Maps and Jacobians

The generic local observation map $\Delta^c : \mathbb{SE}(3) \times \mathbb{SE}(3) \to \mathbb{SE}(3)$ calculates the relative position and rotation between the source and target nodes:

$$\Delta^c\big((\mathbf{p}_i, \mathbf{R}_i), (\mathbf{p}_j, \mathbf{R}_j)\big) = (\mathbf{p}_j - \mathbf{p}_i, \mathbf{R}_i^T \mathbf{R}_j) \tag{42}$$

To construct the rigidity matrix, we compute the analytical Jacobian parameterized locally using the Lie algebra $\mathfrak{se}(3)$, with variations defined as $\delta\mathbf{x} = [\delta\mathbf{p}^T, \delta\boldsymbol{\theta}^T]^T \in \mathbb{R}^6$.

POSITIONAL JACOBIAN: Since the relative position is defined strictly as the difference in global coordinates, its Jacobian is the linear difference $\delta\mathbf{p}_{ij} = \delta\mathbf{p}_j - \delta\mathbf{p}_i$. This yields state-invariant partial derivatives of $-\mathbf{I}_3$ and $\mathbf{I}_3$, strictly independent of the rotational variations.

ROTATIONAL JACOBIAN: For the relative rotation $\mathbf{R}_{ij} = \mathbf{R}_i^T \mathbf{R}_j$, the differential of a transposed rotation evaluates to $\delta(\mathbf{R}^T) = (\delta\mathbf{R})^T = -[\delta\boldsymbol{\theta}]_\times \mathbf{R}^T$. The total differential expands as:

$$\begin{aligned}
\delta\mathbf{R}_{ij} &= \delta(\mathbf{R}_i^T)\mathbf{R}_j + \mathbf{R}_i^T \delta\mathbf{R}_j \\
&= -[\delta\boldsymbol{\theta}_i]_\times \mathbf{R}_i^T \mathbf{R}_j + \mathbf{R}_i^T \mathbf{R}_j [\delta\boldsymbol{\theta}_j]_\times \\
&= -[\delta\boldsymbol{\theta}_i]_\times \mathbf{R}_{ij} + \mathbf{R}_{ij} [\delta\boldsymbol{\theta}_j]_\times
\end{aligned} \tag{43}$$

Equating this with the native right-trivialized variation $\delta\mathbf{R}_{ij} = \mathbf{R}_{ij}[\delta\boldsymbol{\theta}_{ij}]_\times$ yields:

$$\mathbf{R}_{ij}[\delta\boldsymbol{\theta}_{ij}]_\times = -[\delta\boldsymbol{\theta}_i]_\times \mathbf{R}_{ij} + \mathbf{R}_{ij}[\delta\boldsymbol{\theta}_j]_\times \tag{44}$$

Pre-multiplying by $\mathbf{R}_{ij}^T$ and applying the Adjoint property $\mathbf{R}^T[\mathbf{v}]_\times \mathbf{R} = [\mathbf{R}^T\mathbf{v}]_\times$, we map the matrices back to vectors in $\mathbb{R}^3$:

$$\begin{aligned}
[\delta\boldsymbol{\theta}_{ij}]_\times &= -[\mathbf{R}_{ij}^T \delta\boldsymbol{\theta}_i]_\times + [\delta\boldsymbol{\theta}_j]_\times \\
\delta\boldsymbol{\theta}_{ij} &= -\mathbf{R}_{ij}^T \delta\boldsymbol{\theta}_i + \delta\boldsymbol{\theta}_j
\end{aligned} \tag{45}$$

ASSEMBLING THE GENERIC JACOBIAN BLOCK: Let the padded filtered state for a generic single edge $e_k = (i, j)$ be denoted as

$$\tilde{\mathbf{e}}_k^{c*} = \big((\tilde{\mathbf{p}}_i^*, \tilde{\mathbf{R}}_i^*), (\tilde{\mathbf{p}}_j^*, \tilde{\mathbf{R}}_j^*)\big) = \big((\mathbf{p}_i^*, \tilde{\mathbf{R}}_i^*), (\mathbf{p}_j^*, \tilde{\mathbf{R}}_j^*)\big).$$

By combining the Jacobians, the generic Jacobian block evaluated at this state is formulated as:

$$\begin{aligned} J_\Delta^c(\tilde{\mathbf{e}}_k^{c*}) &= \begin{bmatrix} \frac{\partial \mathbf{p}_{ij}}{\partial \mathbf{p}_i} & \frac{\partial \mathbf{p}_{ij}}{\partial \theta_i} & \frac{\partial \mathbf{p}_{ij}}{\partial \mathbf{p}_j} & \frac{\partial \mathbf{p}_{ij}}{\partial \theta_j} \\ \frac{\partial \theta_{ij}}{\partial \mathbf{p}_i} & \frac{\partial \theta_{ij}}{\partial \theta_i} & \frac{\partial \theta_{ij}}{\partial \mathbf{p}_j} & \frac{\partial \theta_{ij}}{\partial \theta_j} \end{bmatrix} \\ &= \begin{bmatrix} -\mathbf{I}_3 & \mathbf{0}_{3\times3} & \mathbf{I}_3 & \mathbf{0}_{3\times3} \\ \mathbf{0}_{3\times3} & -(\tilde{\mathbf{R}}_{ij}^*)^T & \mathbf{0}_{3\times3} & \mathbf{I}_3 \end{bmatrix} \end{aligned} \tag{46}$$

The direct sum structure of the tangent spaces dictates a strict block architecture for the Jacobian matrix, as explained at the beginning of the chapter. Consequently, the matrix naturally partitions into the distinct nodal observation blocks $J_{\Delta,i}^c$ and $J_{\Delta,j}^c$, taking the exact form:

$$J_\Delta^c = \begin{bmatrix} J_{\Delta,i}^c & J_{\Delta,j}^c \end{bmatrix}. \tag{47}$$

Furthermore, due to the complete absence of cross-domain mixing, these nodal blocks mathematically collapse into a strictly block-diagonal configuration:

$$J_{\Delta,i}^c = \mathrm{blockdiag}(J_{\Delta,p,i}^c, J_{\Delta,R,i}^c), \qquad J_{\Delta,j}^c = \mathrm{blockdiag}(J_{\Delta,p,j}^c, J_{\Delta,R,j}^c), \tag{48}$$

where the generic positional operators evaluate universally to $J_{\Delta,p,i}^c = -\mathbf{I}_3$ and $J_{\Delta,p,j}^c = \mathbf{I}_3$, whereas the rotational sub-blocks $J_{\Delta,R,i}^c$ and $J_{\Delta,R,j}^c$ evaluate dynamically based on the specific measurement modality.

Evaluating this generic map and its partitioned Jacobian at the specific operational points dictated by our modality-dependent filtration yields:

- **Distance Edge (**dist**):** Both attitudes are padded with the identity matrix ($\tilde{\mathbf{R}}_i^* = \tilde{\mathbf{R}}_j^* = \mathbf{I}_3$), collapsing the relative rotation to $\tilde{\mathbf{R}}_{ij}^* = \mathbf{I}_3$. Crucially, this padding causes the Jacobian to become completely state-invariant. We thus drop the evaluation argument:

$$\Delta_{\mathrm{dist}}^c\big((\mathbf{p}_i^*, \mathbf{I}_3), (\mathbf{p}_j^*, \mathbf{I}_3)\big) = (\mathbf{p}_j^* - \mathbf{p}_i^*, \mathbf{I}_3) \tag{49}$$

$$J_{\Delta,\mathrm{dist}}^c = \begin{bmatrix} -\mathbf{I}_3 & \mathbf{0}_{3\times3} & \mathbf{I}_3 & \mathbf{0}_{3\times3} \\ \mathbf{0}_{3\times3} & -\mathbf{I}_3 & \mathbf{0}_{3\times3} & \mathbf{I}_3 \end{bmatrix} \tag{50}$$

  Here, $J_{\Delta,R,i}^c = -\mathbf{I}_3$ and $J_{\Delta,R,j}^c = \mathbf{I}_3$.

- **Bearing Edge (**bear**):** Only the target attitude is padded ($\tilde{\mathbf{R}}_j^* = \mathbf{I}_3$). The relative rotation isolates the inverse of the filtered source's attitude ($\tilde{\mathbf{R}}_{ij}^* = (\mathbf{R}_i^*)^T$). The Jacobian retains a strict dependence on the source node's state:

$$\Delta_{\mathrm{bear}}^c\big((\mathbf{p}_i^*, \mathbf{R}_i^*), (\mathbf{p}_j^*, \mathbf{I}_3)\big) = (\mathbf{p}_j^* - \mathbf{p}_i^*, (\mathbf{R}_i^*)^T) \tag{51}$$

$$J_{\Delta,\mathrm{bear}}^c(\tilde{\mathbf{e}}_k^{c*}) = \begin{bmatrix} -\mathbf{I}_3 & \mathbf{0}_{3\times3} & \mathbf{I}_3 & \mathbf{0}_{3\times3} \\ \mathbf{0}_{3\times3} & -\mathbf{R}_i^* & \mathbf{0}_{3\times3} & \mathbf{I}_3 \end{bmatrix} \tag{52}$$

Here, the rotational sub-blocks explicitly evaluate to $J^c_{\Delta,R,i}(\tilde{\mathbf{e}}^{c*}_k) = -\mathbf{R}^*_i$ and $J^c_{\Delta,R,j} = \mathbf{I}_3$.

- **Mixed Edge (**mix**):** Because the target's attitude remains unobservable and padded ($\tilde{\mathbf{R}}^*_j = \mathbf{I}_3$), the observation mapping and its state-dependent Jacobian sub-blocks are structurally identical to the pure bearing case:

$$\Delta^c_{\text{mix}}\big((\mathbf{p}^*_i, \mathbf{R}^*_i), (\mathbf{p}^*_j, \mathbf{I}_3)\big) = (\mathbf{p}^*_j - \mathbf{p}^*_i, (\mathbf{R}^*_i)^T) \tag{53}$$

$$J^c_{\Delta,\text{mix}}(\tilde{\mathbf{e}}^{c*}_k) = \begin{bmatrix} -\mathbf{I}_3 & \mathbf{0}_{3\times3} & \mathbf{I}_3 & \mathbf{0}_{3\times3} \\ \mathbf{0}_{3\times3} & -\mathbf{R}^*_i & \mathbf{0}_{3\times3} & \mathbf{I}_3 \end{bmatrix} \tag{54}$$

Global Observation Jacobian Assembly

The global observation map $\boldsymbol{\Delta}^c_{\text{emb}}$ applies the local evaluation to every edge simultaneously:

$$\begin{aligned} \boldsymbol{\Delta}^c_{\text{emb}} :\ & (\$\mathbb{E}(3) \times \$\mathbb{E}(3))^m \to \$\mathbb{E}(3)^m \\ & (e_1, \dots, e_m) \mapsto \big(\Delta^c(e_1), \dots, \Delta^c(e_m)\big) \end{aligned} \tag{55}$$

Since edge observations are computed independently across the network, the global Jacobian $\mathbf{J}^c_{\boldsymbol{\Delta}}(\tilde{\mathbf{e}}^{c*}) \in \mathbb{R}^{6m\times12m}$ is strictly block-diagonal. In its most general form, it is assembled by explicitly concatenating the local observation Jacobians ordered by the edge index $k = 1, \dots, m$:

$$\mathbf{J}^c_{\boldsymbol{\Delta}}(\tilde{\mathbf{e}}^{c*}) = \text{blockdiag}\left(J^c_\Delta(\tilde{\mathbf{e}}^{c*}_1), \dots, J^c_\Delta(\tilde{\mathbf{e}}^{c*}_m)\right) \tag{56}$$

However, the most efficient algebraic representation depends fundamentally on whether the underlying local Jacobians evaluate to constant matrices or retain state dependence:

- **Distance Network:** As established above, for a homogeneous distance network, the local Jacobian $J^c_{\Delta,\text{dist}}$ evaluates to a strictly constant matrix. Therefore, the general block-diagonal formulation elegantly collapses into a Kronecker product, allowing us to formally drop the global evaluation argument:

$$\mathbf{J}^c_{\boldsymbol{\Delta},\text{dist}} = \mathbf{I}_m \otimes J^c_{\Delta,\text{dist}} \tag{57}$$

- **Bearing Network:** Conversely, in a homogeneous bearing network, the local Jacobian retains an explicit state dependence via $\mathbf{R}^*_i$. The Kronecker product cannot be used, and the global matrix must be explicitly assembled via state-dependent concatenation:

$$\mathbf{J}^c_{\boldsymbol{\Delta},\text{bear}}(\tilde{\mathbf{e}}^{c*}) = \text{blockdiag}\left(J^c_{\Delta,\text{bear}}(\tilde{\mathbf{e}}^{c*}_1), \dots, J^c_{\Delta,\text{bear}}(\tilde{\mathbf{e}}^{c*}_m)\right) \tag{58}$$

- **Mixed Network:** In a graph featuring multiple modalities, the concatenated blocks dynamically adapt to both the specific measurement type ($\text{mod}_k \in \{\text{dist}, \text{bear}, \text{mix}\}$) and local state:

$$\mathbf{J}^c_{\boldsymbol{\Delta}}(\tilde{\mathbf{e}}^{c*}) = \text{blockdiag}\left(J^c_{\Delta,\text{mod}_1}(\tilde{\mathbf{e}}^{c*}_1), \dots, J^c_{\Delta,\text{mod}_m}(\tilde{\mathbf{e}}^{c*}_m)\right) \tag{59}$$

4.4.4 Coupled Measurement Maps

The measurement maps translate the relative edge quantities into specific sensor readings within the codomain $\mathcal{Y}$. Let $\mathbf{q}_{ij}^{*} = \frac{\tilde{\mathbf{p}}_{ij}^{*}}{\|\tilde{\mathbf{p}}_{ij}^{*}\|} = \frac{\mathbf{p}_{ij}^{*}}{\|\mathbf{p}_{ij}^{*}\|}$ denote the normalized relative position vector.

Local Measurement Maps and Jacobians

Let the nominal relative observation state for the k-th edge be $\mathbf{o}_k^{c*} = (\tilde{\mathbf{p}}_{ij}^{*}, \tilde{\mathbf{R}}_{ij}^{*}) = (\mathbf{p}_{ij}^{*}, \tilde{\mathbf{R}}_{ij}^{*})$. We formally define the generic local measurement map

$$\eta_{\mathrm{mod}_k}^{c} : \mathbb{SE}(3) \to \mathcal{Y} \tag{60}$$

which yields the nominal sensor reading $\mathbf{y}_k^{*} \in \mathcal{Y}$:

$$\eta_{\mathrm{mod}_k}^{c}(\mathbf{o}_k^{c*}) = \mathbf{y}_k^{*} \tag{61}$$

Dictated by the direct sum structure of this relative tangent space, the Jacobian $J_{\eta,\mathrm{mod}_k}^{c}(\mathbf{o}_k^{c*})$ naturally partitions into distinct positional and rotational column blocks:

$$J_{\eta,\mathrm{mod}_k}^{c}(\mathbf{o}_k^{c*}) = \left[J_{\eta,\mathrm{mod}_k,p}^{c}(\mathbf{o}_k^{c*}) \quad J_{\eta,\mathrm{mod}_k,R}^{c}(\mathbf{o}_k^{c*}) \right]. \tag{62}$$

Depending on the active sensory modality, evaluating this Jacobian yields blocks that directly project onto the corresponding sub-spaces without loss of information:

- **Distance Modality (**dist**):** The measurement map $\eta_{\mathrm{dist}}^{c} : \mathbb{SE}(3) \to \mathbb{R}_{>0}$ extracts the Euclidean norm of the relative position:

  $$\eta_{\mathrm{dist}}^{c}(\mathbf{p}_{ij}^{*}, \tilde{\mathbf{R}}_{ij}^{*}) = \|\mathbf{p}_{ij}^{*}\| = d_{ij}^{*} \tag{63}$$

  To compute the exact differential of the distance, we express the Euclidean norm algebraically as $d_{ij} = (\mathbf{p}_{ij}^{T}\mathbf{p}_{ij})^{\frac{1}{2}}$. Applying the chain rule, the differential δd_{ij} evaluates to:

  $$\delta d_{ij} = \delta\left((\mathbf{p}_{ij}^{T}\mathbf{p}_{ij})^{\frac{1}{2}}\right) = \frac{1}{2}(\mathbf{p}_{ij}^{T}\mathbf{p}_{ij})^{-\frac{1}{2}}\delta\big(\mathbf{p}_{ij}^{T}\mathbf{p}_{ij}\big). \tag{64}$$

  Using the product rule on the inner product, we obtain:

  $$\delta\big(\mathbf{p}_{ij}^{T}\mathbf{p}_{ij}\big) = \delta\mathbf{p}_{ij}^{T}\mathbf{p}_{ij} + \mathbf{p}_{ij}^{T}\delta\mathbf{p}_{ij} = 2\mathbf{p}_{ij}^{T}\delta\mathbf{p}_{ij}. \tag{65}$$

Substituting this result back into the differential of the norm yields:

$$\begin{aligned} \delta d_{ij} &= \frac{1}{2}\frac{1}{\|\mathbf{p}_{ij}\|}\left(2\mathbf{p}_{ij}^T\delta\mathbf{p}_{ij}\right) \\ &= \frac{\mathbf{p}_{ij}^T}{\|\mathbf{p}_{ij}\|}\delta\mathbf{p}_{ij}. \end{aligned} \tag{66}$$

Evaluated at the nominal operational point, we explicitly recognize the normalized line-of-sight vector $\mathbf{q}_{ij}^* = \frac{\mathbf{p}_{ij}^*}{\|\mathbf{p}_{ij}^*\|}$. The differential is therefore computed via the pure product with this unit vector:

$$\delta d_{ij} = (\mathbf{q}_{ij}^*)^T\delta\mathbf{p}_{ij}. \tag{67}$$

Given that the scalar distance is invariant to rotational perturbations $\delta\boldsymbol{\theta}_{ij}$, the 1×6 local Jacobian zeroes out the rotational block.

The Jacobian reults in :

$$J_{\eta,\text{dist}}^c(\mathbf{o}_k^{c*}) = \begin{bmatrix}(\mathbf{q}_{ij}^*)^T & \mathbf{0}_{1\times 3}\end{bmatrix} \tag{68}$$

where $J_{\eta,\text{dist},p}^c(\mathbf{o}_k^{c*}) = (\mathbf{q}_{ij}^*)^T$ and $J_{\eta,\text{dist},R}^c = \mathbf{0}_{1\times 3}$. Note that while rotationally invariant, it strictly depends on the spatial configuration via $\mathbf{q}_{ij}^*$:

- **Bearing Modality (**bear**):** The measurement map $\eta_{\text{bear}}^c : \mathbb{SE}(3) \to \mathbb{L}$ calculates the line-of-sight direction in the source's local frame. Utilizing the evaluated relative state ($\tilde{\mathbf{R}}_{ij}^* = (\mathbf{R}_i^*)^T$), we have:

$$\eta_{\text{bear}}^c(\mathbf{p}_{ij}^*, \tilde{\mathbf{R}}_{ij}^*) = \frac{\tilde{\mathbf{R}}_{ij}^*\mathbf{p}_{ij}^*}{\|\mathbf{p}_{ij}^*\|} = \mathbf{b}_{ij}^* \tag{69}$$

To compute the exact differential of this normalized vector, let us define the unnormalized local relative position as $\mathbf{v} = \tilde{\mathbf{R}}_{ij}\mathbf{p}_{ij}$. Since rotation matrices preserve the Euclidean norm, we have $\|\mathbf{v}\| = \|\tilde{\mathbf{R}}_{ij}\mathbf{p}_{ij}\| = \|\mathbf{p}_{ij}\|$. The bearing vector is therefore purely the normalization $\mathbf{b}_{ij} = \frac{\mathbf{v}}{\|\mathbf{v}\|}$.

Applying the multivariate product rule to compute the differential $\delta\mathbf{b}_{ij}$, we get:

$$\delta\mathbf{b}_{ij} = \delta\left(\mathbf{v}\|\mathbf{v}\|^{-1}\right) = \delta\mathbf{v}\|\mathbf{v}\|^{-1} + \mathbf{v}\,\delta\left(\|\mathbf{v}\|^{-1}\right). \tag{70}$$

Knowing that the Euclidean norm is defined as $\|\mathbf{v}\| = (\mathbf{v}^T\mathbf{v})^{\frac{1}{2}}$, its differential evaluates to:

$$\delta\left(\|\mathbf{v}\|\right) = \frac{1}{2}(\mathbf{v}^T\mathbf{v})^{-\frac{1}{2}}(2\mathbf{v}^T\delta\mathbf{v}) = \frac{\mathbf{v}^T}{\|\mathbf{v}\|}\delta\mathbf{v} = \mathbf{b}_{ij}^T\delta\mathbf{v}. \tag{71}$$

Using the chain rule, the differential of the inverse norm is:

$$\delta\big(\|\mathbf{v}\|^{-1}\big) = -\|\mathbf{v}\|^{-2}\delta\big(\|\mathbf{v}\|\big) = -\|\mathbf{v}\|^{-2}\mathbf{b}_{ij}^T\delta\mathbf{v}. \tag{72}$$

Substituting this back into the product rule expression yields:

$$\begin{aligned}
\delta\mathbf{b}_{ij} &= \frac{\delta\mathbf{v}}{\|\mathbf{v}\|} - \mathbf{v}\|\mathbf{v}\|^{-2}\mathbf{b}_{ij}^T\delta\mathbf{v} \\
&= \frac{\delta\mathbf{v}}{\|\mathbf{v}\|} - \frac{\mathbf{v}}{\|\mathbf{v}\|}\frac{\mathbf{b}_{ij}^T}{\|\mathbf{v}\|}\delta\mathbf{v} \\
&= \frac{1}{\|\mathbf{v}\|}\mathbf{I}_3\delta\mathbf{v} - \frac{1}{\|\mathbf{v}\|}\mathbf{b}_{ij}\mathbf{b}_{ij}^T\delta\mathbf{v} \\
&= \frac{1}{\|\mathbf{v}\|}\left(\mathbf{I}_3 - \mathbf{b}_{ij}\mathbf{b}_{ij}^T\right)\delta\mathbf{v}.
\end{aligned} \tag{73}$$

We explicitly recognize the orthogonal projector matrix onto the tangent space of the sphere at $\mathbf{b}_{ij}$, denoted as $\mathbf{\Pi}_{\mathbf{b}_{ij}} = \mathbf{I}_3 - \mathbf{b}_{ij}\mathbf{b}_{ij}^T$. Substituting $\|\mathbf{v}\| = \|\mathbf{p}_{ij}\|$ and the linear differential $\delta\mathbf{v} = \delta(\tilde{\mathbf{R}}_{ij}\mathbf{p}_{ij}) = \delta\tilde{\mathbf{R}}_{ij}\mathbf{p}_{ij} + \tilde{\mathbf{R}}_{ij}\delta\mathbf{p}_{ij}$, we obtain:

$$\delta\mathbf{b}_{ij} = \frac{1}{\|\mathbf{p}_{ij}\|}\mathbf{\Pi}_{\mathbf{b}_{ij}}\big(\delta\tilde{\mathbf{R}}_{ij}\mathbf{p}_{ij} + \tilde{\mathbf{R}}_{ij}\delta\mathbf{p}_{ij}\big). \tag{74}$$

Substituting $\delta\mathbf{R}_{ij} = \mathbf{R}_{ij}[\delta\boldsymbol{\theta}_{ij}]_\times$ and exploiting $[\delta\boldsymbol{\theta}_{ij}]_\times\mathbf{p}_{ij} = -[\mathbf{p}_{ij}]_\times\delta\boldsymbol{\theta}_{ij}$, we obtain:

$$\delta\mathbf{b}_{ij} = \frac{1}{\|\mathbf{p}_{ij}\|}\mathbf{\Pi}_{\mathbf{b}_{ij}}\big(\mathbf{R}_{ij}\delta\mathbf{p}_{ij} - \mathbf{R}_{ij}[\mathbf{p}_{ij}]_\times\delta\boldsymbol{\theta}_{ij}\big) \tag{75}$$

Evaluating this at the propagated nominal point yields the 3×6 local Jacobian:

$$J^c_{\eta,\text{bear}}(\mathbf{o}_k^{c*}) = \frac{1}{\|\mathbf{p}_{ij}^*\|}\left[\mathbf{\Pi}_{\mathbf{b}_{ij}^*}(\mathbf{R}_i^*)^T \quad -\mathbf{\Pi}_{\mathbf{b}_{ij}^*}(\mathbf{R}_i^*)^T[\mathbf{p}_{ij}^*]_\times\right] \tag{76}$$

where $J^c_{\eta,\text{bear},p}(\mathbf{o}_k^{c*}) = \frac{1}{\|\mathbf{p}_{ij}^*\|}\mathbf{\Pi}_{\mathbf{b}_{ij}^*}(\mathbf{R}_i^*)^T$ and $J^c_{\eta,\text{bear},R}(\mathbf{o}_k^{c*}) = -\frac{1}{\|\mathbf{p}_{ij}^*\|}\mathbf{\Pi}_{\mathbf{b}_{ij}^*}(\mathbf{R}_i^*)^T[\mathbf{p}_{ij}^*]_\times$.

- **Mixed Modality (**mix**):** To maintain a homogeneous global space in heterogeneous networks, every edge maps uniformly via $\eta^c_{\text{mix}} : \mathbb{SE}(3) \to \mathbb{L} \times \mathbb{R}_{>0}$. The measurement function concatenates the active measurements and pads missing ones with arbitrary dummy constants ($\mathbf{u}_0 \in \mathbb{L}$, $d_0 \in \mathbb{R}_{>0}$):

$$\eta^c_{\text{mix}}(\mathbf{o}_k^{c*}) = \begin{cases} \begin{bmatrix} \mathbf{u}_0 \\ \eta^c_{\text{dist}}(\mathbf{o}_k^{c*}) \end{bmatrix} & \text{if edge } k \text{ is distance} \\ \begin{bmatrix} \eta^c_{\text{bear}}(\mathbf{o}_k^{c*}) \\ d_0 \end{bmatrix} & \text{if edge } k \text{ is bearing} \\ \begin{bmatrix} \eta^c_{\text{bear}}(\mathbf{o}_k^{c*}) \\ \eta^c_{\text{dist}}(\mathbf{o}_k^{c*}) \end{bmatrix} & \text{if edge } k \text{ measures both} \end{cases} \tag{77}$$

As the Jacobian of any constant dummy value evaluates identically to zero ($\delta\mathbf{u}_0 = \mathbf{0}$, $\delta d_0 = 0$), the local Jacobian block cleanly assembles by stacking the active sub-blocks and zeroing out the missing ones:

$$J^c_{\eta,\mathrm{mix}}(\mathbf{o}^{c*}_k) = \begin{cases} \begin{bmatrix} \mathbf{0}_{3\times3} & \mathbf{0}_{3\times3} \\ J^c_{\eta,\mathrm{dist},p}(\mathbf{o}^{c*}_k) & J^c_{\eta,\mathrm{dist},R}(\mathbf{o}^{c*}_k) \end{bmatrix} & \text{if edge } k \text{ is distance} \\ \begin{bmatrix} J^c_{\eta,\mathrm{bear},p}(\mathbf{o}^{c*}_k) & J^c_{\eta,\mathrm{bear},R}(\mathbf{o}^{c*}_k) \\ \mathbf{0}_{1\times3} & \mathbf{0}_{1\times3} \end{bmatrix} & \text{if edge } k \text{ is bearing} \\ \begin{bmatrix} J^c_{\eta,\mathrm{bear},p}(\mathbf{o}^{c*}_k) & J^c_{\eta,\mathrm{bear},R}(\mathbf{o}^{c*}_k) \\ J^c_{\eta,\mathrm{dist},p}(\mathbf{o}^{c*}_k) & J^c_{\eta,\mathrm{dist},R}(\mathbf{o}^{c*}_k) \end{bmatrix} & \text{if edge } k \text{ measures both} \end{cases} \tag{78}$$

Global Measurement Map and Jacobian Assembly

The global measurement map $\boldsymbol{\eta}^c_{\mathrm{emb}}$ aggregates the independent sensor readings into the full measurement vector:

$$\begin{aligned} \boldsymbol{\eta}^c_{\mathrm{emb}} : \mathbb{SE}(3)^m &\to \mathcal{Y}^m \\ (o_1, \dots, o_m) &\mapsto \left(\eta^c_{\mathrm{mod}_1}(o_1), \dots, \eta^c_{\mathrm{mod}_m}(o_m)\right) \end{aligned} \tag{79}$$

Since the measurement of each edge is completely independent, the global measurement Jacobian $\mathbf{J}^c_{\boldsymbol{\eta}}(\mathbf{o}^{c*})$ is strictly block-diagonal. In its most general form, it is assembled by explicitly concatenating the local measurement Jacobians ordered by the edge index $k = 1, \dots, m$:

$$\mathbf{J}^c_{\boldsymbol{\eta}}(\mathbf{o}^{c*}) = \mathrm{blockdiag}\left(J^c_{\eta,\mathrm{mod}_1}(\mathbf{o}^{c*}_1), \dots, J^c_{\eta,\mathrm{mod}_m}(\mathbf{o}^{c*}_m)\right). \tag{80}$$

Given that each local measurement Jacobian (whether distance, bearing, or mixed) inherently relies on the spatial coordinates of its respective edge (via $\mathbf{p}^*_{ij}$ or $\mathbf{q}^*_{ij}$), explicit state dependence is universally preserved. Consequently, the Kronecker product ($\otimes$) cannot be utilized even in fully homogeneous networks. Thus, this overarching block-diagonal formulation applies directly to all network configurations, dynamically adapting its internal block dimensions based on the specific modality of each edge:

- **Distance Network:** The global measurement map is

$$\boldsymbol{\eta}^c_{\mathrm{emb,dist}} : \mathbb{SE}(3)^m \to (\mathbb{R}_{>0})^m \tag{81}$$

Applying the general formula, the global Jacobian $\mathbf{J}^c_{\boldsymbol{\eta},\mathrm{dist}}(\mathbf{o}^{c*}) \in \mathbb{R}^{m\times 6m}$ becomes:

$$\mathbf{J}^c_{\boldsymbol{\eta},\mathrm{dist}}(\mathbf{o}^{c*}) = \mathrm{blockdiag}^m_{k=1}\left(J^c_{\eta,\mathrm{dist}}(\mathbf{o}^{c*}_k)\right) \tag{82}$$

- **Bearing Network:** The global measurement map is

$$\boldsymbol{\eta}^{c}_{\mathrm{emb,bear}} : \mathbb{SE}(3)^m \to \mathbb{L}^m \tag{83}$$

Applying the general formula, the global Jacobian $\mathbf{J}^c_{\eta,\mathrm{bear}}(\mathbf{o}^{c*}) \in \mathbb{R}^{3m\times 6m}$ becomes:

$$\mathbf{J}^c_{\eta,\mathrm{bear}}(\mathbf{o}^{c*}) = \mathrm{blockdiag}_{k=1}^{m}\left(J^c_{\eta,\mathrm{bear}}(\mathbf{o}^{c*}_k)\right) \tag{84}$$

- **Mixed Network:** To maintain structural consistency, the global measurement map pads the codomain uniformly, yielding

$$\boldsymbol{\eta}^{c}_{\mathrm{emb,mix}} : \mathbb{SE}(3)^m \to (\mathbb{L}\times\mathbb{R}_{>0})^m \tag{85}$$

The global Jacobian $\mathbf{J}^c_{\eta}(\mathbf{o}^{c*}) \in \mathbb{R}^{4m\times 6m}$ thus remains a perfectly symmetric sequence of 4×6 blocks across the entire network:

$$\mathbf{J}^c_{\eta}(\mathbf{o}^{c*}) = \mathrm{blockdiag}_{k=1}^{m}\left(J^c_{\eta,\mathrm{mod}_k}(\mathbf{o}^{c*}_k)\right) \tag{86}$$

where $\mathrm{mod}_k \in \{\mathrm{dist}, \mathrm{bear}, \mathrm{mix}\}$.

4.4.5 Coupled Rigidity Matrix Assembly

To motivate the structure of the tangent spaces utilized in our derivation, we must first recognize that the global measurement model is the composition of four distinct smooth maps. Let $\overline{\mathscr{D}}^c = \mathbb{SE}(3)^n$ be the global coupled state manifold, and $\mathscr{Y}^c$ the global measurement manifold.

The measurement function resulting from the embedded coupled functor realization $\mathbf{h}^c : \overline{\mathscr{D}}^c \to \mathscr{Y}^c$ factorizes exactly into the categorical sequence:

$$\mathbf{h}^c = \boldsymbol{\eta}^c_{\mathrm{emb}} \circ \boldsymbol{\Delta}^c_{\mathrm{emb}} \circ \boldsymbol{\gamma}^c_{\mathrm{emb}} \circ \boldsymbol{\sigma}^c_{\mathrm{emb}}. \tag{87}$$

To compute the Jacobian of this composite map via the chain rule, the embedded coupled rigidity matrix is defined as the ordered product of the individual Jacobians, each evaluated at its respective propagated evaluation point:

$$\mathbf{R}^c(\mathbf{x}^{c*}) = \mathbf{J}^c_{\eta}(\mathbf{o}^{c*}) \cdot \mathbf{J}^c_{\Delta}(\tilde{\mathbf{e}}^{c*}) \cdot \mathbf{J}^c_{\gamma} \cdot \mathbf{J}^c_{\sigma}. \tag{88}$$

Rather than evaluating this product monolithically, we adopt a systematic multistep structural factorization. This allows us to highlight different structural properties of the resulting matrix and provides a methodological way to construct it.

First, we completely isolate the measurement dependent components from their topological allocation across the network's agents. Specifically, we define an *edge-wise dense* intermediate matrix $\mathbf{R}^c_{\mathrm{local}}(\mathbf{x}^{c*})$ prior to agent distribution:

$$\mathbf{R}^c(\mathbf{x}^{c*}) = \underbrace{\mathbf{J}^c_{\eta}(\mathbf{o}^{c*}) \cdot \mathbf{J}^c_{\Delta}(\tilde{\mathbf{e}}^{c*}) \cdot \mathbf{J}^c_{\gamma}}_{\mathbf{R}^c_{\mathrm{local}}(\mathbf{x}^{c*})} \cdot \underbrace{\mathbf{J}^c_{\sigma}}_{\text{Agent Distribution}}. \tag{89}$$

We structure the assembly into four distinct algebraic steps. In each step, explicitly identifying the domain and codomain of the underlying map dictates the strict hierarchical partition of the associated tangent spaces, ultimately forcing the resulting matrices into the structured forms explained at the beginning of the chapter.

Step 1: Local Edge-Wise Kinematics

We first evaluate the mapping at the local level for a generic k-th directed edge $e_k = (i, j)$. This corresponds to analyzing the local measurement map

$$h^c_{\text{local},k} : \mathbb{SE}(3) \times \mathbb{SE}(3) \to \mathscr{Y}_k \tag{90}$$

which maps the states of the interacting pair to generate the specific local measurement.

We compute the Jacobian of the map $h^c_{\text{local},k}$ and we obtain the local dense row block $r^c_{\text{mod}_k}(\mathbf{e}^{c*}_k)$:

$$\begin{aligned} r^c_{\text{mod}_k}(\mathbf{e}^{c*}_k) &= J^c_{\eta,\text{mod}_k}(\mathbf{o}^{c*}_k) \cdot J^c_{\Delta,\text{mod}_k}(\tilde{\mathbf{e}}^{c*}_k) \cdot J^c_{\gamma,\text{mod}_k} \\ &= \left[\begin{array}{cc|cc} r^c_{\text{mod}_k,\mathbf{p}_i}(\mathbf{e}^{c*}_k) & r^c_{\text{mod}_k,\boldsymbol{\theta}_i}(\mathbf{e}^{c*}_k) & r^c_{\text{mod}_k,\mathbf{p}_j}(\mathbf{e}^{c*}_k) & r^c_{\text{mod}_k,\boldsymbol{\theta}_j}(\mathbf{e}^{c*}_k) \end{array} \right] \\ &= \left[\begin{array}{c|c} r^c_{\text{mod}_k,i}(\mathbf{e}^{c*}_k) & r^c_{\text{mod}_k,j}(\mathbf{e}^{c*}_k) \end{array} \right]. \end{aligned} \tag{91}$$

As established by the hierarchical geometric decomposition of the edge tangent space explained at the beginning of the chapter, this 12-column dense block perfectly mirrors the physical structure of the interaction. At the highest level, the block decouples into two independent 6-column macro-blocks, representing the full 6-DOF state variations of the source agent i and the target agent j. In turn, each of these nodal macro-blocks explicitly subdivides into two 3-column sub-blocks, isolating the purely translational and purely rotational kinematic contributions within each individual agent.

To explicitly verify that the generic block inherently obeys this strict hierarchical partition, we perform the matrix expansion in two distinct algebraic derivations.

1. NODAL PARTITIONING (SOURCE VS. TARGET): We first evaluate the decoupling for the edge into source (i) and target (j) streams. The measurement Jacobian J^c_{η,mod_k} operates downstream on the unified 6-DOF relative state. The kinematic observation map $J^c_{\Delta,\text{mod}_k}$ inherently splits into a 1×2 block matrix acting on the two distinct agents, while the filtration mask $J^c_{\gamma,\text{mod}_k}$ is strictly block-diagonal across the nodes. Expanding these matrices yields:

$$
\begin{aligned}
r^c_{\text{mod}_k}(\mathbf{e}^{c*}_k) &= J^c_{\eta,\text{mod}_k}(\mathbf{o}^{c*}_k) \cdot J^c_{\Delta,\text{mod}_k}(\tilde{\mathbf{e}}^{c*}_k) \cdot J^c_{\gamma,\text{mod}_k} \\
&= J^c_{\eta,\text{mod}_k}(\mathbf{o}^{c*}_k) \begin{bmatrix} J^c_{\Delta,i}(\tilde{\mathbf{e}}^{c*}_k) & J^c_{\Delta,j}(\tilde{\mathbf{e}}^{c*}_k) \end{bmatrix} \begin{bmatrix} J^c_{\gamma,i} & \mathbf{0}_{6\times6} \\ \mathbf{0}_{6\times6} & J^c_{\gamma,j} \end{bmatrix} \\
&= J^c_{\eta,\text{mod}_k}(\mathbf{o}^{c*}_k) \left[J^c_{\Delta,i}(\tilde{\mathbf{e}}^{c*}_k) J^c_{\gamma,i} \;\middle|\; J^c_{\Delta,j}(\tilde{\mathbf{e}}^{c*}_k) J^c_{\gamma,j} \right] \\
&= \left[J^c_{\eta,\text{mod}_k}(\mathbf{o}^{c*}_k) J^c_{\Delta,i}(\tilde{\mathbf{e}}^{c*}_k) J^c_{\gamma,i} \;\middle|\; J^c_{\eta,\text{mod}_k}(\mathbf{o}^{c*}_k) J^c_{\Delta,j}(\tilde{\mathbf{e}}^{c*}_k) J^c_{\gamma,j} \right] \\
&= \left[r^c_{\text{mod}_k,i}(\mathbf{e}^{c*}_k) \;\middle|\; r^c_{\text{mod}_k,j}(\mathbf{e}^{c*}_k) \right].
\end{aligned} \tag{92}
$$

2. GEOMETRIC PARTITIONING (POSITION VS. ROTATION): We expose the internal positional and rotational kinematics within these isolated nodal blocks. Because the filtration and observation mappings do not mix translations and rotations, their local 6-DOF Jacobians $J^c_{\Delta,i}$ and $J^c_{\gamma,i}$ are strictly block-diagonal. Partitioning the measurement Jacobian J^c_{η,mod_k} into its positional and rotational columns, we expand the generic source nodal block $r^c_{\text{mod}_k,i}$:

$$
\begin{aligned}
r^c_{\text{mod}_k,i}(\mathbf{e}^{c*}_k) &= J^c_{\eta,\text{mod}_k}(\mathbf{o}^{c*}_k) J^c_{\Delta,i}(\tilde{\mathbf{e}}^{c*}_k) J^c_{\gamma,i} \\
&= \begin{bmatrix} J^c_{\eta,\text{mod}_k,p}(\mathbf{o}^{c*}_k) & J^c_{\eta,\text{mod}_k,R}(\mathbf{o}^{c*}_k) \end{bmatrix} \begin{bmatrix} J^c_{\Delta,p,i} & \mathbf{0}_{3\times3} \\ \mathbf{0}_{3\times3} & J^c_{\Delta,R,i}(\tilde{\mathbf{e}}^{c*}_k) \end{bmatrix} \begin{bmatrix} J^c_{\gamma,p,i} & \mathbf{0}_{3\times3} \\ \mathbf{0}_{3\times3} & J^c_{\gamma,R,i} \end{bmatrix} \\
&= \begin{bmatrix} J^c_{\eta,\text{mod}_k,p}(\mathbf{o}^{c*}_k) & J^c_{\eta,\text{mod}_k,R}(\mathbf{o}^{c*}_k) \end{bmatrix} \begin{bmatrix} J^c_{\Delta,p,i} J^c_{\gamma,p,i} & \mathbf{0}_{3\times3} \\ \mathbf{0}_{3\times3} & J^c_{\Delta,R,i}(\tilde{\mathbf{e}}^{c*}_k) J^c_{\gamma,R,i} \end{bmatrix} \\
&= \begin{bmatrix} J^c_{\eta,\text{mod}_k,p}(\mathbf{o}^{c*}_k) J^c_{\Delta,p,i} J^c_{\gamma,p,i} & J^c_{\eta,\text{mod}_k,R}(\mathbf{o}^{c*}_k) J^c_{\Delta,R,i}(\tilde{\mathbf{e}}^{c*}_k) J^c_{\gamma,R,i} \end{bmatrix} \\
&= \begin{bmatrix} r^c_{\text{mod}_k,\mathbf{p}_i}(\mathbf{e}^{c*}_k) & r^c_{\text{mod}_k,\boldsymbol{\theta}_i}(\mathbf{e}^{c*}_k) \end{bmatrix}.
\end{aligned} \tag{93}
$$

By applying the same expansion to the target node j, the full 12-column dense block cleanly reassembles into its four fundamental 3-DOF kinematic contributions:

$$
r^c_{\text{mod}_k}(\mathbf{e}^{c*}_k) = \left[r^c_{\text{mod}_k,\mathbf{p}_i}(\mathbf{e}^{c*}_k) \;\; r^c_{\text{mod}_k,\boldsymbol{\theta}_i}(\mathbf{e}^{c*}_k) \;\middle|\; r^c_{\text{mod}_k,\mathbf{p}_j}(\mathbf{e}^{c*}_k) \;\; r^c_{\text{mod}_k,\boldsymbol{\theta}_j}(\mathbf{e}^{c*}_k) \right]. \tag{94}
$$

Depending on the measurement modality, the explicit analytical evaluation of these coupled blocks yields:

- **Distance Modality (1×12 local block):** The local dense block for the generic edge k is obtained by multiplying the edge-specific coupled Jacobians. We explicitly expand their matrix product using the analytical Jacobians computed previously to obtain:

$$
\begin{aligned}
r^c_{\text{dist}}(\mathbf{e}^{c*}_k) &= J^c_{\eta,\text{dist}}(\mathbf{o}^{c*}_k) \cdot J^c_{\Delta,\text{dist}} \cdot J^c_{\gamma,\text{dist}} \\
&= \begin{bmatrix} (\mathbf{q}^*_{ij})^T & \mathbf{0}_{1\times3} \end{bmatrix} \begin{bmatrix} -\mathbf{I}_3 & \mathbf{0} & \mathbf{I}_3 & \mathbf{0} \\ \mathbf{0} & -\mathbf{I}_3 & \mathbf{0} & \mathbf{I}_3 \end{bmatrix} \begin{bmatrix} \mathbf{I}_3 & \mathbf{0} & \mathbf{0} & \mathbf{0} \\ \mathbf{0} & \mathbf{0}_{3\times3} & \mathbf{0} & \mathbf{0} \\ \mathbf{0} & \mathbf{0} & \mathbf{I}_3 & \mathbf{0} \\ \mathbf{0} & \mathbf{0} & \mathbf{0} & \mathbf{0}_{3\times3} \end{bmatrix} \\
&= \begin{bmatrix} (\mathbf{q}^*_{ij})^T & \mathbf{0}_{1\times3} \end{bmatrix} \begin{bmatrix} -\mathbf{I}_3 & \mathbf{0}_{3\times3} & \mathbf{I}_3 & \mathbf{0}_{3\times3} \\ \mathbf{0} & \mathbf{0}_{3\times3} & \mathbf{0} & \mathbf{0}_{3\times3} \end{bmatrix} \\
&= \left[\begin{array}{cc|cc} -(\mathbf{q}^*_{ij})^T & \mathbf{0}_{1\times3} & (\mathbf{q}^*_{ij})^T & \mathbf{0}_{1\times3} \end{array}\right] \\
&= \left[\begin{array}{c|c} r^c_{\text{dist},i}(\mathbf{e}^{c*}_k) & r^c_{\text{dist},j}(\mathbf{e}^{c*}_k) \end{array}\right].
\end{aligned} \tag{95}
$$

As demonstrated, the extensive padding applied by the filtration mask perfectly zeroes out both rotational columns prior to the final measurement projection.

- **Bearing Modality (3×12 local block):** The local Jacobians for the bearing modality retain explicit state dependence. Substituting the analytical expression for the measurement Jacobian computed previously, and multiplying the 6×12 observation matrix by the 12×12 filtration matrix, rigorously isolates the unobservable target attitude before the final projection:

$$
\begin{aligned}
r^c_{\text{bear}}(\mathbf{e}^{c*}_k) &= J^c_{\eta,\text{bear}}(\mathbf{o}^{c*}_k) \cdot J^c_{\Delta,\text{bear}}(\tilde{\mathbf{e}}^{c*}_k) \cdot J^c_{\gamma,\text{bear}} \\
&= \begin{bmatrix} \frac{1}{\|\mathbf{p}^*_{ij}\|}\mathbf{\Pi}_{\mathbf{b}^*_{ij}}(\mathbf{R}^*_i)^T & -\frac{1}{\|\mathbf{p}^*_{ij}\|}\mathbf{\Pi}_{\mathbf{b}^*_{ij}}(\mathbf{R}^*_i)^T[\mathbf{p}^*_{ij}]_\times \end{bmatrix} \\
&\quad \cdot \begin{bmatrix} -\mathbf{I}_3 & \mathbf{0} & \mathbf{I}_3 & \mathbf{0} \\ \mathbf{0} & -\mathbf{R}^*_i & \mathbf{0} & \mathbf{I}_3 \end{bmatrix} \begin{bmatrix} \mathbf{I}_3 & \mathbf{0} & \mathbf{0} & \mathbf{0} \\ \mathbf{0} & \mathbf{I}_3 & \mathbf{0} & \mathbf{0} \\ \mathbf{0} & \mathbf{0} & \mathbf{I}_3 & \mathbf{0} \\ \mathbf{0} & \mathbf{0} & \mathbf{0} & \mathbf{0}_{3\times3} \end{bmatrix} \\
&= \begin{bmatrix} \frac{1}{\|\mathbf{p}^*_{ij}\|}\mathbf{\Pi}_{\mathbf{b}^*_{ij}}(\mathbf{R}^*_i)^T & -\frac{1}{\|\mathbf{p}^*_{ij}\|}\mathbf{\Pi}_{\mathbf{b}^*_{ij}}(\mathbf{R}^*_i)^T[\mathbf{p}^*_{ij}]_\times \end{bmatrix} \begin{bmatrix} -\mathbf{I}_3 & \mathbf{0} & \mathbf{I}_3 & \mathbf{0}_{3\times3} \\ \mathbf{0} & -\mathbf{R}^*_i & \mathbf{0} & \mathbf{0}_{3\times3} \end{bmatrix} \\
&= \left[\begin{array}{cc|cc} -\frac{1}{\|\mathbf{p}^*_{ij}\|}\mathbf{\Pi}_{\mathbf{b}^*_{ij}}(\mathbf{R}^*_i)^T & \frac{1}{\|\mathbf{p}^*_{ij}\|}\mathbf{\Pi}_{\mathbf{b}^*_{ij}}(\mathbf{R}^*_i)^T[\mathbf{p}^*_{ij}]_\times\mathbf{R}^*_i & \frac{1}{\|\mathbf{p}^*_{ij}\|}\mathbf{\Pi}_{\mathbf{b}^*_{ij}}(\mathbf{R}^*_i)^T & \mathbf{0}_{3\times3} \end{array}\right].
\end{aligned} \tag{96}
$$

While the positional blocks are already in their fully resolved analytical form, the source node's rotational block allows for further simplification. Let us extract and evaluate this specific term:

$$-J^c_{\eta,\text{bear},R}(\mathbf{o}^{c*}_k)\mathbf{R}^*_i = \frac{1}{\|\mathbf{p}^*_{ij}\|}\mathbf{\Pi}_{\mathbf{b}^*_{ij}}\Big((\mathbf{R}^*_i)^T[\mathbf{p}^*_{ij}]_\times\mathbf{R}^*_i\Big). \tag{97}$$

Applying the Adjoint property $(\mathbf{R}^*_i)^T[\mathbf{p}^*_{ij}]_\times\mathbf{R}^*_i = [(\mathbf{R}^*_i)^T\mathbf{p}^*_{ij}]_\times = \|\mathbf{p}^*_{ij}\|[\mathbf{b}^*_{ij}]_\times$, the scalar norm cleanly cancels out:

$$-J^c_{\eta,\text{bear},R}(\mathbf{o}^{c*}_k)\mathbf{R}^*_i = \mathbf{\Pi}_{\mathbf{b}^*_{ij}}[\mathbf{b}^*_{ij}]_\times. \tag{98}$$

Using the orthogonal projection identity $\mathbf{\Pi}_{\mathbf{b}^*_{ij}}[\mathbf{b}^*_{ij}]_\times = [\mathbf{b}^*_{ij}]_\times$, this rotational derivative elegantly reduces to the pure skew-symmetric matrix:

$$-J^c_{\eta,\text{bear},R}(\mathbf{o}^{c*}_k)\mathbf{R}^*_i = [\mathbf{b}^*_{ij}]_\times. \tag{99}$$

Substituting this simplified rotational block back into the vector yields the final compact local row:

$$\begin{aligned} r^c_{\text{bear}}(\mathbf{e}^{c*}_k) &= \left[\begin{array}{cc|cc} -\frac{1}{\|\mathbf{p}^*_{ij}\|}\mathbf{\Pi}_{\mathbf{b}^*_{ij}}(\mathbf{R}^*_i)^T & [\mathbf{b}^*_{ij}]_\times & \frac{1}{\|\mathbf{p}^*_{ij}\|}\mathbf{\Pi}_{\mathbf{b}^*_{ij}}(\mathbf{R}^*_i)^T & \mathbf{0}_{3\times3} \end{array}\right] \\ &= \left[\begin{array}{c|c} r^c_{\text{bear},i}(\mathbf{e}^{c*}_k) & r^c_{\text{bear},j}(\mathbf{e}^{c*}_k) \end{array}\right]. \end{aligned} \tag{100}$$

- **Mixed Modality (**4×12 **local block):** Leveraging the dummy-padding structure of the mixed measurement map, the local block cleanly stacks the respective positional and rotational evaluations for the source and target nodes vertically:

$$\begin{aligned} r^c_{\text{mix}}(\mathbf{e}^{c*}_k) &= \begin{cases} \left[\begin{array}{c|c} \mathbf{0}_{3\times6} & \mathbf{0}_{3\times6} \\ \hline \multicolumn{2}{c}{r^c_{\text{dist}}(\mathbf{e}^{c*}_k)} \end{array}\right] = \left[\begin{array}{c|c} \mathbf{0}_{3\times6} & \mathbf{0}_{3\times6} \\ r^c_{\text{dist},i}(\mathbf{e}^{c*}_k) & r^c_{\text{dist},j}(\mathbf{e}^{c*}_k) \end{array}\right] & \text{(if edge } k \text{ is distance)} \\ \left[\begin{array}{c|c} \multicolumn{2}{c}{r^c_{\text{bear}}(\mathbf{e}^{c*}_k)} \\ \hline \mathbf{0}_{1\times6} & \mathbf{0}_{1\times6} \end{array}\right] = \left[\begin{array}{c|c} r^c_{\text{bear},i}(\mathbf{e}^{c*}_k) & r^c_{\text{bear},j}(\mathbf{e}^{c*}_k) \\ \mathbf{0}_{1\times6} & \mathbf{0}_{1\times6} \end{array}\right] & \text{(if edge } k \text{ is bearing)} \\ \begin{bmatrix} r^c_{\text{bear}}(\mathbf{e}^{c*}_k) \\ r^c_{\text{dist}}(\mathbf{e}^{c*}_k) \end{bmatrix} = \left[\begin{array}{c|c} r^c_{\text{bear},i}(\mathbf{e}^{c*}_k) & r^c_{\text{bear},j}(\mathbf{e}^{c*}_k) \\ r^c_{\text{dist},i}(\mathbf{e}^{c*}_k) & r^c_{\text{dist},j}(\mathbf{e}^{c*}_k) \end{array}\right] & \text{(if edge } k \text{ measures both)} \end{cases} \\ &= \left[\begin{array}{c|c} r^c_{\text{mix},i}(\mathbf{e}^{c*}_k) & r^c_{\text{mix},j}(\mathbf{e}^{c*}_k) \end{array}\right]. \end{aligned} \tag{101}$$

Step 2: Global Edge-Wise Assembly

Combining all these local Jacobian blocks without the topological distribution dictated by the graph yields the intermediate global block-diagonal matrix. This overarching algebraic operator corresponds to the differential of the uncoupled global map:

$$\mathbf{h}^{c}_{\text{local}} : \overline{\mathscr{M}}^{c}_{e} = (\$\mathbb{E}(3) \times \$\mathbb{E}(3))^{m} \to \mathscr{Y}^{c} \tag{102}$$

which evaluates all individual edge states mapping them directly into the full measurement space.

Because the measurement, observation, and filtration maps process each edge independently while maintaining the global geometric factorization, their global Jacobians evaluate as strictly partitioned block-diagonal operators.

To formulate the intermediate global edge-wise matrix $\mathbf{R}^{c}_{\text{local}}(\mathbf{x}^{c*})$, we exploit a standard property: the product of block-diagonal matrices is a block-diagonal matrix whose blocks are simply the products of the corresponding constituent blocks.

Consequently, this operation natively assembles into a wide, structurally ordered block-diagonal matrix:

$$\begin{aligned}
\mathbf{R}^{c}_{\text{local}}(\mathbf{x}^{c*}) &= \text{blockdiag}^{m}_{k=1}\left(J^{c}_{\eta,\text{mod}_k}(\mathbf{o}^{c*}_{k})\right) \cdot \text{blockdiag}^{m}_{k=1}\left(J^{c}_{\Delta,\text{mod}_k}(\tilde{\mathbf{e}}^{c*}_{k})\right) \\
&\qquad \cdot \text{blockdiag}^{m}_{k=1}\left(J^{c}_{\gamma,\text{mod}_k}\right) \\
&= \text{blockdiag}^{m}_{k=1}\left(J^{c}_{\eta,\text{mod}_k}(\mathbf{o}^{c*}_{k}) \cdot J^{c}_{\Delta,\text{mod}_k}(\tilde{\mathbf{e}}^{c*}_{k}) \cdot J^{c}_{\gamma,\text{mod}_k}\right) \\
&= \text{blockdiag}^{m}_{k=1}\left(r^{c}_{k}(\mathbf{e}^{c*}_{k})\right).
\end{aligned} \tag{103}$$

Depending on the network configuration, this intermediate coupled matrix takes the specific dimensions $\mathbb{R}^{m\times 12m}$ (Distance), $\mathbb{R}^{3m\times 12m}$ (Bearing), or $\mathbb{R}^{4m\times 12m}$ (Mixed).

Step 3: Topological Jacobian and Agent Distribution (Domain Expansion)

Having established the local edge-wise kinematics, we now mathematically inject the graph incidence to expand the mapping's domain. We achieve this by initially considering the entire network of agents while isolating the measurement of the single k-th edge $e_k = (i, j)$, thereby formalizing the topological distribution of the interacting agents for this specific edge.

This corresponds to analyzing the isolated global measurement map:

$$\mathbf{h}^{c}_{k} : \overline{\mathscr{D}}^{c} \to \mathscr{Y}_{k}. \tag{104}$$

While the codomain of this mapping remains restricted to the local measurement space $\mathcal{Y}_k$ of the single k-th edge, its domain expands to encompass the entire state space of the network.

By computing the Jacobian $[\mathbf{R}^c(\mathbf{x}^{c*})]_k$ of this specific map $\mathbf{h}_k^c$, we establish how the localized kinematic blocks are distributed across all the agents.

As previously demonstrated, the global natively coupled tangent space inherently factorizes into a sequentially ordered direct sum, natively grouping the 3-DOF positional and 3-DOF rotational contributions agent by agent. Because this global state vector is fundamentally partitioned into n distinct 6-DOF column blocks, the Jacobian $[\mathbf{R}^c(\mathbf{x}^{c*})]_k$ extracts the exact geometric contribution of the required agents directly from this global direct sum.

Physically, since the mapping $\mathbf{h}_k^c$ evaluates the edge $e_k = (i, j)$, which depends exclusively on its source node i and target node j, its partial derivative with respect to any other agent in the network is identically zero. Conversely, its non-zero partial derivatives with respect to i and j coincide exactly with the local kinematic blocks derived previously in Step 1. Therefore, injecting the topology simply requires taking these local blocks and accurately distributing them into their correct global coordinates. This yields a highly sparse row structure: the resulting global row will contain the local 6-DOF dense blocks strictly at the i-th and j-th block-indices, padded by zero-blocks everywhere else.

To realize this precise sparse placement, we recall the topological distribution map. Its local Jacobian can be gracefully expressed using the coupled 6-DOF block-selector operators $(\mathbf{u}_i^T \otimes \mathbf{I}_6)$. Specifically, the k-th local block row for a generic edge $e_k = (i, j)$ is formulated as the incidence-selection matrix:

$$[\mathbf{J}_\sigma^c]_k = \begin{bmatrix} \mathbf{u}_i^T \otimes \mathbf{I}_6 \\ \mathbf{u}_j^T \otimes \mathbf{I}_6 \end{bmatrix} \in \mathbb{R}^{12\times 6n}. \tag{105}$$

Consequently, the full global topological Jacobian is simply represented as the direct vertical stacking of these m edge-wise components:

$$\mathbf{J}_\sigma^c = \begin{bmatrix} [\mathbf{J}_\sigma^c]_1 \\ \vdots \\ [\mathbf{J}_\sigma^c]_m \end{bmatrix}. \tag{106}$$

By post-multiplying the dense 12-column local block $r_k^c(\mathbf{e}_k^{c*})$ by its corresponding topological block $[\mathbf{J}_\sigma^c]_k$, the isolated source and target components are mapped into their precise global columns within the full $6n$-column global sparse vector $[\mathbf{R}^c(\mathbf{x}^{c*})]_k$:

$$\begin{aligned}
[\mathbf{R}^c(\mathbf{x}^{c*})]_k &= r_k^c(\mathbf{e}_k^{c*}) \cdot [\mathbf{J}_\sigma^c]_k \\
&= \left[r_{k,i}^c(\mathbf{e}_k^{c*}) \;\middle|\; r_{k,j}^c(\mathbf{e}_k^{c*}) \right] \begin{bmatrix} \mathbf{u}_i^T \otimes \mathbf{I}_6 \\ \mathbf{u}_j^T \otimes \mathbf{I}_6 \end{bmatrix} \\
&= r_{k,i}^c(\mathbf{e}_k^{c*})\big(\mathbf{u}_i^T \otimes \mathbf{I}_6\big) + r_{k,j}^c(\mathbf{e}_k^{c*})\big(\mathbf{u}_j^T \otimes \mathbf{I}_6\big).
\end{aligned} \tag{107}$$

Depending on the measurement modality, this inner product yields the precise global row structures:

- **Global Distance Row** ($1 \times 6n$):

$$[\mathbf{R}^c_{\text{dist}}(\mathbf{x}^{c*})]_k = \begin{bmatrix} -(\mathbf{q}^*_{ij})^T & \mathbf{0}_{1\times3} \end{bmatrix} \left(\mathbf{u}_i^T \otimes \mathbf{I}_6\right) + \begin{bmatrix} (\mathbf{q}^*_{ij})^T & \mathbf{0}_{1\times3} \end{bmatrix} \left(\mathbf{u}_j^T \otimes \mathbf{I}_6\right). \quad (108)$$

- **Global Bearing Row** ($3 \times 6n$):

$$\begin{aligned} [\mathbf{R}^c_{\text{bear}}(\mathbf{x}^{c*})]_k &= \begin{bmatrix} -\frac{1}{\|\mathbf{p}^*_{ij}\|}\mathbf{\Pi}_{\mathbf{b}^*_{ij}}(\mathbf{R}^*_i)^T & [\mathbf{b}^*_{ij}]_\times \end{bmatrix} \left(\mathbf{u}_i^T \otimes \mathbf{I}_6\right) \\ &\quad + \begin{bmatrix} \frac{1}{\|\mathbf{p}^*_{ij}\|}\mathbf{\Pi}_{\mathbf{b}^*_{ij}}(\mathbf{R}^*_i)^T & \mathbf{0}_{3\times3} \end{bmatrix} \left(\mathbf{u}_j^T \otimes \mathbf{I}_6\right). \end{aligned} \quad (109)$$

- **Global Mixed Row** ($4 \times 6n$):

$$[\mathbf{R}^c_{\text{mix}}(\mathbf{x}^{c*})]_k = \begin{cases} \begin{bmatrix} \mathbf{0}_{3\times6n} \\ [\mathbf{R}^c_{\text{dist}}(\mathbf{x}^{c*})]_k \end{bmatrix} & \text{(if edge } k \text{ is distance)} \\ \begin{bmatrix} [\mathbf{R}^c_{\text{bear}}(\mathbf{x}^{c*})]_k \\ \mathbf{0}_{1\times6n} \end{bmatrix} & \text{(if edge } k \text{ is bearing)} \\ \begin{bmatrix} [\mathbf{R}^c_{\text{bear}}(\mathbf{x}^{c*})]_k \\ [\mathbf{R}^c_{\text{dist}}(\mathbf{x}^{c*})]_k \end{bmatrix} & \text{(if edge } k \text{ measures both)} \end{cases} \quad (110)$$

Step 4: Full Network Integration (Codomain Integration)

We now incorporate all measurement contributions by aggregating the edge-wise components derived in Step 3 across the entire graph. While Step 3 successfully expanded the domain onto the globally coupled agent state space, we must now integrate the codomain to account for the complete sensory network.

As previously established, the coupled embedded rigidity matrix $\mathbf{R}^c(\mathbf{x}^{c*})$ represents the exact differential of the overarching measurement function $\mathbf{h}^c : \overline{\mathscr{D}}^c \to \mathscr{Y}^c$. The direct sum structure of the tangent spaces dictates that the columns of the resulting matrix are structurally forced to partition sequentially by agent, with each 6-DOF column block encapsulating the full pose variation of a specific node. Because the intermediate edge-wise matrix $\mathbf{R}^c_{\text{local}}(\mathbf{x}^{c*})$ is exclusively block-diagonal and the topological Jacobian $\mathbf{J}^c_\sigma$ is constructed by vertically stacked block rows, the full algebraic evaluation of their product rigorously preserves this agent-centric column partition.

The matrix multiplication collapses into an ordered vertical stacking that applies the local dense blocks independently to their respective incidence rows. This operation effectively stacks the individual measurement codomains, yielding the exact global sparse rows derived in Step 3:

$$\begin{aligned} \mathbf{R}^c(\mathbf{x}^{c*}) &= \mathbf{R}^c_{\text{local}}(\mathbf{x}^{c*}) \cdot \mathbf{J}^c_\sigma \\ &= \text{blockdiag}_{k=1}^m \left(r^c_k(\mathbf{e}^{c*}_k) \right) \cdot \begin{bmatrix} [\mathbf{J}^c_\sigma]_1 \\ \vdots \\ [\mathbf{J}^c_\sigma]_m \end{bmatrix} \\ &= \begin{bmatrix} r^c_1(\mathbf{e}^{c*}_1) \cdot [\mathbf{J}^c_\sigma]_1 \\ \vdots \\ r^c_m(\mathbf{e}^{c*}_m) \cdot [\mathbf{J}^c_\sigma]_m \end{bmatrix} = \begin{bmatrix} [\mathbf{R}^c(\mathbf{x}^{c*})]_1 \\ \vdots \\ [\mathbf{R}^c(\mathbf{x}^{c*})]_m \end{bmatrix}. \end{aligned} \tag{111}$$

Thus, depending on the specific modalities distributed across the MAS, the final embedded coupled rigidity matrix $\mathbf{R}^c(\mathbf{x}^{c*})$ is formally assembled by vertically stacking the modality-specific rows:

- **Distance MAS:** The matrix $\mathbf{R}^c_{\text{dist}}(\mathbf{x}^{c*}) \in \mathbb{R}^{m \times 6n}$ is constructed entirely of sparse $1 \times 6n$ distance rows:

$$\mathbf{R}^c_{\text{dist}}(\mathbf{x}^{c*}) = \begin{bmatrix} [\mathbf{R}^c_{\text{dist}}(\mathbf{x}^{c*})]_1 \\ \vdots \\ [\mathbf{R}^c_{\text{dist}}(\mathbf{x}^{c*})]_m \end{bmatrix} \tag{112}$$

- **Bearing MAS:** The matrix $\mathbf{R}^c_{\text{bear}}(\mathbf{x}^{c*}) \in \mathbb{R}^{3m \times 6n}$ is constructed entirely of sparse $3 \times 6n$ bearing rows:

$$\mathbf{R}^c_{\text{bear}}(\mathbf{x}^{c*}) = \begin{bmatrix} [\mathbf{R}^c_{\text{bear}}(\mathbf{x}^{c*})]_1 \\ \vdots \\ [\mathbf{R}^c_{\text{bear}}(\mathbf{x}^{c*})]_m \end{bmatrix} \tag{113}$$

- **Mixed MAS:** The matrix $\mathbf{R}^c_{\text{mix}}(\mathbf{x}^{c*}) \in \mathbb{R}^{4m \times 6n}$ is uniformly assembled by vertically stacking the sparse $4 \times 6n$ padded rows, cleanly preserving structural alignment across the 6-DOF agent columns even where measurements are locally absent:

$$\mathbf{R}^c_{\text{mix}}(\mathbf{x}^{c*}) = \begin{bmatrix} [\mathbf{R}^c_{\text{mix}}(\mathbf{x}^{c*})]_1 \\ \vdots \\ [\mathbf{R}^c_{\text{mix}}(\mathbf{x}^{c*})]_m \end{bmatrix} \tag{114}$$

4.5 DECOUPLED EMBEDDED RIGIDITY MATRIX STRUCTURE

In this section, we investigate the fully pose-decoupled embedded functor realization, denoted as $\mathscr{F}^d$. By exploiting the Cartesian factorization of the global state space throughout the entire sequence, we explicitly derive the algebraic structure of the decoupled rigidity matrix, highlighting the advantageous properties that emerge from isolating translational and rotational kinematics.

4.5.1 Decoupled Topological Distribution Map

In the decoupled space, the topological map strictly separates the routing of positions and attitudes. The global state vector is mapped into two independent streams via $\boldsymbol{\sigma}^d_{\text{emb}} = \boldsymbol{\sigma}^d_{\text{emb},p} \times \boldsymbol{\sigma}^d_{\text{emb},R}$, where:

$$\boldsymbol{\sigma}^d_{\text{emb},p} : (\mathbb{R}^3)^n \to \left(\mathbb{R}^3 \times \mathbb{R}^3\right)^m, \quad \boldsymbol{\sigma}^d_{\text{emb},R} : \mathbb{SO}(3)^n \to (\mathbb{SO}(3) \times \mathbb{SO}(3))^m. \tag{115}$$

Consequently, the joint decoupled map evaluates to:

$$\begin{aligned} \boldsymbol{\sigma}^d_{\text{emb}} : (\mathbb{R}^3)^n \times \mathbb{SO}(3)^n &\to \left(\mathbb{R}^3 \times \mathbb{R}^3\right)^m \times (\mathbb{SO}(3) \times \mathbb{SO}(3))^m \\ (\mathbf{p}, \mathbf{R}) &\mapsto \left(\boldsymbol{\sigma}^d_{\text{emb},p}(\mathbf{p}), \boldsymbol{\sigma}^d_{\text{emb},R}(\mathbf{R})\right). \end{aligned} \tag{116}$$

Because this topological routing relies solely on fixed linear selection, its Jacobian is entirely state-invariant. Dropping the evaluation argument, the local Jacobian block for the k-th edge $e_k = (i, j)$ elegantly splits into a block-diagonal structure containing two identical selection matrices:

$$\left[J^d_\sigma\right]_k = \begin{bmatrix} S_{e_k} & \mathbf{0} \\ \mathbf{0} & S_{e_k} \end{bmatrix}, \tag{117}$$

where $S_{e_k} \in \mathbb{R}^{6\times 3n}$ is the standard incidence-selection matrix. Using the decoupled block-selector operators, it is rigorously formulated as:

$$S_{e_k} = \begin{bmatrix} \mathbf{u}_i^T \otimes \mathbf{I}_3 \\ \mathbf{u}_j^T \otimes \mathbf{I}_3 \end{bmatrix}. \tag{118}$$

To construct the full global matrix $\mathbf{J}^d_{\boldsymbol{\sigma}}$, we define the global incidence-selection matrix $\mathbf{S} \in \mathbb{R}^{6m\times 3n}$ by vertically stacking the individual translational (or rotational) edge blocks. Preserving the macroscopic factorization, the constant global Jacobian evaluates to a strict block-diagonal structure:

$$\mathbf{S} = \begin{bmatrix} S_{e_1} \\ S_{e_2} \\ \vdots \\ S_{e_m} \end{bmatrix}, \quad \mathbf{J}^d_{\boldsymbol{\sigma}} = \begin{bmatrix} \mathbf{S} & \mathbf{0} \\ \mathbf{0} & \mathbf{S} \end{bmatrix} \in \mathbb{R}^{12m\times 6n}. \tag{119}$$

4.5.2 Decoupled Task Filtration

Local Filtration Maps and Jacobians

At the local level, let the nominal decoupled edge state for a specific k-th edge be $\mathbf{e}_k^{d*} = \big((\mathbf{p}_i^*, \mathbf{p}_j^*), (\mathbf{R}_i^*, \mathbf{R}_j^*)\big)$. The task filtration map $\gamma_{\text{mod}_k}^d = \gamma_p^d \times \gamma_R^d$ removes unmeasured quantities and replaces them with a neutral padding, yielding

$$\tilde{\mathbf{e}}_k^{d*} = \big((\tilde{\mathbf{p}}_i^*, \tilde{\mathbf{p}}_j^*), (\tilde{\mathbf{R}}_i^*, \tilde{\mathbf{R}}_j^*)\big) = \big((\mathbf{p}_i^*, \mathbf{p}_j^*), (\tilde{\mathbf{R}}_i^*, \tilde{\mathbf{R}}_j^*)\big).$$

Formally, the independent translational and rotational local filtration maps are defined as:

$$\gamma_p^d : \mathbb{R}^3 \times \mathbb{R}^3 \to \mathbb{R}^3 \times \mathbb{R}^3 \tag{120}$$

$$\gamma_R^d : \mathbb{SO}(3) \times \mathbb{SO}(3) \to \mathbb{SO}(3) \times \mathbb{SO}(3) \tag{121}$$

Because the padding mechanisms do not interfere, all cross-domain derivatives are strictly zero. We can evaluate their independent Jacobians directly.

For the positional stream, the spatial coordinates are universally required and never filtered. Thus, γ_p^d acts as a perfect identity mapping. Its Jacobian is a strictly constant matrix that is completely independent of the evaluation point. Structurally, it splits cleanly for the source i and target j:

$$J_{\gamma,p}^d(\mathbf{e}_k^{d*}) \equiv J_{\gamma,p}^d = \begin{bmatrix} J_{\gamma,p,i}^d & \mathbf{0} \\ \mathbf{0} & J_{\gamma,p,j}^d \end{bmatrix} = \text{blockdiag}(\mathbf{I}_3, \mathbf{I}_3). \tag{122}$$

For the rotational stream, the mapping γ_R^d either preserves a rotation (yielding an identity derivative block) or masks it with constant padding (yielding a zero derivative block). Because masking is fundamentally a linear or constant operation, its Jacobian $J_{\gamma,R,\text{mod}_k}^d$ is also a strictly state-invariant constant matrix that partitions natively by agent:

$$J_{\gamma,R,\text{mod}_k}^d(\mathbf{e}_k^{d*}) \equiv J_{\gamma,R,\text{mod}_k}^d = \begin{bmatrix} J_{\gamma,R,i}^d & \mathbf{0} \\ \mathbf{0} & J_{\gamma,R,j}^d \end{bmatrix}. \tag{123}$$

The joint local filtration Jacobian $J_{\gamma,\text{mod}_k}^d$ is assembled as a strict block-diagonal concatenation of these two invariant components:

$$J_{\gamma,\text{mod}_k}^d = \begin{bmatrix} J_{\gamma,p}^d & \mathbf{0} \\ \mathbf{0} & J_{\gamma,R,\text{mod}_k}^d \end{bmatrix}. \tag{124}$$

Evaluating the modal mappings at the specific operational points yields the exact matrix blocks:

- **Distance Edge (**dist**):** Both attitudes are unobservable and padded ($\tilde{\mathbf{R}}_i^* = \tilde{\mathbf{R}}_j^* = \mathbf{I}_3$).

$$\gamma^d_{\text{dist}}(\mathbf{e}_k^{d*}) = \big((\mathbf{p}_i^*, \mathbf{p}_j^*),\ (\mathbf{I}_3, \mathbf{I}_3)\big) \tag{125}$$

  Because the rotational mapping masks both states, its local sub-blocks evaluate to $J^d_{\gamma,R,i} = \mathbf{0}_{3\times3}$ and $J^d_{\gamma,R,j} = \mathbf{0}_{3\times3}$. The Jacobian is entirely null: $J^d_{\gamma,R,\text{dist}} = \text{blockdiag}(\mathbf{0}_{3\times3}, \mathbf{0}_{3\times3})$. The full invariant block-diagonal Jacobian naturally emerges as:

$$J^d_{\gamma,\text{dist}} = \begin{bmatrix} \mathbf{I}_3 & \mathbf{0} & \mathbf{0} & \mathbf{0} \\ \mathbf{0} & \mathbf{I}_3 & \mathbf{0} & \mathbf{0} \\ \mathbf{0} & \mathbf{0} & \mathbf{0}_{3\times3} & \mathbf{0} \\ \mathbf{0} & \mathbf{0} & \mathbf{0} & \mathbf{0}_{3\times3} \end{bmatrix} = \text{blockdiag}\left(\mathbf{I}_3, \mathbf{I}_3, \mathbf{0}_{3\times3}, \mathbf{0}_{3\times3}\right). \tag{126}$$

- **Bearing Edge (**bear**):** Only the target's attitude is unobservable and padded ($\tilde{\mathbf{R}}_i^* = \mathbf{R}_i^*$, $\tilde{\mathbf{R}}_j^* = \mathbf{I}_3$).

$$\gamma^d_{\text{bear}}(\mathbf{e}_k^{d*}) = \big((\mathbf{p}_i^*, \mathbf{p}_j^*),\ (\mathbf{R}_i^*, \mathbf{I}_3)\big) \tag{127}$$

  The rotational Jacobian preserves the source attitude ($J^d_{\gamma,R,i} = \mathbf{I}_3$) while masking the target ($J^d_{\gamma,R,j} = \mathbf{0}_{3\times3}$), yielding $J^d_{\gamma,R,\text{bear}} = \text{blockdiag}(\mathbf{I}_3, \mathbf{0}_{3\times3})$. The joint local Jacobian cleanly assembles into:

$$J^d_{\gamma,\text{bear}} = \text{blockdiag}\left(\mathbf{I}_3, \mathbf{I}_3, \mathbf{I}_3, \mathbf{0}_{3\times3}\right). \tag{128}$$

- **Mixed Edge (**mix**):** Similar to the bearing edge, the target's orientation is unobservable ($\tilde{\mathbf{R}}_i^* = \mathbf{R}_i^*$, $\tilde{\mathbf{R}}_j^* = \mathbf{I}_3$).

$$\gamma^d_{\text{mix}}(\mathbf{e}_k^{d*}) = \big((\mathbf{p}_i^*, \mathbf{p}_j^*),\ (\mathbf{R}_i^*, \mathbf{I}_3)\big) \tag{129}$$

  Consequently, the individual rotational Jacobian perfectly mirrors the bearing case:

$$J^d_{\gamma,\text{mix}} = \text{blockdiag}\left(\mathbf{I}_3, \mathbf{I}_3, \mathbf{I}_3, \mathbf{0}_{3\times3}\right). \tag{130}$$

Global Filtration Map and Jacobian Assembly

Extending this formulation globally, the task filtration map $\boldsymbol{\gamma}^d_{\text{emb}} = \boldsymbol{\gamma}^d_p \times \boldsymbol{\gamma}^d_R$ acts concurrently on all m edges:

$$\boldsymbol{\gamma}^d_p : \ \left(\mathbb{R}^3 \times \mathbb{R}^3\right)^m \to \left(\mathbb{R}^3 \times \mathbb{R}^3\right)^m \tag{131}$$

$$\boldsymbol{\gamma}^d_R : \ (\mathbb{SO}(3) \times \mathbb{SO}(3))^m \to (\mathbb{SO}(3) \times \mathbb{SO}(3))^m \tag{132}$$

Because the filtration of each edge is independent and state-invariant, the global Jacobian $\mathbf{J}^d_{\boldsymbol{\gamma}} \in \mathbb{R}^{12m\times12m}$ keeps the modal streams rigorously isolated in a constant macro block-diagonal configuration:

$$\mathbf{J}^d_{\boldsymbol{\gamma}} = \begin{bmatrix} \text{blockdiag}_{k=1}^m \left(J^d_{\gamma,p}\right) & \mathbf{0} \\ \mathbf{0} & \text{blockdiag}_{k=1}^m \left(J^d_{\gamma,R,\text{mod}_k}\right) \end{bmatrix}. \tag{133}$$

Crucially, because positional coordinates are never padded in our setup, the local positional Jacobian $J^d_{\gamma,p}$ is universally constant across all sensing paradigms. Consequently, the upper-left positional macro-block can always be factored using the Kronecker product ($\mathbf{I}_m \otimes J^d_{\gamma,p}$). Furthermore, because filtration relies strictly on linear masking or constant padding, the local rotational Jacobians $J^d_{\gamma,R}$ are also strictly state-invariant. Leveraging the Kronecker product ($\otimes$) for homogeneous replication, we obtain:

- **Distance Network:** The global Jacobian replicates the independent positional and rotational distance masks. We exploit a double Kronecker structure:

$$\mathbf{J}^d_{\boldsymbol{\gamma},\text{dist}} = \begin{bmatrix} \mathbf{I}_m \otimes J^d_{\gamma,p} & \mathbf{0} \\ \mathbf{0} & \mathbf{I}_m \otimes J^d_{\gamma,R,\text{dist}} \end{bmatrix}. \tag{134}$$

- **Bearing Network:** The rotational mask remains invariant, allowing full Kronecker replication:

$$\mathbf{J}^d_{\boldsymbol{\gamma},\text{bear}} = \begin{bmatrix} \mathbf{I}_m \otimes J^d_{\gamma,p} & \mathbf{0} \\ \mathbf{0} & \mathbf{I}_m \otimes J^d_{\gamma,R,\text{bear}} \end{bmatrix}. \tag{135}$$

- **Mixed Network:** In heterogeneous graphs, the global Jacobian retains the Kronecker product for the universal positional stream, while dynamically assembling the specific local mask in the rotational stream:

$$\mathbf{J}^d_{\boldsymbol{\gamma}} = \begin{bmatrix} \mathbf{I}_m \otimes J^d_{\gamma,p} & \mathbf{0} \\ \mathbf{0} & \text{blockdiag}^m_{k=1}\left(J^d_{\gamma,R,\text{mod}_k}\right) \end{bmatrix}. \tag{136}$$

4.5.3 Decoupled Edge Observation

The observation map computes the relative kinematics for each edge directly within the decoupled geometric space, relying on the filtered inputs.

Local Observation Maps and Jacobians

Let the padded filtered state for a generic single edge $e_k = (i,j)$ be denoted as $\tilde{\mathbf{e}}^{d*}_k = \big((\tilde{\mathbf{p}}^*_i, \tilde{\mathbf{p}}^*_j), (\tilde{\mathbf{R}}^*_i, \tilde{\mathbf{R}}^*_j)\big) = \big((\mathbf{p}^*_i, \mathbf{p}^*_j), (\tilde{\mathbf{R}}^*_i, \tilde{\mathbf{R}}^*_j)\big)$. The map $\Delta^d = \Delta^d_p \times \Delta^d_R$ computes the relative kinematics by processing the streams separately:

$$\Delta^d_p : \mathbb{R}^3 \times \mathbb{R}^3 \to \mathbb{R}^3 \tag{137}$$

$$\Delta^d_R : \mathbb{SO}(3) \times \mathbb{SO}(3) \to \mathbb{SO}(3) \tag{138}$$

yielding the joint local evaluation:

$$\begin{aligned} \Delta^d : \ & \left(\mathbb{R}^3 \times \mathbb{R}^3\right) \times (\mathbb{SO}(3) \times \mathbb{SO}(3)) \to \mathbb{R}^3 \times \mathbb{SO}(3) \\ & \left((\mathbf{p}_i, \mathbf{p}_j), (\mathbf{R}_i, \mathbf{R}_j)\right) \mapsto \left(\mathbf{p}_j - \mathbf{p}_i,\ \mathbf{R}_i^T \mathbf{R}_j\right). \end{aligned} \tag{139}$$

Given that Δ_p^d depends exclusively on the positional states and Δ_R^d exclusively on the rotational states, all cross-domain derivatives are strictly zero.

For the positional stream, the differential is simply a linear difference $\delta \mathbf{p}_{ij} = \delta \mathbf{p}_j - \delta \mathbf{p}_i$. Consequently, its Jacobian evaluates to a strictly constant matrix, explicitly split into source and target derivatives ($J^d_{\Delta,p,i}$ and $J^d_{\Delta,p,j}$), independent of the evaluation point:

$$J^d_{\Delta,p}(\tilde{\mathbf{e}}_k^{d*}) \equiv J^d_{\Delta,p} = \begin{bmatrix} J^d_{\Delta,p,i} & J^d_{\Delta,p,j} \end{bmatrix} = \begin{bmatrix} -\mathbf{I}_3 & \mathbf{I}_3 \end{bmatrix} \tag{140}$$

For the rotational stream, the Jacobian derived previously yields a matrix that generally retains an explicit state dependence, naturally split into $J^d_{\Delta,R,i}$ and $J^d_{\Delta,R,j}$:

$$J^d_{\Delta,R}(\tilde{\mathbf{e}}_k^{d*}) = \begin{bmatrix} J^d_{\Delta,R,i}(\tilde{\mathbf{e}}_k^{d*}) & J^d_{\Delta,R,j}(\tilde{\mathbf{e}}_k^{d*}) \end{bmatrix} = \begin{bmatrix} -(\tilde{\mathbf{R}}_{ij}^*)^T & \mathbf{I}_3 \end{bmatrix} \tag{141}$$

The joint local observation Jacobian $J^d_\Delta(\tilde{\mathbf{e}}_k^{d*})$ is assembled as a strict block-diagonal combination of these decoupled components:

$$J^d_\Delta(\tilde{\mathbf{e}}_k^{d*}) = \begin{bmatrix} J^d_{\Delta,p} & \mathbf{0}_{3\times 6} \\ \mathbf{0}_{3\times 6} & J^d_{\Delta,R}(\tilde{\mathbf{e}}_k^{d*}) \end{bmatrix} = \begin{bmatrix} -\mathbf{I}_3 & \mathbf{I}_3 & \mathbf{0}_{3\times 3} & \mathbf{0}_{3\times 3} \\ \mathbf{0}_{3\times 3} & \mathbf{0}_{3\times 3} & -(\tilde{\mathbf{R}}_{ij}^*)^T & \mathbf{I}_3 \end{bmatrix}. \tag{142}$$

Evaluating this generic mapping at the specified filtration operational points yields the modal blocks:

- **Distance Edge (**dist**):** Both attitudes are filtered and padded ($\tilde{\mathbf{R}}_i^* = \tilde{\mathbf{R}}_j^* = \mathbf{I}_3$). The relative rotation natively collapses to $\tilde{\mathbf{R}}_{ij}^* = \mathbf{I}_3$. Crucially, this filtering and padding action causes the rotational Jacobian to become state-invariant as well, allowing us to drop its evaluation argument:

$$\Delta^d_{\text{dist}}\left((\mathbf{p}_i^*, \mathbf{p}_j^*), (\mathbf{I}_3, \mathbf{I}_3)\right) = \left(\mathbf{p}_j^* - \mathbf{p}_i^*,\ \mathbf{I}_3\right) \tag{143}$$

$$J^d_{\Delta,R,\text{dist}}(\tilde{\mathbf{e}}_k^{d*}) \equiv J^d_{\Delta,R,\text{dist}} = \begin{bmatrix} -\mathbf{I}_3 & \mathbf{I}_3 \end{bmatrix} \tag{144}$$

$$J^d_{\Delta,\text{dist}} = \begin{bmatrix} J^d_{\Delta,p} & \mathbf{0}_{3\times 6} \\ \mathbf{0}_{3\times 6} & J^d_{\Delta,R,\text{dist}} \end{bmatrix} \tag{145}$$

  where $J^d_{\Delta,R,i} = -\mathbf{I}_3$ and $J^d_{\Delta,R,j} = \mathbf{I}_3$.

- **Bearing Edge (**bear**):** Only the target attitude is padded ($\tilde{\mathbf{R}}_j^* = \mathbf{I}_3$), yielding $\tilde{\mathbf{R}}_{ij}^* = (\mathbf{R}_i^*)^T$. The rotational Jacobian retains its state dependence on the source node:

$$\Delta^d_{\text{bear}}\left((\mathbf{p}_i^*, \mathbf{p}_j^*), (\mathbf{R}_i^*, \mathbf{I}_3)\right) = \left(\mathbf{p}_j^* - \mathbf{p}_i^*,\ (\mathbf{R}_i^*)^T\right) \tag{146}$$

$$J^d_{\Delta,R,\text{bear}}(\tilde{\mathbf{e}}_k^{d*}) = \begin{bmatrix} -\mathbf{R}_i^* & \mathbf{I}_3 \end{bmatrix} \tag{147}$$

$$J^d_{\Delta,\text{bear}}(\tilde{\mathbf{e}}_k^{d*}) = \begin{bmatrix} J^d_{\Delta,p} & \mathbf{0}_{3\times 6} \\ \mathbf{0}_{3\times 6} & J^d_{\Delta,R,\text{bear}}(\tilde{\mathbf{e}}_k^{d*}) \end{bmatrix} \tag{148}$$

  where $J^d_{\Delta,R,i}(\tilde{\mathbf{e}}_k^{d*}) = -\mathbf{R}_i^*$ and $J^d_{\Delta,R,j} = \mathbf{I}_3$.

- **Mixed Edge** (mix)**:** Because the target's attitude remains unobservable ($\tilde{\mathbf{R}}_j^* = \mathbf{I}_3$), the observation mapping and its Jacobian are structurally identical to the pure bearing case:

$$\Delta^d_{\text{mix}}\big((\mathbf{p}_i^*, \mathbf{p}_j^*), (\mathbf{R}_i^*, \mathbf{I}_3)\big) = \big(\mathbf{p}_j^* - \mathbf{p}_i^*, (\mathbf{R}_i^*)^T\big) \tag{149}$$

$$J^d_{\Delta,R,\text{mix}}(\tilde{\mathbf{e}}_k^{d*}) = \begin{bmatrix} -\mathbf{R}_i^* & \mathbf{I}_3 \end{bmatrix} \tag{150}$$

$$J^d_{\Delta,\text{mix}}(\tilde{\mathbf{e}}_k^{d*}) = \begin{bmatrix} J^d_{\Delta,p} & \mathbf{0}_{3\times 6} \\ \mathbf{0}_{3\times 6} & J^d_{\Delta,R,\text{mix}}(\tilde{\mathbf{e}}_k^{d*}) \end{bmatrix} \tag{151}$$

Global Observation Jacobian Assembly

The global edge observation map $\boldsymbol{\Delta}^d_{\text{emb}} = \boldsymbol{\Delta}^d_p \times \boldsymbol{\Delta}^d_R$ concurrently computes the relative kinematics across all m edges:

$$\boldsymbol{\Delta}^d_p : \ \big(\mathbb{R}^3 \times \mathbb{R}^3\big)^m \to \big(\mathbb{R}^3\big)^m \tag{152}$$

$$\boldsymbol{\Delta}^d_R : \ (\mathbb{SO}(3) \times \mathbb{SO}(3))^m \to (\mathbb{SO}(3))^m \tag{153}$$

producing the joint global mapping:

$$\boldsymbol{\Delta}^d_{\text{emb}} : \ \big(\mathbb{R}^3 \times \mathbb{R}^3\big)^m \times (\mathbb{SO}(3) \times \mathbb{SO}(3))^m \to \big(\mathbb{R}^3\big)^m \times (\mathbb{SO}(3))^m . \tag{154}$$

As structural decoupling is maintained globally, the total observation Jacobian $\mathbf{J}^d_{\boldsymbol{\Delta}}(\tilde{\mathbf{e}}^{d*})$ perfectly separates all translational observations from all rotational observations, retaining a strict macro block-diagonal form. In its most general representation, it is assembled by explicitly concatenating the decoupled local mappings ordered by the edge index $k = 1, \dots, m$:

$$\mathbf{J}^d_{\boldsymbol{\Delta}}(\tilde{\mathbf{e}}^{d*}) = \begin{bmatrix} \text{blockdiag}_{k=1}^m \big(J^d_{\Delta,p}\big) & \mathbf{0} \\ \mathbf{0} & \text{blockdiag}_{k=1}^m \big(J^d_{\Delta,R}(\tilde{\mathbf{e}}_k^{d*})\big) \end{bmatrix}. \tag{155}$$

A fundamental structural advantage of this formulation is that the local positional Jacobian $J^d_{\Delta,p}$ is universally constant across all edges and all sensing paradigms. Consequently, the upper-left positional macro-block can always be factored compactly using the Kronecker product ($\mathbf{I}_m \otimes J^d_{\Delta,p}$). The algebraic assembly of the lower-right rotational macro-block, however, depends on whether the underlying measurement modality preserves or removes state dependence:

- **Distance Network:** For a homogeneous distance network, the rotational mapping is completely filtered and padded, yielding the state-invariant local block $J^d_{\Delta,R,\text{dist}}$. Since neither stream depends on the evaluation state, the general formulation elegantly collapses into Kronecker products for both macro-blocks:

$$\mathbf{J}^d_{\boldsymbol{\Delta},\text{dist}} = \begin{bmatrix} \mathbf{I}_m \otimes J^d_{\Delta,p} & \mathbf{0} \\ \mathbf{0} & \mathbf{I}_m \otimes J^d_{\Delta,R,\text{dist}} \end{bmatrix} \tag{156}$$

- **Bearing Network:** In a homogeneous bearing network, the rotational Jacobian $J^d_{\Delta,R,\mathrm{bear}}$ retains an explicit dependence on the source agent's attitude. Consequently, while the positional macro-block is factored via the Kronecker product, the rotational macro-block requires explicit state-dependent concatenation:

$$\mathbf{J}^d_{\Delta,\mathrm{bear}}(\tilde{\mathbf{e}}^{d*}) = \begin{bmatrix} \mathbf{I}_m \otimes J^d_{\Delta,p} & \mathbf{0} \\ \mathbf{0} & \mathrm{blockdiag}_{k=1}^m \left(J^d_{\Delta,R,\mathrm{bear}}(\tilde{\mathbf{e}}^{d*}_k)\right) \end{bmatrix} \tag{157}$$

- **Mixed Network:** In a graph featuring multiple measurement modalities, the rotational macro-block dynamically adapts to both the specific measurement type of each edge and its local state. The positional block remains universally invariant:

$$\mathbf{J}^d_{\Delta}(\tilde{\mathbf{e}}^{d*}) = \begin{bmatrix} \mathbf{I}_m \otimes J^d_{\Delta,p} & \mathbf{0} \\ \mathbf{0} & \mathrm{blockdiag}_{k=1}^m \left(J^d_{\Delta,R,\mathrm{mod}_k}(\tilde{\mathbf{e}}^{d*}_k)\right) \end{bmatrix} \tag{158}$$

4.5.4 Decoupled Measurement Maps

Following the extraction of the relative kinematics, we define the decoupled measurement maps. This is the stage where the previously isolated positional and rotational streams are fused into a single physical observation within the specific measurement codomain $\mathcal{Y}$.

Local Measurement Maps and Jacobians

At the local level for a k-th edge, let the nominal decoupled relative state be explicitly denoted as $\mathbf{o}^{d*}_k = (\tilde{\mathbf{p}}^*_{ij}, \tilde{\mathbf{R}}^*_{ij}) = (\mathbf{p}^*_{ij}, \tilde{\mathbf{R}}^*_{ij})$. We formally define the generic local measurement map

$$\eta^d_{\mathrm{mod}_k} : \mathbb{R}^3 \times \mathbb{SO}(3) \to \mathcal{Y} \tag{159}$$

which yields the nominal sensor reading $\mathbf{y}^*_k \in \mathcal{Y}$:

$$\eta^d_{\mathrm{mod}_k}(\mathbf{o}^{d*}_k) = \mathbf{y}^*_k \tag{160}$$

Its local Jacobian $J^d_{\eta,\mathrm{mod}_k}(\mathbf{o}^{d*}_k)$ is a structured block-row matrix mapping variations of the isolated positional and rotational vectors directly into the measurement's tangent space. Dictated by the direct sum structure of this relative tangent space, the Jacobian naturally partitions into distinct positional and rotational column blocks:

$$J^d_{\eta,\mathrm{mod}_k}(\mathbf{o}^{d*}_k) = \left[J^d_{\eta,\mathrm{mod}_k,p}(\mathbf{o}^{d*}_k) \;\middle|\; J^d_{\eta,\mathrm{mod}_k,R}(\mathbf{o}^{d*}_k) \right]. \tag{161}$$

Depending on the active sensory modality, evaluating this Jacobian yields blocks that directly project onto the corresponding sub-spaces without loss of information:

- **Distance Modality (**dist**):** The measurement map $\eta^d_{\text{dist}} : \mathbb{R}^3 \times \mathbb{SO}(3) \to \mathbb{R}_{>0}$ extracts the Euclidean norm of the relative position:

$$\eta^d_{\text{dist}}(\mathbf{p}^*_{ij}, \tilde{\mathbf{R}}^*_{ij}) = \|\mathbf{p}^*_{ij}\| = d^*_{ij} \tag{162}$$

  As derived in the coupled formulation, the Jacobian evaluates to $\delta d_{ij} = (\mathbf{q}^*_{ij})^T \delta \mathbf{p}_{ij}$. Since the measurement depends purely on translation and is inherently invariant to rotational perturbations, the rotational block naturally nullifies. Mapped into the decoupled format, the local Jacobian explicitly defines $J^d_{\eta,\text{dist},p}$ and $J^d_{\eta,\text{dist},R}$:

$$J^d_{\eta,\text{dist}}(\mathbf{o}^{d*}_k) = \left[(\mathbf{q}^*_{ij})^T \;\middle|\; \mathbf{0}_{1\times 3} \right]. \tag{163}$$

- **Bearing Modality (**bear**):** The measurement map $\eta^d_{\text{bear}} : \mathbb{R}^3 \times \mathbb{SO}(3) \to \mathbb{L}$ intricately couples relative position and source orientation to calculate the local line-of-sight direction. Utilizing the evaluated relative state ($\tilde{\mathbf{R}}^*_{ij} = (\mathbf{R}^*_i)^T$), we have:

$$\eta^d_{\text{bear}}(\mathbf{p}^*_{ij}, \tilde{\mathbf{R}}^*_{ij}) = \frac{\tilde{\mathbf{R}}^*_{ij}\mathbf{p}^*_{ij}}{\|\mathbf{p}^*_{ij}\|} = \mathbf{b}^*_{ij} \tag{164}$$

  The Jacobian preserves the identical algebraic structure derived previously. By separating the positional multiplier from the rotational multiplier, we obtain the decoupled local Jacobian, thereby isolating $J^d_{\eta,\text{bear},p}$ and $J^d_{\eta,\text{bear},R}$:

$$J^d_{\eta,\text{bear}}(\mathbf{o}^{d*}_k) = \frac{1}{\|\mathbf{p}^*_{ij}\|} \left[\mathbf{\Pi}_{\mathbf{b}^*_{ij}} (\mathbf{R}^*_i)^T \;\middle|\; -\mathbf{\Pi}_{\mathbf{b}^*_{ij}} (\mathbf{R}^*_i)^T [\mathbf{p}^*_{ij}]_\times \right]. \tag{165}$$

- **Mixed Modality (**mix**):** To maintain a homogeneous global space in heterogeneous networks, every edge maps uniformly via $\eta^d_{\text{mix}} : \mathbb{R}^3 \times \mathbb{SO}(3) \to \mathbb{L} \times \mathbb{R}_{>0}$. Depending on edge k's specific capability, the measurement function concatenates the active measurements and pads missing ones with abstract dummy constants ($\mathbf{u}_0 \in \mathbb{L}$, $d_0 \in \mathbb{R}_{>0}$):

$$\eta^d_{\text{mix}}(\mathbf{o}^{d*}_k) = \begin{cases} \begin{bmatrix} \mathbf{u}_0 \\ \eta^d_{\text{dist}}(\mathbf{o}^{d*}_k) \end{bmatrix} & \text{if edge } k \text{ is distance} \\ \begin{bmatrix} \eta^d_{\text{bear}}(\mathbf{o}^{d*}_k) \\ d_0 \end{bmatrix} & \text{if edge } k \text{ is bearing} \\ \begin{bmatrix} \eta^d_{\text{bear}}(\mathbf{o}^{d*}_k) \\ \eta^d_{\text{dist}}(\mathbf{o}^{d*}_k) \end{bmatrix} & \text{if edge } k \text{ measures both} \end{cases} \tag{166}$$

  Since differentials of dummy constants evaluate identically to zero, substituting the linear mapping representations yields a uniform 4×6 local Jacobian block.

Due to the underlying decoupling, this naturally splits into distinct positional and rotational sub-blocks, $J^d_{\eta,\text{mix},p}$ and $J^d_{\eta,\text{mix},R}$:

$$J^d_{\eta,\text{mix}}(\mathbf{o}^{d*}_k) = \begin{cases} \left[\begin{array}{c|c} \mathbf{0}_{3\times3} & \mathbf{0}_{3\times3} \\ J^d_{\eta,\text{dist},p}(\mathbf{o}^{d*}_k) & \mathbf{0}_{1\times3} \end{array}\right] & \text{if edge } k \text{ is distance} \\ \left[\begin{array}{c|c} J^d_{\eta,\text{bear},p}(\mathbf{o}^{d*}_k) & J^d_{\eta,\text{bear},R}(\mathbf{o}^{d*}_k) \\ \mathbf{0}_{1\times3} & \mathbf{0}_{1\times3} \end{array}\right] & \text{if edge } k \text{ is bearing} \\ \left[\begin{array}{c|c} J^d_{\eta,\text{bear},p}(\mathbf{o}^{d*}_k) & J^d_{\eta,\text{bear},R}(\mathbf{o}^{d*}_k) \\ J^d_{\eta,\text{dist},p}(\mathbf{o}^{d*}_k) & \mathbf{0}_{1\times3} \end{array}\right] & \text{if edge } k \text{ measures both} \end{cases} \tag{167}$$

Global Measurement Map and Jacobian Assembly

Having established the local measurement mechanics, we extend the formulation globally across all m edges. The global measurement map aggregates the independent sensor readings into the full measurement vector:

$$\begin{aligned} \boldsymbol{\eta}^d_{\text{emb}} : (\mathbb{R}^3)^m \times (\mathbb{SO}(3))^m &\to \mathcal{Y}^m \qquad (168) \\ (o_1, \ldots, o_m) &\mapsto \left(\eta^d_{\text{mod}_1}(o_1), \ldots, \eta^d_{\text{mod}_m}(o_m)\right) \end{aligned}$$

Dictated by the macroscopic decoupling of the tangent space, the generic global measurement Jacobian $\mathbf{J}^d_{\boldsymbol{\eta}}(\mathbf{o}^{d*})$ takes the form of a wide block matrix composed of two large block-diagonal sections, perfectly segregating the physical domains:

$$\begin{aligned} \mathbf{J}^d_{\boldsymbol{\eta}}(\mathbf{o}^{d*}) &= \left[\begin{array}{c|c} \text{blockdiag}^m_{k=1}\left(J^d_{\eta,\text{mod}_k,p}(\mathbf{o}^{d*}_k)\right) & \text{blockdiag}^m_{k=1}\left(J^d_{\eta,\text{mod}_k,R}(\mathbf{o}^{d*}_k)\right) \end{array}\right] \\ &= \left[\begin{array}{c|c} \mathbf{J}^d_{\boldsymbol{\eta},p}(\mathbf{o}^{d*}) & \mathbf{J}^d_{\boldsymbol{\eta},R}(\mathbf{o}^{d*}) \end{array}\right]. \qquad (169) \end{aligned}$$

Given that every measurement depends on the relative positional state $\mathbf{p}^*_{ij}$ (and bearings depend on $\mathbf{R}^*_i$ as well), all active local Jacobian blocks are strictly state-dependent. Thus, explicit block-diagonal concatenation is mandated universally, adapting its internal blocks based on the modality of each individual edge k:

- **Distance Network:** The global measurement map is

$$\boldsymbol{\eta}^d_{\text{emb,dist}} : (\mathbb{R}^3)^m \times (\mathbb{SO}(3))^m \to (\mathbb{R}_{>0})^m \tag{170}$$

Applying the general formula, the global Jacobian $\mathbf{J}^d_{\boldsymbol{\eta},\text{dist}}(\mathbf{o}^{d*}) \in \mathbb{R}^{m\times 6m}$ becomes:

$$\mathbf{J}^d_{\boldsymbol{\eta},\text{dist}}(\mathbf{o}^{d*}) = \left[\text{blockdiag}_{k=1}^m \left(J^d_{\eta,\text{dist},p}(\mathbf{o}^{d*}_k) \right) \;\middle|\; \mathbf{0}_{m\times 3m} \right] \tag{171}$$

- **Bearing Network:** The global measurement map is

$$\boldsymbol{\eta}^d_{\text{emb,bear}} : (\mathbb{R}^3)^m \times (\mathbb{SO}(3))^m \to \mathbb{L}^m \tag{172}$$

Applying the general formula, the global Jacobian $\mathbf{J}^d_{\boldsymbol{\eta},\text{bear}}(\mathbf{o}^{d*}) \in \mathbb{R}^{3m\times 6m}$ becomes:

$$\mathbf{J}^d_{\boldsymbol{\eta},\text{bear}}(\mathbf{o}^{d*}) = \left[\text{blockdiag}_{k=1}^m \left(J^d_{\eta,\text{bear},p}(\mathbf{o}^{d*}_k) \right) \;\middle|\; \text{blockdiag}_{k=1}^m \left(J^d_{\eta,\text{bear},R}(\mathbf{o}^{d*}_k) \right) \right] \tag{173}$$

- **Mixed Network:** To maintain structural consistency, the global measurement map pads the codomain uniformly, yielding

$$\boldsymbol{\eta}^d_{\text{emb,mix}} : (\mathbb{R}^3)^m \times (\mathbb{SO}(3))^m \to (\mathbb{L} \times \mathbb{R}_{>0})^m \tag{174}$$

The global Jacobian $\mathbf{J}^d_{\boldsymbol{\eta}}(\mathbf{o}^{d*}) \in \mathbb{R}^{4m\times 6m}$ becomes:

$$\mathbf{J}^d_{\boldsymbol{\eta}}(\mathbf{o}^{d*}) = \left[\text{blockdiag}_{k=1}^m \left(J^d_{\eta,\text{mod}_k,p}(\mathbf{o}^{d*}_k) \right) \;\middle|\; \text{blockdiag}_{k=1}^m \left(J^d_{\eta,\text{mod}_k,R}(\mathbf{o}^{d*}_k) \right) \right] \tag{175}$$

where $\text{mod}_k \in \{\text{dist}, \text{bear}, \text{mix}\}$.

4.5.5 Decoupled Rigidity Matrix Assembly

Mirroring the coupled formulation, the construction of the embedded decoupled rigidity matrix $\mathbf{R}^d(\mathbf{x}^{d*})$ inherently relies on the differential geometry of the MAS. To rigorously motivate the structure of the tangent spaces utilized in our derivation, we must first recognize that the global decoupled measurement model is the composition of four distinct smooth maps. Let $\overline{\mathscr{D}}^d = (\mathbb{R}^3)^n \times (\mathbb{SO}(3))^n$ be the global decoupled state manifold, and $\mathscr{Y}^d$ the global measurement manifold.

The measurement function resulting from the embedded decoupled functor realization $\mathbf{h}^d : \overline{\mathscr{D}}^d \to \mathscr{Y}^d$ factorizes exactly into the categorical sequence:

$$\mathbf{h}^d = \boldsymbol{\eta}^d_{\text{emb}} \circ \boldsymbol{\Delta}^d_{\text{emb}} \circ \boldsymbol{\gamma}^d_{\text{emb}} \circ \boldsymbol{\sigma}^d_{\text{emb}}. \tag{176}$$

To compute the Jacobian of this composite map via the chain rule, the embedded decoupled rigidity matrix is defined as the ordered product of the individual Jacobians, each evaluated at its respective propagated evaluation point:

$$\mathbf{R}^d(\mathbf{x}^{d*}) = \mathbf{J}^d_{\boldsymbol{\eta}}(\mathbf{o}^{d*}) \cdot \mathbf{J}^d_{\Delta}(\tilde{\mathbf{e}}^{d*}) \cdot \mathbf{J}^d_{\boldsymbol{\gamma}} \cdot \mathbf{J}^d_{\boldsymbol{\sigma}}. \tag{177}$$

Rather than evaluating this product monolithically, we adopt a systematic multistep structural factorization. This allows us to highlight different structural properties of the resulting matrix and provides a methodological way to construct it.

First, we completely isolate the measurement dependent components from their allocation across the network's agents. Specifically, we define an *edge-wise dense* intermediate matrix $\mathbf{R}^d_{\text{local}}(\mathbf{x}^{d*})$ prior to agent distribution:

$$\mathbf{R}^d(\mathbf{x}^{d*}) = \underbrace{\mathbf{J}^d_{\boldsymbol{\eta}}(\mathbf{o}^{d*}) \cdot \mathbf{J}^d_{\Delta}(\tilde{\mathbf{e}}^{d*}) \cdot \mathbf{J}^d_{\boldsymbol{\gamma}}}_{\mathbf{R}^d_{\text{local}}(\mathbf{x}^{d*})} \cdot \underbrace{\mathbf{J}^d_{\boldsymbol{\sigma}}}_{\text{Agent Distribution}}. \tag{178}$$

We structure the assembly into four distinct algebraic steps. In each step, explicitly identifying the domain and codomain of the underlying map dictates the strict hierarchical partition of the associated tangent spaces, ultimately forcing the resulting matrices into the structured forms explained at the beginning of the chapter.

Step 1: Local Edge-Wise Kinematics

We first evaluate the mapping at the local level for a generic k-th directed edge $e_k = (i, j)$. This corresponds to analyzing the local measurement map

$$h^d_{\text{local},k} : (\mathbb{R}^3 \times \mathbb{R}^3) \times (\mathbb{SO}(3) \times \mathbb{SO}(3)) \to \mathcal{Y}_k \tag{179}$$

which maps the states of the interacting pair to generate the specific local measurement.

We compute the Jacobian of the map $h^d_{\text{local},k}$ and we obtain the local dense row block $r^d_{\text{mod}_k}(\mathbf{e}^{d*}_k)$:

$$\begin{aligned} r^d_{\text{mod}_k}(\mathbf{e}^{d*}_k) &= J^d_{\eta,\text{mod}_k}(\mathbf{o}^{d*}_k) \cdot J^d_{\Delta,\text{mod}_k}(\tilde{\mathbf{e}}^{d*}_k) \cdot J^d_{\gamma,\text{mod}_k} \\ &= \left[\begin{array}{cc|cc} r^d_{\text{mod}_k,\mathbf{p}_i}(\mathbf{e}^{d*}_k) & r^d_{\text{mod}_k,\mathbf{p}_j}(\mathbf{e}^{d*}_k) & r^d_{\text{mod}_k,\boldsymbol{\theta}_i}(\mathbf{e}^{d*}_k) & r^d_{\text{mod}_k,\boldsymbol{\theta}_j}(\mathbf{e}^{d*}_k) \end{array} \right] \\ &= \left[\begin{array}{c|c} r^d_{\text{mod}_k,p}(\mathbf{e}^{d*}_k) & r^d_{\text{mod}_k,R}(\mathbf{e}^{d*}_k) \end{array} \right]. \end{aligned} \tag{180}$$

As established by the hierarchical decomposition of the decoupled edge tangent space explained at the beginning of the chapter, this 12-column dense block perfectly mirrors the physical structure of the interaction. At the highest level, the block decouples into two independent 6-column macro-blocks, representing the purely translational and purely rotational streams. In turn, each of these geometric streams explicitly subdivides into two 3-column sub-blocks, isolating the individual 3-DOF kinematic contributions of the source agent i and the target agent j.

To explicitly verify that the generic block inherently obeys this strict hierarchical partition, we perform the matrix expansion in two distinct algebraic derivations.

1. Geometric partitioning (position vs. rotation): We first evaluate the decoupling of the edge into independent positional and rotational streams. The measurement Jacobian $J^d_{\eta,\mathrm{mod}_k}$ inherently partitions into positional and rotational columns. Crucially, the kinematic observation map $J^d_{\Delta,\mathrm{mod}_k}$ and the filtration mask $J^d_{\gamma,\mathrm{mod}_k}$ are strictly block-diagonal across these two distinct physical domains. Expanding these matrices yields:

$$
\begin{aligned}
r^d_{\mathrm{mod}_k}(\mathbf{e}^{d*}_k) &= \left[J^d_{\eta,\mathrm{mod}_k,p}(\mathbf{o}^{d*}_k) \;\middle|\; J^d_{\eta,\mathrm{mod}_k,R}(\mathbf{o}^{d*}_k) \right] \begin{bmatrix} J^d_{\Delta,p} & \mathbf{0}_{3\times 6} \\ \mathbf{0}_{3\times 6} & J^d_{\Delta,R,\mathrm{mod}_k}(\tilde{\mathbf{e}}^{d*}_k) \end{bmatrix} \begin{bmatrix} J^d_{\gamma,p} & \mathbf{0}_{6\times 6} \\ \mathbf{0}_{6\times 6} & J^d_{\gamma,R,\mathrm{mod}_k} \end{bmatrix} \\
&= \left[J^d_{\eta,\mathrm{mod}_k,p}(\mathbf{o}^{d*}_k) \;\middle|\; J^d_{\eta,\mathrm{mod}_k,R}(\mathbf{o}^{d*}_k) \right] \begin{bmatrix} J^d_{\Delta,p} J^d_{\gamma,p} & \mathbf{0}_{3\times 6} \\ \mathbf{0}_{3\times 6} & J^d_{\Delta,R,\mathrm{mod}_k}(\tilde{\mathbf{e}}^{d*}_k) J^d_{\gamma,R,\mathrm{mod}_k} \end{bmatrix} \\
&= \left[J^d_{\eta,\mathrm{mod}_k,p}(\mathbf{o}^{d*}_k) J^d_{\Delta,p} J^d_{\gamma,p} \;\middle|\; J^d_{\eta,\mathrm{mod}_k,R}(\mathbf{o}^{d*}_k) J^d_{\Delta,R,\mathrm{mod}_k}(\tilde{\mathbf{e}}^{d*}_k) J^d_{\gamma,R,\mathrm{mod}_k} \right] \\
&= \left[r^d_{\mathrm{mod}_k,p}(\mathbf{e}^{d*}_k) \;\middle|\; r^d_{\mathrm{mod}_k,R}(\mathbf{e}^{d*}_k) \right].
\end{aligned}
\tag{181}
$$

2. Nodal partitioning (source vs. target): Next, we expose the internal nodal kinematics within these isolated geometric macro-domains. Because the filtration and observation mappings process the two agents independently, their domain-specific Jacobians inherently split into a 1×2 observation mapping and a strictly block-diagonal filtration mask. Expanding the generic positional macro-block $r^d_{\mathrm{mod}_k,p}$ yields:

$$
\begin{aligned}
r^d_{\mathrm{mod}_k,p}(\mathbf{e}_k^{d*}) &= J^d_{\eta,\mathrm{mod}_k,p}(\mathbf{o}_k^{d*}) \cdot J^d_{\Delta,p} \cdot J^d_{\gamma,p} \\
&= J^d_{\eta,\mathrm{mod}_k,p}(\mathbf{o}_k^{d*}) \begin{bmatrix} J^d_{\Delta,p,i} & J^d_{\Delta,p,j} \end{bmatrix} \begin{bmatrix} J^d_{\gamma,p,i} & \mathbf{0}_{3\times3} \\ \mathbf{0}_{3\times3} & J^d_{\gamma,p,j} \end{bmatrix} \\
&= J^d_{\eta,\mathrm{mod}_k,p}(\mathbf{o}_k^{d*}) \begin{bmatrix} J^d_{\Delta,p,i} J^d_{\gamma,p,i} & J^d_{\Delta,p,j} J^d_{\gamma,p,j} \end{bmatrix} \\
&= \begin{bmatrix} J^d_{\eta,\mathrm{mod}_k,p}(\mathbf{o}_k^{d*}) J^d_{\Delta,p,i} J^d_{\gamma,p,i} & J^d_{\eta,\mathrm{mod}_k,p}(\mathbf{o}_k^{d*}) J^d_{\Delta,p,j} J^d_{\gamma,p,j} \end{bmatrix} \\
&= \begin{bmatrix} r^d_{\mathrm{mod}_k,\mathbf{p}_i}(\mathbf{e}_k^{d*}) & r^d_{\mathrm{mod}_k,\mathbf{p}_j}(\mathbf{e}_k^{d*}) \end{bmatrix}.
\end{aligned} \tag{182}
$$

By applying an analogous expansion to the rotational macro-block, the full 12-column dense block cleanly reassembles into its four fundamental 3-DOF kinematic contributions, strictly preserving the macroscopic physical decoupling:

$$
r^d_{\mathrm{mod}_k}(\mathbf{e}_k^{d*}) = \left[\begin{array}{cc|cc} r^d_{\mathrm{mod}_k,\mathbf{p}_i}(\mathbf{e}_k^{d*}) & r^d_{\mathrm{mod}_k,\mathbf{p}_j}(\mathbf{e}_k^{d*}) & r^d_{\mathrm{mod}_k,\boldsymbol{\theta}_i}(\mathbf{e}_k^{d*}) & r^d_{\mathrm{mod}_k,\boldsymbol{\theta}_j}(\mathbf{e}_k^{d*}) \end{array} \right]. \tag{183}
$$

Depending on the measurement modality, we explicitly evaluate the decoupled streams by multiplying the corresponding analytical Jacobians computed previously:

- **Distance Modality (**1×12 **local block):**
  - *Positional Block ($r^d_{\mathrm{dist},p}$):* The state-dependent measurement positional Jacobian distributes cleanly across the constant linear observation difference:

$$
\begin{aligned}
r^d_{\mathrm{dist},p}(\mathbf{e}_k^{d*}) &= J^d_{\eta,\mathrm{dist},p}(\mathbf{o}_k^{d*}) \cdot J^d_{\Delta,p} \cdot J^d_{\gamma,p} \\
&= \left((\mathbf{q}_{ij}^*)^T\right) \begin{bmatrix} -\mathbf{I}_3 & \mathbf{I}_3 \end{bmatrix} \begin{bmatrix} \mathbf{I}_3 & \mathbf{0} \\ \mathbf{0} & \mathbf{I}_3 \end{bmatrix} \\
&= \begin{bmatrix} -(\mathbf{q}_{ij}^*)^T & (\mathbf{q}_{ij}^*)^T \end{bmatrix}.
\end{aligned} \tag{184}
$$

  - *Rotational Block ($r^d_{\mathrm{dist},R}$):* Due to the scalar nature of distance mapping ($J^d_{\eta,\mathrm{dist},R} = \mathbf{0}_{1\times3}$) and the full rotational filtration mask, the entire rotational kinematic chain naturally nullifies:

$$
\begin{aligned}
r^d_{\mathrm{dist},R}(\mathbf{e}_k^{d*}) &= J^d_{\eta,\mathrm{dist},R}(\mathbf{o}_k^{d*}) \cdot J^d_{\Delta,R,\mathrm{dist}} \cdot J^d_{\gamma,R,\mathrm{dist}} \\
&= \left(\mathbf{0}_{1\times3}\right) \begin{bmatrix} -\mathbf{I}_3 & \mathbf{I}_3 \end{bmatrix} \begin{bmatrix} \mathbf{0}_{3\times3} & \mathbf{0} \\ \mathbf{0} & \mathbf{0}_{3\times3} \end{bmatrix} \\
&= \begin{bmatrix} \mathbf{0}_{1\times3} & \mathbf{0}_{1\times3} \end{bmatrix} = \mathbf{0}_{1\times6}.
\end{aligned} \tag{185}
$$

Concatenating these evaluated blocks constructs the fully decoupled macro-blocks and the final compact row:

$$
\begin{aligned}
r^d_{\mathrm{dist}}(\mathbf{e}^{d*}_k) &= \left[\begin{array}{cc|cc} -(\mathbf{q}^*_{ij})^T & (\mathbf{q}^*_{ij})^T & \mathbf{0}_{1\times3} & \mathbf{0}_{1\times3} \end{array}\right] \\
&= \left[\begin{array}{c|c} r^d_{\mathrm{dist},p}(\mathbf{e}^{d*}_k) & r^d_{\mathrm{dist},R}(\mathbf{e}^{d*}_k) \end{array}\right].
\end{aligned} \tag{186}
$$

- **Bearing Modality (**3×12 **local block):**
  - *Positional Block* ($r^d_{\mathrm{bear},p}$)*:* The positional components cleanly distributes through the observation mapping:

$$
\begin{aligned}
r^d_{\mathrm{bear},p}(\mathbf{e}^{d*}_k) &= J^d_{\eta,\mathrm{bear},p}(\mathbf{o}^{d*}_k) \cdot J^d_{\Delta,p} \cdot J^d_{\gamma,p} \\
&= \left(\frac{1}{\|\mathbf{p}^*_{ij}\|} \mathbf{\Pi}_{\mathbf{b}^*_{ij}} (\mathbf{R}^*_i)^T \right) \begin{bmatrix} -\mathbf{I}_3 & \mathbf{I}_3 \end{bmatrix} \begin{bmatrix} \mathbf{I}_3 & \mathbf{0} \\ \mathbf{0} & \mathbf{I}_3 \end{bmatrix} \\
&= \begin{bmatrix} -\frac{1}{\|\mathbf{p}^*_{ij}\|} \mathbf{\Pi}_{\mathbf{b}^*_{ij}} (\mathbf{R}^*_i)^T & \frac{1}{\|\mathbf{p}^*_{ij}\|} \mathbf{\Pi}_{\mathbf{b}^*_{ij}} (\mathbf{R}^*_i)^T \end{bmatrix}.
\end{aligned} \tag{187}
$$

  - *Rotational Block* ($r^d_{\mathrm{bear},R}$)*:* The target node's attitude is completely unobservable, meaning the invariant filtration mask naturally zeroes it out ($\mathbf{0}_{3\times3}$). The state-dependent matrix product evaluates sequentially as follows:

$$
\begin{aligned}
r^d_{\mathrm{bear},R}(\mathbf{e}^{d*}_k) &= J^d_{\eta,\mathrm{bear},R}(\mathbf{o}^{d*}_k) \cdot J^d_{\Delta,R,\mathrm{bear}}(\tilde{\mathbf{e}}^{d*}_k) \cdot J^d_{\gamma,R,\mathrm{bear}} \\
&= \left(-\frac{1}{\|\mathbf{p}^*_{ij}\|} \mathbf{\Pi}_{\mathbf{b}^*_{ij}} (\mathbf{R}^*_i)^T [\mathbf{p}^*_{ij}]_\times \right) \begin{bmatrix} -\mathbf{R}^*_i & \mathbf{I}_3 \end{bmatrix} \begin{bmatrix} \mathbf{I}_3 & \mathbf{0} \\ \mathbf{0} & \mathbf{0}_{3\times3} \end{bmatrix} \\
&= \left(-\frac{1}{\|\mathbf{p}^*_{ij}\|} \mathbf{\Pi}_{\mathbf{b}^*_{ij}} (\mathbf{R}^*_i)^T [\mathbf{p}^*_{ij}]_\times \right) \begin{bmatrix} -\mathbf{R}^*_i & \mathbf{0}_{3\times3} \end{bmatrix} \\
&= \begin{bmatrix} \frac{1}{\|\mathbf{p}^*_{ij}\|} \mathbf{\Pi}_{\mathbf{b}^*_{ij}} \left((\mathbf{R}^*_i)^T [\mathbf{p}^*_{ij}]_\times \mathbf{R}^*_i \right) & \mathbf{0}_{3\times3} \end{bmatrix}.
\end{aligned} \tag{188}
$$

  By applying the identical Adjoint property $(\mathbf{R}^*_i)^T [\mathbf{p}^*_{ij}]_\times \mathbf{R}^*_i = [(\mathbf{R}^*_i)^T \mathbf{p}^*_{ij}]_\times = \|\mathbf{p}^*_{ij}\| [\mathbf{b}^*_{ij}]_\times$, the scalar norm cleanly cancels out:

$$
r^d_{\mathrm{bear},R}(\mathbf{e}^{d*}_k) = \begin{bmatrix} \mathbf{\Pi}_{\mathbf{b}^*_{ij}} [\mathbf{b}^*_{ij}]_\times & \mathbf{0}_{3\times3} \end{bmatrix}. \tag{189}
$$

  Finally, using the orthogonal projection identity $\mathbf{\Pi}_{\mathbf{b}^*_{ij}} [\mathbf{b}^*_{ij}]_\times = [\mathbf{b}^*_{ij}]_\times$, this matrix elegantly simplifies to the pure skew-symmetric form, completely bypassing redundant derivations:

$$
r^d_{\mathrm{bear},R}(\mathbf{e}^{d*}_k) = \begin{bmatrix} [\mathbf{b}^*_{ij}]_\times & \mathbf{0}_{3\times3} \end{bmatrix}. \tag{190}
$$

Concatenating these fully resolved streams constructs the final local row:

$$\begin{aligned} r^d_{\text{bear}}(\mathbf{e}^{d*}_k) &= \left[-\frac{1}{\|\mathbf{p}^*_{ij}\|}\mathbf{\Pi}_{\mathbf{b}^*_{ij}}(\mathbf{R}^*_i)^T \quad \frac{1}{\|\mathbf{p}^*_{ij}\|}\mathbf{\Pi}_{\mathbf{b}^*_{ij}}(\mathbf{R}^*_i)^T \;\middle|\; [\mathbf{b}^*_{ij}]_\times \quad \mathbf{0}_{3\times 3} \right] \\ &= \left[r^d_{\text{bear},p}(\mathbf{e}^{d*}_k) \;\middle|\; r^d_{\text{bear},R}(\mathbf{e}^{d*}_k) \right]. \end{aligned} \tag{191}$$

- **Mixed Modality (**4×12 **local block):** Leveraging the dummy-padding structure of the mixed measurement map, the local block cleanly stacks the respective positional and rotational evaluations for the distance and bearing components vertically:

$$\begin{aligned} r^d_{\text{mix}}(\mathbf{e}^{d*}_k) &= \begin{cases} \begin{bmatrix} \mathbf{0}_{3\times 6} & \mathbf{0}_{3\times 6} \\ \multicolumn{2}{c}{r^d_{\text{dist}}(\mathbf{e}^{d*}_k)} \end{bmatrix} = \left[\begin{array}{c|c} \mathbf{0}_{3\times 6} & \mathbf{0}_{3\times 6} \\ r^d_{\text{dist},p}(\mathbf{e}^{d*}_k) & r^d_{\text{dist},R}(\mathbf{e}^{d*}_k) \end{array}\right] & \text{(if edge } k \text{ is distance)} \\ \begin{bmatrix} \multicolumn{2}{c}{r^d_{\text{bear}}(\mathbf{e}^{d*}_k)} \\ \mathbf{0}_{1\times 6} & \mathbf{0}_{1\times 6} \end{bmatrix} = \left[\begin{array}{c|c} r^d_{\text{bear},p}(\mathbf{e}^{d*}_k) & r^d_{\text{bear},R}(\mathbf{e}^{d*}_k) \\ \mathbf{0}_{1\times 6} & \mathbf{0}_{1\times 6} \end{array}\right] & \text{(if edge } k \text{ is bearing)} \\ \begin{bmatrix} r^d_{\text{bear}}(\mathbf{e}^{d*}_k) \\ r^d_{\text{dist}}(\mathbf{e}^{d*}_k) \end{bmatrix} = \left[\begin{array}{c|c} r^d_{\text{bear},p}(\mathbf{e}^{d*}_k) & r^d_{\text{bear},R}(\mathbf{e}^{d*}_k) \\ r^d_{\text{dist},p}(\mathbf{e}^{d*}_k) & r^d_{\text{dist},R}(\mathbf{e}^{d*}_k) \end{array}\right] & \text{(if edge } k \text{ measures both)} \end{cases} \\ &= \left[r^d_{\text{mix},p}(\mathbf{e}^{d*}_k) \;\middle|\; r^d_{\text{mix},R}(\mathbf{e}^{d*}_k) \right]. \end{aligned} \tag{192}$$

Step 2: Global Edge-Wise Assembly

Combining all these local maps without the topological distribution dictated by the graph yields the intermediate algebraic operator. This overarching operator corresponds to the global map

$$\mathbf{h}^d_{\text{local}} : \overline{\mathcal{M}}^d_e = (\mathbb{R}^3 \times \mathbb{R}^3)^m \times (\mathbb{SO}(3) \times \mathbb{SO}(3))^m \to \mathcal{Y}^d \tag{193}$$

which evaluates all individual edge states mapping them directly into the full measurement space.

Because the measurement, observation, and filtration maps process each edge independently while maintaining the global factorization, their global Jacobians evaluate as strictly partitioned block-diagonal operators.

To formulate the intermediate global edge-wise matrix $\mathbf{R}^d_{\text{local}}(\mathbf{x}^{d*})$, we exploit a standard property: the product of block-diagonal matrices is a block-diagonal matrix whose blocks are simply the products of the corresponding constituent blocks.

Consequently, this operation natively assembles into a wide, structurally ordered matrix characterized by two entirely separated block-diagonal macro-blocks (one accumulating all positional kinematics, and one for all rotational kinematics):

$$\begin{aligned}\mathbf{R}^d_{\text{local}}(\mathbf{x}^{d*}) &= \mathbf{J}^d_{\boldsymbol{\eta}}(\mathbf{o}^{d*}) \cdot \mathbf{J}^d_{\Delta}(\tilde{\mathbf{e}}^{d*}) \cdot \mathbf{J}^d_{\boldsymbol{\gamma}} \\ &= \left[\begin{array}{c|c} \mathbf{J}^d_{\boldsymbol{\eta},p}(\mathbf{o}^{d*}) & \mathbf{J}^d_{\boldsymbol{\eta},R}(\mathbf{o}^{d*}) \end{array}\right] \begin{bmatrix} \mathbf{J}^d_{\Delta,p} & \mathbf{0} \\ \mathbf{0} & \mathbf{J}^d_{\Delta,R}(\tilde{\mathbf{e}}^{d*}) \end{bmatrix} \begin{bmatrix} \mathbf{J}^d_{\boldsymbol{\gamma},p} & \mathbf{0} \\ \mathbf{0} & \mathbf{J}^d_{\boldsymbol{\gamma},R} \end{bmatrix} \\ &= \left[\begin{array}{c|c} \mathbf{J}^d_{\boldsymbol{\eta},p}(\mathbf{o}^{d*})\mathbf{J}^d_{\Delta,p}\mathbf{J}^d_{\boldsymbol{\gamma},p} & \mathbf{J}^d_{\boldsymbol{\eta},R}(\mathbf{o}^{d*})\mathbf{J}^d_{\Delta,R}(\tilde{\mathbf{e}}^{d*})\mathbf{J}^d_{\boldsymbol{\gamma},R} \end{array}\right] \\ &= \left[\begin{array}{c|c} \operatorname{blockdiag}_{k=1}^m \left(r^d_{\text{mod}_k,p}(\mathbf{e}^{d*}_k)\right) & \operatorname{blockdiag}_{k=1}^m \left(r^d_{\text{mod}_k,R}(\mathbf{e}^{d*}_k)\right) \end{array}\right] \\ &= \left[\begin{array}{c|c} \mathbf{R}^d_{\text{local},p}(\mathbf{x}^{d*}) & \mathbf{R}^d_{\text{local},R}(\mathbf{x}^{d*}) \end{array}\right]. \end{aligned} \tag{194}$$

Depending on the network configuration, this intermediate decoupled matrix takes the specific dimensions $\mathbb{R}^{m\times 12m}$ (Distance), $\mathbb{R}^{3m\times 12m}$ (Bearing), or $\mathbb{R}^{4m\times 12m}$ (Mixed).

Step 3: Topological Jacobian and Agent Distribution (Domain Expansion)

Having established the local edge-wise kinematics, we now mathematically inject the graph incidence to expand the mapping's domain. We achieve this by initially considering the entire network of agents while isolating the measurement of the single k-th edge $e_k = (i, j)$, thereby formalizing the topological distribution of the interacting agents for this specific edge.

This corresponds to analyzing the isolated global measurement map:

$$\mathbf{h}^d_k : \overline{\mathscr{D}}^d \to \mathscr{Y}_k. \tag{195}$$

While the codomain of this mapping remains restricted to the local measurement space $\mathscr{Y}_k$ of the single k-th edge, its domain expands to encompass the entire state space of the network.

By computing the Jacobian $[\mathbf{R}^d(\mathbf{x}^{d*})]_k$ of this specific map $\mathbf{h}^d_k$, we establish how the localized kinematic blocks are distributed across all the agents.

Because this global state vector is fundamentally partitioned into all network positions followed by all network rotations, the Jacobian $[\mathbf{R}^d(\mathbf{x}^{d*})]_k$ applies independently to the translational and rotational sub-spaces without any cross-domain interference.

Physically, since the mapping $\mathbf{h}_k^d$ evaluates the edge $e_k = (i, j)$, which depends exclusively on its source node i and target node j, its partial derivative with respect to any other agent in the network is identically zero. Conversely, its non-zero partial derivatives with respect to i and j coincide exactly with the local kinematic blocks derived previously in Step 1. Therefore, injecting the topology simply requires taking these local blocks and accurately distributing them into their correct global coordinates. This yields a highly sparse row structure: the resulting global row will contain the local 3-DOF positional blocks and 3-DOF rotational blocks strictly at their corresponding i-th and j-th block-indices within their respective macro-domains, padded by zero-blocks everywhere else.

To realize this precise sparse placement, we recall the topological distribution map. The local Jacobian block for the k-th edge $e_k = (i, j)$ is

$$\left[J_\sigma^d\right]_k = \begin{bmatrix} S_{e_k} & \mathbf{0} \\ \mathbf{0} & S_{e_k} \end{bmatrix} \qquad \text{where} \quad S_{e_k} = \begin{bmatrix} \mathbf{u}_i^T \otimes \mathbf{I}_3 \\ \mathbf{u}_j^T \otimes \mathbf{I}_3 \end{bmatrix} \tag{196}$$

To global matrix $\mathbf{J}_\sigma^d$:

$$\mathbf{S} = \begin{bmatrix} S_{e_1} \\ S_{e_2} \\ \vdots \\ S_{e_m} \end{bmatrix}, \quad \mathbf{J}_\sigma^d = \begin{bmatrix} \mathbf{S} & \mathbf{0} \\ \mathbf{0} & \mathbf{S} \end{bmatrix} \in \mathbb{R}^{12m \times 6n}. \tag{197}$$

Leveraging the decoupled 3-DOF block-selector operators $(\mathbf{u}_i^T \otimes \mathbf{I}_3)$, we map the isolated source and target edge blocks into their precise global columns.

By post-multiplying the dense 12-column decoupled local block $r_{\text{mod}_k}^d(\mathbf{e}_k^{d*})$ by its corresponding topological block $[\mathbf{J}_\sigma^d]_k$, the isolated positional and rotational components are mapped simultaneously into their precise global columns. Exploiting the block-diagonal structure of both the decoupled edge kinematics and the topological router, the multiplication cleanly factorizes into the two independent geometric streams:

$$\begin{aligned}
[\mathbf{R}^d(\mathbf{x}^{d*})]_k &= r_{\text{mod}_k}^d(\mathbf{e}_k^{d*}) \cdot [\mathbf{J}_\sigma^d]_k \\
&= \left[r_{\text{mod}_k,p}^d(\mathbf{e}_k^{d*}) \;\middle|\; r_{\text{mod}_k,R}^d(\mathbf{e}_k^{d*}) \right] \begin{bmatrix} \mathbf{S}_{e_k} & \mathbf{0} \\ \mathbf{0} & \mathbf{S}_{e_k} \end{bmatrix} \\
&= \left[r_{\text{mod}_k,p}^d(\mathbf{e}_k^{d*}) \cdot \mathbf{S}_{e_k} \;\middle|\; r_{\text{mod}_k,R}^d(\mathbf{e}_k^{d*}) \cdot \mathbf{S}_{e_k} \right] \\
&= \left[[\mathbf{R}_p^d(\mathbf{x}^{d*})]_k \;\middle|\; [\mathbf{R}_R^d(\mathbf{x}^{d*})]_k \right].
\end{aligned} \tag{198}$$

Expanding the products explicitly defines the global positional block $[\mathbf{R}_p^d(\mathbf{x}^{d*})]_k \in \mathbb{R}^{\dim(\mathcal{Y}_k) \times 3n}$ and the global rotational block $[\mathbf{R}_R^d(\mathbf{x}^{d*})]_k \in \mathbb{R}^{\dim(\mathcal{Y}_k) \times 3n}$ independently for the k-th edge. By substituting the partitioned local blocks and the decoupled incidence matrix, we explicitly compute the block-matrix multiplication for the positional stream:

$$\begin{aligned}
[\mathbf{R}_p^d(\mathbf{x}^{d*})]_k &= r^d_{\mathrm{mod}_k,p}(\mathbf{e}_k^{d*}) \cdot \mathbf{S}_{e_k} \\
&= \begin{bmatrix} r^d_{\mathrm{mod}_k,\mathbf{p}_i}(\mathbf{e}_k^{d*}) & r^d_{\mathrm{mod}_k,\mathbf{p}_j}(\mathbf{e}_k^{d*}) \end{bmatrix} \begin{bmatrix} \mathbf{u}_i^T \otimes \mathbf{I}_3 \\ \mathbf{u}_j^T \otimes \mathbf{I}_3 \end{bmatrix} \\
&= r^d_{\mathrm{mod}_k,\mathbf{p}_i}(\mathbf{e}_k^{d*})\big(\mathbf{u}_i^T \otimes \mathbf{I}_3\big) + r^d_{\mathrm{mod}_k,\mathbf{p}_j}(\mathbf{e}_k^{d*})\big(\mathbf{u}_j^T \otimes \mathbf{I}_3\big). \qquad (199)
\end{aligned}$$

Following the exact same algebraic logic, the rotational mapping distributes its source and target kinematic blocks into their global coordinates:

$$\begin{aligned}
[\mathbf{R}_R^d(\mathbf{x}^{d*})]_k &= r^d_{\mathrm{mod}_k,R}(\mathbf{e}_k^{d*}) \cdot \mathbf{S}_{e_k} \\
&= \begin{bmatrix} r^d_{\mathrm{mod}_k,\boldsymbol{\theta}_i}(\mathbf{e}_k^{d*}) & r^d_{\mathrm{mod}_k,\boldsymbol{\theta}_j}(\mathbf{e}_k^{d*}) \end{bmatrix} \begin{bmatrix} \mathbf{u}_i^T \otimes \mathbf{I}_3 \\ \mathbf{u}_j^T \otimes \mathbf{I}_3 \end{bmatrix} \\
&= r^d_{\mathrm{mod}_k,\boldsymbol{\theta}_i}(\mathbf{e}_k^{d*})\big(\mathbf{u}_i^T \otimes \mathbf{I}_3\big) + r^d_{\mathrm{mod}_k,\boldsymbol{\theta}_j}(\mathbf{e}_k^{d*})\big(\mathbf{u}_j^T \otimes \mathbf{I}_3\big). \qquad (200)
\end{aligned}$$

Applying this modular allocation, we obtain the explicit analytical forms for the sparse global row blocks specific to each modality:

- **Global Distance Row ($1 \times 6n$):** The rotational variations have no effect on the distance, hence the rotational block is globally null ($\mathbf{0}_{1\times 3n}$):

  $$\begin{aligned}
  [\mathbf{R}^d_{\mathrm{dist},p}(\mathbf{x}^{d*})]_k &= -(\mathbf{q}_{ij}^*)^T\big(\mathbf{u}_i^T \otimes \mathbf{I}_3\big) + (\mathbf{q}_{ij}^*)^T\big(\mathbf{u}_j^T \otimes \mathbf{I}_3\big) \qquad (201)\\
  [\mathbf{R}^d_{\mathrm{dist},R}(\mathbf{x}^{d*})]_k &= \mathbf{0}_{1\times 3n}
  \end{aligned}$$

  yielding

  $$[\mathbf{R}^d_{\mathrm{dist}}(\mathbf{x}^{d*})]_k = \left[[\mathbf{R}^d_{\mathrm{dist},p}(\mathbf{x}^{d*})]_k \;\middle|\; [\mathbf{R}^d_{\mathrm{dist},R}(\mathbf{x}^{d*})]_k \right]. \qquad (202)$$

- **Global Bearing Row ($3 \times 6n$):**

  $$\begin{aligned}
  [\mathbf{R}^d_{\mathrm{bear},p}(\mathbf{x}^{d*})]_k &= -\frac{1}{\|\mathbf{p}_{ij}^*\|}\boldsymbol{\Pi}_{\mathbf{b}_{ij}^*}(\mathbf{R}_i^*)^T\big(\mathbf{u}_i^T \otimes \mathbf{I}_3\big) + \frac{1}{\|\mathbf{p}_{ij}^*\|}\boldsymbol{\Pi}_{\mathbf{b}_{ij}^*}(\mathbf{R}_i^*)^T\big(\mathbf{u}_j^T \otimes \mathbf{I}_3\big) \qquad (203)\\
  [\mathbf{R}^d_{\mathrm{bear},R}(\mathbf{x}^{d*})]_k &= [\mathbf{b}_{ij}^*]_\times\big(\mathbf{u}_i^T \otimes \mathbf{I}_3\big) + \mathbf{0}_{3\times 3n} \qquad (204)
  \end{aligned}$$

  yielding

  $$[\mathbf{R}^d_{\mathrm{bear}}(\mathbf{x}^{d*})]_k = \left[[\mathbf{R}^d_{\mathrm{bear},p}(\mathbf{x}^{d*})]_k \;\middle|\; [\mathbf{R}^d_{\mathrm{bear},R}(\mathbf{x}^{d*})]_k \right]. \qquad (205)$$

- **Global Mixed Row** ($4 \times 6n$):

$$[\mathbf{R}^d_{\mathrm{mix}}(\mathbf{x}^{d*})]_k = \begin{cases} \left[\begin{array}{c|c} \mathbf{0}_{3\times 3n} & \mathbf{0}_{3\times 3n} \\ [\mathbf{R}^d_{\mathrm{dist},p}(\mathbf{x}^{d*})]_k & [\mathbf{R}^d_{\mathrm{dist},R}(\mathbf{x}^{d*})]_k \end{array}\right] & \text{(if edge } k \text{ is distance)} \\ \left[\begin{array}{c|c} [\mathbf{R}^d_{\mathrm{bear},p}(\mathbf{x}^{d*})]_k & [\mathbf{R}^d_{\mathrm{bear},R}(\mathbf{x}^{d*})]_k \\ \mathbf{0}_{1\times 3n} & \mathbf{0}_{1\times 3n} \end{array}\right] & \text{(if edge } k \text{ is bearing)} \\ \left[\begin{array}{c|c} [\mathbf{R}^d_{\mathrm{bear},p}(\mathbf{x}^{d*})]_k & [\mathbf{R}^d_{\mathrm{bear},R}(\mathbf{x}^{d*})]_k \\ [\mathbf{R}^d_{\mathrm{dist},p}(\mathbf{x}^{d*})]_k & [\mathbf{R}^d_{\mathrm{dist},R}(\mathbf{x}^{d*})]_k \end{array}\right] & \text{(if edge } k \text{ measures both)} \end{cases} \tag{206}$$

Step 4: Full Network Integration (Codomain Integration)

We now incorporate all measurement contributions by aggregating the edge-wise components derived in Step 3 across the entire graph. While Step 3 successfully expanded the domain onto the globally decoupled agent state space, we must now integrate the codomain to account for the complete sensory network.

As previously established, the decoupled embedded rigidity matrix $\mathbf{R}^d(\mathbf{x}^{d*})$ represents the exact differential of the overarching measurement function $\mathbf{h}^d : \overline{\mathscr{D}}^d \to \mathscr{Y}^d$. The direct sum structure of the tangent spaces dictates that the columns of the resulting matrix are structurally forced to partition into a positional left macro-block and a rotational right macro-block. Because the intermediate edge-wise matrix $\mathbf{R}^d_{\mathrm{local}}(\mathbf{x}^{d*})$ is exclusively block-diagonal within its separated macro-domains, the full evaluation of its product with the decoupled topological Jacobian rigorously preserves this horizontal separation.

The matrix multiplication collapses into an ordered vertical stacking that applies the local dense blocks independently to their respective incidence rows. This operation effectively stacks the individual measurement codomains, yielding the exact global sparse rows derived in Step 3:

$$
\begin{aligned}
\mathbf{R}^d(\mathbf{x}^{d*}) &= \mathbf{R}^d_{\text{local}}(\mathbf{x}^{d*}) \cdot \mathbf{J}^d_{\sigma} \\
&= \left[\mathbf{R}^d_{\text{local},p}(\mathbf{x}^{d*}) \;\middle|\; \mathbf{R}^d_{\text{local},R}(\mathbf{x}^{d*}) \right] \begin{bmatrix} \mathbf{S} & \mathbf{0} \\ \mathbf{0} & \mathbf{S} \end{bmatrix} \\
&= \left[\mathbf{R}^d_{\text{local},p}(\mathbf{x}^{d*}) \cdot \mathbf{S} \;\middle|\; \mathbf{R}^d_{\text{local},R}(\mathbf{x}^{d*}) \cdot \mathbf{S} \right] \\
&= \left[\begin{array}{c|c} \text{blockdiag}_{k=1}^{m} \left(r^d_{\text{mod}_k,p}(\mathbf{e}_k^{d*}) \right) \begin{bmatrix} \mathbf{S}_{e_1} \\ \vdots \\ \mathbf{S}_{e_m} \end{bmatrix} & \text{blockdiag}_{k=1}^{m} \left(r^d_{\text{mod}_k,R}(\mathbf{e}_k^{d*}) \right) \begin{bmatrix} \mathbf{S}_{e_1} \\ \vdots \\ \mathbf{S}_{e_m} \end{bmatrix} \end{array} \right] \\
&= \left[\begin{array}{c|c} r^d_{\text{mod}_1,p}(\mathbf{e}_1^{d*}) \cdot \mathbf{S}_{e_1} & r^d_{\text{mod}_1,R}(\mathbf{e}_1^{d*}) \cdot \mathbf{S}_{e_1} \\ \vdots & \vdots \\ r^d_{\text{mod}_m,p}(\mathbf{e}_m^{d*}) \cdot \mathbf{S}_{e_m} & r^d_{\text{mod}_m,R}(\mathbf{e}_m^{d*}) \cdot \mathbf{S}_{e_m} \end{array} \right] \\
&= \left[\begin{array}{c|c} [\mathbf{R}^d_p(\mathbf{x}^{d*})]_1 & [\mathbf{R}^d_R(\mathbf{x}^{d*})]_1 \\ \vdots & \vdots \\ [\mathbf{R}^d_p(\mathbf{x}^{d*})]_m & [\mathbf{R}^d_R(\mathbf{x}^{d*})]_m \end{array} \right] = \left[\mathbf{R}^d_p(\mathbf{x}^{d*}) \;\middle|\; \mathbf{R}^d_R(\mathbf{x}^{d*}) \right] \\
&= \begin{bmatrix} [\mathbf{R}^d(\mathbf{x}^{d*})]_1 \\ \vdots \\ [\mathbf{R}^d(\mathbf{x}^{d*})]_m \end{bmatrix}.
\end{aligned}
\tag{207}
$$

By exposing the block formulation defined previously, we definitively reveal the overarching decoupled architecture that cleanly separates the translational and rotational MASs across the entire network:

- **Distance MAS:** The matrix $\mathbf{R}^d_{\text{dist}}(\mathbf{x}^{d*}) \in \mathbb{R}^{m \times 6n}$ is constructed entirely of sparse $1 \times 6n$ distance rows:

$$
\begin{aligned}
\mathbf{R}^d_{\text{dist}}(\mathbf{x}^{d*}) &= \begin{bmatrix} [\mathbf{R}^d_{\text{dist}}(\mathbf{x}^{d*})]_1 \\ \vdots \\ [\mathbf{R}^d_{\text{dist}}(\mathbf{x}^{d*})]_m \end{bmatrix} \\
&= \left[\begin{array}{c|c} [\mathbf{R}^d_{\text{dist},p}(\mathbf{x}^{d*})]_1 & [\mathbf{R}^d_{\text{dist},R}(\mathbf{x}^{d*})]_1 \\ \vdots & \vdots \\ [\mathbf{R}^d_{\text{dist},p}(\mathbf{x}^{d*})]_m & [\mathbf{R}^d_{\text{dist},R}(\mathbf{x}^{d*})]_m \end{array} \right] \\
&= \left[\mathbf{R}^d_{\text{dist},p}(\mathbf{x}^{d*}) \;\middle|\; \mathbf{R}^d_{\text{dist},R}(\mathbf{x}^{d*}) \right].
\end{aligned}
\tag{208}
$$

- **Bearing MAS:** The matrix $\mathbf{R}^d_{\text{bear}}(\mathbf{x}^{d*}) \in \mathbb{R}^{3m\times 6n}$ is constructed entirely of sparse $3 \times 6n$ bearing rows:

$$\mathbf{R}^d_{\text{bear}}(\mathbf{x}^{d*}) = \begin{bmatrix} [\mathbf{R}^d_{\text{bear}}(\mathbf{x}^{d*})]_1 \\ \vdots \\ [\mathbf{R}^d_{\text{bear}}(\mathbf{x}^{d*})]_m \end{bmatrix}$$

$$= \left[\begin{array}{c|c} [\mathbf{R}^d_{\text{bear},p}(\mathbf{x}^{d*})]_1 & [\mathbf{R}^d_{\text{bear},R}(\mathbf{x}^{d*})]_1 \\ \vdots & \vdots \\ [\mathbf{R}^d_{\text{bear},p}(\mathbf{x}^{d*})]_m & [\mathbf{R}^d_{\text{bear},R}(\mathbf{x}^{d*})]_m \end{array}\right]$$

$$= \left[\begin{array}{c|c} \mathbf{R}^d_{\text{bear},p}(\mathbf{x}^{d*}) & \mathbf{R}^d_{\text{bear},R}(\mathbf{x}^{d*}) \end{array}\right]. \tag{209}$$

- **Mixed MAS:** The matrix $\mathbf{R}^d_{\text{mix}}(\mathbf{x}^{d*}) \in \mathbb{R}^{4m\times 6n}$ is uniformly assembled by vertically stacking the sparse $4 \times 6n$ padded rows for all m edges, seamlessly integrating zero-blocks where measurements are locally absent:

$$\mathbf{R}^d_{\text{mix}}(\mathbf{x}^{d*}) = \begin{bmatrix} [\mathbf{R}^d_{\text{mix}}(\mathbf{x}^{d*})]_1 \\ \vdots \\ [\mathbf{R}^d_{\text{mix}}(\mathbf{x}^{d*})]_m \end{bmatrix}$$

$$= \left[\begin{array}{c|c} [\mathbf{R}^d_{\text{mix},p}(\mathbf{x}^{d*})]_1 & [\mathbf{R}^d_{\text{mix},R}(\mathbf{x}^{d*})]_1 \\ \vdots & \vdots \\ [\mathbf{R}^d_{\text{mix},p}(\mathbf{x}^{d*})]_m & [\mathbf{R}^d_{\text{mix},R}(\mathbf{x}^{d*})]_m \end{array}\right]$$

$$= \left[\begin{array}{c|c} \mathbf{R}^d_{\text{mix},p}(\mathbf{x}^{d*}) & \mathbf{R}^d_{\text{mix},R}(\mathbf{x}^{d*}) \end{array}\right]. \tag{210}$$

Remark 4.1. The edge-wise dense local blocks $r^c_k(\mathbf{e}^{c*}_k)$ and $r^d_{\text{mod}_k}(\mathbf{e}^{d*}_k)$ encapsulate the strictly local kinematics for each individual edge to cleanly capture the full 6-DOF coupled dynamics or the structurally separated positional and rotational variations. Combining these dense edge-wise blocks with the network discrete incidence list mathematically encodes the same information as the full global rigidity matrix. This factorization completely avoids the transmission of uninformative zero blocks inflated by topological sparsity. We can communicate only these information and each agent can then independently reassemble the complete global rigidity matrix locally.

4.6 RIGIDITY MATRICES RELATION VIA NATURAL DIFFEOMORPHISM

The commutative diagram presented at the beginning of this chapter is not merely a structural illustration; it dictates the exact analytical relationship between the coupled and decoupled formulations of the framework. By tracing the paths of the diagram, the overarching decoupled measurement function $\mathbf{h}^d$ (induced by the decoupled functor realization) can be rigorously expressed as the composition of the natively coupled measurement function $\mathbf{h}^c$ (induce by the coupled functor realization) with the global domain diffeomorphism. Since the final measurement codomain $\mathcal{Y}^m$ is physically identical in both formulations (yielding an identity transformation on the output), the commutative relation globally reduces to:

$$\mathbf{h}^d = \mathbf{h}^c \circ \phi_{\mathcal{V}}^{-1}. \tag{211}$$

This compositional equivalence allows us to directly map the differential properties between the two spaces. Let $\mathbf{x}^{c*} \in \mathbb{SE}(3)^n$ be the nominal coupled state and $\mathbf{x}^{d*} \in (\mathbb{R}^3)^n \times \mathbb{SO}(3)^n$ be the corresponding nominal decoupled state, strictly related by $\mathbf{x}^{c*} = \phi_{\mathcal{V}}^{-1}(\mathbf{x}^{d*})$. By applying the multivariate chain rule on manifolds evaluated at these respective nominal points, we relate the Jacobian of the decoupled measurement function to the Jacobian of the coupled measurement function:

$$\mathbf{J}_{\mathbf{h}^d}(\mathbf{x}^{d*}) = \mathbf{J}_{\mathbf{h}^c}(\mathbf{x}^{c*}) \cdot \mathbf{J}_{\phi_{\mathcal{V}}^{-1}}(\mathbf{x}^{d*}). \tag{212}$$

Substituting the respective global rigidity matrices into this identity (since $\mathbf{R}^d \equiv \mathbf{J}_{\mathbf{h}^d}$ and $\mathbf{R}^c \equiv \mathbf{J}_{\mathbf{h}^c}$), we obtain:

$$\mathbf{R}^d(\mathbf{x}^{d*}) = \mathbf{R}^c(\mathbf{x}^{c*}) \cdot \mathbf{P}^{-1} \tag{213}$$

where, by the Inverse Function Theorem, $\mathbf{P}^{-1} = \mathbf{J}_{\phi_{\mathcal{V}}^{-1}}(\mathbf{x}^{d*})$ corresponds to the inverse of $\mathbf{P} = \mathbf{J}_{\phi_{\mathcal{V}}}(\mathbf{x}^{c*}) \in \mathbb{R}^{6n\times 6n}$, which is the Jacobian of the forward state diffeomorphism mapping the coupled tangent space $T(\mathbb{SE}(3)^n)$ into the decoupled tangent space $T((\mathbb{R}^3)^n \times \mathbb{SO}(3)^n)$.

Crucially, because the local Lie algebra parameterization $[\delta\mathbf{p}^T, \delta\boldsymbol{\theta}^T]^T \in \mathbb{R}^6$ is identical for both domains, the state diffeomorphism $\phi_{\mathcal{V}}$ acts merely as a macroscopic topological router. Formally, the map rearranges the Cartesian product:

$$\begin{aligned} \phi_{\mathcal{V}} :\ \mathbb{SE}(3)^n &\xrightarrow{\cong} (\mathbb{R}^3)^n \times \mathbb{SO}(3)^n \\ \big((\mathbf{p}_1, \mathbf{R}_1), \dots, (\mathbf{p}_n, \mathbf{R}_n)\big) &\mapsto \big((\mathbf{p}_1, \dots, \mathbf{p}_n), (\mathbf{R}_1, \dots, \mathbf{R}_n)\big) \end{aligned} \tag{214}$$

In the coupled tangent space, translational and rotational variations are interleaved per agent:

$$\delta\mathbf{x}^c = \begin{bmatrix} \delta\mathbf{p}_1^T & \delta\boldsymbol{\theta}_1^T & \dots & \delta\mathbf{p}_n^T & \delta\boldsymbol{\theta}_n^T \end{bmatrix}^T. \tag{215}$$

In the decoupled tangent space, they are rigorously segregated into macroscopic positional and rotational blocks:

$$\delta \mathbf{x}^d = \left[\delta \mathbf{p}_1^T \quad \dots \quad \delta \mathbf{p}_n^T \;\middle|\; \delta \boldsymbol{\theta}_1^T \quad \dots \quad \delta \boldsymbol{\theta}_n^T\right]^T. \tag{216}$$

Consequently, the transformation matrix $\mathbf{P}$ mapping the coupled variations to the decoupled variations ($\delta \mathbf{x}^d = \mathbf{P} \delta \mathbf{x}^c$) is strictly a constant, linear **Permutation Matrix**. To compute it analytically, we define the standard positional and rotational selection matrices for a single $\mathbb{SE}(3)$ twist:

$$\mathbf{E}_p = \begin{bmatrix} \mathbf{I}_3 & \mathbf{0}_{3\times 3} \end{bmatrix} \in \mathbb{R}^{3\times 6}, \quad \mathbf{E}_R = \begin{bmatrix} \mathbf{0}_{3\times 3} & \mathbf{I}_3 \end{bmatrix} \in \mathbb{R}^{3\times 6} \tag{217}$$

Applying these selectors simultaneously to all n agents via the Kronecker product ($\otimes$), the global $6n \times 6n$ permutation matrix is explicitly constructed as:

$$\mathbf{P} = \begin{bmatrix} \mathbf{I}_n \otimes \mathbf{E}_p \\ \mathbf{I}_n \otimes \mathbf{E}_R \end{bmatrix} = \left[\begin{array}{ccccccc} \mathbf{I}_3 & \mathbf{0}_{3\times 3} & \mathbf{0}_{3\times 3} & \mathbf{0}_{3\times 3} & \dots & \mathbf{0}_{3\times 3} & \mathbf{0}_{3\times 3} \\ \mathbf{0}_{3\times 3} & \mathbf{0}_{3\times 3} & \mathbf{I}_3 & \mathbf{0}_{3\times 3} & \dots & \mathbf{0}_{3\times 3} & \mathbf{0}_{3\times 3} \\ \vdots & \vdots & \vdots & \vdots & \ddots & \vdots & \vdots \\ \mathbf{0}_{3\times 3} & \mathbf{0}_{3\times 3} & \mathbf{0}_{3\times 3} & \mathbf{0}_{3\times 3} & \dots & \mathbf{I}_3 & \mathbf{0}_{3\times 3} \\ \hline \mathbf{0}_{3\times 3} & \mathbf{I}_3 & \mathbf{0}_{3\times 3} & \mathbf{0}_{3\times 3} & \dots & \mathbf{0}_{3\times 3} & \mathbf{0}_{3\times 3} \\ \mathbf{0}_{3\times 3} & \mathbf{0}_{3\times 3} & \mathbf{0}_{3\times 3} & \mathbf{I}_3 & \dots & \mathbf{0}_{3\times 3} & \mathbf{0}_{3\times 3} \\ \vdots & \vdots & \vdots & \vdots & \ddots & \vdots & \vdots \\ \mathbf{0}_{3\times 3} & \mathbf{0}_{3\times 3} & \mathbf{0}_{3\times 3} & \mathbf{0}_{3\times 3} & \dots & \mathbf{0}_{3\times 3} & \mathbf{I}_3 \end{array}\right] \tag{218}$$

A fundamental property of permutation matrices is that they are structurally orthogonal ($\mathbf{P}^{-1} = \mathbf{P}^T$). The algebraic relation between the rigidity matrices can thus be elegantly rewritten as a mere column reordering:

$$\mathbf{R}^d(\mathbf{x}^{d*}) = \mathbf{R}^c(\mathbf{x}^{c*}) \cdot \mathbf{P}^T. \tag{219}$$

Conversely, one can effortlessly recover the rigidity matrix of the natively coupled system by computing the simpler decoupled rigidity matrix first, and then applying the inverse column permutation:

$$\mathbf{R}^c(\mathbf{x}^{c*}) = \mathbf{R}^d(\mathbf{x}^{d*}) \cdot \mathbf{P}. \tag{220}$$

PRESERVATION OF INFINITESIMAL Φ-RIGIDITY: Right-multiplying a matrix by a full-rank non-singular matrix acts as an isomorphism on its kernel, perfectly preserving both its rank and the dimension of its nullity. Therefore, we formally state that:

$$\dim\ker\left(\mathbf{R}^d(\mathbf{x}^{d*})\right) \equiv \dim\ker\left(\mathbf{R}^d(\mathbf{x}^{d*}) \cdot \mathbf{P}\right) \equiv \dim\ker\left(\mathbf{R}^c(\mathbf{x}^{c*})\right). \tag{221}$$

Recall that a framework is defined as infinitesimally Φ-rigid if and only if the dimension of the rigidity matrix's kernel exactly matches the dimension of the trivial motion space generated by the symmetry group action, i.e., $\dim\ker \mathbf{R} = \dim \mathrm{Im}(d\Phi_{\mathbf{x}}|_e)$.

Because the dimension of this trivial motion space $\mathrm{Im}(d\Phi_{\mathbf{x}}|_e)$ is an intrinsic geometric property of the configuration, it is strictly invariant under the diffeomorphism, which inherently acts as a change of coordinate parameterization.

Consequently, since the diffeomorphism maintains the dimension equality condition, infinitesimal Φ-rigidity is preserved under this diffeomorphism.

5 | CASE STUDIES

We consider the following functors realization commutative diagram:

$$
\begin{tikzcd}
& \text{Agents Space} & \text{Edges Space} & \text{Task Edges Space} & \text{Observation Space} & \text{Measurement Space} \\
\textbf{Kinematic} & \prod_{i=1}^{n} \mathcal{D}_i \arrow[r, shift left, "\sigma_{kin}"] \arrow[d, hook, shift left, "\iota_{\alpha,V}"] & \prod_{k=1}^{m} \left(\mathcal{D}_{s(e_k)} \times \mathcal{D}_{t(e_k)}\right) \arrow[l, shift left, "\mu_{kin}"] \arrow[r, "\gamma_{kin}"] \arrow[d, hook, shift left, "\iota_{\alpha,E}"] & \prod_{k=1}^{m} \left(\mathcal{T}_{s(e_k)} \times \mathcal{T}_{t(e_k)}\right) \arrow[r, "\Delta_{kin}"] \arrow[d, hook, shift left, "\iota_{\alpha,T}"] & \prod_{k=1}^{m} \mathcal{O}_k \arrow[r, "\eta_{kin}"] \arrow[d, hook, shift left, "\iota_{\alpha,O}"] & \prod_{k=1}^{m} \mathcal{M}_k \arrow[d, hook, shift left, "\iota_{\alpha,M}"] \\
\textbf{Augmented} & \prod_{i=1}^{n} \left(\mathcal{D}_i \times \Theta_i\right) \arrow[r, shift left, "\sigma_{aug}"] \arrow[u, two heads, shift left, "\rho_{\alpha,V}"] \arrow[d, hook, shift left, "\iota_{\epsilon,V}"] & \prod_{k=1}^{m} \prod_{j \in \{s(e_k),t(e_k)\}} \left(\mathcal{D}_j \times \Theta_j\right) \arrow[l, shift left, "\mu_{aug}"] \arrow[r, "\gamma_{aug}"] \arrow[u, two heads, shift left, "\rho_{\alpha,E}"] \arrow[d, hook, shift left, "\iota_{\epsilon,E}"] & \prod_{k=1}^{m} \left(\mathcal{T}_{s(e_k)} \times \mathcal{T}_{t(e_k)}\right) \arrow[r, "\Delta_{aug}"] \arrow[u, two heads, shift left, "\rho_{\alpha,T}"] \arrow[d, hook, shift left, "\iota_{\epsilon,T}"] & \prod_{k=1}^{m} \mathcal{O}_k \arrow[r, "\eta_{aug}"] \arrow[u, two heads, shift left, "\rho_{\alpha,O}"] \arrow[d, hook, shift left, "\iota_{\epsilon,O}"] & \prod_{k=1}^{m} \mathcal{M}_k \arrow[u, two heads, shift left, "\rho_{\alpha,M}"] \arrow[d, hook, shift left, "\iota_{\epsilon,M}"] \\
\textbf{Embedded} & \mathbb{SE}(3)^n \arrow[r, shift left, "\sigma_{emb}"] \arrow[u, two heads, shift left, "\rho_{\epsilon,V}"] & \left(\mathbb{SE}(3) \times \mathbb{SE}(3)\right)^m \arrow[l, shift left, "\mu_{emb}"] \arrow[r, "\gamma_{emb}"] \arrow[u, two heads, shift left, "\rho_{\epsilon,E}"] & \left(\mathbb{SE}(3) \times \mathbb{SE}(3)\right)^m \arrow[r, "\Delta_{emb}"] \arrow[u, two heads, shift left, "\rho_{\epsilon,T}"] & \mathbb{SE}(3)^m \arrow[r, "\eta_{emb}"] \arrow[u, two heads, shift left, "\rho_{\epsilon,O}"] & \mathcal{Y}^m \arrow[u, two heads, shift left, "\rho_{\epsilon,M}"]
\end{tikzcd}
$$

5.1 INTRODUCTION

In the following, two case studies are presented to illustrate how the hybrid rigidity framework can be applied to solve complex modeling and analysis problems. The first case study focuses on a heterogeneous MAS utilizing mixed measurements, specifically combining 2-dimensional spatial distances with 3-dimensional spatial bearings. The second case study examines a MAS composed of agents restricted to moving along distinct straight lines (1D submanifolds) while being mutually constrained by 3-dimensional spatial distance measurements.

These case studies highlight the innovative capabilities of the proposed framework. From a practical perspective, these examples illustrate the precise mechanism by which extrinsic parameters are injected into the state embedding and measurement processes. They also showcase how the commutativity between different functorial realizations provides a powerful, rigorous analytical tool. Ultimately, this analysis confirms a core theoretical claim: by integrating extrinsic information, the framework can accurately map disparate agent states into a common abstract homogeneous space. This embedding process and the pipeline structure, characterized by an explicit filtration action, enable the formulation of measurement maps that are no longer strictly bound to the agents' full intrinsic kinematics. Instead, they allow the framework to selectively evaluate a specific subset of their state or seamlessly incorporate external data to satisfy complex physical constraints.

Both case studies share the same fundamental objective and analytical methodology, which are outlined below before detailing the specific scenarios:

5.1.1 Goal

The objective of this analysis is to verify whether the MAS, equipped with a specific sensing network, allows only those continuous motions that strictly preserve its shape, namely the Euclidean distances between all pairs of agents.

5.1.2 Methodology

We construct the embedded rigidity matrix within the completely homogenized $\mathbb{SE}(3)$ space, leveraging the generalized structural framework developed in the previous chapter.

To execute this operation, we must first explicitly define the state embedding functions and their respective Jacobians. This allows us to map the agents' states into $\mathbb{SE}(3)$, yielding a common homogeneous representation while rigorously establishing the exact relationship between the native kinematic state space and the embedded representations. To clearly expose how the structural constraints and extrinsic hardware parameters enter the analytical formulation, this embedding is performed in two sequential stages: first, from the minimal native kinematic space to the augmented space; and second, from the augmented space to the fully embedded $\mathbb{SE}(3)$ space.

Furthermore, to formally connect this embedded rigidity matrix with its augmented and kinematic counterparts, we explicitly derive the measurement retraction functions and their corresponding Jacobians. This inverse mapping is similarly executed in stages: first, from the abstract embedded space back to the augmented space; and finally, from the augmented space down to the minimal kinematic space.

This systematic approach allows us to analytically derive all three rigidity matrices associated with their respective functorial realizations.

5.1.3 Common Assumptions

Throughout this analysis, it is assumed that:

- no collinear configurations occur;
- no spatial inter-agent collisions occur.

Note that this analysis strictly inherits all the conventions established in the previous chapter.

5.2 EXAMPLE 1

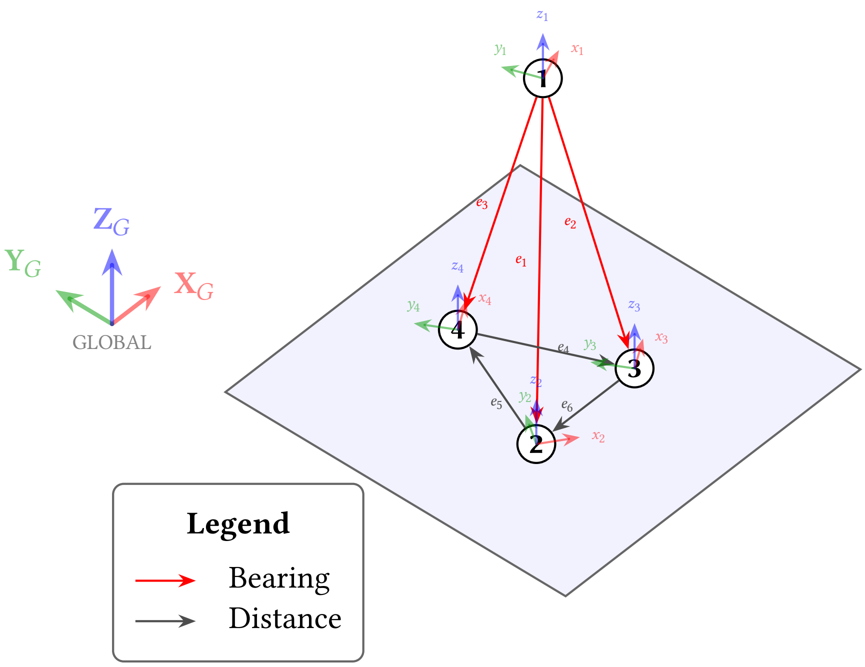

5.2.1 System Description

This example investigates a heterogeneous MAS comprising three planar UGVs and one UAV. The three ground agents operate on a 2D plane and are mutually constrained by distance measurements, establishing a non-collinear triangular formation. The UAV, operating in the 3D workspace, is constrained to the ground formation strictly through relative bearing measurements.

5.2.2 Agents

We consider a MAS composed of $n = 4$ agents evolving on heterogeneous manifolds. The agents are categorized as follows:

- **Ground Agents ($v_i, i \in \{2, 3, 4\}$):** These agents operate on a flat horizontal plane, and their pose can be fully represented by an element in $\mathbb{SE}(2)$. To account for their operation within a 3D environment, their augmented agent space is defined as the manifold $P_i = \mathbb{SE}(2) \times \mathbb{R}$, which extends their planar state with the constant height of the horizontal plane $h \in \mathbb{R}$. Thus, their augmented state is characterized by $\mathbf{q}_i = (\mathbf{p}_i, \theta_i, h) \in P_i$, where $\mathbf{p}_i = (x_i, y_i) \in \mathbb{R}^2$ is the planar position and $\theta_i \in \mathbb{SO}(2)$ is the orientation.
- **Aerial Agent (v_1):** Its full pose is characterized by an element of $\mathbb{SE}(3)$. Since this fully describes its 3D position and orientation, there is no need for additional parameters. In other words, its augmented agent space naturally coincides with its native space, defined directly as $P_1 = \mathbb{SE}(3)$. Its state is represented by $\mathbf{x}_1 = (\mathbf{p}_1, \mathbf{R}_1) \in P_1$, where $\mathbf{p}_1 \in \mathbb{R}^3$ is the 3D position and $\mathbf{R}_1 \in \mathbb{SO}(3)$ is the rotation matrix representing its attitude.

5.2.3 Agent Embedding Maps

To analyze rigidity in a unified mathematical framework, the agents' native kinematic states must be mapped into the common global space $\mathbb{SE}(3)$. Following the categorical pipeline established previously, this process is rigorously decomposed into two sequential natural transformations: first, a parametric expansion via $\iota_{\alpha,\mathbb{V}}$ that maps the native states into the augmented space; and second, the application of topological padding via $\iota_{\epsilon,\mathbb{V}}$ to embed these augmented states into the final embedding space.

Stage 1: Kinematic-to-Augmented

The first stage expands the minimal native kinematic state $\mathbf{x}_i \in \mathscr{D}_i$ with the specific extrinsic hardware parameters required for the task, forming the augmented state $\mathbf{q}_i$.

AERIAL AGENT (v_1): For the fully actuated aerial agent, the native space is already $\mathscr{D}_1 = \mathbb{SE}(3)$, and no extra parameters are required to define its full pose in 3D space. The augmented state is identical to the kinematic state, hence the embedding is the identity map:

$$\begin{aligned} \iota_{\alpha,1} :\ & \mathbb{SE}(3) \hookrightarrow \mathbb{SE}(3) \\ & \mathbf{x}_1 \mapsto \mathbf{q}_1 = \mathbf{x}_1 \end{aligned} \tag{1}$$

Parameterizing the native variation as $\delta\mathbf{x}_1 = [\delta\mathbf{p}_1^T, \delta\boldsymbol{\theta}_1^T]^T \in \mathbb{R}^6$, the corresponding Jacobian is simply the identity matrix:

$$J_{\iota_{\alpha,1}} = \frac{\partial \iota_{\alpha,1}}{\partial \mathbf{x}_1} = \mathbf{I}_6 \in \mathbb{R}^{6\times 6} \tag{2}$$

GROUND AGENTS (v_2, v_3, v_4): For the ground agents, the native kinematic space is $\mathscr{D}_i = \mathbb{SE}(2)$, with each element identified by $\mathbf{x}_i = (\mathbf{p}_{i,xy}, \theta_i)$, where $\mathbf{p}_{i,xy} \in \mathbb{R}^2$ denotes the planar position and $\theta_i \in \mathbb{SO}(2)$ represents the orientation. However, they operate on a horizontal plane shifted by a structural height parameter $h_i \in \mathbb{R}$. The resulting map is:

$$\begin{aligned} \iota_{\alpha,i} :\ & \mathbb{SE}(2) \hookrightarrow \mathbb{SE}(2) \times \mathbb{R} \\ & \mathbf{x}_i \mapsto \mathbf{q}_i = (\mathbf{x}_i, h_i) = (\mathbf{p}_{i,xy}, \theta_i, h_i) \end{aligned} \tag{3}$$

The kinematic variation is explicitly parameterized as $\delta\mathbf{x}_i = [\delta\mathbf{p}_{i,xy}^T, \delta\theta_i]^T \in \mathbb{R}^3$, while the corresponding augmented variation is $\delta\mathbf{q}_i = [\delta\mathbf{x}_i^T, \delta h_i]^T \in \mathbb{R}^4$. The Jacobian of this expansion safely pads the parametric dimension:

$$J_{\iota_{\alpha,i}} = \frac{\partial \iota_{\alpha,i}}{\partial \mathbf{x}_i} = \begin{bmatrix} \mathbf{I}_3 \\ \mathbf{0}_{1\times 3} \end{bmatrix} \in \mathbb{R}^{4\times 3} \tag{4}$$

GLOBAL KINEMATIC-TO-AUGMENTED MAPPING: To evaluate the network as a whole at this stage, we aggregate the individual agent mappings via Cartesian products, mapping the global kinematic product space $\mathbb{SE}(3) \times \mathbb{SE}(2)^3$ into the global augmented product space $\mathbb{SE}(3) \times (\mathbb{SE}(2) \times \mathbb{R})^3$ via $\iota_{\alpha,\mathrm{V}}$. The global Jacobian is constructed as a block-diagonal matrix, naturally preserving the individual local tangent-space parameterizations:

$$J_{\iota_{\alpha,\mathrm{V}}} = \mathrm{blockdiag}\left(J_{\iota_{\alpha,1}}, J_{\iota_{\alpha,2}}, J_{\iota_{\alpha,3}}, J_{\iota_{\alpha,4}}\right) \in \mathbb{R}^{18\times 15} \tag{5}$$

Stage 2: Augmented-to-Embedded

The second stage resolves dimensional heterogeneity by embedding the augmented states into the common abstract space $\mathbb{SE}(3)$ through a map that structurally transforms the agent augmented states while applying any necessary informationless padding. This process maps the parameterized augmented states $\mathbf{q}_i$ into the uniform ambient manifold $\mathbb{SE}(3)$, yielding the embedded pose $\mathbf{x}_i^e = (\mathbf{p}_i^e, \mathbf{R}_i^e)$.

AERIAL AGENT (v_1): Since the augmented state of the aerial agent is already in $\mathbb{SE}(3)$, the topological embedding is trivially the identity map:

$$\begin{aligned} \iota_{\epsilon,1} : \ & \mathbb{SE}(3) \hookrightarrow \mathbb{SE}(3) \\ & \mathbf{q}_1 \mapsto (\mathbf{p}_1^e, \mathbf{R}_1^e) = \mathbf{x}_1^e \end{aligned} \tag{6}$$

where $\mathbf{p}_1^e = \mathbf{p}_1$ and $\mathbf{R}_1^e = \mathbf{R}_1$.

Reusing the same tangent-space parameterization established previously for both augmented and embedded states, the corresponding Jacobian is simply the identity matrix:

$$J_{\iota_{\epsilon,1}} = \frac{\partial \iota_{\epsilon,1}}{\partial \mathbf{q}_1} = \mathbf{I}_6 \in \mathbb{R}^{6\times 6} \tag{7}$$

GROUND AGENTS (v_2, v_3, v_4): For the ground agents, the embedding map assigns the parameter h_i to the z-axis and completes the 1D orientation into a full 3D rotation matrix around the vertical axis:

$$\begin{aligned} \iota_{\epsilon,i} : \ & \mathbb{SE}(2) \times \mathbb{R} \hookrightarrow \mathbb{SE}(3) \\ \mathbf{q}_i = (\mathbf{p}_{i,xy}, \theta_i, h_i) \mapsto & \left(\underbrace{\begin{bmatrix} \mathbf{p}_{i,xy} \\ h_i \end{bmatrix}}_{\mathbf{p}_i^e}, \underbrace{\begin{bmatrix} \cos\theta_i & -\sin\theta_i & 0 \\ \sin\theta_i & \cos\theta_i & 0 \\ 0 & 0 & 1 \end{bmatrix}}_{\mathbf{R}_i^e} \right) = \mathbf{x}_i^e \end{aligned} \tag{8}$$

To analytically propagate the variations from the augmented space to the global tangent space, let us explicitly define the augmented tangent variation as

$$\delta \mathbf{q}_i = \begin{bmatrix} \delta \mathbf{p}_{i,xy}^T & \delta\theta_i & \delta h_i \end{bmatrix}^T \in \mathbb{R}^4$$

, and the embedded tangent variation as

$$\delta \mathbf{x}_i^e = \begin{bmatrix} (\delta \mathbf{p}_i^e)^T & (\delta \boldsymbol{\theta}_i^e)^T \end{bmatrix}^T \in \mathbb{R}^6.$$

Defining the planar canonical injection matrix $P_2 = \begin{bmatrix} \mathbf{e}_1 & \mathbf{e}_2 \end{bmatrix} \in \mathbb{R}^{3\times 2}$ and the vertical unit vector $\mathbf{e}_3 = \begin{bmatrix} 0 & 0 & 1 \end{bmatrix}^T$, the embedding process can be expressed as $\mathbf{p}_i^e = P_2 \mathbf{p}_{i,xy} + \mathbf{e}_3 h_i$, and the embedded kinematics are expressed as:

$$\delta \mathbf{p}_i^e = P_2 \delta \mathbf{p}_{i,xy} + \mathbf{e}_3 \delta h_i \tag{9}$$

$$\delta \boldsymbol{\theta}_i^e = \mathbf{e}_3 \delta \theta_i \tag{10}$$

Taking the exact differentials with respect to the augmented variables, we construct the 6×4 local Jacobian block. This matrix perfectly isolates the active planar kinematics (left block) from the static structural parameter (right column):

$$J_{\iota_{\epsilon,i}} = \frac{\partial \iota_{\epsilon,i}}{\partial \mathbf{q}_i} = \left[\begin{array}{cc|c} \frac{\partial \mathbf{p}_i^e}{\partial \mathbf{p}_{i,xy}} & \frac{\partial \mathbf{p}_i^e}{\partial \theta_i} & \frac{\partial \mathbf{p}_i^e}{\partial h_i} \\ \frac{\partial \boldsymbol{\theta}_i^e}{\partial \mathbf{p}_{i,xy}} & \frac{\partial \boldsymbol{\theta}_i^e}{\partial \theta_i} & \frac{\partial \boldsymbol{\theta}_i^e}{\partial h_i} \end{array}\right] = \left[\begin{array}{cc|c} P_2 & \mathbf{0}_{3\times 1} & \mathbf{e}_3 \\ \mathbf{0}_{3\times 2} & \mathbf{e}_3 & \mathbf{0}_{3\times 1} \end{array}\right] \in \mathbb{R}^{6\times 4} \tag{11}$$

GLOBAL AUGMENTED-TO-EMBEDDED MAPPING: Similarly, aggregating the second stage via Cartesian products maps the global augmented product space $\mathbb{SE}(3) \times (\mathbb{SE}(2) \times \mathbb{R})^3$ into the homogeneous global embedded space $\mathbb{SE}(3)^4$ via $\iota_{\epsilon,\mathbb{V}}$. The global Jacobian is a block-diagonal matrix that injects the necessary structural zeros to homogenize all agents into $\mathbb{SE}(3)$:

$$J_{\iota_{\epsilon,\mathbb{V}}} = \text{blockdiag}\left(J_{\iota_{\epsilon,1}}, J_{\iota_{\epsilon,2}}, J_{\iota_{\epsilon,3}}, J_{\iota_{\epsilon,4}}\right) \in \mathbb{R}^{24\times 18} \tag{12}$$

5.2.4 Measurement Retraction Maps

Embedded-to-Augmented Measurement Retraction ($\rho_{\mathbb{M},\epsilon}$)

The augmented measurement space is identical to the embedded homogeneous measurement space $\mathcal{Y} = \mathbb{L} \times \mathbb{R}_{>0}$. Here, $\mathbb{L} \subset \mathbb{R}^3$ defines the set where the bearing measurements reside (specifically adopted over the intrinsic $\mathbb{S}^2$ to circumvent geometric singularities) while $\mathbb{R}_{>0}$ represents the codomain for the Euclidean distance measurements.

For each individual network edge k, the retraction map is trivially the identity map:

$$\begin{aligned} \rho^k_{\mathbb{M},\epsilon} : \mathbb{L} \times \mathbb{R}_{>0} &\to \mathbb{L} \times \mathbb{R}_{>0} \\ \mathbf{y}_{emb,k} &\mapsto \mathbf{y}_{emb,k} \end{aligned} \tag{13}$$

Parameterizing the local tangent variation as $\delta\mathbf{y}_{emb,k} = [\delta\mathbf{b}_k^T, \delta d_k]^T \in \mathbb{R}^4$, the corresponding local Jacobian block is simply the 4×4 identity matrix $\mathbf{I}_4$.

GLOBAL EMBEDDED-TO-AUGMENTED MAPPING: To evaluate the network measurements as a whole at this stage, we aggregate the individual edge mappings via Cartesian products, mapping the global embedded measurement product space into the global augmented measurement space via $\rho_{\mathbb{M},\epsilon} : (\mathbb{L} \times \mathbb{R}_{>0})^6 \to (\mathbb{L} \times \mathbb{R}_{>0})^6$.

Parameterizing the global tangent variation as $\delta\mathbf{y}_{emb} \in \mathbb{R}^{24}$ via the concatenation of the local variations, and naturally preserving the individual local tangent-space parameterizations, the global Jacobian is constructed as a block-diagonal matrix of identities, yielding the global identity matrix:

$$J_{\rho_{\mathbb{M},\epsilon}} = \text{blockdiag}\left(\mathbf{I}_4, \dots, \mathbf{I}_4\right) = \mathbf{I}_{24} \in \mathbb{R}^{24\times 24} \tag{14}$$

Augmented-to-Kinematic Measurement Retraction ($\rho_{\alpha,\mathbb{M}}$)

The augmented-to-kinematic measurement retraction map isolates the true physical observation specific to each sensor type. It acts as the left-inverse of the kinematic measurement embedding map, restoring the true informational dimension of the network.

Depending on the specific measurement modality of the edge, we define a local retraction map that projects the padded homogeneous state $(\mathbf{b}_{ij}, d_{ij}) \in \mathbb{L} \times \mathbb{R}_{>0}$ onto its active physical components.

For edges corresponding to **bearing measurements**, the physical state resides strictly in $\mathbb{L}$. The retraction map discards the padded distance component:

$$\begin{aligned} \rho^b_{\alpha,\mathbb{M}} : \mathbb{L} \times \mathbb{R}_{>0} &\to \mathbb{L} \\ (\mathbf{b}_{ij}, d_{ij}) &\mapsto \mathbf{b}_{ij} \end{aligned} \tag{15}$$

For edges corresponding to **Euclidean distance measurements**, the physical state resides strictly in $\mathbb{R}_{>0}$. The retraction map discards the padded dummy bearing vector:

$$\begin{aligned} \rho^d_{\alpha,\mathbb{M}} : \mathbb{L} \times \mathbb{R}_{>0} &\to \mathbb{R}_{>0} \\ (\mathbf{b}_{ij}, d_{ij}) &\mapsto d_{ij} \end{aligned} \tag{16}$$

Let the local tangent variation of the extended measurement be explicitly parameterized as $\delta y_{ij} = [\delta \mathbf{b}_{ij}^T, \delta d_{ij}]^T \in \mathbb{R}^4$.

The **bearing retraction map** preserves the 3-dimensional variation of the bearing vector $\delta \mathbf{b}_{ij}$ while systematically zeroing out the scalar distance variation δd_{ij}. Therefore, its corresponding local Jacobian block is a constant 3×4 extraction matrix:

$$J_{\rho^b_{\alpha,\mathbb{M}}} = \frac{\partial \rho^b_{\alpha,\mathbb{M}}}{\partial y_{ij}} = \begin{bmatrix} \mathbf{I}_3 & \mathbf{0}_{3\times 1} \end{bmatrix} \in \mathbb{R}^{3\times 4} \tag{17}$$

Conversely, the **distance retraction map** preserves only the scalar distance variation δd_{ij} and discards the 3-dimensional bearing variation $\delta \mathbf{b}_{ij}$. Its corresponding local Jacobian block is a constant 1×4 extraction matrix:

$$J_{\rho^d_{\alpha,\mathbb{M}}} = \frac{\partial \rho^d_{\alpha,\mathbb{M}}}{\partial y_{ij}} = \begin{bmatrix} \mathbf{0}_{1\times 3} & 1 \end{bmatrix} \in \mathbb{R}^{1\times 4} \tag{18}$$

GLOBAL AUGMENTED-TO-KINEMATIC MAPPING: To filter the measurements for the entire network simultaneously, we aggregate the individual local retraction maps into a single global measurement retraction map via $\rho_{\alpha,\mathbb{M}} : (\mathbb{L} \times \mathbb{R}_{>0})^6 \to \mathbb{L}^3 \times \mathbb{R}^3_{>0}$.

Naturally preserving the individual local measurement tangent-space parameterizations defined previously, the global Jacobian is constructed as a block-diagonal matrix from the local extraction blocks:

$$J_{\rho_{\alpha,\mathbb{M}}} = \frac{\partial \rho_{\alpha,\mathbb{M}}}{\partial \mathbf{y}_{emb}} = \text{blockdiag}\left(J_{\rho^b_{\alpha,\mathbb{M}}}, J_{\rho^b_{\alpha,\mathbb{M}}}, J_{\rho^b_{\alpha,\mathbb{M}}}, J_{\rho^d_{\alpha,\mathbb{M}}}, J_{\rho^d_{\alpha,\mathbb{M}}}, J_{\rho^d_{\alpha,\mathbb{M}}}\right) \in \mathbb{R}^{12\times 24} \tag{19}$$

5.2.5 Rigidity Matrix

Embedded Rigidity Matrix (R^{emb})

The Embedded Rigidity Matrix captures the first-order differential constraints of the network strictly within the fully homogeneous extended spaces. It maps the 24-dimensional variations of the structurally padded agents into the 24-dimensional variations of the completely padded abstract measurement space:

$$\delta\mathbf{z}_{\mathbb{E}}^{emb} = R^{emb}\,\delta\mathbf{x}_{\mathbb{V}}^{e}, \quad \text{where } \delta\mathbf{x}_{\mathbb{V}}^{e} \in \mathbb{R}^{24},\ \delta\mathbf{z}_{\mathbb{E}}^{emb} \in \mathbb{R}^{24} \tag{20}$$

To make the block structure explicit, we rely on the tangent space parameterizations established in the previous sections. The padded input state variation vector $\delta\mathbf{x}_{\mathbb{V}}^{e}$ explicitly concatenates the complete $\$\mathbb{E}(3)$ kinematic twists for all $n = 4$ agents (6 DOFs each). Similarly, the padded output variation vector $\delta\mathbf{z}_{\mathbb{E}}^{emb}$ reserves a full 4-dimensional coordinate block for each of the $m = 6$ edges (3 DOFs for the bearing variation embedded in $\mathbb{R}^3$, and 1 DOF for the distance), systematically injecting zeros for the unmeasured complementary components:

$$\delta\mathbf{x}_{\mathbb{V}}^{e} = \begin{bmatrix} \delta\mathbf{x}_1^e \\ \hline \delta\mathbf{x}_2^e \\ \hline \delta\mathbf{x}_3^e \\ \hline \delta\mathbf{x}_4^e \end{bmatrix} = \begin{bmatrix} \delta\mathbf{p}_1^e \\ \delta\boldsymbol{\theta}_1^e \\ \hline \delta\mathbf{p}_2^e \\ \delta\boldsymbol{\theta}_2^e \\ \hline \delta\mathbf{p}_3^e \\ \delta\boldsymbol{\theta}_3^e \\ \hline \delta\mathbf{p}_4^e \\ \delta\boldsymbol{\theta}_4^e \end{bmatrix}, \quad \delta\mathbf{z}_{\mathbb{E}}^{emb} = \begin{bmatrix} \delta\mathbf{z}_{12}^{emb} \\ \hline \delta\mathbf{z}_{13}^{emb} \\ \hline \delta\mathbf{z}_{14}^{emb} \\ \hline\hline \delta\mathbf{z}_{43}^{emb} \\ \hline \delta\mathbf{z}_{24}^{emb} \\ \hline \delta\mathbf{z}_{32}^{emb} \end{bmatrix} = \begin{bmatrix} \delta\mathbf{b}_{12} \\ 0 \\ \hline \delta\mathbf{b}_{13} \\ 0 \\ \hline \delta\mathbf{b}_{14} \\ 0 \\ \hline\hline \mathbf{0}_{3\times 1} \\ \delta d_{43} \\ \hline \mathbf{0}_{3\times 1} \\ \delta d_{24} \\ \hline \mathbf{0}_{3\times 1} \\ \delta d_{32} \end{bmatrix} \tag{21}$$

Using the sequence of categorical mappings established previously, we construct the purely homogeneous Embedded Rigidity Matrix $R^{emb} \in \mathbb{R}^{24\times 24}$ by directly applying the chain rule ($R^{emb} = J_{\eta_{emb}} J_{\Delta_{emb}} J_{\gamma_{emb}} J_{\sigma_{emb}}$). The explicit sparse formulation evaluates to:

$$
R^{emb} = \left[\begin{array}{cc|cc|cc|cc}
-\frac{1}{\|\mathbf{p}_{12}\|}\mathbf{\Pi}_{\mathbf{b}_{12}}\mathbf{R}_1^T & [\mathbf{b}_{12}]_\times & +\frac{1}{\|\mathbf{p}_{12}\|}\mathbf{\Pi}_{\mathbf{b}_{12}}\mathbf{R}_1^T & \mathbf{0}_{3\times3} & \mathbf{0}_{3\times3} & \mathbf{0}_{3\times3} & \mathbf{0}_{3\times3} & \mathbf{0}_{3\times3} \\
\mathbf{0}_{1\times3} & \mathbf{0}_{1\times3} & \mathbf{0}_{1\times3} & \mathbf{0}_{1\times3} & \mathbf{0}_{1\times3} & \mathbf{0}_{1\times3} & \mathbf{0}_{1\times3} & \mathbf{0}_{1\times3} \\
\hline
-\frac{1}{\|\mathbf{p}_{13}\|}\mathbf{\Pi}_{\mathbf{b}_{13}}\mathbf{R}_1^T & [\mathbf{b}_{13}]_\times & \mathbf{0}_{3\times3} & \mathbf{0}_{3\times3} & +\frac{1}{\|\mathbf{p}_{13}\|}\mathbf{\Pi}_{\mathbf{b}_{13}}\mathbf{R}_1^T & \mathbf{0}_{3\times3} & \mathbf{0}_{3\times3} & \mathbf{0}_{3\times3} \\
\mathbf{0}_{1\times3} & \mathbf{0}_{1\times3} & \mathbf{0}_{1\times3} & \mathbf{0}_{1\times3} & \mathbf{0}_{1\times3} & \mathbf{0}_{1\times3} & \mathbf{0}_{1\times3} & \mathbf{0}_{1\times3} \\
\hline
-\frac{1}{\|\mathbf{p}_{14}\|}\mathbf{\Pi}_{\mathbf{b}_{14}}\mathbf{R}_1^T & [\mathbf{b}_{14}]_\times & \mathbf{0}_{3\times3} & \mathbf{0}_{3\times3} & \mathbf{0}_{3\times3} & \mathbf{0}_{3\times3} & +\frac{1}{\|\mathbf{p}_{14}\|}\mathbf{\Pi}_{\mathbf{b}_{14}}\mathbf{R}_1^T & \mathbf{0}_{3\times3} \\
\mathbf{0}_{1\times3} & \mathbf{0}_{1\times3} & \mathbf{0}_{1\times3} & \mathbf{0}_{1\times3} & \mathbf{0}_{1\times3} & \mathbf{0}_{1\times3} & \mathbf{0}_{1\times3} & \mathbf{0}_{1\times3} \\
\hline\hline
\mathbf{0}_{3\times3} & \mathbf{0}_{3\times3} & \mathbf{0}_{3\times3} & \mathbf{0}_{3\times3} & \mathbf{0}_{3\times3} & \mathbf{0}_{3\times3} & \mathbf{0}_{3\times3} & \mathbf{0}_{3\times3} \\
\mathbf{0}_{1\times3} & \mathbf{0}_{1\times3} & \mathbf{0}_{1\times3} & \mathbf{0}_{1\times3} & +\mathbf{q}_{43,xy}^T & \mathbf{0}_{1\times3} & -\mathbf{q}_{43,xy}^T & \mathbf{0}_{1\times3} \\
\hline
\mathbf{0}_{3\times3} & \mathbf{0}_{3\times3} & \mathbf{0}_{3\times3} & \mathbf{0}_{3\times3} & \mathbf{0}_{3\times3} & \mathbf{0}_{3\times3} & \mathbf{0}_{3\times3} & \mathbf{0}_{3\times3} \\
\mathbf{0}_{1\times3} & \mathbf{0}_{1\times3} & -\mathbf{q}_{24,xy}^T & \mathbf{0}_{1\times3} & \mathbf{0}_{1\times3} & \mathbf{0}_{1\times3} & +\mathbf{q}_{24,xy}^T & \mathbf{0}_{1\times3} \\
\hline
\mathbf{0}_{3\times3} & \mathbf{0}_{3\times3} & \mathbf{0}_{3\times3} & \mathbf{0}_{3\times3} & \mathbf{0}_{3\times3} & \mathbf{0}_{3\times3} & \mathbf{0}_{3\times3} & \mathbf{0}_{3\times3} \\
\mathbf{0}_{1\times3} & \mathbf{0}_{1\times3} & +\mathbf{q}_{32,xy}^T & \mathbf{0}_{1\times3} & -\mathbf{q}_{32,xy}^T & \mathbf{0}_{1\times3} & \mathbf{0}_{1\times3} & \mathbf{0}_{1\times3}
\end{array}\right] \tag{22}
$$

where $\mathbf{\Pi}_{\mathbf{b}_{1j}}$ the local orthogonal projector.

Augmented Rigidity Matrix (R^{aug})

The Augmented Rigidity Matrix R^{aug} is obtained by pulling the analysis back to the Augmented Space. This is achieved through both pre-multiplying by the Embedded-to-Augmented Measurement Retraction Jacobian $J_{\rho_{\mathbb{M},\epsilon}}$ and post-multiplying by the global Augmented-to-Embedded Jacobian $J_{\iota_{\epsilon,\mathbb{V}}}$:

$$
R^{aug} = J_{\rho_{\mathbb{M},\epsilon}} R^{emb} J_{\iota_{\epsilon,\mathbb{V}}} = R^{emb} J_{\iota_{\epsilon,\mathbb{V}}} \tag{23}
$$

since $J_{\rho_{\mathbb{M},\epsilon}} = I_{24}$.

Because the measurement retraction is the identity, the output variation vector remains the fully padded 24-dimensional coordinate space ($\delta\mathbf{z}_{\mathbb{E}}^{aug} \equiv \delta\mathbf{z}_{\mathbb{E}}^{emb}$). However, the input vector condenses from 24 to 18 dimensions, reflecting the exact parameterization of the augmented tangent manifolds:

$$
\delta\mathbf{z}_{\mathbb{E}}^{aug} = R^{aug}\,\delta\mathbf{q}_{\mathbb{V}}, \quad \text{where } \delta\mathbf{q}_{\mathbb{V}} \in \mathbb{R}^{18},\ \delta\mathbf{z}_{\mathbb{E}}^{aug} \in \mathbb{R}^{24} \tag{24}
$$

Explicitly defining the local coordinate representations for these augmented tangent spaces, the global input vector $\delta\mathbf{q}_{\mathbb{V}}$ concatenates the 6 coordinate variables of the quadrotor's native $\mathbb{SE}(3)$ twist with the 4 coordinate variables (planar twist + structural height variation) representing the tangent space of each augmented unicycle manifold $SE(2) \times \mathbb{R}$:

$$\delta \mathbf{q}_{\mathbb{V}} = \left[\begin{array}{c} \delta \mathbf{q}_1 \\ \hline \delta \mathbf{q}_2 \\ \hline \delta \mathbf{q}_3 \\ \hline \delta \mathbf{q}_4 \end{array}\right] = \left[\begin{array}{c} \delta \mathbf{p}_1 \\ \delta \boldsymbol{\theta}_1 \\ \hline \delta \mathbf{p}_{2,xy} \\ \delta \theta_2 \\ \delta h_2 \\ \hline \delta \mathbf{p}_{3,xy} \\ \delta \theta_3 \\ \delta h_3 \\ \hline \delta \mathbf{p}_{4,xy} \\ \delta \theta_4 \\ \delta h_4 \end{array}\right] \tag{25}$$

We obtain:

$$R^{aug} = \left[\begin{array}{cc|c|c|c}
-\frac{1}{\|\mathbf{p}_{12}\|}\Pi_{\mathbf{b}_{12}}\mathbf{R}_1^T & [\mathbf{b}_{12}]_\times & \left[+\frac{1}{\|\mathbf{p}_{12}\|}\Pi_{\mathbf{b}_{12}}\mathbf{R}_1^T P_2 \quad \mathbf{0}_{3\times1} \;\middle|\; +\frac{1}{\|\mathbf{p}_{12}\|}\Pi_{\mathbf{b}_{12}}\mathbf{R}_1^T \mathbf{e}_3 \right] & \mathbf{0}_{3\times4} & \mathbf{0}_{3\times4} \\
\mathbf{0}_{1\times3} & \mathbf{0}_{1\times3} & \mathbf{0}_{1\times4} & \mathbf{0}_{1\times4} & \mathbf{0}_{1\times4} \\ \hline
-\frac{1}{\|\mathbf{p}_{13}\|}\Pi_{\mathbf{b}_{13}}\mathbf{R}_1^T & [\mathbf{b}_{13}]_\times & \mathbf{0}_{3\times4} & \left[+\frac{1}{\|\mathbf{p}_{13}\|}\Pi_{\mathbf{b}_{13}}\mathbf{R}_1^T P_2 \quad \mathbf{0}_{3\times1} \;\middle|\; +\frac{1}{\|\mathbf{p}_{13}\|}\Pi_{\mathbf{b}_{13}}\mathbf{R}_1^T \mathbf{e}_3 \right] & \mathbf{0}_{3\times4} \\
\mathbf{0}_{1\times3} & \mathbf{0}_{1\times3} & \mathbf{0}_{1\times4} & \mathbf{0}_{1\times4} & \mathbf{0}_{1\times4} \\ \hline
-\frac{1}{\|\mathbf{p}_{14}\|}\Pi_{\mathbf{b}_{14}}\mathbf{R}_1^T & [\mathbf{b}_{14}]_\times & \mathbf{0}_{3\times4} & \mathbf{0}_{3\times4} & \left[+\frac{1}{\|\mathbf{p}_{14}\|}\Pi_{\mathbf{b}_{14}}\mathbf{R}_1^T P_2 \quad \mathbf{0}_{3\times1} \;\middle|\; +\frac{1}{\|\mathbf{p}_{14}\|}\Pi_{\mathbf{b}_{14}}\mathbf{R}_1^T \mathbf{e}_3 \right] \\
\mathbf{0}_{1\times3} & \mathbf{0}_{1\times3} & \mathbf{0}_{1\times4} & \mathbf{0}_{1\times4} & \mathbf{0}_{1\times4} \\ \hline\hline
\mathbf{0}_{3\times3} & \mathbf{0}_{3\times3} & \mathbf{0}_{3\times4} & \mathbf{0}_{3\times4} & \mathbf{0}_{3\times4} \\
\mathbf{0}_{1\times3} & \mathbf{0}_{1\times3} & \mathbf{0}_{1\times4} & \left[+\mathbf{q}_{43,xy}^T \quad 0 \;\middle|\; 0 \right] & \left[-\mathbf{q}_{43,xy}^T \quad 0 \;\middle|\; 0 \right] \\ \hline
\mathbf{0}_{3\times3} & \mathbf{0}_{3\times3} & \mathbf{0}_{3\times4} & \mathbf{0}_{3\times4} & \mathbf{0}_{3\times4} \\
\mathbf{0}_{1\times3} & \mathbf{0}_{1\times3} & \left[-\mathbf{q}_{24,xy}^T \quad 0 \;\middle|\; 0 \right] & \mathbf{0}_{1\times4} & \left[+\mathbf{q}_{24,xy}^T \quad 0 \;\middle|\; 0 \right] \\ \hline
\mathbf{0}_{3\times3} & \mathbf{0}_{3\times3} & \mathbf{0}_{3\times4} & \mathbf{0}_{3\times4} & \mathbf{0}_{3\times4} \\
\mathbf{0}_{1\times3} & \mathbf{0}_{1\times3} & \left[+\mathbf{q}_{32,xy}^T \quad 0 \;\middle|\; 0 \right] & \left[-\mathbf{q}_{32,xy}^T \quad 0 \;\middle|\; 0 \right] & \mathbf{0}_{1\times4}
\end{array}\right] \tag{26}$$

Kinematic Rigidity Matrix (R^{kin})

To reach the Kinematic Rigidity Matrix, we must execute the final categorical reduction on both sides simultaneously.

We right-multiply by the Kinematic-to-Augmented Jacobian $J_{\iota_{\alpha,\mathbb{V}}}$ to discard the structural height parameters, mapping the input domain down to the minimal 15-dimensional native kinematic space.

Simultaneously, we left-multiply by the Augmented-to-Kinematic Measurement Retraction Jacobian $J_{\rho_{\alpha,\mathbb{M}}}$ to extract only the physically meaningful measurement dimensions, removing the zeros introduced by the informationless padding:

$$R^{kin} = J_{\rho_{\alpha,\mathbb{M}}} R^{aug} J_{\iota_{\alpha,\mathbb{V}}} = J_{\rho_{\alpha,\mathbb{M}}} J_{\rho_{\mathbb{M},\varepsilon}} R^{emb} J_{\iota_{\varepsilon,\mathbb{V}}} J_{\iota_{\alpha,\mathbb{V}}} \tag{27}$$

By enforcing this double reduction, the coordinate parameterizations exactly match the physical tangent spaces of the minimal kinematic manifolds and the true sensor spaces. This yields the final, minimal physical mapping:

$$\delta \mathbf{z}_{\mathbb{E}} = R^{kin} \, \delta \mathbf{x}_{\mathbb{V}}, \quad \text{where } \delta \mathbf{x}_{\mathbb{V}} \in \mathbb{R}^{15}, \; \delta \mathbf{z}_{\mathbb{E}} \in \mathbb{R}^{12} \tag{28}$$

Here, both the input state vector and the output measurement vector are completely stripped of their informationless padding. The minimal kinematic input vector $\delta\mathbf{x}_{\mathbb{V}}$ groups solely the true actuatable coordinate twists (6 DOFs for the aerial agent, 3 planar DOFs for each ground agent). Conversely, the physical output vector $\delta\mathbf{z}_{\mathbb{E}}$ retains only the active variations for each specific sensor (3 dimensions for the bearing edges, 1 dimension for the distance edges):

$$\delta\mathbf{x}_{\mathbb{V}} = \left[\begin{array}{c} \delta\mathbf{x}_1 \\ \hline \delta\mathbf{x}_2 \\ \hline \delta\mathbf{x}_3 \\ \hline \delta\mathbf{x}_4 \end{array}\right] = \left[\begin{array}{c} \delta\mathbf{p}_1 \\ \delta\boldsymbol{\theta}_1 \\ \hline \delta\mathbf{p}_{2,xy} \\ \delta\theta_2 \\ \hline \delta\mathbf{p}_{3,xy} \\ \delta\theta_3 \\ \hline \delta\mathbf{p}_{4,xy} \\ \delta\theta_4 \end{array}\right], \quad \delta\mathbf{z}_{\mathbb{E}} = \left[\begin{array}{c} \delta\mathbf{z}_{12} \\ \hline \delta\mathbf{z}_{13} \\ \hline \delta\mathbf{z}_{14} \\ \hline\hline \delta\mathbf{z}_{43} \\ \hline \delta\mathbf{z}_{24} \\ \hline \delta\mathbf{z}_{32} \end{array}\right] = \left[\begin{array}{c} \delta\mathbf{b}_{12} \\ \hline \delta\mathbf{b}_{13} \\ \hline \delta\mathbf{b}_{14} \\ \hline\hline \delta d_{43} \\ \hline \delta d_{24} \\ \hline \delta d_{32} \end{array}\right] \tag{29}$$

The sparse 24×18 matrix is thereby elegantly compressed into its true 12×15 physical dimensionality:

$$R^{kin} = \left[\begin{array}{cc|c|c|c} -\frac{1}{\|\mathbf{p}_{12}\|}\Pi_{\mathbf{b}_{12}}\mathbf{R}_1^T & [\mathbf{b}_{12}]_\times & \left[+\frac{1}{\|\mathbf{p}_{12}\|}\Pi_{\mathbf{b}_{12}}\mathbf{R}_1^T P_2 \quad \mathbf{0}_{3\times1}\right] & \mathbf{0}_{3\times3} & \mathbf{0}_{3\times3} \\ \hline -\frac{1}{\|\mathbf{p}_{13}\|}\Pi_{\mathbf{b}_{13}}\mathbf{R}_1^T & [\mathbf{b}_{13}]_\times & \mathbf{0}_{3\times3} & \left[+\frac{1}{\|\mathbf{p}_{13}\|}\Pi_{\mathbf{b}_{13}}\mathbf{R}_1^T P_2 \quad \mathbf{0}_{3\times1}\right] & \mathbf{0}_{3\times3} \\ \hline -\frac{1}{\|\mathbf{p}_{14}\|}\Pi_{\mathbf{b}_{14}}\mathbf{R}_1^T & [\mathbf{b}_{14}]_\times & \mathbf{0}_{3\times3} & \mathbf{0}_{3\times3} & \left[+\frac{1}{\|\mathbf{p}_{14}\|}\Pi_{\mathbf{b}_{14}}\mathbf{R}_1^T P_2 \quad \mathbf{0}_{3\times1}\right] \\ \hline\hline \mathbf{0}_{1\times3} & \mathbf{0}_{1\times3} & \mathbf{0}_{1\times3} & \left[+\mathbf{q}_{43,xy}^T \quad 0\right] & \left[-\mathbf{q}_{43,xy}^T \quad 0\right] \\ \hline \mathbf{0}_{1\times3} & \mathbf{0}_{1\times3} & \left[-\mathbf{q}_{24,xy}^T \quad 0\right] & \mathbf{0}_{1\times3} & \left[+\mathbf{q}_{24,xy}^T \quad 0\right] \\ \hline \mathbf{0}_{1\times3} & \mathbf{0}_{1\times3} & \left[+\mathbf{q}_{32,xy}^T \quad 0\right] & \left[-\mathbf{q}_{32,xy}^T \quad 0\right] & \mathbf{0}_{1\times3} \end{array}\right] \tag{30}$$

5.2.6 Infinitesimal Φ-Rigidity Analysis

Theorem 5.1. *Let $\mathscr{D}_{kin}$ be the purely kinematic state space of the network, where the state of the aerial agent is $\mathbf{x}_1 = (\mathbf{p}_1, \mathbf{R}_1) \in \mathbb{SE}(3)$ and the state of each planar ground agent is $\mathbf{x}_j = (\mathbf{p}_{j,xy}, \theta_j) \in \mathbb{SE}(2)$ for $j \in \{2, 3, 4\}$.*

Let $\tilde{\mathscr{D}} \subset \mathscr{D}_{kin}$ be the set of generic configurations $\mathbf{x}$ satisfying two conditions:

(H1) *The ground positions $\mathbf{p}_{2,xy}, \mathbf{p}_{3,xy}, \mathbf{p}_{4,xy}$ are non-collinear.*

(H2) *The matrix*

$$M(\mathbf{x}) = \begin{bmatrix} \mathbf{p}_{12}^T\mathbf{p}_{32} & \mathbf{p}_{13}^T\mathbf{p}_{23} & 0 \\ \mathbf{p}_{12}^T\mathbf{p}_{42} & 0 & \mathbf{p}_{14}^T\mathbf{p}_{24} \\ 0 & \mathbf{p}_{13}^T\mathbf{p}_{43} & \mathbf{p}_{14}^T\mathbf{p}_{34} \end{bmatrix}$$

is nonsingular ($\det M(\mathbf{x}) \neq 0$). Equivalently, the aerial agent does not lie on the danger cylinder *of the ground triangle, the classical critical locus of P3P problem.*

(H3) *Spatial non-collision of agents.*

Let us consider the group $G = \mathbb{SE}(2)\times\mathbb{SO}(2)^3$, where $\mathbb{SE}(2)$ governs the global formation motion, while $\mathbb{SO}(2)^3$ accounts for the independent local rotational symmetries.

A generic element $g \in G$ is parameterized as

$$g = (g_{se2}, \beta_2, \beta_3, \beta_4)$$

Here, $g_{se2} = (\mathbf{t}, \alpha) \in \mathbb{SE}(2)$ represents the global planar translation $\mathbf{t} \in \mathbb{R}^2$ and the global yaw rotation $\alpha \in \mathbb{SO}(2)$. The terms $\beta_j \in \mathbb{SO}(2)$ for $j \in \{2, 3, 4\}$ represent the independent local rotations of the individual ground agents.

The global planar movement translates the aerial agent along the horizontal plane and rotates it around the vertical axis, while remaining completely independent of the local ground symmetries. Let $\mathbf{R}_z(\alpha) \in \mathbb{SO}(3)$ denote the standard 3D rotation matrix around the Z axis. The action is evaluated as:

$$\Phi_1(g, \mathbf{x}_1) = \left(\mathbf{R}_z(\alpha)\mathbf{p}_1 + \begin{bmatrix}\mathbf{t}\\0\end{bmatrix}, \mathbf{R}_z(\alpha)\mathbf{R}_1\right)$$

Each ground agent is subjected to the global rotation and translation of the group $\mathbb{SE}(2)$, to which the unobservable local rotation of the specific node is linearly appended. Let $\mathbf{R}_{2D}(\alpha) \in \mathbb{SO}(2)$ denote the planar rotation matrix. The action evaluates to:

$$\Phi_j(g, \mathbf{x}_j) = \left(\mathbf{R}_{2D}(\alpha)\mathbf{p}_{j,xy} + \mathbf{t}, \theta_j + \alpha + \beta_j\right)$$

The overall group action on the complete network state $\mathbf{x} = (\mathbf{x}_1, \mathbf{x}_2, \mathbf{x}_3, \mathbf{x}_4) \in \mathscr{D}_{kin}$ is obtained by concatenating the individual transformations:

$$\Phi(g, \mathbf{x}) = \left(\Phi_1(g, \mathbf{x}_1), \Phi_2(g, \mathbf{x}_2), \Phi_3(g, \mathbf{x}_3), \Phi_4(g, \mathbf{x}_4)\right)$$

Note that this action is shape-preserving for the framework, as it is composed of the action of elements in $\mathbb{SE}(2)$ *that rigidly transform the global formation, and independent local symmetries in* $\mathbb{SO}(2)$ *that act exclusively on the heading of the ground agents without altering their positions. Consequently, the shape of the formation remains strictly invariant.*

Under this decomposition, the kinematic rigidity matrix $R^{kin} \in \mathbb{R}^{12\times 15}$ *takes the sparse block form:*

$$R^{kin} = \begin{bmatrix} \mathbf{A}(\mathbf{x}) & \mathbf{B}(\mathbf{x}) \\ \mathbf{0}_{3\times 6} & \mathbf{C}(\mathbf{x}) \end{bmatrix} \tag{31}$$

where $\mathbf{A} \in \mathbb{R}^{9\times 6}$ *collects the bearing-row derivatives with respect to the aerial twist* $\delta\mathbf{x}_1$*, and* $\mathbf{C} \in \mathbb{R}^{3\times 9}$ *collects the distance-row derivatives with respect to the ground twist* $\delta\mathbf{x}_G$*.*

The smooth framework family over the generic domain $\tilde{\mathscr{D}}$ *is infinitesimally* Φ*-rigid.*

Proof. rank$(\mathbf{C}) = 3$ **under (H1)**
Because distance measurements are invariant to agent orientations, the heading columns of $\mathbf{C}$ (corresponding to $\delta\theta_2, \delta\theta_3, \delta\theta_4$) are identically zero. Defining the normalized relative 2D position vectors as $\mathbf{q}_{kj} := \frac{\mathbf{p}_{j,xy}-\mathbf{p}_{k,xy}}{\|\mathbf{p}_{j,xy}-\mathbf{p}_{k,xy}\|}$, the 3×9 ground rigidity sub-matrix $\mathbf{C}$ evaluating the ground agent triangle edges $(4,3)$, $(2,4)$, and $(3,2)$ is explicitly written as:

$$\mathbf{C} = \left[\begin{array}{cc|cc|cc} \mathbf{0}_{1\times 2} & 0 & +\mathbf{q}_{43}^T & 0 & -\mathbf{q}_{43}^T & 0 \\ -\mathbf{q}_{24}^T & 0 & \mathbf{0}_{1\times 2} & 0 & +\mathbf{q}_{24}^T & 0 \\ +\mathbf{q}_{32}^T & 0 & -\mathbf{q}_{32}^T & 0 & \mathbf{0}_{1\times 2} & 0 \end{array}\right] \tag{32}$$

We extract the relevant 3×6 sub-matrix $\mathbf{C}'$ acting purely on the translational variations $(\delta\mathbf{p}_{2,xy}, \delta\mathbf{p}_{3,xy}, \delta\mathbf{p}_{4,xy})$ by discarding the null heading columns:

$$\mathbf{C}' = \begin{bmatrix} \mathbf{0}_{1\times 2} & +\mathbf{q}_{43}^T & -\mathbf{q}_{43}^T \\ -\mathbf{q}_{24}^T & \mathbf{0}_{1\times 2} & +\mathbf{q}_{24}^T \\ +\mathbf{q}_{32}^T & -\mathbf{q}_{32}^T & \mathbf{0}_{1\times 2} \end{bmatrix} \tag{33}$$

To prove that under assumption (H1) the matrix $\mathbf{C}'$ is full rank, we proceed by contradiction.

Let R_1, R_2, R_3 denote the three row-blocks of $\mathbf{C}'$.

$$R_1 = \begin{bmatrix} \mathbf{0}_{1\times 2} & +\mathbf{q}_{43}^T & -\mathbf{q}_{43}^T \end{bmatrix} \tag{34}$$

$$R_2 = \begin{bmatrix} -\mathbf{q}_{24}^T & \mathbf{0}_{1\times 2} & +\mathbf{q}_{24}^T \end{bmatrix} \tag{35}$$

$$R_3 = \begin{bmatrix} +\mathbf{q}_{32}^T & -\mathbf{q}_{32}^T & \mathbf{0}_{1\times 2} \end{bmatrix} \tag{36}$$

$$\tag{37}$$

Assume there exists a linear dependence of the rows such that $\mu_1 R_1 + \mu_2 R_2 + \mu_3 R_3 = \mathbf{0}^T$ for some scalars $\mu_1, \mu_2, \mu_3 \in \mathbb{R}$ with μ_1, μ_2, μ_3 not be simultaneously all zero.

Evaluating this sum explicitly, column-block by column-block, yields the following system of independent vector equations:

$$\mu_2(-\mathbf{q}_{24}^T) + \mu_3(+\mathbf{q}_{32}^T) = \mathbf{0}^T \quad \Longrightarrow \quad \mu_3\mathbf{q}_{32}^T = \mu_2\mathbf{q}_{24}^T \tag{38}$$

$$\mu_1(+\mathbf{q}_{43}^T) + \mu_3(-\mathbf{q}_{32}^T) = \mathbf{0}^T \quad \Longrightarrow \quad \mu_1\mathbf{q}_{43}^T = \mu_3\mathbf{q}_{32}^T \tag{39}$$

$$\mu_1(-\mathbf{q}_{43}^T) + \mu_2(+\mathbf{q}_{24}^T) = \mathbf{0}^T \quad \Longrightarrow \quad \mu_2\mathbf{q}_{24}^T = \mu_1\mathbf{q}_{43}^T \tag{40}$$

By the transitive property of equality, transposing the terms into column vectors directly yields the strict vector equality:

$$\mu_1\mathbf{q}_{43} = \mu_2\mathbf{q}_{24} = \mu_3\mathbf{q}_{32} =: \mathbf{u} \tag{41}$$

If this common vector is non-zero ($\mathbf{u} \neq \mathbf{0}$), it geometrically requires the three directional edge vectors to be strictly parallel ($\mathbf{q}_{43} \parallel \mathbf{q}_{24} \parallel \mathbf{q}_{32}$). This implies that the three ground nodes lie on a single straight line, directly contradicting Assumption (H1).

Therefore, the common vector must be zero ($\mathbf{u} = \mathbf{0}$). Since the nodes are spatially distinct (H3), their relative unit vectors are non-zero ($\mathbf{q}_{43}, \mathbf{q}_{24}, \mathbf{q}_{32} \neq \mathbf{0}$). This forces the scalars to identically vanish, admitting only the unique trivial solution $\mu_1 = \mu_2 = \mu_3 = 0$.

The rows of $\mathbf{C}'$ are linearly independent, meaning $\text{rank}(\mathbf{C}') = 3$. Because $\mathbf{C}'$ is obtained from $\mathbf{C}$ solely by removing identically zero columns, an algebraic operation that does not alter the rank of the matrix, it strictly holds that $\text{rank}(\mathbf{C}) = \text{rank}(\mathbf{C}') = 3$.

$\text{rank}(\mathbf{A}) = 6$ **under (H1,H2)**
We analyze the null space condition $\mathbf{A}\delta\mathbf{x}_1 = \mathbf{0}$. Note that this analysis falls within the classical domain of the Perspective-3-Point (P3P) problem.

Let $\mathbf{v}, \boldsymbol{\omega} \in \mathbb{R}^3$ be the local translational and rotational twist components of the aerial agent. The homogeneous bearing constraint $\delta\mathbf{b}_{1j} = \mathbf{0}$ for target $j \in \{2, 3, 4\}$ reduces to:

$$\delta\mathbf{b}_{1j} = \mathbf{\Pi}_{\mathbf{b}_{1j}}(\mathbf{v} + \boldsymbol{\omega} \times (\mathbf{R}_1^T\mathbf{p}_{1j})) = \mathbf{0} \iff \mathbf{v} + \boldsymbol{\omega} \times (\mathbf{R}_1^T\mathbf{p}_{1j}) = \lambda_j(\mathbf{R}_1^T\mathbf{p}_{1j}), \quad \lambda_j \in \mathbb{R}. \tag{42}$$

This exact equivalence holds because $\mathbf{\Pi}_{\mathbf{b}_{1j}}$ is the orthogonal projection matrix onto the plane perpendicular to the line-of-sight vector. If the projection of the velocity vector onto this perpendicular plane is identically zero, the vector itself must lie entirely along the optical ray. Consequently, it can be expressed strictly as a scalar multiple λ_j of the relative position vector expressed in the local frame.

To prove $\ker(\mathbf{A}) = \{\mathbf{0}\}$, we must show that $\mathbf{v} = \boldsymbol{\omega} = \mathbf{0}$ is the unique solution.

We first isolate the rotational component by evaluating the constraint for a pair of distinct targets, j and k, and subtracting them to rigorously eliminate the translational velocity $\mathbf{v}$:

$$\boldsymbol{\omega} \times \mathbf{R}_1^T(\mathbf{p}_{1j} - \mathbf{p}_{1k}) = \lambda_j \mathbf{R}_1^T \mathbf{p}_{1j} - \lambda_k \mathbf{R}_1^T \mathbf{p}_{1k} \tag{43}$$

To completely eliminate the angular velocity $\boldsymbol{\omega}$ and isolate the scalar multipliers, we project this vector equation onto the relative position vector $\mathbf{R}_1^T(\mathbf{p}_{1j} - \mathbf{p}_{1k})$ by applying the inner product to both sides.

Leveraging the fundamental cross-product property, the left-hand side identically vanishes:

$$\begin{aligned}
0 &= (\mathbf{R}_1^T(\mathbf{p}_{1j} - \mathbf{p}_{1k}))^T(\lambda_j \mathbf{R}_1^T \mathbf{p}_{1j} - \lambda_k \mathbf{R}_1^T \mathbf{p}_{1k}) \\
0 &= \lambda_j \|\mathbf{R}_1^T \mathbf{p}_{1j}\|^2 - \lambda_k (\mathbf{R}_1^T \mathbf{p}_{1j})^T(\mathbf{R}_1^T \mathbf{p}_{1k}) - \lambda_j (\mathbf{R}_1^T \mathbf{p}_{1k})^T(\mathbf{R}_1^T \mathbf{p}_{1j}) + \lambda_k \|\mathbf{R}_1^T \mathbf{p}_{1k}\|^2 \\
0 &= \lambda_j(\|\mathbf{R}_1^T \mathbf{p}_{1j}\|^2 - (\mathbf{R}_1^T \mathbf{p}_{1j})^T(\mathbf{R}_1^T \mathbf{p}_{1k})) + \lambda_k(\|\mathbf{R}_1^T \mathbf{p}_{1k}\|^2 - (\mathbf{R}_1^T \mathbf{p}_{1j})^T(\mathbf{R}_1^T \mathbf{p}_{1k}))
\end{aligned} \tag{44}$$

Because the rotation matrix $\mathbf{R}_1$ is orthogonal, inner products are fully invariant: $\|\mathbf{R}_1^T \mathbf{p}_{1j}\|^2 = \|\mathbf{p}_{1j}\|^2$ and $(\mathbf{R}_1^T \mathbf{p}_{1j})^T(\mathbf{R}_1^T \mathbf{p}_{1k}) = \mathbf{p}_{1j}^T \mathbf{p}_{1k}$. Substituting these absolute coordinates directly yields:

$$0 = \lambda_j \mathbf{p}_{1j}^T(\mathbf{p}_{1j} - \mathbf{p}_{1k}) + \lambda_k \mathbf{p}_{1k}^T(\mathbf{p}_{1k} - \mathbf{p}_{1j}) \tag{45}$$

Defining the relative ground vectors bidirectionally as $\mathbf{p}_{kj} := \mathbf{p}_j - \mathbf{p}_k = \mathbf{p}_{1j} - \mathbf{p}_{1k}$ and $\mathbf{p}_{jk} := \mathbf{p}_{1k} - \mathbf{p}_{1j}$, we can elegantly rewrite the relation as a sum of inner products:

$$0 = \lambda_j \mathbf{p}_{1j}^T \mathbf{p}_{kj} + \lambda_k \mathbf{p}_{1k}^T \mathbf{p}_{jk} \tag{46}$$

Evaluating this relation sequentially for the three distinct agent pairs $(2,3)$, $(2,4)$, and $(3,4)$ yields a homogeneous linear system in terms of $\boldsymbol{\lambda} = [\lambda_2, \lambda_3, \lambda_4]^T$:

$$\underbrace{\begin{bmatrix} \mathbf{p}_{12}^T \mathbf{p}_{32} & \mathbf{p}_{13}^T \mathbf{p}_{23} & 0 \\ \mathbf{p}_{12}^T \mathbf{p}_{42} & 0 & \mathbf{p}_{14}^T \mathbf{p}_{24} \\ 0 & \mathbf{p}_{13}^T \mathbf{p}_{43} & \mathbf{p}_{14}^T \mathbf{p}_{34} \end{bmatrix}}_{M(\mathbf{x})} \begin{bmatrix} \lambda_2 \\ \lambda_3 \\ \lambda_4 \end{bmatrix} = \begin{bmatrix} 0 \\ 0 \\ 0 \end{bmatrix} \tag{47}$$

For a non-trivial solution $\boldsymbol{\lambda} \neq \mathbf{0}$ to exist, the matrix $M(\mathbf{x})$ must be singular, demanding $\det M(\mathbf{x}) = 0$.

By Assumption (H2), $\det M(\mathbf{x}) \neq 0$. This strictly forces $\boldsymbol{\lambda} = \mathbf{0}$.

Substituting $\lambda_j = 0$ back into the fundamental bearing constraint (Equation 42) yields the homogeneous linear system for the twist components $\mathbf{x}_1 = [\mathbf{v}^T, \boldsymbol{\omega}^T]^T$:

$$\begin{bmatrix} \mathbf{I}_3 & -[\mathbf{R}_1^T \mathbf{p}_{12}]_\times \\ \mathbf{I}_3 & -[\mathbf{R}_1^T \mathbf{p}_{13}]_\times \\ \mathbf{I}_3 & -[\mathbf{R}_1^T \mathbf{p}_{14}]_\times \end{bmatrix} \begin{bmatrix} \mathbf{v} \\ \boldsymbol{\omega} \end{bmatrix} = \mathbf{0} \tag{48}$$

where $[\mathbf{R}_1^T \mathbf{p}_{1j}]_\times$ denotes the skew-symmetric matrix associated with the rotated relative position vector.

To formally prove that the coefficient matrix has full column rank (6), let us assume by contradiction that there exists a non-zero twist vector $\mathbf{x}_1 = [\mathbf{v}^T, \boldsymbol{\omega}^T]^T \neq \mathbf{0}$ satisfying the system:

$$\mathbf{v} + \boldsymbol{\omega} \times (\mathbf{R}_1^T \mathbf{p}_{1j}) = \mathbf{0}, \quad \forall j \in \{2, 3, 4\} \tag{49}$$

Subtracting this relation for the pairs $(2, 3)$ and $(2, 4)$ eliminates the translational velocity $\mathbf{v}$ and yields:

$$\boldsymbol{\omega} \times (\mathbf{R}_1^T \mathbf{p}_{32}) = \mathbf{0} \quad \text{and} \quad \boldsymbol{\omega} \times (\mathbf{R}_1^T \mathbf{p}_{42}) = \mathbf{0} \tag{50}$$

Assuming $\boldsymbol{\omega} \neq \mathbf{0}$, these cross-products require both rotated relative position vectors $\mathbf{R}_1^T \mathbf{p}_{32}$ and $\mathbf{R}_1^T \mathbf{p}_{42}$ to be parallel to the direction of $\boldsymbol{\omega}$. Because the orthogonal transformation $\mathbf{R}_1$ preserves collinearity and linear independence, if both rotated vectors are parallel to $\boldsymbol{\omega}$, they must be parallel to each other. This implies the existence of a scalar $k \in \mathbb{R}$ such that $\mathbf{p}_{42} = k\mathbf{p}_{32}$, meaning the ground position vectors $\mathbf{p}_2$, $\mathbf{p}_3$, and $\mathbf{p}_4$ lie on a single straight line.

However, this directly contradicts Assumption (H1), which states that the ground agents are strictly non-collinear. Therefore, the initial assumption must be false, forcing $\boldsymbol{\omega} = \mathbf{0}$. Substituting $\boldsymbol{\omega} = \mathbf{0}$ back into the original system immediately yields $\mathbf{v} = \mathbf{0}$. Thus, $\mathbf{x}_1 = \mathbf{0}$ is the unique solution, proving that the coefficient matrix has full column rank (6), $\ker(\mathbf{A}) = \{\mathbf{0}\}$, and $\operatorname{rank}(\mathbf{A}) = 6$.

Summarizing, we have established that $\mathbf{A}$ has full column rank (6) and $\mathbf{C}$ has full row rank (3).

A general fact about block upper-triangular matrices gives a lower bound on the total rank, regardless of the coupling matrix $\mathbf{B}$:

$$\operatorname{rank}(R^{kin}(\mathbf{x})) \geq \operatorname{rank}(\mathbf{A}) + \operatorname{rank}(\mathbf{C}) = 9, \qquad \text{i.e.,} \qquad \dim\ker(R^{kin}(\mathbf{x})) \leq 15 - 9 = 6. \tag{51}$$

Measurement Φ-Invariance
The structural distances and bearings are intrinsically invariant under the global rigid-body actions applied to the entire formation, and are physically unaffected by the local $\mathbb{SO}(2)^3$ heading variations of the ground agents.

Consequently, by the local infinitesimal orbit-kernel inclusion:

$$\mathrm{Im}(d\Phi_{\mathbf{x}}|_e) \subseteq \ker R^{kin}(\mathbf{x})$$

this implies that

$$\dim(\mathrm{Im}(d\Phi_{\mathbf{x}}|_e)) \leq \dim(\ker R^{kin}(\mathbf{x}))$$

Because the three ground agents are non-collinear (H1), no global planar transformation other than the identity can leave all their coordinates simultaneously unchanged, and independent variations in the ground agents' headings directly alter the state without affecting their positions. This guarantees that the group action Φ is free at any $\mathbf{x} \in \tilde{\mathscr{D}}$, so:

$$\dim(\mathrm{Im}(d\Phi_{\mathbf{x}}|_e)) = \dim(G) = 6. \tag{52}$$

This implies that

$$6 \leq \dim(\ker R^{kin}(\mathbf{x}))$$

Combining the two bounds:

$$\begin{cases} \dim\ker(R^{kin}(\mathbf{x})) \geq \dim(\mathrm{Im}(d\Phi_{\mathbf{x}}|_e)) = 6 \\ \dim\ker(R^{kin}(\mathbf{x})) \leq 6 \end{cases} \tag{53}$$

Hence equality holds: $\dim\ker(R^{kin}(\mathbf{x})) = 6$ exactly (so $\mathrm{rank}(R^{kin}(\mathbf{x})) = 9$ exactly).

By the dimensional equality for the infinitesimal Φ-rigidity condition, since

$$\dim\mathrm{Im}(d\Phi_{\mathbf{x}}|_e) = \dim\ker(R^{kin}(\mathbf{x}))$$

the framework is infinitesimally Φ-rigid. Since the choice of the node configuration is arbitrary in $\tilde{\mathscr{D}}$, the smooth framework family over $\tilde{\mathscr{D}}$ is infinitesimally Φ-rigid. $\square$

5.3 EXAMPLE 2

5.3.1 Introduction

We consider a system of three agents, each strictly constrained to move along a pre-defined distinct straight rail. This physical restriction acts as a holonomic constraint, fundamentally reducing the state space of each agent to a one-dimensional active manifold. Consequently, the intrinsic state of the i-th agent is fully parameterized by a single scalar $s_i \in \mathbb{R}$, representing its position along the rail. The direction of motion is implicitly captured by the sign of its instantaneous velocity $\dot{s}_i$, thus requiring no additional spatial heading parameter in the active state.

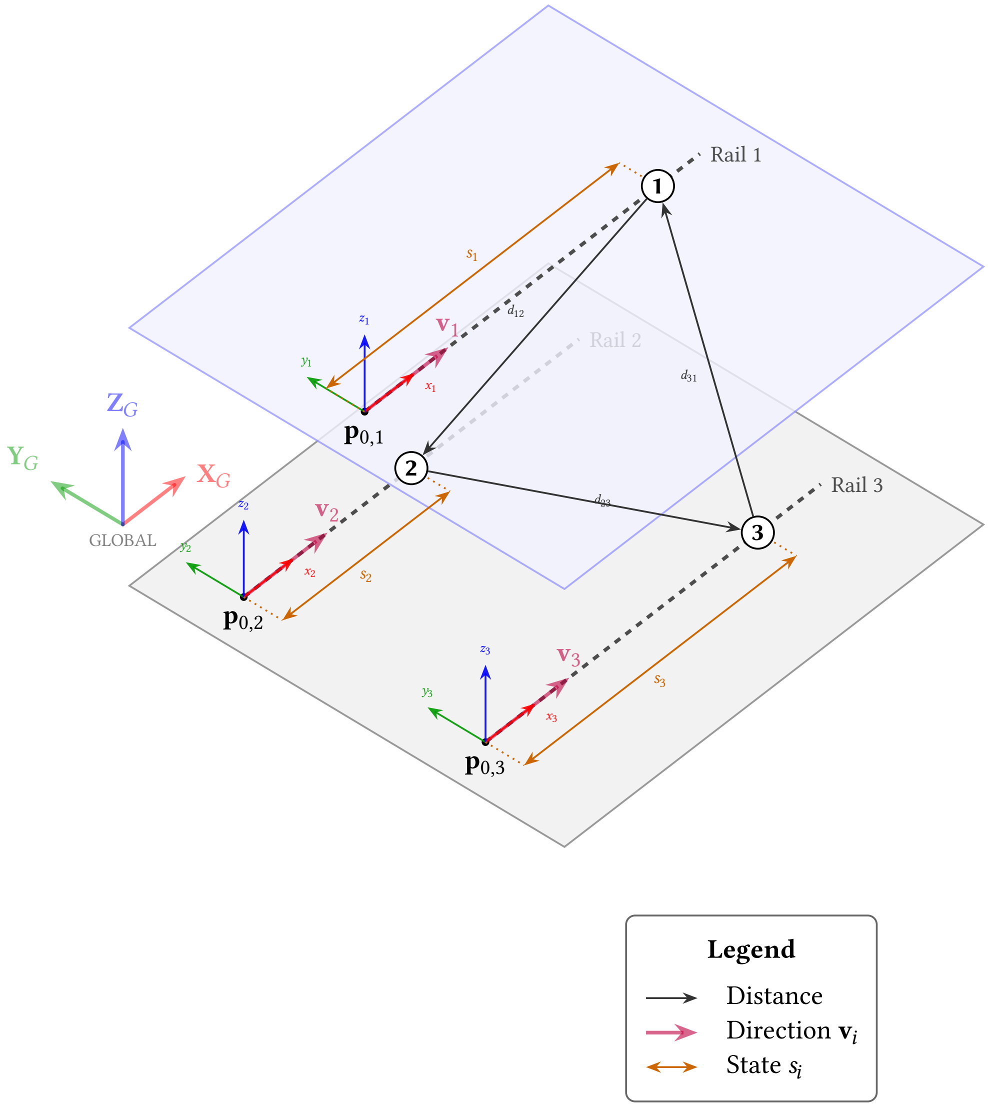

5.4 SYSTEM DESCRIPTION

To correctly embed the agent's state from its natural 1D domain into $\mathbb{SE}(3)$, we must formalize the spatial geometry of the constraining rails. Since a rail cannot be uniquely defined merely by a direction vector $\mathbf{v}_i \in \mathbb{L}$ and requires a reference point to compute the 1-dimensional state, we completely parameterize the i-th straight rail using a fixed reference frame in the world space, represented by a pose tuple $T_{rail,i} = (\mathbf{p}_{0,i}, R_{rail,i}) \in \mathbb{SE}(3)$, where $\mathbf{p}_{0,i} \in \mathbb{R}^3$ is the arbitrary geometric origin of the rail, and $R_{rail,i} \in \mathbb{SO}(3)$ defines its spatial orientation. Conventionally, we align the local x-axis of $R_{rail,i}$ with the longitudinal direction of the rail, yielding $\mathbf{v}_i = R_{rail,i}\mathbf{e}_1 \in \mathbb{L}$.

The structural parameter space defining the physical constraint is therefore the manifold $\Theta_i = \mathbb{SE}(3)$. The augmented space P_i for the i-th agent, coupling its internal dynamic state with its structural rail parameters, is the product manifold:

$$P_i = \mathscr{D}_i \times \Theta_i = \mathbb{R} \times \mathbb{SE}(3) \tag{54}$$

5.4.1 Agent Embedding Maps

Kinematic-to-Augmented Map ($\iota_{\alpha,i}$)

The first stage injects the active 1D kinematic state $s_i \in \mathbb{R}$ into the augmented space P_i, binding it to a specific physical constraint configuration. Given a fixed structural rail parameter $T_{rail,i} \in \mathbb{SE}(3)$, we define the kinematic-to-augmented mapping as:

$$\begin{aligned} \iota_{\alpha,i}:\ & \mathbb{R} \to \mathbb{R} \times \mathbb{SE}(3) \\ & s_i \mapsto (s_i, T_{rail,i}) \end{aligned} \tag{55}$$

To analyze the differential behavior of this first stage, we parameterize the native variation as $\delta s_i \in \mathbb{R}$ and the augmented variation as $\delta\mathbf{q}_i = [\delta s_i^T, \delta\mathbf{x}_{rail,i}^T]^T \in \mathbb{R}^7$, where $\delta\mathbf{x}_{rail,i} = [\delta\mathbf{p}_{0,i}^T, \delta\boldsymbol{\theta}_{rail,i}^T]^T$. Because the structural rail parameters $T_{rail,i}$ are strictly fixed during the purely active kinematic evolution of the agent, they do not vary with respect to the kinematic state s_i. Thus, the corresponding Jacobian $J_{\iota_{\alpha,i}} \in \mathbb{R}^{7\times1}$ is:

$$J_{\iota_{\alpha,i}} = \frac{\partial \iota_{\alpha,i}}{\partial s_i} = \begin{bmatrix} 1 \\ \mathbf{0}_{6\times1} \end{bmatrix} \tag{56}$$

GLOBAL KINEMATIC-TO-AUGMENTED MAPPING: To evaluate the network as a whole at this stage, we aggregate the individual agent mappings via Cartesian products, mapping the global kinematic product space $\mathbb{R}^3$ into the global augmented product space $(\mathbb{R}\times\mathbb{SE}(3))^3$ via $\iota_{\alpha,\mathbb{V}}$. Naturally preserving the individual local tangent-space parameterizations, the global Jacobian is constructed as a block-diagonal matrix:

$$J_{\iota_{\alpha,\mathbb{V}}} = \operatorname{blockdiag}\left(J_{\iota_{\alpha,1}}, J_{\iota_{\alpha,2}}, J_{\iota_{\alpha,3}}\right) \in \mathbb{R}^{21\times3} \tag{57}$$

Augmented-to-Embedded Map ($\iota_{\epsilon,i}$)

The second stage translates the fully defined augmented state into a global pose in $\mathbb{SE}(3)$. We first define the local motion embedding map, where the intrinsic state s_i acts as a pure translation along the local x-axis:

$$\begin{aligned} T_{local,i} :\ & \mathbb{R} \to \mathbb{SE}(3) \\ & s_i \mapsto (s_i \mathbf{e}_1, \mathbf{I}_3) \end{aligned} \tag{58}$$

The augmented-to-embedded function evaluates the full global pose by composing the structural rail frame with the local state embedding. Formally, it maps the entire augmented space P_i to $\mathbb{SE}(3)$:

$$\begin{aligned} \iota_{\epsilon,i} :\ & \mathbb{R} \times \mathbb{SE}(3) \to \mathbb{SE}(3) \\ & (s_i, T_{rail,i}) \mapsto T_{rail,i} \circ T_{local,i}(s_i) = \left(\mathbf{p}_{0,i} + s_i \mathbf{v}_i, R_{rail,i}\right) = (\mathbf{p}_i^e, \mathbf{R}_i^e) = \mathbf{x}_i^e \end{aligned} \tag{59}$$

where $\mathbf{v}_i = R_{rail,i}\mathbf{e}_1$. This map establishes the exact geometric correspondence between the coupled agent-rail parameters and the full spatial pose.

We evaluate the differential kinematics of this map. In $\mathbb{SE}(3)$, the spatial variation of the global embedded pose is represented by the twist $\delta\mathbf{x}_i^e = \left[(\delta\mathbf{p}_i^e)^T \quad (\delta\boldsymbol{\theta}_i^e)^T\right]^T \in \mathbb{R}^6$. By applying the total differential to the map $\iota_{\varepsilon,i}$ over the augmented space P_i, the global twist emerges as a linear combination of the active state variation $\delta s_i \in \mathbb{R}$ and the structural parameter variation $\delta\mathbf{x}_{rail,i} = \left[\delta\mathbf{p}_{0,i}^T \quad \delta\boldsymbol{\theta}_{rail,i}^T\right]^T \in \mathbb{R}^6$, grouped as $\delta\mathbf{q}_i = [\delta s_i, \delta\mathbf{x}_{rail,i}^T]^T$:

$$\delta\mathbf{x}_i^e = \frac{\partial \iota_{\varepsilon,i}}{\partial s_i}\delta s_i + \frac{\partial \iota_{\varepsilon,i}}{\partial \mathbf{x}_{rail,i}}\delta\mathbf{x}_{rail,i} \tag{60}$$

To compute the exact blocks of this total Jacobian, we evaluate the positional and rotational components independently:

- **Position Variation:** The global position is $\mathbf{p}_i^e = \mathbf{p}_{0,i} + s_i\mathbf{v}_i$. The rail direction vector $\mathbf{v}_i$ is intrinsically tied to the rail's orientation, specifically $\mathbf{v}_i = R_{rail,i}\mathbf{e}_1$. If the rail frame undergoes a structural right-trivialized rotation $\delta\boldsymbol{\theta}_{rail,i}$ defined in its local body frame, the direction vector varies as $\delta\mathbf{v}_i = \delta(R_{rail,i}\mathbf{e}_1) = R_{rail,i}[\delta\boldsymbol{\theta}_{rail,i}]_\times\mathbf{e}_1 = -R_{rail,i}[\mathbf{e}_1]_\times\delta\boldsymbol{\theta}_{rail,i}$. Therefore, the total differential of the position evaluates to:

$$\delta\mathbf{p}_i^e = \mathbf{v}_i\delta s_i + \delta\mathbf{p}_{0,i} - s_i R_{rail,i}[\mathbf{e}_1]_\times\delta\boldsymbol{\theta}_{rail,i} \tag{61}$$

- **Attitude Variation:** Because the local mapping assumes no internal rotation relative to the rail, the global attitude of the agent is strictly identical to the structural attitude of the rail. Hence, $\delta\boldsymbol{\theta}_i^e = \delta\boldsymbol{\theta}_{rail,i}$.

Assembling these differential relations, the total local embedding Jacobian $J_{\iota_{\epsilon,i}} \in \mathbb{R}^{6\times7}$ maps the full 7-dimensional augmented variation vector $[\delta s_i, \delta \mathbf{x}_{rail,i}^T]^T$ to the 6-dimensional spatial twist $\delta \mathbf{x}_i^e = \left[(\delta \mathbf{p}_i^e)^T \quad (\delta \boldsymbol{\theta}_i^e)^T\right]^T$:

$$J_{\iota_{\epsilon,i}} = \frac{\partial \iota_{\epsilon,i}}{\partial \mathbf{q}_i} = \left[\begin{array}{c|cc} \mathbf{v}_i & \mathbf{I}_3 & -s_i R_{rail,i}[\mathbf{e}_1]_\times \\ \mathbf{0}_{3\times1} & \mathbf{0}_{3\times3} & \mathbf{I}_3 \end{array}\right] \in \mathbb{R}^{6\times7} \tag{62}$$

GLOBAL AUGMENTED-TO-EMBEDDED MAPPING: To evaluate the network as a whole, we aggregate the individual agent mapping stages via Cartesian products, mapping the global augmented product space $(\mathbb{R} \times \mathbb{SE}(3))^3$ into the homogeneous global embedded space $\mathbb{SE}(3)^3$ via $\iota_{\epsilon,\mathbb{V}}$. Naturally preserving the individual local tangent-space parameterizations, the global Jacobian is constructed as a block-diagonal matrix:

$$J_{\iota_{\epsilon,\mathbb{V}}} = \text{blockdiag}\left(J_{\iota_{\epsilon,1}}, J_{\iota_{\epsilon,2}}, J_{\iota_{\epsilon,3}}\right) \in \mathbb{R}^{18\times21} \tag{63}$$

5.4.2 Measurement Retraction Maps

Embedded-to-Augmented Measurement Retraction ($\rho_{\mathbb{M},\epsilon}$)

The augmented measurement space is identical to the embedded homogeneous measurement space $\mathcal{Y} = \mathbb{R}^3_{>0}$ (comprising pure distance measurements for the network topology).

For each individual network edge k, the retraction map is trivially the identity map:

$$\begin{aligned} \rho^k_{\mathbb{M},\epsilon} : \mathbb{R}_{>0} &\to \mathbb{R}_{>0} \\ d_k &\mapsto d_k \end{aligned} \tag{64}$$

Parameterizing the local tangent variation as $\delta d_k \in \mathbb{R}$, the corresponding local Jacobian block is simply the scalar identity matrix 1.

GLOBAL EMBEDDED-TO-AUGMENTED MAPPING: To evaluate the network measurements as a whole at this stage, we aggregate the individual edge mappings via Cartesian products, mapping the global embedded measurement space into the global augmented measurement space via $\rho_{\mathbb{M},\epsilon} : \mathbb{R}^3_{>0} \to \mathbb{R}^3_{>0}$.

Parameterizing the global tangent variation as $\delta \mathbf{y}_{emb} \in \mathbb{R}^3$ via the concatenation of the local variations, and naturally preserving the individual local tangent-space parameterizations, the global Jacobian is constructed as a block-diagonal matrix of identities, yielding the global identity matrix:

$$J_{\rho_{\mathbb{M},\epsilon}} = \text{blockdiag}\left(1, 1, 1\right) = \mathbf{I}_3 \in \mathbb{R}^{3\times3} \tag{65}$$

Augmented-to-Kinematic Measurement Retraction ($\rho_{\alpha,\mathbb{M}}$)

The augmented-to-kinematic measurement retraction map isolates the true physical observation specific to each sensor type. Since the physical distance sensor measures the spatial separation directly between the agents without being altered by the structural rail parameters, the local retraction map preserves the observed value directly:

$$\begin{aligned} \rho^d_{\alpha,\mathbb{M}} : \mathbb{R}_{>0} &\to \mathbb{R}_{>0} \\ d_{ij} &\mapsto d_{ij} \end{aligned} \tag{66}$$

To analytically propagate this definition to the tangent space, let the local tangent variation be parameterized as $\delta d_{ij} \in \mathbb{R}$. Its corresponding local Jacobian block is trivially the scalar identity:

$$J_{\rho^d_{\alpha,\mathbb{M}}} = \frac{\partial \rho^d_{\alpha,\mathbb{M}}}{\partial d_{ij}} = 1 \in \mathbb{R}^{1\times 1} \tag{67}$$

GLOBAL AUGMENTED-TO-KINEMATIC MAPPING: To filter the measurements for the entire network simultaneously, we aggregate the individual local retraction maps into a single global measurement retraction map via $\rho_{\alpha,\mathbb{M}} : \mathbb{R}^3_{>0} \to \mathbb{R}^3_{>0}$.

Naturally preserving the individual local measurement tangent-space parameterizations defined previously, the global Jacobian is constructed as a block-diagonal matrix from the local extraction blocks:

$$J_{\rho_{\alpha,\mathbb{M}}} = \frac{\partial \rho_{\alpha,\mathbb{M}}}{\partial \mathbf{y}_{emb}} = \text{blockdiag}\left(1, 1, 1\right) = \mathbf{I}_3 \in \mathbb{R}^{3\times 3} \tag{68}$$

The resulting dimension correctly reflects the preservation of the 3-dimensional physical distance measurement space.

5.4.3 Rigidity Matrix

Embedded Rigidity Matrix (R^{emb})

The Embedded Rigidity Matrix captures the first-order differential constraints of the network strictly within the fully homogeneous extended spaces. It maps the 18-dimensional variations of the structurally embedded agents into the 3-dimensional variations of the abstract measurement space. It is fundamentally defined as the Jacobian of the embedded measurement function $h_{emb} : \mathbb{SE}(3)^3 \to (\mathbb{R}_{>0})^3$:

$$\delta \mathbf{z}^{emb}_{\mathbb{E}} = R^{emb}\, \delta \mathbf{x}^e_{\mathbb{V}}, \quad \text{where } \delta \mathbf{x}^e_{\mathbb{V}} \in \mathbb{R}^{18},\ \delta \mathbf{z}^{emb}_{\mathbb{E}} \in \mathbb{R}^3 \tag{69}$$

By locally identifying the abstract variations with coordinate vectors in Euclidean space, the input state variation vector $\delta \mathbf{x}^e_{\mathbb{V}}$ concatenates the complete $\mathbb{SE}(3)$ kinematic twists for all $n = 3$ agents (6 DOFs each). Since distance measurements inherently map to $\mathbb{R}_{>0}$, no dummy padding is required in the abstract measurement space, and the output vector $\delta\mathbf{z}_{\mathbb{E}}^{emb}$ simply stacks the $m = 3$ distance variations:

$$\delta\mathbf{x}_{\mathbb{V}}^{e} = \begin{bmatrix} \delta\mathbf{x}_1^e \\ \hline \delta\mathbf{x}_2^e \\ \hline \delta\mathbf{x}_3^e \end{bmatrix} = \begin{bmatrix} \delta\mathbf{p}_1^e \\ \delta\boldsymbol{\theta}_1^e \\ \hline \delta\mathbf{p}_2^e \\ \delta\boldsymbol{\theta}_2^e \\ \hline \delta\mathbf{p}_3^e \\ \delta\boldsymbol{\theta}_3^e \end{bmatrix}, \quad \delta\mathbf{z}_{\mathbb{E}}^{emb} = \begin{bmatrix} \delta\mathbf{z}_{12}^{emb} \\ \hline \delta\mathbf{z}_{23}^{emb} \\ \hline \delta\mathbf{z}_{31}^{emb} \end{bmatrix} = \begin{bmatrix} \delta d_{12} \\ \hline \delta d_{23} \\ \hline \delta d_{31} \end{bmatrix} \tag{70}$$

Using the sequence of categorical mappings established previously, we construct the purely homogeneous Embedded Rigidity Matrix $R^{emb} \in \mathbb{R}^{3\times 18}$ by directly applying the chain rule to the composed maps ($R^{emb} = J_{\eta_{emb}} J_{\Delta_{emb}} J_{\gamma_{emb}} J_{\sigma_{emb}}$). This explicit sparse formulation evaluates to:

$$R^{emb} = \left[\begin{array}{cc|cc|cc} -\mathbf{q}_{12}^T & \mathbf{0}_{1\times 3} & \mathbf{q}_{12}^T & \mathbf{0}_{1\times 3} & \mathbf{0}_{1\times 3} & \mathbf{0}_{1\times 3} \\ \hline \mathbf{0}_{1\times 3} & \mathbf{0}_{1\times 3} & -\mathbf{q}_{23}^T & \mathbf{0}_{1\times 3} & \mathbf{q}_{23}^T & \mathbf{0}_{1\times 3} \\ \hline \mathbf{q}_{31}^T & \mathbf{0}_{1\times 3} & \mathbf{0}_{1\times 3} & \mathbf{0}_{1\times 3} & -\mathbf{q}_{31}^T & \mathbf{0}_{1\times 3} \end{array}\right] \tag{71}$$

Augmented Rigidity Matrix (R^{aug})

The Augmented Rigidity Matrix R^{aug} is obtained by pulling the analysis back to the Augmented Space. This is achieved through both pre-multiplying by the Embedded-to-Augmented Measurement Retraction Jacobian $J_{\rho_{\mathbb{M},\epsilon}}$ and post-multiplying by the global Augmented-to-Embedded Jacobian $J_{\iota_{\epsilon,\mathbb{V}}}$:

$$R^{aug} = J_{\rho_{\epsilon,\mathbb{M}}} R^{emb} J_{\iota_{\epsilon,\mathbb{V}}} = R^{emb} J_{\iota_{\epsilon,\mathbb{V}}} \tag{72}$$

since $J_{\rho_{\epsilon,\mathbb{M}}} = \mathbf{I}_3$.

Because the measurement retraction is the identity, the output variation vector remains $\mathbb{R}^3$. However, the input vector expands to 21 dimensions, concatenating the 7 variables of each agent's augmented tangent manifold (the intrinsic 1D kinematic velocity δs_i, and the 6-DoF structural rail variation $\delta\mathbf{p}_{0,i}, \delta\boldsymbol{\theta}_{rail,i}$):

$$\delta\mathbf{z}_{\mathbb{E}}^{aug} = R^{aug}\,\delta\mathbf{q}_{\mathbb{V}}, \quad \text{where } \delta\mathbf{q}_{\mathbb{V}} = \begin{bmatrix} \delta\mathbf{q}_1 \\ \hline \delta\mathbf{q}_2 \\ \hline \delta\mathbf{q}_3 \end{bmatrix} = \begin{bmatrix} \delta s_1 \\ \delta\mathbf{p}_{0,1} \\ \delta\boldsymbol{\theta}_{rail,1} \\ \hline \delta s_2 \\ \delta\mathbf{p}_{0,2} \\ \delta\boldsymbol{\theta}_{rail,2} \\ \hline \delta s_3 \\ \delta\mathbf{p}_{0,3} \\ \delta\boldsymbol{\theta}_{rail,3} \end{bmatrix} \in \mathbb{R}^{21} \tag{73}$$

We obtain

$$R^{aug} = \left[\begin{array}{c|cc|c|cc|c|cc} -\mathbf{q}_{12}^T\mathbf{v}_1 & -\mathbf{q}_{12}^T & s_1\mathbf{q}_{12}^T R_{rail,1}[\mathbf{e}_1]_\times & +\mathbf{q}_{12}^T\mathbf{v}_2 & +\mathbf{q}_{12}^T & -s_2\mathbf{q}_{12}^T R_{rail,2}[\mathbf{e}_1]_\times & 0 & \mathbf{0}_{1\times3} & \mathbf{0}_{1\times3} \\ \hline 0 & \mathbf{0}_{1\times3} & \mathbf{0}_{1\times3} & -\mathbf{q}_{23}^T\mathbf{v}_2 & -\mathbf{q}_{23}^T & s_2\mathbf{q}_{23}^T R_{rail,2}[\mathbf{e}_1]_\times & +\mathbf{q}_{23}^T\mathbf{v}_3 & +\mathbf{q}_{23}^T & -s_3\mathbf{q}_{23}^T R_{rail,3}[\mathbf{e}_1]_\times \\ \hline +\mathbf{q}_{31}^T\mathbf{v}_1 & +\mathbf{q}_{31}^T & -s_1\mathbf{q}_{31}^T R_{rail,1}[\mathbf{e}_1]_\times & 0 & \mathbf{0}_{1\times3} & \mathbf{0}_{1\times3} & -\mathbf{q}_{31}^T\mathbf{v}_3 & -\mathbf{q}_{31}^T & s_3\mathbf{q}_{31}^T R_{rail,3}[\mathbf{e}_1]_\times \end{array}\right] \tag{74}$$

Kinematic Rigidity Matrix (R^{kin})

Formally, we right-multiply by the Kinematic-to-Augmented Jacobian $J_{\iota_{\alpha,\mathbb{V}}}$ to discard the structural rail parameter variations, mapping the input domain strictly down to the minimal 3-dimensional native kinematic space. Simultaneously, we left-multiply by the Augmented-to-Kinematic Retraction Jacobian$J_{\rho_{\alpha,\mathbb{M}}} = \mathbf{I}_3$:

$$\begin{aligned} R^{kin} &= J_{\rho_{\alpha,\mathbb{M}}} R^{aug} J_{\iota_{\alpha,\mathbb{V}}} = R^{aug} J_{\iota_{\alpha,\mathbb{V}}} \\ &= J_{\rho_{\alpha,\mathbb{M}}} J_{\rho_{\epsilon,\mathbb{M}}} R^{emb} J_{\iota_{\epsilon,\mathbb{V}}} J_{\iota_{\alpha,\mathbb{V}}} \end{aligned} \tag{75}$$

By enforcing this double reduction, the coordinate parameterizations exactly match the physical tangent spaces of the minimal kinematic manifolds and the true sensor spaces.

The resulting mapping restricts the input vector $\delta\mathbf{s}$ solely to the true 1D actuatable coordinate velocities for each agent ($\delta\mathbf{s} = [\delta s_1, \delta s_2, \delta s_3]^T \in \mathbb{R}^3$):

$$\delta\mathbf{z}_{\mathbb{E}} = R^{kin}\,\delta\mathbf{s}, \quad \text{where } \delta\mathbf{s} \in \mathbb{R}^3,\ \delta\mathbf{z}_{\mathbb{E}} \in \mathbb{R}^3 \tag{76}$$

On the columns, the right-multiplication gracefully deletes the entire 6-column environmental parametric block of every agent, isolating the pure active scalar kinematic entries. The sparse 3×21 matrix is thereby elegantly compressed into its minimal 3×3 physical dimensionality:

$$R^{kin} = \left[\begin{array}{c|c|c} -\mathbf{q}_{12}^T\mathbf{v}_1 & \mathbf{q}_{12}^T\mathbf{v}_2 & 0 \\ \hline 0 & -\mathbf{q}_{23}^T\mathbf{v}_2 & \mathbf{q}_{23}^T\mathbf{v}_3 \\ \hline \mathbf{q}_{31}^T\mathbf{v}_1 & 0 & -\mathbf{q}_{31}^T\mathbf{v}_3 \end{array}\right] \tag{77}$$

5.4.4 Kernel Rigidity Matrix and Infinitesimal Rigidity Analysis

$$\det(R) = \det \left[\begin{array}{c|c|c} -\mathbf{q}_{12}^T\mathbf{v}_1 & \mathbf{q}_{12}^T\mathbf{v}_2 & 0 \\ \hline 0 & -\mathbf{q}_{23}^T\mathbf{v}_2 & \mathbf{q}_{23}^T\mathbf{v}_3 \\ \hline \mathbf{q}_{31}^T\mathbf{v}_1 & 0 & -\mathbf{q}_{31}^T\mathbf{v}_3 \end{array} \right]$$
$$= (-\mathbf{q}_{12}^T\mathbf{v}_1)(-\mathbf{q}_{23}^T\mathbf{v}_2)(-\mathbf{q}_{31}^T\mathbf{v}_3) + (\mathbf{q}_{12}^T\mathbf{v}_2)(\mathbf{q}_{23}^T\mathbf{v}_3)(\mathbf{q}_{31}^T\mathbf{v}_1) \tag{78}$$

Depending on the structural alignment of the underlying infrastructure, the formation exhibits different rigidity properties. We categorize the topology of the rails into the following three cases:

- **Globally Parallel Infrastructure** ($\mathbf{v}_1 = \mathbf{v}_2 = \mathbf{v}_3 = \mathbf{v}$): The highly symmetric baseline scenario where all infrastructural constraints share a common spatial orientation.
- **Singular Deviation** ($\mathbf{v}_1 \neq \mathbf{v}_2 = \mathbf{v}_3 = \mathbf{v}$): A case in which exactly two rails are parallel while the third one possesses a distinct spatial orientation. Since the underlying interaction topology is a fully symmetric triangular graph, any arrangement of this type differs from the others merely by a permutation of the node indices, which mathematically corresponds to an automorphism of the graph. Because these permutations yield completely isomorphic systems with identical rigidity properties, we can arbitrarily assign the unique, non-parallel constraint to the first agent without any loss of generality.
- **General Spatial Configuration** ($\mathbf{v}_i \neq \mathbf{v}_j \quad \forall i \neq j$): The fully asymmetric scenario where the directional vectors of the rails are pairwise linearly independent.

In the subsequent analysis, we strictly impose the following geometric assumptions to prevent trivial structural degeneracies:

Assumption 5.1. **Non-Collinear Assumption (Non-Degenerate Framework):** The three agents do not lie on a single one-dimensional line in space. Consequently, any pair of adjacent edge vectors (e.g., $\mathbf{q}_{ij}$ and $\mathbf{q}_{jk}$) are strictly linearly independent. This guarantees that the triangular framework spans a valid 2D internal plane, preventing trivial folding flexes and kinematic blind spots.

Before starting with the kernel analysis of the rigidity matrix, we establish a highly powerful geometric property inherent to the triangular framework, which will be utilized extensively throughout the subsequent proofs.

Property 5.1 (Triangle Loop Closure). For any closed triangular framework defined by three agents located at distinct spatial coordinates $\mathbf{p}_1, \mathbf{p}_2, \mathbf{p}_3 \in \mathbb{R}^3$, the sum of the relative position p_{ij} vectors along the cyclic directed graph is identically zero.

$$p_{12} + p_{23} + p_{31} = 0 \tag{79}$$

Expressed in terms of the unit directional edge vectors $\mathbf{q}_{ij} = \frac{\mathbf{p}_j - \mathbf{p}_i}{\|\mathbf{p}_j - \mathbf{p}_i\|}$ and their corresponding scalar edge lengths $\|\mathbf{p}_{ij}\|$, the closure constraint is given by:

$$\|\mathbf{p}_{12}\|\mathbf{q}_{12} + \|\mathbf{p}_{23}\|\mathbf{q}_{23} + \|\mathbf{p}_{31}\|\mathbf{q}_{31} = \mathbf{0} \tag{80}$$

Proof. Let $\mathbf{p}_{ij} = \mathbf{p}_j - \mathbf{p}_i$ denote the relative position vector directed from source agent i to target agent j. We evaluate the cyclic sum of the relative position vectors along the closed perimeter of the triangle:

$$S = \mathbf{p}_{12} + \mathbf{p}_{23} + \mathbf{p}_{31} \tag{81}$$

Expanding each relative vector into the absolute spatial coordinates of the agents yields a telescoping sum:

$$\begin{aligned} S &= (\mathbf{p}_2 - \mathbf{p}_1) + (\mathbf{p}_3 - \mathbf{p}_2) + (\mathbf{p}_1 - \mathbf{p}_3) \\ &= (\mathbf{p}_2 - \mathbf{p}_2) + (\mathbf{p}_3 - \mathbf{p}_3) + (\mathbf{p}_1 - \mathbf{p}_1) \\ &= \mathbf{0} \end{aligned} \tag{82}$$

By the definition of the Euclidean norm, any non-zero relative position vector can be uniquely decomposed into its scalar length and its unit directional vector: $\mathbf{p}_{ij} = \|\mathbf{p}_{ij}\|\mathbf{q}_{ij}$. Substituting this decomposition into the zero-sum identity produces the desired geometric relation:

$$\|\mathbf{p}_{12}\|\mathbf{q}_{12} + \|\mathbf{p}_{23}\|\mathbf{q}_{23} + \|\mathbf{p}_{31}\|\mathbf{q}_{31} = \mathbf{0} \tag{83}$$

This strictly dictates that the scaled directional vectors of any physically realizable closed triangular framework are linearly dependent, structurally interlocking the spatial geometry of the network. □

For this work, we analyze only the case $\mathbf{v}_1 = \mathbf{v}_2 = \mathbf{v}_3 = \mathbf{v}$. Other case will be addressed in future work.

5.4.5 Globally Parallel Infrastructure ($\mathbf{v}_1 = \mathbf{v}_2 = \mathbf{v}_3 = \mathbf{v}$)

Assuming a globally parallel rail infrastructure where all agent constraints share the same directional vector ($\mathbf{v}_1 = \mathbf{v}_2 = \mathbf{v}_3 = \mathbf{v}$), we can definitively analyze the structural integrity of the formation.

By invoking the Triangle Loop Closure (Property 5.1), we can project the cyclic sum of the framework's edges directly onto the common rail vector $\mathbf{v}$:

$$\|\mathbf{p}_{12}\|(\mathbf{q}_{12}^T\mathbf{v}) + \|\mathbf{p}_{23}\|(\mathbf{q}_{23}^T\mathbf{v}) + \|\mathbf{p}_{31}\|(\mathbf{q}_{31}^T\mathbf{v}) = 0 \tag{84}$$

From this linear dependence, it is immediately evident that if any two edges of the triangle are orthogonal to the rail vector (e.g., $\mathbf{q}_{12}^T\mathbf{v} = 0$ and $\mathbf{q}_{23}^T\mathbf{v} = 0$), the projection of the third edge must also identically vanish since its scalar length is strictly positive ($\|\mathbf{p}_{31}\|(\mathbf{q}_{31}^T\mathbf{v}) = 0 \implies \mathbf{q}_{31}^T\mathbf{v} = 0$).

Geometrically, if two spanning edges of a non-degenerate triangle are orthogonal to a common vector $\mathbf{v}$, the entire internal plane containing the framework is orthogonal to $\mathbf{v}$, strictly mandating the orthogonality of the third edge.

The rigidity matrix for this globally parallel thus becomes:

$$R = \left[\begin{array}{c|c|c} -\mathbf{q}_{12}^T\mathbf{v} & \mathbf{q}_{12}^T\mathbf{v} & 0 \\ \hline 0 & -\mathbf{q}_{23}^T\mathbf{v} & \mathbf{q}_{23}^T\mathbf{v} \\ \hline \mathbf{q}_{31}^T\mathbf{v} & 0 & -\mathbf{q}_{31}^T\mathbf{v} \end{array}\right] \tag{85}$$

By expanding this homogeneous 3×3 system, its determinant is computed directly as:

$$\begin{aligned} \det(R) &= \det\left[\begin{array}{c|c|c} -\mathbf{q}_{12}^T\mathbf{v} & \mathbf{q}_{12}^T\mathbf{v} & 0 \\ \hline 0 & -\mathbf{q}_{23}^T\mathbf{v} & \mathbf{q}_{23}^T\mathbf{v} \\ \hline \mathbf{q}_{31}^T\mathbf{v} & 0 & -\mathbf{q}_{31}^T\mathbf{v} \end{array}\right] \\ &= (-\mathbf{q}_{12}^T\mathbf{v})(-\mathbf{q}_{23}^T\mathbf{v})(-\mathbf{q}_{31}^T\mathbf{v}) + (\mathbf{q}_{12}^T\mathbf{v})(\mathbf{q}_{23}^T\mathbf{v})(\mathbf{q}_{31}^T\mathbf{v}) \\ &= -(\mathbf{q}_{12}^T\mathbf{v})(\mathbf{q}_{23}^T\mathbf{v})(\mathbf{q}_{31}^T\mathbf{v}) + (\mathbf{q}_{12}^T\mathbf{v})(\mathbf{q}_{23}^T\mathbf{v})(\mathbf{q}_{31}^T\mathbf{v}) \\ &= 0 \end{aligned} \tag{86}$$

Because the determinant evaluates identically to zero independent of the specific agent coordinates, the rigidity matrix is structurally rank-deficient ($\operatorname{rank}(R) \le 2$). The system always admits at least a one-dimensional null space. Consequently, the triangular framework is never infinitesimally anchored when constrained to globally parallel rails.

To explicitly characterize the unobservable velocities, the homogeneous system governing the infinitesimal kinematics $R\delta\mathbf{s} = \mathbf{0}$ simplifies to:

$$\begin{cases} \mathbf{q}_{12}^T\mathbf{v}(\delta s_2 - \delta s_1) = 0 \\ \mathbf{q}_{23}^T\mathbf{v}(\delta s_3 - \delta s_2) = 0 \\ \mathbf{q}_{31}^T\mathbf{v}(\delta s_1 - \delta s_3) = 0 \end{cases} \tag{87}$$

Based on the geometric projection of the framework onto the infrastructure, we distinguish two mutually exclusive kinematic cases: the totally degenerate orthogonal case and the nominal case .

Total Degeneracy (Three Orthogonal Edges)

If $\mathbf{q}_{12}^T\mathbf{v} = \mathbf{q}_{23}^T\mathbf{v} = \mathbf{q}_{31}^T\mathbf{v} = 0$, the entire formation plane is completely orthogonal to the rail vector $\mathbf{v}$. In this specific geometric layout, every coefficient in the system (87) vanishes identically.

As a result, the relative velocity constraints between the agents vanish, reducing the system to $0 \cdot (\delta s_i - \delta s_j) = 0$. Each agent i can adopt any independent scalar speed $\delta s_i \in \mathbb{R}$ without violating the first-order distance measurements. Because all three agents can move freely along their parallel rails, the kernel spans the entire 3D parameter space:

$$\mathcal{N}(R) = \mathbb{R}^3 \tag{88}$$

To rigorously classify this total degeneracy case, we must demonstrate that every kinematically permissible velocity field along the orthogonal rails acts purely as a rigid-body spatial transformation.

Lemma 5.2. *Assume the network configuration is strictly collision-free (guaranteed by the distinct rails assumption) and non-collinear (a structural condition that inherently depends on the spatial placement of the rails). In the orthogonal degenerate case, where the structural plane of the framework is strictly orthogonal to the rail infrastructure, the only possible infinitesimal motions of the constrained formation are rigid-body motions.*

Proof. By hypothesis, the rail directional vector $\mathbf{v}$ is orthogonal to all edge vectors of the triangular formation. Since the framework is non-collinear (Assumption 5.1), any two edges (e.g., $\mathbf{p}_{12} = \mathbf{p}_2 - \mathbf{p}_1$ and $\mathbf{p}_{23} = \mathbf{p}_3 - \mathbf{p}_2$) are linearly independent and uniquely define the internal formation plane, establishing $\mathbf{v}$ as its exact surface normal. Consequently, for any pair of agents, the relative position vector satisfies $(\mathbf{p}_j - \mathbf{p}_i)^T \mathbf{v} = 0$.

An arbitrary unobservable velocity field $\delta \mathbf{s} = [\delta s_1, \delta s_2, \delta s_3]^T \in \mathcal{N}(R)$ maps the infinitesimal agent displacements strictly along the rails: $\delta \mathbf{p}_i = \delta s_i \mathbf{v}$ for $i \in \{1, 2, 3\}$.

We must demonstrate that there exists a unique rigid-body twist $(\mathbf{t}, \boldsymbol{\omega}) \in \mathfrak{se}(3)$ that synthesizes this velocity field via the fundamental kinematic relation:

$$\mathbf{t} + \boldsymbol{\omega} \times \mathbf{p}_i = \delta s_i \mathbf{v} \quad \forall i \in \{1, 2, 3\} \tag{89}$$

Evaluating the velocity difference between any two connected agents yields the structural compatibility condition for the global angular velocity vector $\boldsymbol{\omega}$:

$$\boldsymbol{\omega} \times (\mathbf{p}_j - \mathbf{p}_i) = (\delta s_j - \delta s_i) \mathbf{v} \tag{90}$$

Because the cross product $\boldsymbol{\omega} \times (\mathbf{p}_j - \mathbf{p}_i)$ must generate a vector strictly parallel to the normal vector $\mathbf{v}$, the global angular velocity $\boldsymbol{\omega}$ is algebraically restricted to lie entirely within the internal plane of the formation, this means that $\boldsymbol{\omega}^T \mathbf{v} = 0$. Thus, we can therefore parameterize $\boldsymbol{\omega}$ explicitly as a linear combination of the two non-collinear basis edges:

$$\boldsymbol{\omega} = \alpha \mathbf{p}_{12} + \beta \mathbf{p}_{23} \tag{91}$$

Substituting this parameterization into the compatibility condition (90) for the first edge $\mathbf{p}_{12}$ yields:

$$(\alpha\mathbf{p}_{12} + \beta\mathbf{p}_{23}) \times \mathbf{p}_{12} = \beta(\mathbf{p}_{23} \times \mathbf{p}_{12}) = (\delta s_2 - \delta s_1)\mathbf{v} \tag{92}$$

To rigorously isolate the scalar coefficient β, we project both sides onto the cross-product vector $(\mathbf{p}_{23} \times \mathbf{p}_{12})$:

$$\beta\|\mathbf{p}_{23} \times \mathbf{p}_{12}\|^2 = (\delta s_2 - \delta s_1)(\mathbf{p}_{23} \times \mathbf{p}_{12})^T\mathbf{v} \tag{93}$$

$$\beta = \frac{(\delta s_2 - \delta s_1)(\mathbf{p}_{23} \times \mathbf{p}_{12})^T\mathbf{v}}{\|\mathbf{p}_{23} \times \mathbf{p}_{12}\|^2} \tag{94}$$

Applying the exact same procedure for the second spanning edge $\mathbf{p}_{23}$ yields:

$$(\alpha\mathbf{p}_{12} + \beta\mathbf{p}_{23}) \times \mathbf{p}_{23} = \alpha(\mathbf{p}_{12} \times \mathbf{p}_{23}) = (\delta s_3 - \delta s_2)\mathbf{v} \tag{95}$$

Projecting onto $(\mathbf{p}_{12} \times \mathbf{p}_{23})$ explicitly solves for α:

$$\alpha = \frac{(\delta s_3 - \delta s_2)(\mathbf{p}_{12} \times \mathbf{p}_{23})^T\mathbf{v}}{\|\mathbf{p}_{12} \times \mathbf{p}_{23}\|^2} \tag{96}$$

The denominator $\|\mathbf{p}_{12}\times\mathbf{p}_{23}\|^2$ is strictly non-zero because the agents are non-collinear, guaranteeing the existence of a unique, exact analytical solution for the planar angular velocity:

$$\boldsymbol{\omega} = \left[\frac{(\delta s_3 - \delta s_2)(\mathbf{p}_{12} \times \mathbf{p}_{23})^T\mathbf{v}}{\|\mathbf{p}_{12} \times \mathbf{p}_{23}\|^2}\right]\mathbf{p}_{12} + \left[\frac{(\delta s_2 - \delta s_1)(\mathbf{p}_{23} \times \mathbf{p}_{12})^T\mathbf{v}}{\|\mathbf{p}_{23} \times \mathbf{p}_{12}\|^2}\right]\mathbf{p}_{23} \tag{97}$$

With $\boldsymbol{\omega}$ uniquely determined, we define the uniform global translation vector $\mathbf{t}$ by anchoring the rigid-body parameterization to a reference agent, specifically Agent 1:

$$\mathbf{t} = \delta s_1\mathbf{v} - \boldsymbol{\omega} \times \mathbf{p}_1 \tag{98}$$

Having uniquely constructed the spatial twist pair $(\mathbf{t}, \boldsymbol{\omega})$ strictly from the algebraic structure of the relative velocities, we must formally confirm that evaluating this global parameterization successfully reconstructs the absolute rail velocities for all three agents.

We consider the general rigid-body kinematic equation:

$$\delta\mathbf{p}_i = \begin{bmatrix}\mathbf{I}_3 & -[\mathbf{p}_i]_\times\end{bmatrix}\begin{bmatrix}\mathbf{t} \\ \boldsymbol{\omega}\end{bmatrix} = \mathbf{t} + \boldsymbol{\omega} \times \mathbf{p}_i \tag{99}$$

- **Agent 1:**
Substituting our explicitly constructed $\mathbf{t}$ into (99):

$$\begin{aligned}\delta\mathbf{p}_1 &= \mathbf{t} + \boldsymbol{\omega} \times \mathbf{p}_1 \\ &= (\delta s_1 \mathbf{v} - \boldsymbol{\omega} \times \mathbf{p}_1) + \boldsymbol{\omega} \times \mathbf{p}_1 \\ &= \delta s_1 \mathbf{v}\end{aligned} \tag{100}$$

- **Agent 2:**
Applying the exact same global twist to Agent 2:

$$\begin{aligned}\delta\mathbf{p}_2 &= \mathbf{t} + \boldsymbol{\omega} \times \mathbf{p}_2 \\ &= (\delta s_1 \mathbf{v} - \boldsymbol{\omega} \times \mathbf{p}_1) + \boldsymbol{\omega} \times \mathbf{p}_2 \\ &= \delta s_1 \mathbf{v} + \boldsymbol{\omega} \times (\mathbf{p}_2 - \mathbf{p}_1) \\ &= \delta s_1 \mathbf{v} + \boldsymbol{\omega} \times \mathbf{p}_{12}\end{aligned} \tag{101}$$

By substituting the structural compatibility condition derived in (90), we know $\boldsymbol{\omega} \times \mathbf{p}_{12} = (\delta s_2 - \delta s_1)\mathbf{v}$. Therefore:

$$\begin{aligned}\delta\mathbf{p}_2 &= \delta s_1 \mathbf{v} + (\delta s_2 - \delta s_1)\mathbf{v} \\ &= \delta s_2 \mathbf{v}\end{aligned} \tag{102}$$

- **Agent 3:**
Applying the global twist to Agent 3:

$$\begin{aligned}\delta\mathbf{p}_3 &= \mathbf{t} + \boldsymbol{\omega} \times \mathbf{p}_3 \\ &= (\delta s_1 \mathbf{v} - \boldsymbol{\omega} \times \mathbf{p}_1) + \boldsymbol{\omega} \times \mathbf{p}_3 \\ &= \delta s_1 \mathbf{v} + \boldsymbol{\omega} \times (\mathbf{p}_3 - \mathbf{p}_1)\end{aligned} \tag{103}$$

By vector addition, the relative position $\mathbf{p}_{13}$ can be expanded using the Triangle Loop Closure $\mathbf{p}_{13} = -\mathbf{p}_{31} = \mathbf{p}_{12} + \mathbf{p}_{23}$. Distributing the cross product yields:

$$\begin{aligned}\delta\mathbf{p}_3 &= \delta s_1 \mathbf{v} + \boldsymbol{\omega} \times (\mathbf{p}_{12} + \mathbf{p}_{23}) \\ &= \delta s_1 \mathbf{v} + (\boldsymbol{\omega} \times \mathbf{p}_{12}) + (\boldsymbol{\omega} \times \mathbf{p}_{23})\end{aligned} \tag{104}$$

Substituting the compatibility conditions (90) for both edges:

$$\begin{aligned}\delta\mathbf{p}_3 &= \delta s_1 \mathbf{v} + (\delta s_2 - \delta s_1)\mathbf{v} + (\delta s_3 - \delta s_2)\mathbf{v} \\ &= \delta s_3 \mathbf{v}\end{aligned} \tag{105}$$

Having successfully verified each node, we have proven that substituting our directly derived kinematic variables $\boldsymbol{\omega}$ and $\mathbf{t}$ perfectly reconstructs the respective rail velocities.

Because the unobservable velocity space is perfectly and bijectively synthesized by this exact global rigid-body transformation, all unobservable motions are rigid-body motions. □

Proposition 5.3. *Let $D_{kin} \subset \mathbb{R}^3$ be the purely kinematic state space of the network. We explicitly restrict D_{kin} to the open domain of valid configurations that are strictly collision-free (guaranteed by the distinct rails assumption) and non-collinear (a structural condition that inherently depends on the spatial placement of the rails). The state vector of the agents is $\mathbf{s} = [s_1, s_2, s_3]^T \in D_{kin}$, representing the displacements along their respective rails, with nominal 3D positions $\mathbf{p}_i = \mathbf{p}_{0,i} + s_i\mathbf{v}$.*

We define the symmetry group as $G = \mathbb{R}^3$. A generic element $g \in G$ is parameterized by the virtual velocity coefficients along the rails, $g = (u_1, u_2, u_3)$.

Following the exact analytical rigid-body synthesis derived in the previous Lemma, we explicitly define the corresponding out-of-plane rotational coefficients α and β:

$$\alpha = \frac{(u_3 - u_2)(\mathbf{p}_{12} \times \mathbf{p}_{23})^T\mathbf{v}}{\|\mathbf{p}_{12} \times \mathbf{p}_{23}\|^2} \tag{106}$$

$$\beta = \frac{(u_2 - u_1)(\mathbf{p}_{23} \times \mathbf{p}_{12})^T\mathbf{v}}{\|\mathbf{p}_{23} \times \mathbf{p}_{12}\|^2} \tag{107}$$

These dictate the global angular velocity vector $\boldsymbol{\omega}$ and the global translation vector $\mathbf{t}$ anchored at $\mathbf{p}_1$:

$$\boldsymbol{\omega} = \alpha\mathbf{p}_{12} + \beta\mathbf{p}_{23} \tag{108}$$

$$\mathbf{t} = u_1\mathbf{v} - \boldsymbol{\omega} \times \mathbf{p}_1 \tag{109}$$

The smooth group action $\Phi : G \times D_{kin} \to D_{kin}$ mapping the global state is defined by applying this synthesized rigid-body twist to the agents' spatial positions and projecting the displacement algebraically onto the common rail vector $\mathbf{v}$:

$$\begin{aligned}\Phi(g, \mathbf{s})_i &= s_i + \mathbf{v}^T\Big(\mathbf{t} + \boldsymbol{\omega} \times \mathbf{p}_i\Big) \\ &= s_i + u_1 + \mathbf{v}^T\Big(\boldsymbol{\omega} \times (\mathbf{p}_i - \mathbf{p}_1)\Big)\end{aligned} \tag{110}$$

The smooth framework family over the orthogonal degenerate domain D_{kin} is infinitesimally Φ-rigid.

Proof. We first verify that the framework family is measurement Φ-invariant. The group action $\Phi(g, \mathbf{s})$ effectively applies a spatial translation $\mathbf{t}$ and a rigid-body rotation $\boldsymbol{\omega}$ to the entire formation. By the fundamental definition of rigid-body kinematics, such transformations strictly preserve all relative Euclidean distances between the agents.

Recalling the result established in the previous Lemma, any arbitrary unobservable velocity field $\delta\mathbf{s} \in \ker \mathbf{R}(\mathbf{s})$ is uniquely and bijectively parameterized by exactly one pure translation along the rails and two rotational degrees of freedom (corresponding to the out-of-plane rotations parameterized by α and β). Thus, the dimension of the null space of the rigidity matrix is exactly:

$$\dim \ker \mathbf{R}(\mathbf{s}) = 1 + 2 = 3. \tag{111}$$

Furthermore, the group action $G = \mathbb{R}^3$ exclusively generates continuous rigid-body motions parameterized by 3 degrees of freedom. Because the three agents form a strictly non-collinear configuration, no non-trivial infinitesimal rigid-body motion can leave all three spatial positions simultaneously fixed. This guarantees that the local isotropy subgroup is trivial (meaning the group action is strictly free). Consequently, the differential mapping is fully injective, and the dimension of the trivial motion space matches the dimension of the symmetry group:

$$\dim \left(\mathrm{Im}(d\Phi_{\mathbf{s}}|_e)\right) = \dim(G) = 3. \tag{112}$$

Because the framework is measurement Φ-invariant and

$$\dim \ker \mathbf{R}(\mathbf{s}) = \dim \mathrm{Im}(d\Phi_{\mathbf{s}}|_e) = 3$$

, the dimensional equality condition is strictly satisfied. This confirms that the framework at $\mathbf{s}$ is infinitesimally Φ-rigid. Finally, since the state $\mathbf{s}$ was chosen arbitrarily from the considered domain D_{kin}, we conclude that the entire smooth framework family over this domain is infinitesimally Φ-rigid. $\square$

Nominal (At Most One Orthogonal Edge)

Based on the Triangle Loop Closure derived at the beginning of this section, a non-degenerate triangle cannot possess exactly two edges orthogonal to a common vector(if two entry are zero also the third one must be zero). Consequently, if the system is not totally degenerate (i.e., not all three edges are orthogonal), it must possess either exactly zero or exactly one orthogonal edge.

In both of these nominal scenarios, at least two inner products in (87) are strictly non-zero (e.g., $\mathbf{q}_{12}^T\mathbf{v} \neq 0$ and $\mathbf{q}_{23}^T\mathbf{v} \neq 0$). These non-zero coefficients algebraically force the relative velocity differences to vanish in order to satisfy the homogeneous system. (e.g. if $\mathbf{q}_{12}^T\mathbf{v} \neq 0$ and $\mathbf{q}_{23}^T\mathbf{v} \neq 0$ then $\delta s_1 - \delta s_2 = 0 \implies \delta s_1 = \delta s_2$, and $\delta s_2 - \delta s_3 = 0 \implies \delta s_2 = \delta s_3$, obtaining $\delta s_1 = \delta s_2 = \delta s_3$).

Whether the third edge is orthogonal or not, this chain of equalities strictly dictates that all agents must move synchronously at the exact same speed. The null space thus collapses entirely to a 1-dimensional uniform translation:

$$\mathcal{N}(R) = \text{span}\{\mathbf{1}_3\} \tag{113}$$

Lemma 5.4. *Assume the network configuration is strictly collision-free (guaranteed by the distinct rails assumption) and non-collinear (a structural condition that inherently depends on the spatial placement of the rails). In any nominal non-degenerate case (≤ 1 orthogonal edge), the only possible infinitesimal motions of the rail-constrained framework along the unobservable manifold are rigid-body motions.*

Proof. Any velocity vector residing in the nominal unobservable space takes the form $\delta\mathbf{s} = [\alpha, \alpha, \alpha]^T$, where $\alpha \in \mathbb{R}$ is a uniform scalar velocity. The corresponding 3D spatial velocity for each agent maps this scalar magnitude uniformly along the common infrastructure vector $\mathbf{v}$, yielding $\delta\mathbf{p}_i = \alpha\mathbf{v}$ for $i \in \{1, 2, 3\}$.

To prove that these allowable velocities correspond exclusively to rigid-body motions, we synthesize a trivial global rigid-body twist $(\mathbf{t}, \boldsymbol{\omega}) \in \mathfrak{se}(3)$ by defining a uniform spatial translation strictly along the rails and enforcing zero global rotation:

$$\mathbf{t} = \alpha\mathbf{v}, \tag{114}$$
$$\boldsymbol{\omega} = \mathbf{0}. \tag{115}$$

We now formally verify that this global parameterization successfully reconstructs the absolute spatial velocities for all three agents using the general rigid-body kinematic equation:

$$\delta\mathbf{p}_i = \begin{bmatrix} \mathbf{I}_3 & -[\mathbf{p}_i]_\times \end{bmatrix} \begin{bmatrix} \mathbf{t} \\ \boldsymbol{\omega} \end{bmatrix} = \mathbf{t} + \boldsymbol{\omega} \times \mathbf{p}_i. \tag{116}$$

For every agent $i \in \{1, 2, 3\}$, substituting our explicit twist parameters into the kinematic equation yields:

$$\begin{aligned} \delta\mathbf{p}_i &= \alpha\mathbf{v} + \mathbf{0} \times \mathbf{p}_i \\ &= \alpha\mathbf{v} \\ &= \delta s_i \mathbf{v}. \end{aligned} \tag{117}$$

This confirms that the synthesized kinematic variables $\boldsymbol{\omega}$ and $\mathbf{t}$ perfectly reconstruct the respective rail velocities for all nodes.

Because the 1-dimensional unobservable velocity space is perfectly and bijectively parameterized by this exact global rigid-body translation, no unassigned velocity components remain to induce internal framework deformations. This definitively establishes that any valid infinitesimal motion along the unobservable manifold is necessarily a pure rigid-body motion. □

Proposition 5.5. *Let $D_{kin} \subset \mathbb{R}^3$ be the purely kinematic state space of the network. We explicitly restrict D_{kin} to the open domain of valid configurations that are strictly collision-free (guaranteed by the distinct rails assumption) and non-collinear (a structural condition that inherently depends on the spatial placement of the rails). The state vector of the agents is $\mathbf{s} = [s_1, s_2, s_3]^T \in D_{kin}$ along their respective rails.*

We define the symmetry group as $G = \mathbb{R}$. A generic element $g \in G$ is parameterized as $g = t$, where $t \in \mathbb{R}$ represents the uniform global translation component along the infrastructure.

The smooth group action $\Phi : G \times D_{kin} \to D_{kin}$ mapping the global state is defined purely by the rigid-body translation:

$$\Phi(g, \mathbf{s})_i = s_i + t \tag{118}$$

which can be expressed in vector form as $\Phi(g, \mathbf{s}) = \mathbf{s} + t\mathbf{1}_3$.

The smooth framework family over the nominal domain D_{kin} is infinitesimally Φ-rigid.

Proof. We first verify that the framework family is measurement Φ-invariant. The group action $\Phi(t, \mathbf{s})$ applies a uniform spatial translation t to the entire formation. By the fundamental definition of rigid-body kinematics, such pure translations strictly preserve all relative Euclidean distances between the agents.

Recalling the algebraic result established for the nominal case, the presence of at least two non-orthogonal edges mathematically forces the relative velocity differences to vanish (i.e., $\delta s_1 = \delta s_2 = \delta s_3$). Consequently, any arbitrary unobservable velocity field $\delta\mathbf{s} \in \ker \mathbf{R}(\mathbf{s})$ is uniquely restricted to exactly one pure uniform translation along the rails, i.e., $\ker \mathbf{R}(\mathbf{s}) = \mathrm{span}(\mathbf{1}_3)$. Thus, the dimension of the null space of the rigidity matrix is exactly:

$$\dim \ker \mathbf{R}(\mathbf{s}) = 1. \tag{119}$$

Furthermore, the symmetry group $G = \mathbb{R}$ exclusively generates continuous 1-dimensional rigid-body translations. The differential map $d\Phi_{\mathbf{s}}|_e : \mathbb{R} \to D_{kin}$ associates the Lie algebra scalar t to the corresponding uniform rail velocity vector $\delta\mathbf{s} = t\mathbf{1}_3$. Because $\mathbf{1}_3 \neq \mathbf{0}$, the condition $t\mathbf{1}_3 = \mathbf{0}$ strictly implies $t = 0$. This guarantees that the local isotropy subgroup is trivial (meaning the group action is strictly free). Consequently, the differential mapping is fully injective, and the dimension of the trivial motion space matches the dimension of the symmetry group:

$$\dim\left(\mathrm{Im}(d\Phi_{\mathbf{s}}|_e)\right) = \dim(G) = 1. \tag{120}$$

Because the framework is measurement Φ-invariant and

$$\dim \ker \mathbf{R}(\mathbf{s}) = \dim \mathrm{Im}(d\Phi_{\mathbf{s}}|_e) = 1$$

, the dimensional equality condition is strictly satisfied. This confirms that the framework at **s** is infinitesimally Φ-rigid. Finally, since the state **s** was chosen arbitrarily from the considered domain D_{kin}, we conclude that the entire smooth framework family over this domain is infinitesimally Φ-rigid. □

6 CONCLUSIONS AND FUTURE WORK

6.1 CONCLUSIONS

This thesis introduced the Hybrid Rigidity framework, a novel abstract mathematical formulation that unifies heterogeneous MASs and mixed-measurement sensing topologies into a single, cohesive theory. The framework constitutes a rigorous generalization of existing rigidity paradigms, which emerge naturally as special cases within it.

The introduction of group theory to define a new notion of rigidity provided the mathematical machinery necessary to formalize mixed measurements. A substantial contribution of this work lies in the characterization of the measurement function, which elegantly encapsulates the underlying complexity of handling heterogeneous agents and sensors. Rather than treating it as a monolithic entity, the measurement process was rigorously deconstructed into a strictly ordered composition of intermediate smooth maps. By detailing how this measurement function handles heterogeneity in both agents and sensing modalities, category theory provided a natural and rigorous language. It allowed us to formally express the structural relations holding between the intermediate steps of the modeling chain, as well as between the different pipeline realizations required to manage system heterogeneity.

The integration of extrinsic parameters allows the framework to overcome the classical limitation requiring measurements to depend exclusively on intrinsic agent states. Crucially, the reformulated measurement function is no longer constrained to process the entirety of the agents' kinematics: it can instead evaluate only a specific subset of the state information, or conversely, enrich it with external data. This yields a highly flexible architecture for modeling complex physical constraints and interactive systems.

As emphasized throughout this work, the proposed functorial characterizations serve primarily as a foundational baseline. The underlying categorical architecture is modular and flexible by design: one is free to generate a completely new base category to describe different modeling processes, define additional functorial realizations, characterize them according to specific analytical needs, and link them via natural transformations, provided the resulting architecture coherently describes the physical problem under analysis.

Building on the embedded formulation on homogeneous spaces, the thesis explicitly derived the algebraic structure of the embedded rigidity matrices for pure distance, pure bearing, and mixed distance-bearing measurements. This result holds for any

MAS employing the proposed Embedded Functor realization. Moreover, the approach is inherently non-restrictive, as it relies on a maximal realization within the Special Euclidean group $\mathbb{SE}(3)$. This algebraic foundation thus provides a powerful tool for establishing generalized structural results in future work.

Finally, the theoretical framework was validated through targeted case studies. These demonstrated how the framework can be deployed to analyze networks characterized by heterogeneous agents and mixed-measurement topologies, as well as formations of agents constrained to specific submanifolds, such as agents confined to parallel linear rails. This confirms the framework's broad applicability and effectiveness in formally modeling constrained, real-world physical systems.

6.2 FUTURE WORK: ALGORITHMIC DESIGN

The theoretical flexibility of the Hybrid Rigidity framework opens several critical avenues for future research, particularly in bridging the gap between structural analysis and algorithmic synthesis:

- **From Analysis to Synthesis:** The formulation presented thus far inherently addresses an *analysis* problem: given a predefined framework, we verify whether it is rigid with respect to a given Lie group action Φ operating on the agents' configuration space. However, this mathematical foundation naturally paves the way for the inverse problem. Suppose we are given a system of n agents that must be made rigid with respect to a specific group action Φ. The dual challenge lies in systematically designing the graph topology and assigning the appropriate measurement functions to the edges in order to achieve Φ-rigidity for a desired family of smooth ordered frameworks.
- **Optimal Network Design:** Using the mixed-measurement framework to synthesize sensing topologies that achieve specific design targets, such as minimizing hardware costs while maximizing fault tolerance, structural robustness, and guaranteeing the desired rigidity properties. This approach would exploit the asymmetric capabilities of heterogeneous agents to optimally allocate sensing tasks across the network.
- **Distributed Control Synthesis:** Developing novel nonlinear cooperative control and network localization laws within this new framework. The algebraic transparency of the proposed framework provides a direct foundation for designing gradient-based control strategies, which can be further enriched by modern mathematical techniques such as geometric control or Port-Hamiltonian systems.
- **Submanifold-Constrained Dynamics:** Formalizing the concept of rigidity for submanifold-constrained dynamics, namely MASs whose states are intrinsically restricted to specific geometric submanifolds. While introduced in this

work, this concept requires further mathematical investigation and formalization. Future efforts will involve extending the control and localization architectures to explicitly account for and enforce these geometric constraints.

- **Cross-Manifold Dynamics:** Leveraging the abstract embedding framework to address the complex coordination of MASs experiencing discontinuous state-space transitions, drawing upon Hybrid Dynamics and Control Theory. This explicitly targets scenarios where agents dynamically switch the manifolds they inhabit during operation (e.g., a ground vehicle in $S\mathbb{E}(2)$ abruptly transitioning between intersecting planar surfaces with different orientation constraints). Future research will investigate whether the proposed unified embedding space can provide the mathematical foundation to model these discontinuous cross-manifold jumps, exploring how the global rigidity formalism and cooperative control laws might be preserved across such topological transitions.

- **Robustness Analysis:** To successfully bridge the sim-to-real gap, the stability of the hybrid rigidity properties must be rigorously investigated across several critical dimensions:

  - *Parameter Variations:* Analyzing robustness against dynamic extrinsic and intrinsic parameter variations. This direction will explicitly exploit the enhanced resilience provided by combining different sensing modalities to effectively mitigate traditional unimodal vulnerabilities.

  - *Communication Constraints and Delays:* Investigating the impact of bandwidth limitations, packet loss, and time delays on the structural cohesion of the network. Addressing these challenges necessitates the integration and application of advanced networked control systems tools.

  - *Measurement Noise and Stochastic Rigidity:* Addressing real-world sensor inaccuracies by extending the current deterministic framework. This requires formally redefining rigidity theory within a rigorous stochastic mathematical setting to properly model, analyze, and filter uncertainties, ultimately enabling robust state estimation and reliable control of the overall system.

- **Large-Scale Swarms and Continuum Limits:** Extending the proposed distributed algorithms to tackle complex large-scale networks and mean-field problems. This includes formalizing the rigidity conditions for the continuum limit of MASs, where the discrete network transitions into a continuous spatial density, thereby enabling the macroscopic control of massive robotic swarms.

- **Observability and Controllability:** Investigating how invariants and underlying symmetries govern the structural observability and controllability of the overall MAS.

- **Symmetry-Breaking Mechanisms:** Formally investigating how the strategic integration of heterogeneous measurements can systematically break spatial ambiguities (such as scale or reflection symmetries) to naturally anchor formations without requiring absolute reference frames.

6.3 FUTURE WORK: INFORMATION RIGIDITY

Beyond traditional spatial formation control, the framework's ability to process partial manifold data and integrate extrinsic information via the Augmented realization suggests a profound paradigm shift:

- **Measurement Space Parameterization:** Extending the integration of extrinsic parameters and offsets beyond the agent state space directly into the measurement space and the intermediate stages of the modeling chain. This expansion will allow for more complex sensor modeling, accommodating heterogeneous sensing hardware with intrinsic offsets or non-ideal calibrations.
- **Extrinsic Variables in Control Design:** Enabling the development of control algorithms that leverage both agent kinematics and external variables to achieve specific collective objectives. These algorithms can drive source-seeking behaviors where agents coordinate under rigidity-like constraints to locate the origin of temperature or pollution fields. Furthermore, this approach can optimize the overall coverage of a MAS equipped with extrinsic or communication sensors while rigorously preserving its structural coordination.
- **Dynamic Movements and Design Synthesis:** Leveraging group-based Φ-rigidity to explore formations that preserve desired dynamic movements rather than static shapes. This introduces a novel design problem: synthesizing MAS structure and control laws specifically engineered to achieve and guarantee these permitted dynamic behaviors.
- **Local and Subgraph Symmetries:** While classical rigidity typically deals with global framework symmetries, the enhanced generality of this hybrid framework allows for the emergence of local and subgraph-specific behavior. This requires a formal characterization of such localized invariances as they naturally arise in mixed-signal sensor networks.
- **Counting Rules and Rank Conditions:** Classical rigidity theorems, such as Laman's and Maxwell's, are fundamentally restricted to Euclidean spaces and systems that are strictly homogeneous in both agents and measurements. Overcoming these limitations requires formulating novel combinatorial tools specifically tailored for non-Euclidean ambient spaces and networks that are heterogeneous in both agent kinematics and measurement modalities.
- **Information Rigidity and General Systems Control:** Formalizing the concept of "Information Rigidity" by extending traditional frameworks beyond purely spatial formations. In this generalized paradigm, structural cohesion

is no longer dictated by rigid geometric shapes, but rather by the preservation of distributed information and specific system properties. This shift allows for the definition of generalized metrics that consist of different information beyond purely geometric quantities and standard one-to-one agent mappings to incorporate multi-source and/or multi-target measurements. By introducing these novel measurement paradigms tailored to distributed variables, the framework can be actively leveraged to induce desired collective behaviors while accounting for complex agent interactions. Extending this concept to general distributed networks offers a novel mathematical perspective for revisiting and resolving standard distributed control problems, such as the regulation of physical fields (e.g., environmental temperature), as well as entirely new ones.

A GRAPH THEORY

Definition A.1 (Directed Graph). A *directed graph* $\mathcal{G} = (\mathcal{V}, \mathcal{E})$ is an ordered pair consisting of a finite set of vertices $\mathcal{V}$ and a set of directed edges $\mathcal{E} \subseteq \mathcal{V} \times \mathcal{V}$. An element $v \in \mathcal{V}$ is called a vertex or a node. An element $(j, i) \in \mathcal{E}$ explicitly indicates an edge directed *from* vertex j *to* vertex i. In this context, j is called the source and i is called the target of the edge.

Definition A.2 (Neighborhood in Directed Graphs). In a directed graph $\mathcal{G} = (\mathcal{V}, \mathcal{E})$, the neighborhood of a vertex $v_i \in \mathcal{V}$ is strictly partitioned based on the orientation of the edges:

- The *in-neighborhood* $\mathcal{N}_i^{\text{in}}$ consists of all source vertices that have an edge directed towards v_i:
$$\mathcal{N}_i^{\text{in}} = \{v_j \in \mathcal{V} \mid (v_j, v_i) \in \mathcal{E}\}. \tag{1}$$
- The *out-neighborhood* $\mathcal{N}_i^{\text{out}}$ consists of all target vertices to which v_i directs an edge:
$$\mathcal{N}_i^{\text{out}} = \{v_j \in \mathcal{V} \mid (v_i, v_j) \in \mathcal{E}\}. \tag{2}$$

Correspondingly, the cardinalities of these sets, denoted as $d^{\text{in}}(v_i) = |\mathcal{N}_i^{\text{in}}|$ and $d^{\text{out}}(v_i) = |\mathcal{N}_i^{\text{out}}|$, are defined as the *in-degree* and *out-degree* of v_i, respectively.

Definition A.3 (Undirected Graph). An *undirected graph* $\mathcal{G} = (\mathcal{V}, \mathcal{E})$ is a graph where the connections between vertices are bidirectional. Formally, the edge set $\mathcal{E}$ consists of *unordered* pairs of distinct vertices, denoted as $\{i, j\}$ rather than the ordered pair (i, j). Alternatively, it can be viewed as a directed graph satisfying a symmetry property: if a directed edge (i, j) exists from vertex i to vertex j, then the reverse edge (j, i) is also present.

Definition A.4 (Neighborhood in Undirected Graphs). Given an undirected graph $\mathcal{G} = (\mathcal{V}, \mathcal{E})$ and a vertex $v_i \in \mathcal{V}$, the *neighborhood* of v_i, denoted by $\mathcal{N}_i$, is defined as the set of all adjacent vertices directly connected to v_i. Formally:

$$\mathcal{N}_i = \{v_j \in \mathcal{V} \mid \{v_i, v_j\} \in \mathcal{E}\}. \tag{3}$$

The cardinality of this set, $d(v_i) = |\mathcal{N}_i|$, is referred to as the *degree* of vertex v_i.

Definition A.5 (Simple Graph)**.** A *simple graph* is a (directed or undirected) graph that contains no self-loops (edges connecting a vertex to itself) and no multiple edges (more than one edge connecting the exact same pair of vertices in the same direction). In the mathematical modeling of multi-agent sensing networks, interaction topologies are standardly assumed to be simple finite graphs, ensuring that the edge set $\mathscr{E}$ strictly represents unique pairwise physical interactions.

Definition A.6 (Complete Graph)**.** The *complete graph* with n vertices, denoted by K_n, is a special undirected graph in which every pair of distinct vertices is connected by a unique edge. Consequently, its edge set $\mathscr{E}$ contains all possible $\frac{n(n-1)}{2}$ unordered pairs of vertices.

Definition A.7 (Finite Graph)**.** A *finite graph* is a graph characterized by a finite number of vertices and edges. Formally, both the cardinality of the vertex set, denoted as $|\mathscr{V}| = n$, and the cardinality of the edge set, denoted as $|\mathscr{E}| = m$, are finite integers.

Definition A.8 (Labeled Graph)**.** A finite (directed or undirected) graph $\mathscr{G} = (\mathscr{V}, \mathscr{E})$ is defined as a *labeled graph* when its vertices and edges are assigned unique, distinct identifiers. This property ensures that each abstract entity within the network is uniquely distinguishable from the others, although it does not inherently impose any mathematical sequence or numerical mapping.

Definition A.9 (Indexed Graph)**.** A labeled graph $\mathscr{G} = (\mathscr{V}, \mathscr{E})$ is defined as an *indexed graph* when its unique identifiers are bijectively mapped to the standard finite index sets $\mathscr{I}_{\mathscr{V}} = \{1, \ldots, n\}$ and $\mathscr{I}_{\mathscr{E}} = \{1, \ldots, m\}$, where n and m denote the total number of vertices and edges, respectively. Under this mapping, the vertex and edge sets are formally enumerated as $\mathscr{V} = \{v_1, \ldots, v_n\}$ and $\mathscr{E} = \{e_1, \ldots, e_m\}$.

Definition A.10 (Ordered Graph)**.** An indexed graph $\mathscr{G} = (\mathscr{V}, \mathscr{E})$ is defined as an *ordered graph* when a strict total order, naturally induced by its index sets, is explicitly imposed on its vertices and edges. Consequently, $\mathscr{V}$ and $\mathscr{E}$ are no longer treated as unordered sets, but rather as mathematically ordered tuples, denoted by the tuple notation $\mathscr{V} = (v_1, \ldots, v_n)$ and $\mathscr{E} = (e_1, \ldots, e_m)$.

B CATEGORY THEORY

Definition B.1 (Category)**.** A category $\mathscr{C}$ consists of the following data:

- A class of objects, denoted by $\mathrm{ob}(\mathscr{C})$.
- A class of morphisms (also known as arrows or maps), denoted by $\mathrm{mor}(\mathscr{C})$. Each morphism f is associated with a unique source object $a \in \mathrm{ob}(\mathscr{C})$ and a unique target object $b \in \mathrm{ob}(\mathscr{C})$. We write $f : a \to b$ to indicate this relationship.
- A binary operation called *composition of morphisms*. For any three objects $a, b, c \in \mathrm{ob}(\mathscr{C})$, the composition operator is defined as a function:

  $$\circ : \mathrm{hom}_{\mathscr{C}}(b, c) \times \mathrm{hom}_{\mathscr{C}}(a, b) \to \mathrm{hom}_{\mathscr{C}}(a, c)$$

  The composition of a morphism $f : a \to b$ and a morphism $g : b \to c$ is denoted as $g \circ f : a \to c$.

Furthermore, this data must satisfy two fundamental axioms:

- **Associativity**: For any sequence of morphisms $f : a \to b$, $g : b \to c$, and $h : c \to d$, the composition is associative:

  $$h \circ (g \circ f) = (h \circ g) \circ f$$

- **Identity**: For every object $x \in \mathrm{ob}(\mathscr{C})$, there exists a unique identity morphism $\mathrm{id}_x : x \to x$ such that for any morphism $f : a \to x$, we have $\mathrm{id}_x \circ f = f$, and for any morphism $g : x \to b$, we have $g \circ \mathrm{id}_x = g$.

Definition B.2 (Functor)**.** A functor is a structure-preserving map between categories. Specifically, a *covariant functor* F from a category $\mathscr{C}$ to a category $\mathscr{D}$, denoted $F : \mathscr{C} \to \mathscr{D}$, is an association that maps:

- Each object $X \in \mathrm{ob}(\mathscr{C})$ to a corresponding object $F(X) \in \mathrm{ob}(\mathscr{D})$.
- Each morphism $f : X \to Y$ in $\mathscr{C}$ to a corresponding morphism $F(f) : F(X) \to F(Y)$ in $\mathscr{D}$.

This mapping must satisfy the following structural properties:

- **Identity preservation**: $F(id_X) = id_{F(X)}$ for every object $X \in \mathrm{ob}(\mathscr{C})$.
- **Composition preservation**: $F(g \circ f) = F(g) \circ F(f)$ for all morphisms $f : X \to Y$ and $g : Y \to Z$ in $\mathscr{C}$.

Definition B.3 (Contravariant Functor)**.** A *contravariant functor* behaves analogously to a covariant functor but explicitly reverses the direction of the morphisms. If $f : X \to Y$ is a morphism in $\mathscr{C}$, then the contravariant functor yields $F(f) : F(Y) \to F(X)$ in $\mathscr{D}$. The composition rule is accordingly reversed: $F(g \circ f) = F(f) \circ F(g)$.

Definition B.4 (Natural Transformation)**.** A *natural transformation* provides a rigorous mathematical translation between two functors while strictly preserving the internal morphisms of the categories involved.

Let $F, G : \mathscr{C} \to \mathscr{D}$ be two covariant functors acting between categories $\mathscr{C}$ and $\mathscr{D}$. A natural transformation $\eta : F \Rightarrow G$ assigns to every object $X \in \mathrm{ob}(\mathscr{C})$ a morphism $\eta_X : F(X) \to G(X)$ in $\mathscr{D}$, referred to as the *component* of η at X.

This family of morphisms must satisfy a structural compatibility condition: for any two objects $X, Y \in \mathrm{ob}(\mathscr{C})$ and any morphism $f \in \hom_{\mathscr{C}}(X, Y)$, the identity $\eta_Y \circ F(f) = G(f) \circ \eta_X$ must hold. Equivalently, this dictates that the following diagram in $\mathscr{D}$ commutes:

$$\begin{tikzcd}
F(X) \arrow[r, "F(f)"] \arrow[d, "\eta_X"'] & F(Y) \arrow[d, "\eta_Y"] \\
G(X) \arrow[r, "G(f)"'] & G(Y)
\end{tikzcd}$$

Figure B.1: Commutative square illustrating the naturality condition for $\eta : F \Rightarrow G$.

C GROUP THEORY

Definition C.1 (Group)**.** A *group* is a set G equipped with a binary operation $\cdot : G \times G \to G$, mapping an ordered pair (g, h) to an element $g \cdot h$ (often denoted simply as gh), satisfying the following four axioms:

1. **Closure:** For all $g, h \in G$, the product $g \cdot h \in G$.
2. **Associativity:** For all $f, g, h \in G$, $(f \cdot g) \cdot h = f \cdot (g \cdot h)$.
3. **Identity Element:** There exists a unique element $e \in G$ such that for every $g \in G$, $e \cdot g = g \cdot e = g$.
4. **Inverse Element:** For each $g \in G$, there exists a unique element $g^{-1} \in G$ such that $g \cdot g^{-1} = g^{-1} \cdot g = e$.

Definition C.2 (Lie Group)**.** A *Lie group* is a set G equipped simultaneously with the structure of a group and the structure of a smooth manifold, satisfying the following compatibility conditions between its algebraic and topological frameworks:

1. The multiplication map $\mu : G \times G \to G$, induced by the group's binary operation via the assignment $(g, h) \mapsto g \cdot h$, is a smooth (C^∞) map, where $G \times G$ is endowed with the standard product manifold structure.
2. The inversion map $\iota : G \to G$, defined by the assignment $g \mapsto g^{-1}$, is a smooth (C^∞) map.

This compatibility between algebraic and topological structures ensures that continuous group operations do not introduce singularities.

Definition C.3 (Smooth Group Action)**.** Let G be a Lie group with identity element e, and let M be a smooth manifold.
A *smooth left action* of G on M is a smooth (C^∞) map $\theta : G \times M \to M$, conventionally denoted as $\theta(g, p) = g \cdot p$, that satisfies the following two axioms for all $g, h \in G$ and $p \in M$:

1. **Identity:** $e \cdot p = p$.
2. **Compatibility:** $g \cdot (h \cdot p) = (gh) \cdot p$.

Analogously, a *smooth right action* is a smooth (C^∞) map $\phi : M \times G \to M$, conventionally denoted as $\phi(p, g) = p \cdot g$, that satisfies the following two axioms for all $g, h \in G$ and $p \in M$:

1. **Identity:** $p \cdot e = p$.
2. **Compatibility:** $(p \cdot g) \cdot h = p \cdot (gh)$.

In the context of spatial transformations and geometric control, left actions are predominantly adopted. Therefore, throughout this work, we will simply use the term *action* or *group action* to denote a left group action unless explicitly stated otherwise.

Remark C.1 (Relation between Left and Right Actions). If $\rho : M \times G \to M$ is a right group action, then the map $\theta : G \times M \to M$ defined by $\theta(g, p) = \rho(p, g^{-1})$ constitutes a valid left group action. Consequently, any theoretical result derived under the assumption of a left group action applies equivalently to right group actions, justifying our standard choice without loss of generality.

Definition C.4 (G-space)**.** A smooth manifold M equipped with a smooth (left or right) action of a Lie group G is called a *G-space*.

Definition C.5 (Isotropy Group)**.** Let $\theta : G \times M \to M$ be an action of a Lie group G on a manifold M. The *isotropy group* (or *stabilizer*) G_p of a point $p \in M$ is the subgroup consisting of all elements in G that fix p. Formally:

$$G_p = \{g \in G \mid \theta_g(p) = p\} \tag{1}$$

Definition C.6 (Orbit)**.** Let M be a G-space equipped with a smooth left action $\theta : G \times M \to M$, conventionally denoted by $\theta(g, p) = g \cdot p$. The *orbit* of a point $p \in M$, denoted as $\mathrm{Orb}(p)$ or $G \cdot p$, is the subset of the manifold defined by:

$$\mathrm{Orb}(p) = \{g \cdot p \in M \mid g \in G\} \subseteq M \tag{2}$$

Geometrically, $\mathrm{Orb}(p)$ forms an immersed smooth submanifold of M, representing the locus of all points reachable from p through the continuous action of the group G.

Remark C.2 (Equivalence Relation and Orbit Space). The group action induces a natural equivalence relation on the manifold M. Two points $p, q \in M$ are defined to be equivalent if they belong to the same orbit. Because of the fundamental group axioms, this relation is reflexive, symmetric, and transitive. Consequently, the orbits constitute a mathematical partition of M, dividing the space into mutually disjoint equivalence classes. The set of all these orbits is called the *orbit space* or *quotient space*, and is denoted by M/G.

Definition C.7 (Lie Algebra)**.** Associated with every Lie group G is its *Lie algebra*, conventionally denoted by the Fraktur letter $\mathfrak{g}$. The Lie algebra is a vector space canonically identified with the tangent space to the group manifold at its identity element e, such that $\mathfrak{g} \cong T_e G$. It completely captures the local, first-order algebraic and topological structure of the group G in the vicinity of the identity.

BIBLIOGRAPHY

[1] L. Euler, *Leonhardi Euleri Opera postuma mathematica et physica anno MDCCCXLIV detecta*. Petropoli: Eggers, 1862, vol. 1, pp. 494–496.

[2] A.-L. Cauchy, "Recherche sur les polyèdres—premier mémoire," *Journal de l'École Polytechnique*, vol. 9, pp. 68–86, 1813.

[3] J. C. Maxwell, "On the calculation of the equilibrium and stiffness of frames," *The London, Edinburgh, and Dublin Philosophical Magazine and Journal of Science*, vol. 27, no. 182, pp. 294–299, 1864.

[4] J. C. Maxwell, "On reciprocal figures, frames, and diagrams of forces," *Transactions of the Royal Society of Edinburgh*, vol. 26, no. 1, pp. 1–40, 1870.

[5] G. Laman, "On graphs and rigidity of plane skeletal structures," *Journal of Engineering Mathematics*, vol. 4, no. 4, pp. 331–340, 1970.

[6] L. Asimow and B. Roth, "The rigidity of graphs," *Transactions of the American Mathematical Society*, vol. 245, pp. 279–289, 1978.

[7] L. Asimow and B. Roth, "The rigidity of graphs ii," *Journal of Mathematical Analysis and Applications*, vol. 68, no. 1, pp. 171–190, 1979.

[8] M. F. Thorpe and P. M. Duxbury, Eds., *Rigidity Theory and Applications*. New York, NY, USA: Springer, 1999.

[9] H.-S. Ahn, *Formation Control: Approaches to Distributed Agents*. Berlin, Germany: Springer, 2020.

[10] M. De Queiroz, X. Cai, and M. Feemster, *Formation Control of Multi-Agent Systems: A Graph Rigidity Approach*. Hoboken, NJ, USA: Wiley, 2019.

[11] B. D. Anderson, C. Yu, B. Fidan, and J. M. Hendrickx, "Rigid graph control architectures for autonomous formations," *IEEE Control Systems Magazine*, vol. 28, no. 6, pp. 48–63, 2008.

[12] K.-K. Oh, M.-C. Park, and H.-S. Ahn, "A survey of multi-agent formation control," *Automatica*, vol. 53, pp. 424–440, 2015.

[13] D. Zelazo and M. Mesbahi, "Graph-theoretic methods for the analysis and synthesis of networked dynamic systems," *IEEE Transactions on Automatic Control*, vol. 56, no. 4, pp. 971–982, 2011.

[14] T. Eren et al., "Rigidity, computation, and randomization in network localization," in *IEEE INFOCOM 2004*, IEEE, vol. 4, 2004, pp. 2673–2684.

[15] C. Krick, M. E. Broucke, and B. A. Francis, "Stabilisation of infinitesimally rigid formations of multi-robot networks," *International Journal of Control*, vol. 82, no. 4, pp. 423–439, 2009.

[16] S. Zhao and D. Zelazo, "Translational and scaling formation maneuver control via a bearing-based approach," *IEEE Transactions on Control of Network Systems*, vol. 4, no. 3, pp. 429–438, 2015.

[17] S. Zhao and D. Zelazo, "Bearing rigidity theory and its applications for control and estimation of network systems: Life beyond distance rigidity," *IEEE Control Systems Magazine*, vol. 39, no. 2, pp. 66–83, 2019.

[18] G. Jing, G. Zheng, and L. Wang, "Angle rigidity and its usage to stabilize multi-agent formations in 2d," *IEEE Transactions on Automatic Control*, vol. 64, no. 12, pp. 5148–5155, 2019.

[19] J. M. Hendrickx, B. D. Anderson, J.-C. Delvenne, and V. D. Blondel, "Directed graphs for the analysis of rigidity and persistence in autonomous agent collectives," *International Journal of Robust and Nonlinear Control*, vol. 17, no. 10-11, pp. 960–981, 2007.

[20] S. Zhao and D. Zelazo, "Bearing-based formation stabilization with directed interaction topologies," in *54th IEEE Conference on Decision and Control (CDC)*, IEEE, 2015, pp. 6115–6120.

[21] D. Zelazo, A. Franchi, and P. Robuffo Giordano, "Bearing-only formation control using an $SE(2)$ rigidity theory," in *54th IEEE Conference on Decision and Control (CDC)*, IEEE, 2015, pp. 6121–6126.

[22] G. Michieletto, A. Cenedese, and A. Franchi, "Bearing rigidity theory in SE(3)," in *2016 IEEE 55th Conference on Decision and Control (CDC)*, IEEE, 2016, pp. 5950–5955. DOI: 10.1109/CDC.2016.7799182

[23] G. Michieletto, A. Cenedese, and D. Zelazo, "A unified dissertation on bearing rigidity theory," *IEEE Transactions on Control of Network Systems*, vol. 8, no. 4, pp. 1624–1636, 2021. DOI: 10.1109/TCNS.2021.3077712

[24] G. Stacey and R. Mahony, "The role of symmetry in rigidity analysis: A tool for network localization and formation control," *IEEE Transactions on Automatic Control*, vol. 63, no. 5, pp. 1313–1328, 2018. DOI: 10.1109/TAC.2017.2747760

[25] J. Aspnes et al., "A theory of network localization," *IEEE Transactions on Mobile Computing*, vol. 5, no. 12, pp. 1663–1678, 2006.

[26] S. Zhao and D. Zelazo, "Bearing rigidity and almost global bearing-only formation stabilization," *IEEE Transactions on Automatic Control*, vol. 61, no. 5, pp. 1255–1268, 2016.

[27] S. Zhao and D. Zelazo, "Localizability and distributed protocols for bearing-based network localization in arbitrary dimensions," *Automatica*, vol. 69, pp. 334–341, 2016.

[28] R. M. Haralick, C.-N. Lee, K. Ottenberg, and M. Nölle, "Review and analysis of solutions of the three point perspective pose estimation problem," *International Journal of Computer Vision*, vol. 13, no. 3, pp. 331–356, 1994. DOI: 10.1007/BF02028352 [Online]. Available: https://doi.org/10.1007/BF02028352